RESCUE AND CHARACTERISATION OF OROPOUCHE VIRUS IN MAMMALIAN CELL LINES

Natasha Louise Tilston-Lunel

A Thesis Submitted for the Degree of PhD
at the
University of St Andrews

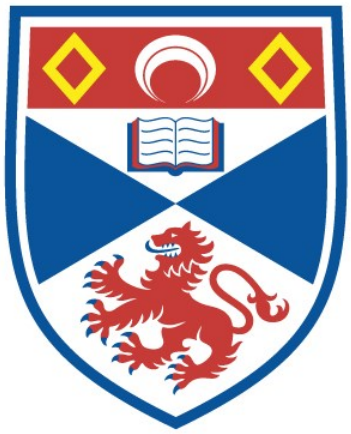

2016

Rescue and characterisation of Oropouche virus in mammalian cell lines

Natasha Louise Tilston-Lunel
BSc, MSc

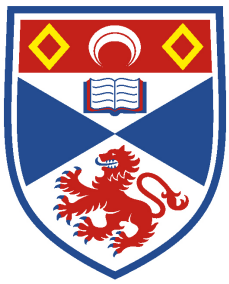

University of
St Andrews

This thesis is submitted in partial fulfilment for the degree of
Doctor of Philosophy
at the
University of St Andrews

November 2015

Rescue and characterisation of Oropouche virus in mammalian cell lines

Natasha Louise Tilston-Lunel

Biomolecular Sciences Research Complex
University of St Andrews
St Andrews, UK

A thesis submitted for the degree of Doctor of Philosophy
in
Molecular Virology

November 2015

Supervisors:
Professor Richard M. Elliott
University of Glasgow, Centre for Virus Research

Professor Richard E. Randall
University of St. Andrews, School of Biology

Abstract

Oropouche virus (OROV) is a medically important orthobunyavirus, which causes frequent outbreaks of a febrile illness in the northern parts of Brazil. However, despite being the cause of an estimated half a million human infections since its first isolation in Trinidad in 1955, details of the molecular biology of this tripartite, negative-sense RNA virus remain limited. The work presented in this thesis has re-determined the nucleotide sequences of OROV strain BeAn19991 (GenBank accession numbers: L, KP052850; M, KP052851 and S, KP052852), and demonstrates that the S segment is significantly longer than the published sequence with an additional 204 nucleotides at the 3' end. Data analysis revealed that there is a critical nucleotide mismatch at position 9 within the base-paired terminal panhandle structure of each genomic segment. Using a combination of deep sequencing and Sanger sequencing the complete genome sequences of 10 field isolates of OROV were also determined for the first time, and led to the identification of a novel OROV reassortant virus. Phylogenetic analysis of these sequences and of published sequences showed that there are two genotypes of OROV, rather than the four genotypes previously proposed. Further work led to the development of a T7-RNA polymerase-driven minigenome and virus-like particle (VLP) production systems for OROV; the information from these was subsequently used to develop a reverse genetics system for OROV. Using reverse genetics, OROV mutants that lack either the non-structural proteins NSm or NSs were generated. *In vitro* growth properties of the OROV mutant lacking NSm were indistinguishable from the wild-type virus, but the NSs mutant was attenuated in growth, particularly in interferon (IFN) competent cells. Further work demonstrated NSs as a viral IFN antagonist and that it's C-terminus is required for this activity. Interestingly, OROV is more resistant to IFN-α treatment than Bunyamwera virus, but this is not related to its NSs protein.

The development of a reverse genetics system for OROV, which is the main human pathogen within the Simbu serogroup of orthobunyaviruses, will prove invaluable for future studies designed to further investigate the molecular pathogenesis of this virus and in the development of attenuated vaccine strains.

Publications based on this thesis

Published

Acrani GO* and **Tilston-Lunel NL***., Spiegal M., Weidmann M., Silva D., Nunes MRT., Elliott RM. (2014). Establishment of a minigenome system for Oropouche virus reveals the S genome segment to be significantly longer than reported previously. *Journal of General Virology*, 95, 513-523.

Tilston-Lunel NL., Hughes J., Acrani GO., da Silva DE., Azevedo RS., Rodrigues SG., Vasconcelos PF., Nunes MR., Elliott RM. (2015). Genetic analysis of members of the species Oropouche virus and identification of a novel M segment sequence. *Journal of General Virology*, 96(7):1636-1650.

Tilston-Lunel NL*., Acrani GO*., Randall RE., Elliott RM. (2015). Generation of recombinant Oropouche viruses lacking the nonstructural protein NSm or NSs, *Journal of Virology*. In Press, Dec 23. pii: JVI.02849-15.

In preparation

Natasha L. Tilston-Lunel, Xiaohong Shi, Richard M. Elliott and Gustavo Olszanski Acrani. Minigenome analysis suggests that Oropouche and Schmallenberg orthobunyaviruses would be capable of reassortment.

Contributed to, but not part of this thesis

Mariana Varela, Ilaria M. Piras, Catrina Mullan, Xiaohong Shi, **Natasha L. Tilston-Lunel**, Rute Maria Dos Santo Pinto, Stephen R. Welch, Felix Kreher, Aislynn Taggart, Stuart J.D. Neil, Richard M. Elliott and Massimo Palmarini. BST-2 is One of the Determinants of Orthobunyavirus Host Range (in preparation).

* co-authors

Acknowledgments

Richard I did it! At 317 pages it's not quite as short as you said it would be! Wish you were here to tell me what you think, but Steve did a good job of reminding me of you and things you probably would have said whilst walking into the office shaking your head at me! I hope you can read it now and be proud. I miss you and I want to thank you for constantly pushing me to do better and encouraging me whenever I doubted myself. I want to thank you for all the times when I came knocking at your office door whether it was for science or for my confusions in life, your support has brought me to where I am today and for that I am truly grateful. I am proud to have been your PhD student Professor Elliott!

I would like to thank Professor Rick Randall, your help and your encouraging words have been crucial for me in these last few months. I thank my collaborator Dr. Gustavo Olszanski Acrani, you my Oropouche buddy! have made this PhD fun. I have enjoyed all the conversations we have had and all the crazy ideas we have shared! You have become a true friend and I will never forget your constant support and kind words. I wish you the very best of luck with starting your own group.

I would like to acknowledge the people who have read this thesis, my supervisor Professor Rick Randall and Dr. Gustavo Olszanski Acrani. Thank you Dr. Isabelle Dietrich for reading my introduction and Dr. Steve Welch for the critical review of my work. Mr. Mark Tilston, the best dad in the world! thank you for putting up with me and proof reading this entire thesis!

I would like to thank past and present Elliott lab members, Dr. Agnieszka Szemiel, Dr. Aitor Navarro, Angela Elliott, Dr. Basma Bahsoun, Dr. Ben Brennan, Dr. Beryl Mazel-Sanchez, Edward Dornan, Elina Koudriakova, Dr. Felix Kreher, Gillian Slack, Dr. Gjon Blakqori, Dr. Ingeborg van Knippenberg, Jill McVee, Junjie Feng, Dr. Ping Li, Dr. Sophie Jegouic, Dr. Steve Welch, Veronica Rezelj and Dr. Xiaohong Shi, for help in the lab and for all the fun times. Agnieszka, Ben and Steve thank you for always answering

questions I had and Agnieszka for always saying ‘there is no such thing as a dumb question’. Angela thank you for always being there to talk to, hopefully that bottle is still OK to drink! I am going to miss all of you and I wish you all the very best in everything.

I also want to acknowledge our collaborators Professor Manfred Weidmann for initial data before I started on this project. Dr. Marcio Roberto Teixeira Nunes and Professor Pedro Vasconcelos for Oropouche virus samples and for resources I used during my stay in your lab. Dr. Daisy da Silva, thank you for helping me in the lab and teaching me how to use the sequencers. I thank everyone at the Evandro Chagas Institute, for trying so very hard to teach me Portuguese! for showing me your culture and most of all making me feel welcome. A special shout-out to the Nunes group - Dr. Daisy da Silva, Dr. Clayton Lima, Dr. Janaina Vasconcelos, Dr. João Vianez, Jedson Cardoso, Keley Nunes, Layanna Oliveira, Rodrigo de Oliveira and Dr. Sandro Patroca Silva. Sandro, I’m sorry I still can’t dance the Samba!

I would like to thank members of my PhD committee Dr. David Jackson and Dr. Rona Ramsay for critical appraisal during my four and nine month review meetings. I thank the Medical Research Council for funding me, and Professor Massimo Palmarini for the support you have given me.

I would not have chosen the path of a PhD had it not been for meeting amazing people like Dr. Chris Skelly, Professor John Edmunds and Professor Tanya Parish. You inspired me and showed me that research is fun! My science school teacher Mrs. Vijaya Kumari, your classes always left me in awe of biology. These four years have been a journey I will always cherish and I want to thank the friends I have made along the way. Especially Andri Vasou, Lee Sherry and Chris Murgatroyd, thank you for all those fun nights in St Andrews! Lee, I know you can’t wait to share a flat with Andri and me again at our next conference! I wish you guys nothing but happiness.

I would like to thank my adopted Brazilian family Daisy da Silva, Regina Andrade, Fcisco da Silva, Tulio da Silva and Katia Andrade for the amazing time I had in Brazil. I'm not exactly sure how I would have survived there without you!

I am humbled by the love and encouragement I've constantly received from all my family and friends, whilst there are so many of you to list a special thanks must be given to Aruna Tilston (ma), Mark Tilston (dad), Chad Tilston, Andrew Tilston-Lunel, Lokajini Kasinathar, Steve Welch, Lisa Monteith and Sumita Sharma. I can't remember a day where I've felt low during these last few months and not received a message of some kind from any one of you. I love you all.

Chad your positivity has always been my motivation. Jini, my soul mate, you have helped me keep my sanity. Lisa, thank you for being such an awesome big sister. Alasdair Monteith, unfortunately I don't think I'll be swimming in money like Beyoncé any time soon! Paris puppy a woof-woof to you too! Mum and dad, I don't even know where to begin, the sacrifices you have made, and your unconditional love and support have made me the person I am today. Thank you.

Andrew Tilston-Lunel, husband I finished first! Now I'm going to miss our "writing-up" coffee breaks to ASDA and our "writing-up" chapatti and fried-egg lunches. It's been fun writing this together and thank you for putting up with me and answering all the science confusions I've had! We've come a long way since we first met in 2004 and I would like to thank you for everything. I wish you nothing but happiness. I love you.

Narendra Kumar Sithiah (11.11.1977 – 07.01.2016)

Forever in our hearts. Until I see you again Naresh mãmã, my pumpkin.

To,

My parents, Mark and Aruna Tilston

And

My mentor and father figure Richard M. Elliott

My three heroes.

I love you.

Declarations

1. Candidate's declarations:

I, *Natasha Louise Tilston-Lunel*, hereby certify that this thesis, which is approximately 46,288 words in length, has been written by me, and that it is the record of work carried out by me, or principally by myself in collaboration with others as acknowledged, and that it has not been submitted in any previous application for a higher degree.

I was admitted as a research student in *September 2011* and as a candidate for the degree of *PhD in Molecular Virology* in *September 2012*; the higher study for which this is a record was carried out in the University of St Andrews between *2012* and *2015*.

Date ……. Signature of candidate ……

2. Supervisor's declaration:

I hereby certify that the candidate has fulfilled the conditions of the Resolution and Regulations appropriate for the degree of ……. in the University of St Andrews and that the candidate is qualified to submit this thesis in application for that degree.

Date……. Signature of supervisor ……

3. Permission for publication:

In submitting this thesis to the University of St Andrews I understand that I am giving permission for it to be made available for use in accordance with the regulations of the University Library for the time being in force, subject to any copyright vested in the work not being affected thereby. I also understand that the title and the abstract will be published, and that a copy of the work may be made and supplied to any bona fide library or research worker, that my thesis will be electronically accessible for personal

or research use unless exempt by award of an embargo as requested below, and that the library has the right to migrate my thesis into new electronic forms as required to ensure continued access to the thesis. To the best of my knowledge, no third-party copyright permissions are required in order to allow such access and migration, and I have requested the appropriate embargo below.

The following is an agreed request by candidate and supervisor regarding the publication of this thesis:

PRINTED COPY

Embargo on all print copy for a period of *1 year* on the following ground:

- Publication would preclude future publication.

Date……

Signature of candidate …… Signature of supervisor……

ELECTRONIC COPY

Embargo on all electronic copy for a period of *1 year* on the following ground:

- Publication would preclude future publication.

Date……

Signature of candidate …… Signature of supervisor……

Table of Contents

List of Tables

List of Figures

List of abbreviations

°C	degrees Celsius (temperature)
3’ UTR	3’ untranslated region
5’ UTR	5’ untranslated region
aa	amino acid
BHK	baby hamster kidney
bp	base pair
BSA	bovine serum albumin
cDNA	complementary DNA
CPE	cytopathic effect
CTD	carboxy-terminal domain
DC-SIGN	Dendritic Cell-Specific Intercellular adhesion molecule-3-Grabbing Non-integrin
DAPI	4’, 6-diamidino-2-phenylindole
DNA	deoxyribonucleic acid
dNTP	deoxyribonucleotide triphosphate
DMEM	Dulbecco’s modified Eagle medium
DMSO	dimethyl sulphoxide
DTT	dithiothreitol
dsRNA	double-stranded RNA
ECL	enhanced chemoluminescence
EDTA	ethylene diamine tetra-acetic acid
eGFP	enhanced GFP
EM	electron microscopy
ER	endoplasmic reticulum
FBS	foetal bovine serum
g	gram
Gn/Gc	glycoproteins Gn and Gc
GMEM	Glasgow modified Eagles media
HRP	horseradish peroxidase
ICTV	International Committee on Taxonomy of Viruses
IFN	interferon
IRES	internal ribosomes entry site
IRF	interferon regulatory factor
ISG	interferon stimulated gene
ISRE	interferon stimulated response element

kDa	kilo Dalton
L	L protein (viral polymerase) or large segment
M	medium segment
M	molar concentration (moles per litre)
MDA5	melanoma differentiation-associated protein 5
MEM	modified Eagles media
mg	milli-gram
min	minutes
ml	milli-litre
mM	milli-molar
M-MLV RT	Moloney murine leukemia virus reverse transcriptase
MOI	multiplicity of infection
mRNA	messenger RNA
N	nucleoprotein
NCS	newborn calf serum
ng	nano-gram
NSm	non-structural medium (non-structural protein encoded on the M segment)
NSs	non-structural small (non-structural protein encoded on the S segment)
nt	nucleotide
ORF	open reading frame
PAMPs	pathogen-associated molecular patterns
PBS	phosphate-buffered saline
PCR	polymerase chain reaction
pfu	particle forming unit
pH	$-\log_{10}[H^+]$
p.i.	post-infection
PKR	protein kinase R
PRR	pattern recognition receptors
p.t.	post-transfection
PVDF	polyvinylidene difluoride
RACE	rapid amplification of cDNA end
RdRp	RNA-dependant RNA-polymerase
RIG-1	retinoic acid inducible gene-1
rpm	revolutions per minute
RNA	ribonucleic acid
RNAP	RNA polymerase
RNP	ribonucleocapsid
RT	room temperature
RT-PCR	reverse-transcription PCR
S	small segment

SDS-PAGE	sodium dodecyl sulphate polyacrylamide gel electrophoresis
STAT1	signal transducers and activators of transcription 1
TFIIH	transcription initiation factor II H
Tm	melting temperature
TPB	typtose phosphate broth
Tris	tris-hygroxymethyly-aminomethane
T7RNAP	T7 RNA polymerase
UTR	un-translated regions
UV	ultra-violet
VLP	virus like particle
vRNA	viral RNA
wt	wild-type

Virus abbreviations:

AKAV	Akabane virus
BUNV	Bunyamwera virus
CCHFV	Crimean-Congo haemorrhagic fever virus
CEV	California encephalitis virus
DENV	Dengue virus
DOBV	Dobrava virus
DUGV	Dugbe virus
EMCV	Encephalomyocarditis virus
HTNV	Hantaan virus
IQTV	Iquitos virus
JATV	Jatobal virus
LACV	La Crosse virus
LENV	Leanyer virus
MDDV	Madre de Dios virus
OROV	Oropouche virus
OYAV	Oya virus
PHV	Prospect Hill virus
PTV	Punta Toro virus
PUUV	Puumala virus
SAV	San Angelo virus
SBV	Schmallenberg virus
SEOV	Seoul virus
SFTSV	Severe fever with thrombocytopenia syndrome virus
SNV	Sin Nombre virus
TAHV	Tahyna virus
TSWV	Tomato spotted wilt virus
UUKV	Uukuniemi virus

Nothing in Biology makes sense except in the light of Evolution

Theodosius Dobzhansky, 1973

Chapter I

General Introduction

Chapter I. General Introduction

Pathogenic viruses have a huge impact on human, animal and plant health causing significant morbidity and mortality, as well as placing a costly burden on economies. Global development in the past century has caused tremendous change bringing the human population in much closer proximity to each other and the surrounding environment than ever before. Human behaviour has altered ecosystems, accelerated climate change and increased our chances of coming into contact with pathogens and their vectors. Some examples of infectious virus spill-overs into the human population include Hendra virus in Australia in 1994 (Murray *et al.*, 1995), Nipah virus in Malaysia in 1997 (Uppal, 2000), H1N1 influenza in Mexico in 2009 (Dawood *et al.*, 2009), severe acute respiratory syndrome coronavirus (SARS-CoV) in China in 2002 (Holmes & Rambaut, 2004), Severe fever with thrombocytopenia syndrome virus (SFTSV) in China in 2010 (Li, 2013) and the Middle East respiratory syndrome coronavirus (MERS-CoV) in Saudi Arabia in 2012 (Raj *et al.*, 2014). This is a trend that is likely to continue. With SARS-CoV and the recent (2013 – 2015) Ebola virus outbreak in West Africa (Gatherer, 2014) we have learnt the potential devastation that these viruses can have once introduced into a naive population. It is therefore of paramount importance that we continue to elucidate the molecular biology of these emerging and re-emerging pathogens, and understand their evolution in our complex society.

The focus of this study has been on the human pathogen Oropouche virus (OROV). OROV belongs to the *Bunyaviridae* family, which also contains the recent emergent viruses Schmallenberg virus (SBV) (Hoffmann *et al.*, 2012) and SFTSV (Zhang *et al.*, 2013). OROV has a geographic distribution in South America where it causes recurring outbreaks of flu-like illness in the Amazonian regions of Brazil. Over half a million OROV infections have occurred in over 30 outbreaks since its isolation in 1955. In an urban environment, OROV is transmitted to humans by the midge *Culicoides paraensis*. The natural host of the virus is the pale-throated three-toed sloth and possibly other non-human primates (Anderson *et al.*, 1961; Pinheiro, 1962). Recently however, OROV has been isolated outside the current known epidemic zone in Brazil (Nunes *et al.*, 2005),

while OROV reassortant viruses capable of infecting humans have been isolated in Peru and Venezuela (Aguilar *et al.*, 2011; Ladner *et al.*, 2014), indicating that OROV may be circulating more widely in South America than previously appreciated. This thesis describes the establishment of a reverse genetics system for OROV and its initial characterisation that will enable us to study this important yet poorly understood emerging viral zoonosis.

The literature review that now follows describes our current understanding of the *Bunyaviridae* family and how these viruses manipulate the human host cell. This is then followed by research so far published on OROV. Developments in bunyavirus reverse genetics are also discussed followed by the specific aims of this PhD project.

1.1 The family *Bunyaviridae*

The *Bunyaviridae* family is one of the largest groups of segmented RNA viruses (Figure 1.1) consisting of over 350 known pathogenic and non-pathogenic members. Based on serological cross-reactivity of each virus, biochemical characteristics and conserved terminal untranslated regions (UTR) in their genome these viruses are further sub-divided into the genera *Orthobunyavirus, Hantavirus, Nairovirus, Phlebovirus and Tospovirus* (Hunt & Calisher, 1979; Elliott & Blakqori, 2011; Elliott & Schmaljohn, 2013). All viruses in general are referred to as bunyaviruses. With the exception of hantaviruses all other members are transmitted to their host primarily by arthropods, mainly sandflies [eg. sandfly fever Sicilian virus (SFSV) in the Mediterranean basin], midges (eg. OROV in South America), mosquitoes [eg. Rift Valley fever virus (RVFV) in Africa or La Crosse encephalitis virus (LACV) in the United States] or ticks [eg. Crimean-Congo haemorrhagic fever virus (CCHFV) in Africa, Asia, Eastern Europe and the Middle East]. *Hantaviruses* for an unknown evolutionary advantage tend to cause persistent asymptomatic infection in rodents and are transmitted onwards to humans via aerosolised rodent urine/faeces; examples include Hantaan virus (HTNV), Seoul virus (SEOV), Puumula virus (PUUV) and Sin Nombre virus (SNV). The *Tospovirus* genera consist of important plant pathogens such as thrips-transmitted

Tomato spotted wilt virus (TSWV) (Elliott & Blakqori, 2011; Elliott & Schmaljohn, 2013).

Bunyaviruses became recognised as a separate family of viruses by the International Committee on Taxonomy of Viruses (ITCV) in 1975 (Elliott & Blakqori, 2011) and it was using a bunyavirus, Bunyamwera virus (BUNV), that in 1996 Bridgen and Elliott made the first breakthrough for segmented negative-sense RNA virus recovery via plasmid DNA alone (Bridgen & Elliott, 1996). BUNV has since become the prototype virus of the *Bunyaviridae* family and initial discoveries made on BUNV by Elliott and colleagues have been crucial to our understanding of how these viruses replicate and manipulate their host cell.

Our continued understanding of this major virus family is important, because it constitutes viruses that are highly pathogenic in humans as well as viruses that can only infect invertebrates, making them an ideal model for comparative RNA virus evolution.

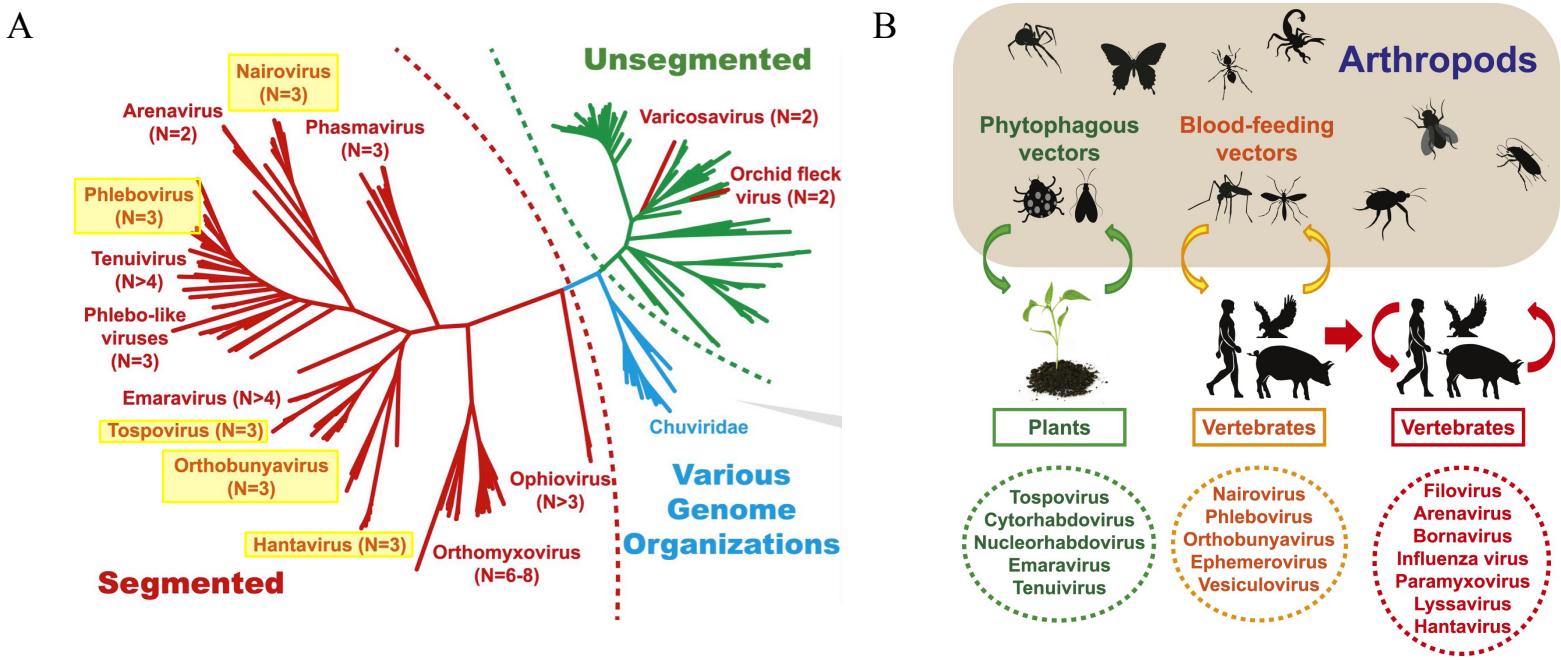

Figure 1. 1. Phylogenetic relationship of RNA viruses.

(A) Unrooted maximum likelihood tree based on the viral polymerase protein. Bunyaviruses are highlighted in yellow and cluster with other segmented RNA virus families (in red). The number of genome segments for each genus is presented in brackets. *Chuviridae* (in blue) consists of viruses that have either a circular genome, or both circular and segmented genome or only linear genomes. (B) Transmission cycles. The image illustrates the various transmission cycles through which arboviruses circulate in nature. These figures were taken from a recent study by Li *et al.* on the diversity of RNA viruses in arthropods (Li *et al.*, 2015).

1.1.1 The bunyavirus virion and genome

All bunyaviruses share a similar genomic organisation and replication strategy. The genome is composed of three single-stranded negative/ambi-sense RNA segments named according to their sizes large (L), medium (M) and small (S). Each segment consists of a coding region flanked by UTRs, which have terminal ends that are partially complementary and give the genome its pseudo-circular appearance (Figure 1.2). It was recently demonstrated that these complementary regions of both 5' and 3' UTRs interact on separate sites in the viral polymerase, a feature now thought to be conserved in all negative strand RNA virus polymerases (Gerlach, 2015). The secondary structure of the UTR functions as a promoter for viral genome replication and transcription (von Bonsdorff & Pettersson, 1975; Raju & Kolakofsky, 1989; Dunn *et al.*, 1995; Elliott & Weber, 2009; Elliott & Blakqori, 2011).

The main bunyavirus structural proteins encoded by all members include the RNA-dependent RNA polymerase (L protein) by the L segment, the glycoproteins Gn and Gc by the M segment and a nucleocapsid (N) protein by the S segment. Some members encode an additional non-structural medium (NSm) protein on the M segment, while some orthobunyaviruses, phleboviruses and tospoviruses encode an additional non-structural small (NSs) protein on the S segment (Elliott & Blakqori, 2011; Elliott & Schmaljohn, 2013). Some new world hantaviruses have now been shown to also encode a putative NSs protein (Vera-Otarola *et al.*, 2012). The L and M segment proteins are encoded in a negative-sense orientation, however the coding strategy used for the S segment proteins differs for certain genera. Phleboviruses and tospoviruses use an ambisense coding strategy. In ambisense, genes are coded both in negative and positive polarities allowing proteins to be translated from separate mRNAs. Orthobunyaviruses have both proteins encoded in overlapping reading frames and so translation of both proteins occurs from the same mRNA transcript (Figure 1.3). The N protein interacts with the genome and with the L protein, as well as the glycoproteins to form the bunyavirus virion (Elliott & Blakqori, 2011; Elliott & Schmaljohn, 2013).

Cryo-electron tomography and microscopy of Uukuniemi (UUKV), RVFV MP12, LACV, BUNV and Tula virus (TULV) depicts a difference in bunyavirus virion morphology between the different genera (Elliott & Schmaljohn, 2013). Phleboviruses appear to be spherical, whilst orthobunyaviruses and hantaviruses are pleomorphic. Hantaviruses can additionally consist of elongated virions (Figure 1.2 B). Common to all bunyaviruses is a lipid envelope, which is about 4 – 5 nm thick and encloses the densely packed ribonucleoprotein (RNP). Gn-Gc heterodimer spikes about 10 – 18 nm in length surround the envelope, with connections going between the RNP and the glycoproteins. The glycoproteins of orthobunyaviruses have a tripodal-like structure; these are arranged as pentamers and hexamers in phleboviruses and as unevenly distributed tetramers in hantaviruses. The virion diameter of BUNV was found to be 108 ± 8 nm (Bowden *et al.*, 2013), that of LACV 75 – 115 nm (Talmon *et al.*, 1987), RVFV MP12 100 nm (Freiberg *et al.*, 2008; Sherman *et al.*, 2009), UUKV 95 – 125 nm (von Bonsdorff & Pettersson, 1975; Hewlett *et al.*, 1977; Overby *et al.*, 2008) and that of TULV 120 – 160 nm (Huiskonen *et al.*, 2010).

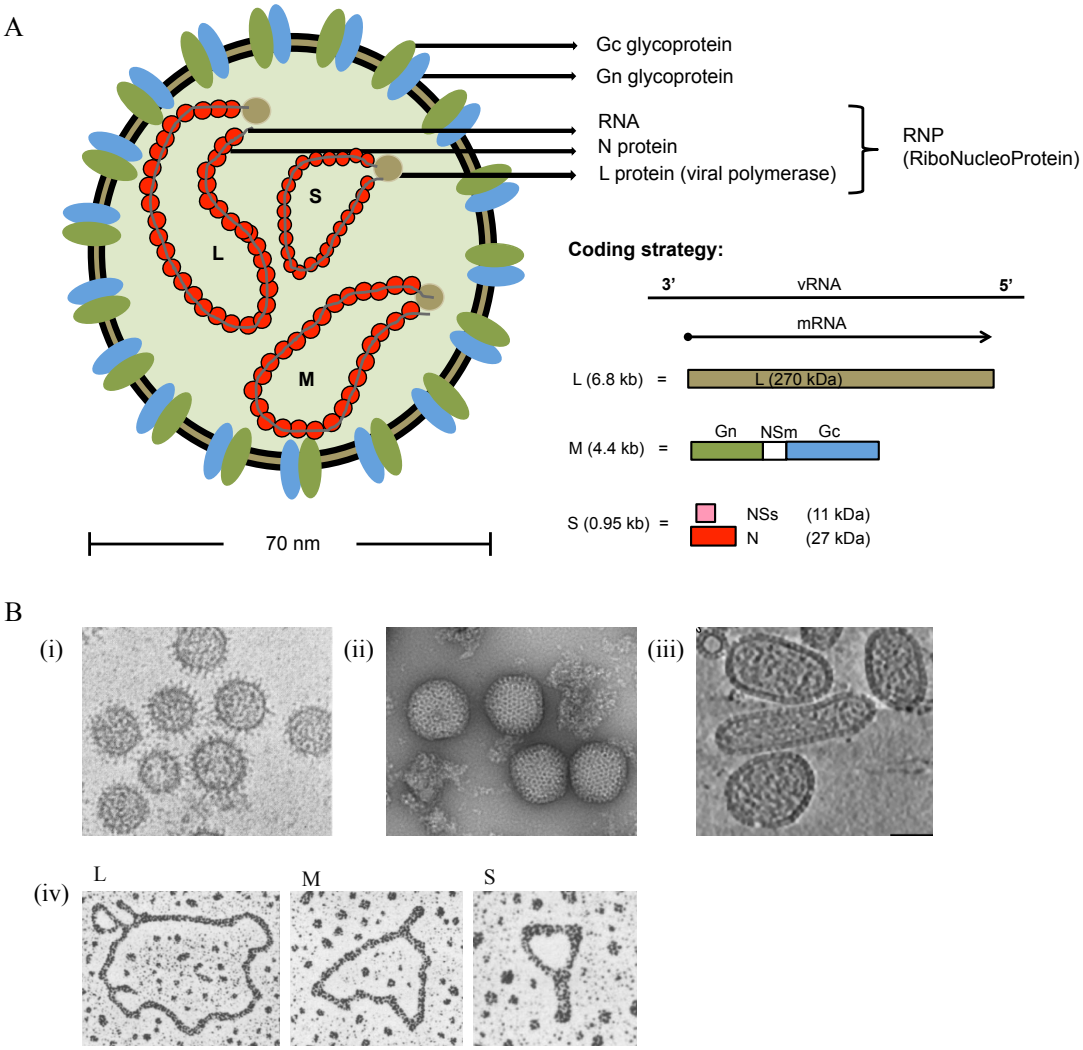

Figure 1. 2. Bunyavirus virion structure.

(A) Schematic diagram showing a bunyavirus virion. Electron microscopy of OROV data estimates that OROV virions are ≈70 nm in diameter (Personal communication, Dr. Gustavo Olszanski Acrani, University of Sao Paulo). On the right is the coding strategy used by OROV along with its genomic segments and expressed proteins. The size of the segments and proteins are given in brackets. (B) Cryo-electron micrographs of virus particles: (i) LACV (Talmon *et al.*, 1987); (ii) RVFV (Huiskonen *et al.*, 2009); (iii) Tula virus (Huiskonen *et al.*, 2010), the image shows an elongated tubular particle; (iv) electron micrographs showing UUKV RNA molecules with panhandle (Hewlett *et al.*, 1977).

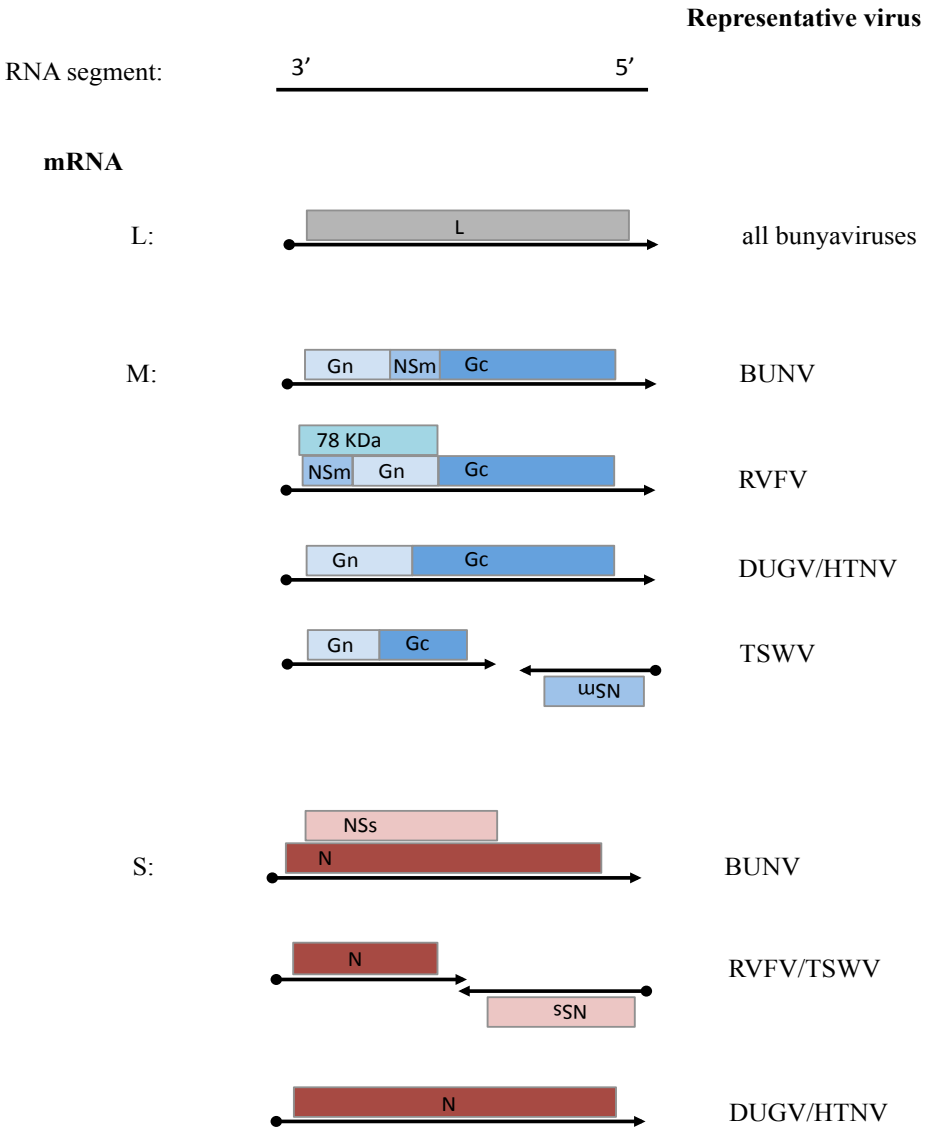

Figure 1. 3. The different coding strategies used by bunyaviruses.

A schematic representation of the various coding strategies of the L, M and S bunyavirus segments. RNA molecules are in the negative-sense orientation 3' – 5'. Representative viruses include Bunyamwera virus (BUNV), Rift Valley fever virus (RVFV), Dugbe virus (DUGV), Hantaan virus (HTNV) and tomato spotted wilt virus (TSWV). mRNA orientation is in the 5' – 3' direction (black arrows). Viral proteins (coloured boxes) include L, polymerase; Gn and Gc, glycoproteins; N, nucleocapsid protein; and the non-structural proteins, NSm and NSs (Elliott & Schmaljohn, 2013).

The protein coding regions

L

The L gene on the L segment encodes an RNA dependent RNA-polymerase (RdRp) that the virus requires in order to transcribe and replicate its genome (Jin & Elliott, 1991). Work in the early 1990's by Jin and Elliott established that the bunyavirus polymerase domain resides in the central region of the protein (Jin & Elliott, 1992, 1993b). This work succeeded in the initial identification of a probable "polymerase module" that appeared to remain evolutionarily conserved in every available RdRp sequence (Poch *et al.*, 1989). Segmented negative strand virus RdRps additionally exhibit endonuclease activity and for bunyaviruses this was identified by isolating positive/coding-sense RNA that contained 5 – 15 nucleotide long host-cell derived capped oligonucleotides at the 5' termini (Patterson *et al.*, 1984; Jin & Elliott, 1993b, a; Garcin *et al.*, 1995). This endonuclease activity termed "cap-snatching" was first identified in Influenza virus (Krug *et al.*; Plotch *et al.*, 1979) and is a transcription initiation method where by short 5' caps from the host pre-mRNAs are cleaved for the purpose of priming viral mRNA synthesis (Reich *et al.*, 2014). The cap-snatching endonuclease domain of the bunyavirus L protein is present at its N-terminus (Muller *et al.*, 1994), and is supported by structural data on LACV (Reguera *et al.*, 2010). Nairoviruses have an Ovarian Tumor (OTU)-domain additionally present before the endonuclease domain around amino acids 29 – 158 (Honig *et al.*, 2004; Kinsella *et al.*, 2004; Capodagli *et al.*, 2011; Devignot *et al.*, 2015). Interestingly this domain is also present in RdRps of several positive-sense RNA viruses, and is implicated in antagonising the host innate immune pathway as discussed in 1.1.3.

The L protein localises in the cytoplasm and around the perinuclear region suggesting an association with intracellular membrane compartments. Co-localisation of the N-protein further suggests that these regions harbour the viral replication complexes (Kukkonen *et al.*, 2004; Shi & Elliott, 2009; Brennan *et al.*, 2011). The sizes of various bunyavirus L proteins are listed in Table 1.1.

M

The M gene encodes a large polyprotein precursor, which is co-translationally cleaved into glycoproteins Gn and Gc (Elliott & Schmaljohn, 2013). The sizes of various bunyavirus M proteins are listed in Table 1.1. Cleavage of the M polyprotein occurs by host signal peptidases and the mature Gn and Gc proteins are transported from the endoplasmic reticulum (ER) as heterodimers to the site of viral budding in the Golgi apparatus (Persson & Pettersson, 1991; Lappin *et al.*, 1994; Elliott & Schmaljohn, 2013). For BUNV the Golgi-targeting and retention signals are found within the Gn protein (Shi & Elliott, 2004). Work on BUNV and HTNV glycoproteins has shown that both Gn and Gc are altered by N-linked glycosylation, and failure to rescue BUNV lacking the Gn N-glycan that is present on its N-termini showed the importance of Gn for proper Gc folding (Shi & Elliott, 2004; Shi *et al.*, 2005). The ER chaperones calnexin and calreticulin have also shown to play a role in HTNV Gn-Gc folding (Shi & Elliott, 2004). HTNV Gn and Gc are of the high-mannose type (Shi & Elliott, 2004), whereas it appears that only the Gn of BUNV, LACV and Inkoo viruses are predominately high-mannose (Shi *et al.*, 2005). The Gn and Gc proteins are responsible for virus entry into a host cell, although it is still uncertain whether both or just one protein is responsible for attachment to the host cell receptor (Cifuentes-Munoz *et al.*, 2014). Computational modelling of the HTNV (Ogino *et al.*, 2004; Tischler *et al.*, 2005) and Sandfly fever virus (Garry & Garry, 2004) glycoproteins implicated Gc as a fusion protein. This was then followed on by experimental evidence using LACV Gc which mapped residues 860 – 1442 as essential for the fusogenic activity (Plassmeyer *et al.*, 2005; Plassmeyer *et al.*, 2007). In BUNV a domain on the C-terminus of Gc around residues 930 to 982 was also mapped as important for cell-to-cell fusion (Shi *et al.*, 2009). Further work on Andes virus also supported the role of Gc in fusion by mapping its activity to residues 115 – 121 (Cifuentes-Munoz *et al.*, 2011). Such fusion proteins are responsible for the virus and host cell membranes to merge, and is an important step in the virus entry process (reviewed in section 1.1.2). A Maguari virus (MAGV) mutant lacking the N-terminal 239 aa of Gc (Pollitt *et al.*, 2006), as well as a BUNV recombinant containing a fluorescent protein in place of the first 346 aa of Gc (Shi *et al.*, 2010) demonstrated Gc N-terminus as dispensable for infectivity of the virus. The crystal structure of RVFV Gc has now recently revealed a three domain protein fold

similar to that of the class II fusion proteins of alphaviruses and flaviviruses, further strengthening the evidence for Gc in fusion (Dessau & Modis, 2013).

In addition to Gn/Gc some bunyaviruses also encode a non-structural protein (NSm) on the M segment (Figure 1.3 and Table 1.1) (Fazakerley *et al.*, 1988; Matsuoka *et al.*, 1988), and from early work using BUNV it was shown that this protein also localises to the Golgi (Nakitare & Elliott, 1993; Shi *et al.*, 2006). A MAGV mutant with two-thirds of its NSm C-terminus missing suggested that the C-terminus of this protein is not crucial for the virus in cell culture (Pollitt *et al.*, 2006). This is also true for SBV, as a large internal deletion in the NSm C-terminus does not affect the virus infectivity even *in vivo* (Kraatz *et al.*, 2015). What role the protein may play in the virus life-cycle in the case of these orthobunyaviruses is still unclear. However, for the phlebovirus RVFV the NSm protein is important for infection in mosquitoes by allowing the virus to cross the midgut barrier (Crabtree *et al.*, 2012; Kading *et al.*, 2014). Additionally, in RVFV the NSm can stay fused to Gn, producing a protein called P78 (Figure 1.3), which also has a role in virus circulation in mosquitoes (Kreher *et al.*, 2014). In tospoviruses the NSm protein has been shown to be important for virus cell-to-cell spread (Kormelink *et al.*, 1994; Storms *et al.*, 1995; Soellick *et al.*, 2000).

S

The S segment mainly encodes the N protein. However, some ortho- and hanta- viruses have evolved to take advantage of the leaky scanning of ribosomes. In these viruses N is encoded from the first AUG site, whilst an additional protein called NSs is encoded from a downstream AUG site on the same mRNA transcript (Fuller & Bishop, 1982; Fuller *et al.*, 1983; Vera-Otarola *et al.*, 2012). In contrast to this, phlebo- and tospo-viruses employ an ambisense coding strategy so that N and NSs can be translated on separate mRNA transcripts from the same genomic segment. Nairoviruses are not known to encode NSs (Elliott & Schmaljohn, 2013). The size of various bunyavirus S segment proteins are listed in Table 1.1.

The NSs protein functions mainly as an interferon (IFN) antagonist (see section 1.1.3 for a detailed explanation), but may also play a role in the regulation of the L protein

(Weber *et al.*, 2001; Elliott & Schmaljohn, 2013; Brennan *et al.*, 2015). The N protein on the other hand is important in the viral life-cycle, interacting with L protein during genome replication and with Gn-Gc during virus particle formation. Due to this, high quantities of N are present in both virions and in the virus infected host cells (Elliott & Schmaljohn, 2013). N is responsible for encapsidating and protecting each vRNA segment in the form of RNPs, and though virions contain genome and antigenome segments there appears to be a preference for genomic encapsidation (Richmond *et al.*, 1998; Osborne & Elliott, 2000). N does this via a signal in the 5' UTR panhandle structure (Osborne & Elliott, 2000; Severson *et al.*, 2001; Mir & Panganiban, 2004) and encapsidation begins via N-N interaction. Using reverse genetics these interacting regions in BUNV N were mapped to residues 1 to 10 of the N-terminus and residues 216 to 233 of the C-terminus, along with a central domain encompassing amino acids 94 to 158 (Leonard *et al.*, 2005; Eifan & Elliott, 2009). Similar N-N oligomerisation and RNA binding have also been suggested for viruses in the tospo- and hanta- virus genera (Uhrig *et al.*, 1999; Kaukinen *et al.*, 2001; Severson *et al.*, 2001; Kaukinen *et al.*, 2003). Protein structural data for several orthobunyavirus N proteins have now confirmed the original BUNV mutagenesis studies. N protein structures for BUNV (Li *et al.*, 2013), leanyer virus (LEAV) (Niu *et al.*, 2013), SBV (Dong *et al.*, 2013b; Dong *et al.*, 2013a) and LACV (Reguera *et al.*, 2013) demonstrate that N forms a tetrameric ring and each of the monomers are folded to contain a globular head domain (made up of N- and C- terminal domains) and flexible arms (N- and C- terminal arms) with a positively charged RNA-binding groove between them (Figure 1.4.A). The groove in each monomer binds 11 bases (Figure 1.4.B). The flexible arm facilitates N-N interaction in a head-to-head and tail-to-tail manner. The N proteins of phleboviruses RVFV (Raymond *et al.*, 2010; Ferron *et al.*, 2011) and Toscana virus (TosV) (Olal *et al.*, 2014) on the other hand form a hexameric ring arrangement with the N-terminal arm of one monomer interacting with the globular domain of another. Each monomer can bind six bases in a similar manner to the orthobunyaviruses. The nairovirus CCHFV that does not encode an NSs protein on the S segment interestingly shares a closer structural homology with arenavirus Lassa virus NP than with other bunyaviruses, specifically at its RNA binding domain (Carter *et al.*, 2012). Additionally, CCHFV N contains a structurally exposed caspase-3 dependent cleavage site (Asp-Glu-Val-Asp) at

its N-terminus, which can result in the cleavage of the N protein. This site was shown to be conserved in several CCHFV strains, although what significance it holds in terms of the virus life-cycle is yet to be determined (Karlberg *et al.*, 2011; Carter *et al.*, 2012).

An interesting deviation from the typical NSs-encoding orthobunyaviruses is Brazoran virus. Its putative NSs ORF is encoded from the first initiation codon prior to N, although using a weak Kozak sequence. This putative protein is 19.6 kDa in size which is larger than the "typical" ≈10 kDa orthobunyavirus NSs protein size. In addition, the C-terminus of N contains a glutamine-rich domain not present in other orthobunyavirus N proteins (Lanciotti *et al.*, 2013). At present it is unclear what the significance of any of these observations are; future functional and structural work on these proteins will however prove useful to understanding the evolution of these diverse bunyaviruses.

Table 1. 1. Bunyavirus protein size

The various proteins (sizes in kDa) encoded by representative members of each genus.

Genus	Virus	L	Gn	Gc	NSm	N	NSs
Hantavirus	Hantaan	247	70	35	0	48	0
Nairovirus	Dugbe	459	35	73	0	50	0
Orthobunyavirus	Bunyamwera	259	32	110	11	26	11
Phlebovirus	Rift Valley fever	238	55	62	14	27	30
Tospovirus	Tomato spotted wilt	332	46	75	34	29	52

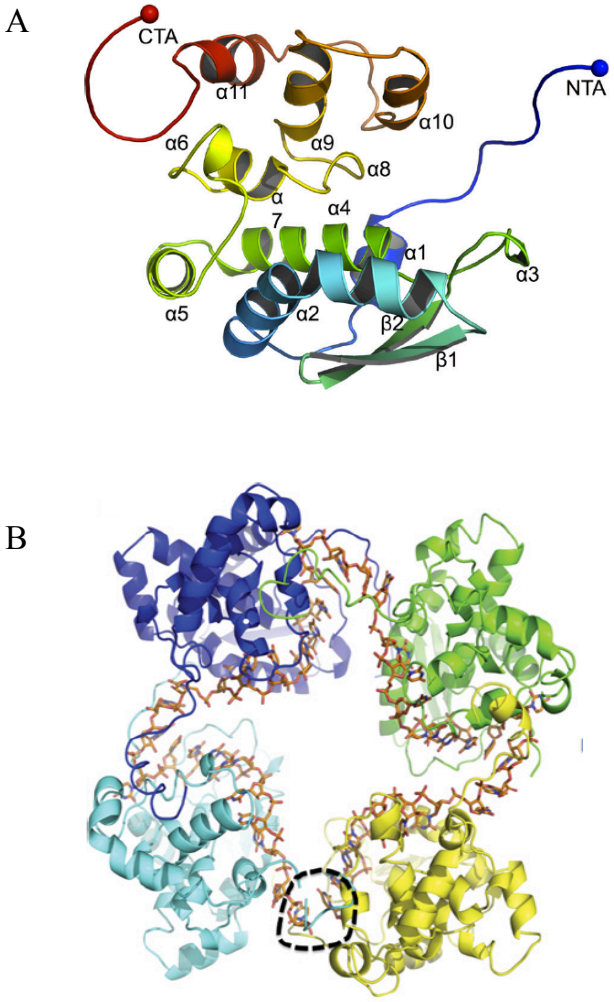

Figure 1. 4. Crystal structure of SBV N.

(A) Protomer structure of SBV N showing the N terminal arm (NTA; blue), a C-terminal domain (CTD) and the C terminal arm (CTA; red). Taken from (Dong *et al.*, 2013a). (B) Tetrameric structure of SBV N–RNA complex. RNA (42 nucleotide, stick form, orange) bound inside the tetrameric SBV N ring, formed by four protomers (blue, green, yellow and cyan). The dotted line shows a gap in the bound RNA. Taken from (Dong *et al.*, 2013b).

The untranslated regions

The bunyavirus UTR contains signals for genome replication, packaging and encapsidation. RNA secondary structures are crucial for such functions. In bunyaviruses, the terminal 3' and 5' ends of each segment are complementary and based on available sequences the first 8 to 11 nucleotides of all three segments are highly conserved within a given genus (Table 1.2). Beyond the conserved nucleotides the sequences and UTR lengths begin to vary and become unique within a segment and a specific virus (Elliott *et al.*, 1991; Kohl *et al.*, 2004a; Barr *et al.*, 2005; Elliott & Schmaljohn, 2013).

Table 1. 2. The terminal UTR consensus sequence of bunyaviruses

Sequences are represented in genomic sense. Some orthobunyaviruses differ from the prototype sequence at positions 8 and 9, which are highlighted in bold. The mismatch at position 9 is highlighted in red.

Genus	Virus		Terminal nucleotides
Hantavirus	Hantaan	3'- 5'-	AUCAUCAUCUG... UAGUAGUAUGC...
Nairovirus	Dugbe	3'- 5'-	AGAGUUUCU... UCUCAAAGA...
Orthobunyavirus	Bunyamwera	3'- 5'-	UCAUCACA**U**GA... AGUAGUG**U**GCU...
Phlebovirus	Rift Valley fever	3'- 5'-	UGUGUUUC... ACACAAAG...
Tospovirus	Tomato spotted wilt	3'- 5'-	UCUCGUUA... AGAGCAAU...

Orthobunyaviruses have a very diverse range of UTR lengths (Table 1.3) and point mutations in any of the first 20 nucleotides can either partially disrupt or completely eliminate promoter activity (Dunn *et al.*, 1995; Kohl *et al.*, 2004a). The sequences upstream of this region are specific to each segment and when disrupted can have a drastic effect on the regulation of the encoded gene. This was demonstrated when Lowen *et al.* created a viable, but highly attenuated recombinant BUNV that was engineered to have its L gene flanked by the M segment UTRs (Lowen *et al.*, 2005). Though the internal regions of the UTR are essential for gene regulation, recombinant

viruses lacking large portions of these sequences are viable (Lowen & Elliott, 2005; Mazel-Sanchez & Elliott, 2012). The minimum requirement for a viable BUNV S segment mutant is a 22-nucleotide 5'-UTR and at least 112 nucleotides at the 3'-terminus (Lowen & Elliott, 2005). Further work on BUNV M revealed that nucleotides 20 to 33 at both termini are important for genome packaging (Kohl *et al.*, 2006). Also the segment-specific sequences appear to have a role in regulation of packaging and co-packaging of each segment into a single virion (Kohl *et al.*, 2006; Terasaki *et al.*, 2011). Recent work on BUNV has now demonstrated that the L protein evolves to some degree in order to accommodate mutations in these UTRs (Mazel-Sanchez & Elliott, 2015)

Table 1. 3. Examples showing the 3' and 5' UTR lengths for different orthobunyaviruses (antigenome sense)

Virus	Serogroup	L		M		S		GenBank Accession No.s
		5'	3'	5'	3'	5'	3'	
Oropouche	Simbu	43	50	31	91	44	218	KP052850-52
Schmallenberg	Simbu	27	90	23	138	31	106	KC355457-59
Leanyer	Simbu	68	180	40	141	67	179	HM627179-81
Brazoran	unclassified	44	126	58	230	71	272	NC_022038-39, KC854416
Bunyamwera	Bunyamwera	50	108	56	100	85	174	NC_001925-27
La Crosse	California encephalitis	61	127	61	140	81	195	NC_004108-10

Bunyaviruses in the genera *Phlebovirus* and *Tospovirus* employ an ambisense strategy to encode proteins from their S, and M and S segments, respectively. Between the two genes on these segments is an intergenic region (IGR) that allows for differential regulation of gene expression and termination (Flick *et al.*, 2004). Phleboviruses and tospoviruses, along with plant infecting tenuiviruses (currently in an unassigned family) are so far the only known viruses to have both negative and ambisense genome segments. It is probable that these viruses form an evolutionary link between the purely segmented negative stranded viruses (*Orthomyxoviridae*) and the purely segmented negative stranded ambisense viruses (*Arenaviridae*) (Nguyen & Haenni, 2003).

1.1.2 The life-cycle of a bunyavirus particle in mammalian cells

Attachment and entry

Similar to other enveloped viruses a bunyavirus virion utilises its glycoproteins Gn and Gc to attach and enter into a host cell. The type of cellular receptor the virion binds to will determine the cell tropism of that virus. Current understanding of host cell receptors for bunyaviruses are limited, however knowledge of the varied cell tropism of some bunyaviruses indicate that these viruses may have evolved to interact with a number of mammalian cell receptors (Elliott & Schmaljohn, 2013). Phleboviruses RVFV, SFTSV, TosV, Punta Toro (PTV) and UUKV, and orthobunyavirus Germiston virus were shown to interact with host cell receptor DC-SIGN (DC [dendritic cell] - specific ICAM [intercellular adhesion molecule] - 3 grabbing non-integrin). DC-SIGN is a receptor present on immature DCs, which reside in peripheral tissues and are likely the first cells to encounter incoming viruses. DC-SIGN is a type II membrane protein with a calcium-dependent lectin extracellular domain likely capable of interacting with the glycosylated sites on the viral glycoproteins (Lozach *et al.*, 2011; Hofmann *et al.*, 2013). This interaction would then trigger a response in the DC causing it to mature into an antigen-presenting cell (Tan & O'Neill, 2005). As number of viruses appear to have evolved to use DC-SIGN as entry into mammalian cells they have also evolved mechanisms of blocking the maturation of these cells (Rogers & Heise, 2009). Phleboviruses RVFV and TosV have also been shown to interact with the proteoglycan heparin sulfate receptor (Jin *et al.*, 2002; de Boer *et al.*, 2012b). Whilst, pathogenic hantaviruses can interact with integrins β_1, β_2 (CR3 and CR4) and β_3 (Gavrilovskaya *et al.*, 1998; Gavrilovskaya *et al.*, 1999; Raftery *et al.*, 2014), as well as Decay-accelerating factor (DAF)/CD55 and gC1qR/p32 (Choi *et al.*, 2008; Krautkramer & Zeier, 2008) for attachment to endothelial and epithelial cells.

Upon attachment bunyaviruses take advantage of the endocytic pathway for internalization. OROV, LACV, HTNV and CCHFV were shown to use the clathrin-mediated endocytotic (CME) pathway (Figure 1.6 A) (Jin *et al.*, 2002; Santos *et al.*, 2008; Simon *et al.*, 2009; Hollidge *et al.*, 2012). CME is used by all cells and is probably the reason why several enveloped viruses use it to gain entry into cells (Figure

1.5 A, step 2). Interestingly, UUKV appears to predominantly use a clathrin-independent pathway to enter A549 (human) and BSC-40 (money) cell-lines (Lozach *et al.*, 2010). Akabane virus (AKV) on the other hand uses the clathrin-independent pathway in bovine-derived cell-lines, whereas in non-bovine cells it seems to use the CME pathway (Bangphoomi *et al.*, 2014).

Membrane fusion

The endocytic pathway follows a pH gradient that can be detected by bunyavirus glycoproteins triggering a conformational change in their structure (Överby *et al.*, 2008). This pH sensing is possible due to protonation of the histidine residues typically found on the viral fusion protein (Kampmann *et al.*, 2006; Mueller *et al.*, 2008). As discussed previously, Gc likely functions as a fusion protein. This is further strengthened by work on RVFV, where certain conserved histidine residues on Gc were found to be important for virus infectivity (de Boer *et al.*, 2012a). Conformational changes in Gc would then mediate fusion between viral and endosomal membranes, hence allowing release of viral RNP into the cell cytoplasm (Figure 1.5 A, step 3) (Mercer *et al.*, 2010; Cosset & Lavillette, 2011). Several enveloped viruses are known to use this mode of penetration (White *et al.*, 1981; Kielian *et al.*, 2010). Detailed work by Lozach *et al*. demonstrated that UUKV is transported from the early endosomes (pH <6.3) to late endosomes (pH <5.3) before infection occurs (Figure 1.6 B). The authors demonstrated that infection was pH dependent since neutralisation of vesicular pH inhibited infection, whilst acidification of the external cell environment was sufficient to trigger fusion of the viral and cell plasma membranes (Lozach *et al.*, 2010). Cell-to-cell fusion has been shown using different bunyaviruses, where over-expression as well as infection induces syncytium formation (Jacoby *et al.*, 1993; Hacker & Hardy, 1997; Ogino *et al.*, 2004; Plassmeyer *et al.*, 2005; Shi *et al.*, 2007).

Transcription and Replication

Bunyaviruses replicate in the host cell cytoplasm and progeny virions mature and bud at the Golgi apparatus, Figure 1.5 A (Shi *et al.*, 2010; Elliott & Schmaljohn, 2013). Upon release of RNP the virion-associated L begins transcription of the genome via a cap-snatching mechanism (Figure 1.5 B). Work on SNV suggests that N can recognise 5' caps of cellular mRNA, which are then cleaved by L (Mir *et al.*, 2008). Work prior to

this using BUNV and RVFV demonstrated that both L and N are together required for active transcription (Dunn *et al.*, 1995; Lopez *et al.*, 1995). As N also encapsidates the genome, structural data suggests that N could potentially expose the UTRs using its flexible arms allowing L to bind (Elliott, 2014). Recent structural data on LACV L bound to vRNA revealed that the terminal 3' and 5' UTR sequences are crucial and that they each bind specific regions in the L molecule, confirming all prior *in vitro* mutagenesis work. The overall crystal structure of L indicates a main globular core, which harbours the RdRp and RNA-binding domains connected to a flexible endonuclease domain by a linker region. The template entry and exit tunnels and the nascent RNA exit tunnels are located in the main globular core (Gerlach *et al.*, 2015).

Transcription occurs prior to replication and unlike transcription, replication occurs in a cap-independent manner. The exact mechanism for switching from cap-dependent to cap-independent initiation is still uncertain, but the possibilities of host cell translation shut-off forcing this switch; or that viral and/or host proteins may be involved in the process have been proposed (Guu *et al.*, 2012; Elliott & Schmaljohn, 2013). In transcription the nascent mRNA terminates upstream of the 5' end, however in replication the nascent strand is processed right to the very end of the 5' termini. Transcription termination signals ubiquitous to all three segments have not been found, but a pentanucleotide sequence 5'-UGUCG-3' in BUNV S segment appears to be able to signal termination (Barr *et al.*, 2006; Ikegami *et al.*, 2007; Blakqori *et al.*, 2012).

Translation commences immediately on the growing nascent mRNA strand and is required to prevent this strand from hybridising to the template and halting transcription. These mRNA species are not poly(A) tailed. The L and S segment mRNAs are translated by free ribosomes, whilst M is translated by membrane-bound ribosomes (Elliott & Schmaljohn, 2013; Elliott, 2014). Once in the replication mode it is suggested that nascent cRNA undergoes immediate circularisation by polymerase dimerisation followed by immediate N encapsidation. This replicative intermediate RNP is known as the antigenome (Figure 1.5.B) and it serves as a template for another round of replication (Gerlach *et al.*, 2015).

Release

The M segment products Gn and Gc are post-translationally modified by N-linked glycosylation. Primary glycosylation takes place at the ER (Elliott & Schmaljohn, 2013; Elliott, 2014). All viral proteins then migrate towards the Golgi and signals in the Gn cytoplasmic tail (CT) help recruit RNP for assembly (Shi *et al.*, 2007; Strandin *et al.*, 2013). Early EM work on UUKV and BUNV demonstrated viral factories at the Golgi complex where these viruses appear to bud (Figure 1.6 B and C) (Kuismanen *et al.*, 1982; Salanueva *et al.*, 2003; Fontana *et al.*, 2008). Mature bunyaviruses are then transported to the plasma membrane in large vesicles via the secretary pathway (Figure 1.6 D) where membrane fusion then enables the virions to exit the host cell (Figure 1.5 A, step 8-10; Figure 1.6 D and E) (Elliott & Schmaljohn, 2013; Elliott, 2014).

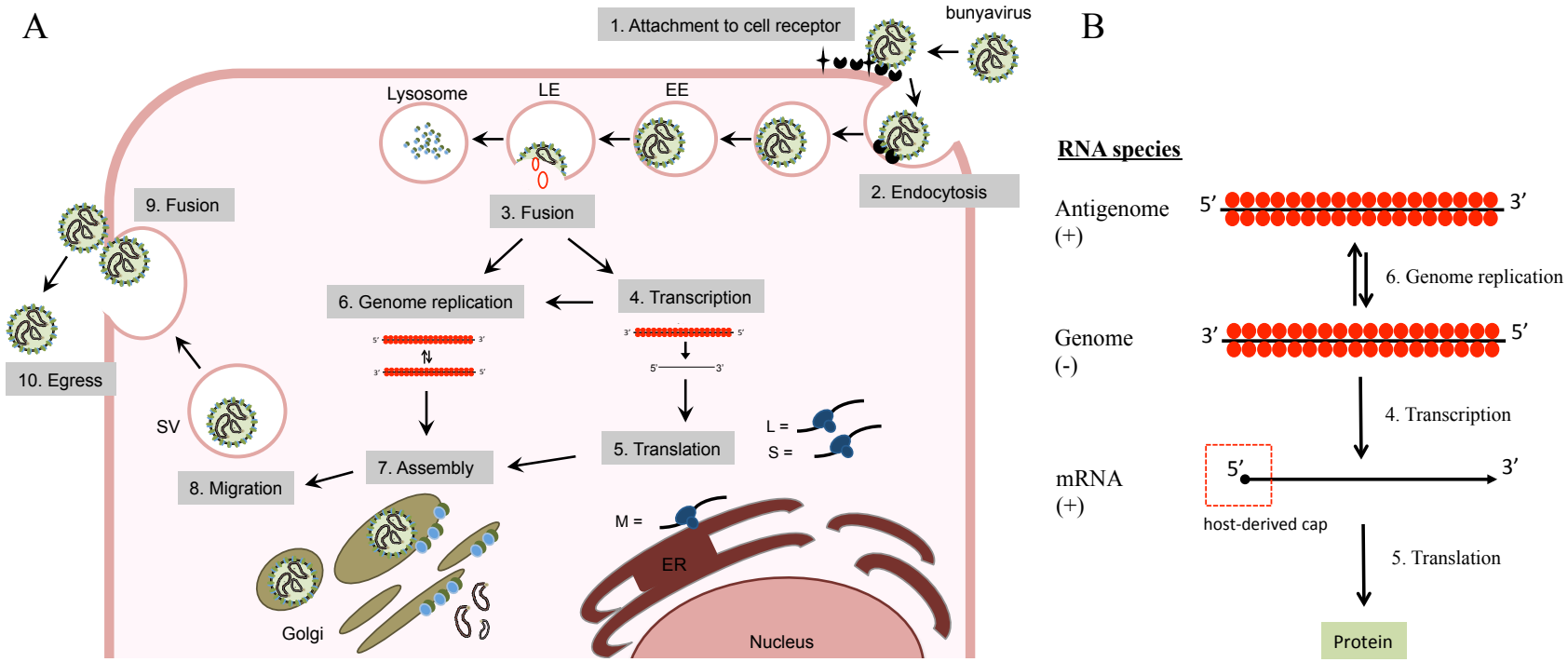

Figure 1. 5. Life cycle of the bunyaviruses.

(A) Schematic diagram of the various stages in a bunyavirus life-cycle. EE, early endosomes; LE, late endosomes; ER, endoplasmic reticulum; SV, secretary vesicles. (B) Transcription and replication of the bunyavirus genome. The genome is in a negative-sense orientation and is transcribed into a replicative intermediate known as the antigenome. Red circles depict the N protein encapsidating the genome/antigenome. The red dashed-box highlights that the mRNA contains 10 – 15 nt long host-derived primers/caps. Numbers correspond to the stages found in (A). Illustrations adapted from (Elliott & Schmaljohn, 2013; Elliott, 2014).

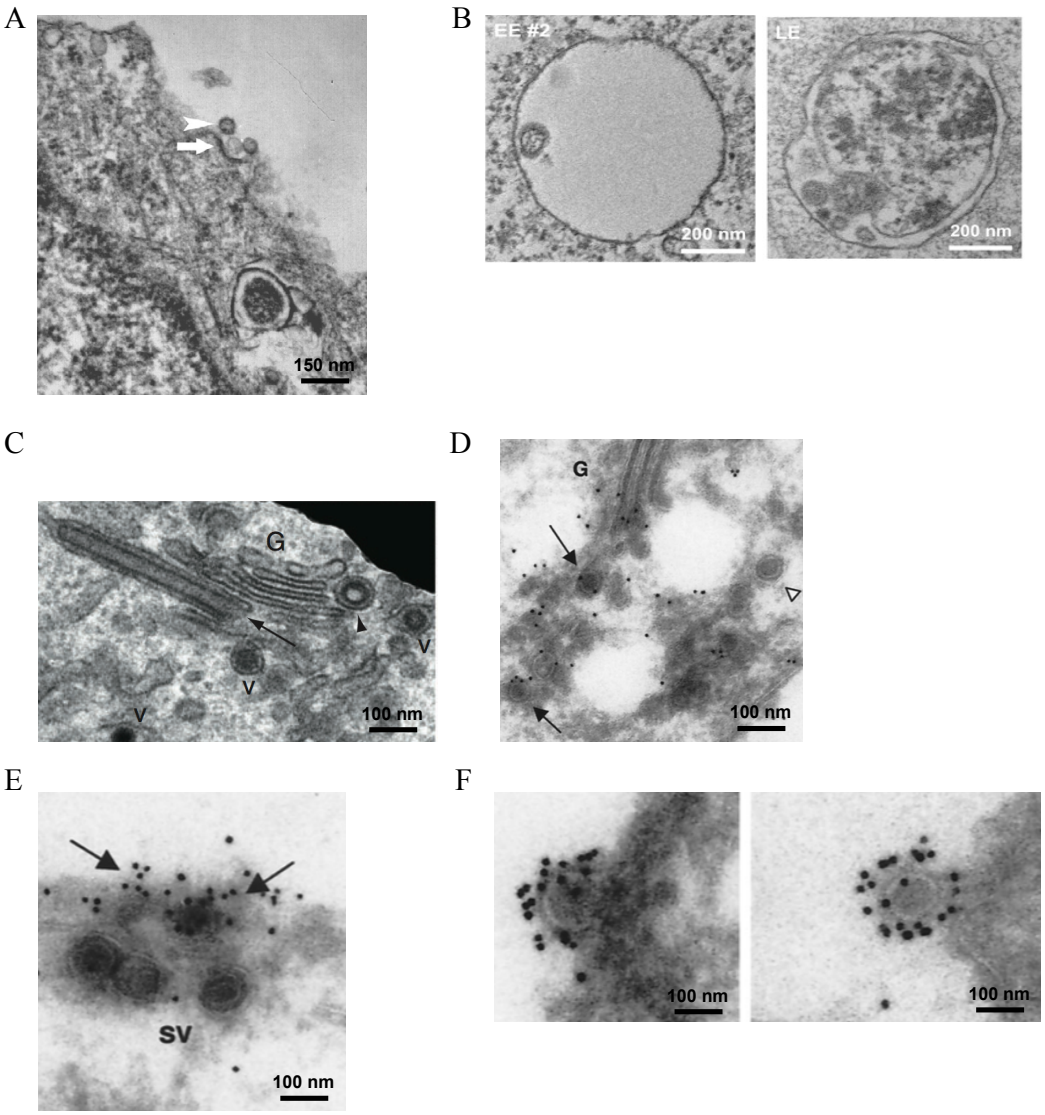

Figure 1. 6. Electron micrographs of bunyavirus entry and exit from the host cell.

(A) OROV (arrowhead) entering HeLa cells via clathrin-coated pits (arrow). Image taken from (Santos *et al.*, 2008). (B) UUKV inside early (EE#2) and late (LE) endosomal vesicles in A549 cells. Image taken from (Lozach *et al.*, 2010). (C) Viral factories of BUNV in the BHK-21 cells. G, Golgi; V, virus particle. The arrows show various tubular and globular structures that form part of the viral factories. Image taken from (Fontana *et al.*, 2008). (D) BUNV inside the Golgi in BHK-21 cells (arrows), post-Golgi area (arrowhead). (E) BUNV exiting BHK-21 cells by secretary vesicles (SV) (F). Exited BUNV attached to the cell surface. Images (D), (E) and (F) were taken from (Salanueva *et al.*, 2003), where the cryosections were labelled with anti-Bunyamwera virus antiserum.

1.1.3 Host responses to bunyavirus infection

Vertebrate and invertebrate cells have evolved to recognise molecular signatures, thereby enabling them to distinguish between "self" and "non-self". In terms of a virus infection, certain distinct features on the viral genome or on their replication intermediate are recognised by "pattern" recognition receptors (PRRs) on or within the host cell. These foreign molecular features are known distinctively as pathogen-associated molecular patterns (PAMPs) and they can set in motion a series of events all geared towards preventing onwards spread of the infection (Ausubel, 2005; Randall & Goodbourn, 2008; Iwasaki, 2012).

The type 1 interferons and bunyaviruses

Mammalian cells can sense the presence of foreign RNA through cellular receptors (PRRs) such as transmembrane toll-like receptors (TLR), and cytosolic receptors RIG-I (retinoic acid-inducible gene 1) and MDA5 (melanoma differentiation-associated protein 5). TLRs are mainly expressed in lymphocytes, dendritic cells, macrophages and epithelial cells. For instance, TLR3 is highly expressed in the endosomes of myeloid dendritic cells and can recognise dsRNA following endocytosis of the virus (Schaefer *et al.*, 2004). RIG-1 and MDA5 on the other hand are more widely expressed. RIG-I receptors recognise short dsRNA with triphosphorylated 5' (5'ppp) ends, whereas MDA5 can recognise long dsRNA structures (Goodbourn *et al.*, 2000; Randall & Goodbourn, 2008; Reikine *et al.*, 2014; Schneider *et al.*, 2014; Hoffmann *et al.*, 2015; Weber, 2015). Recognition by RIG-1 and MDA5 triggers phosphorylation of transcription factors such as the interferon regulatory factors (IRF) IRF-3 and IRF-7, and NF-κB (nuclear factor kappa-light-chain enhancer of activated B cells) via activation of mitochondrial adaptor molecule called Cardif/VISA/MAVS/IPS-1 (CARD adaptor inducing IFN-β/Virus-induced signalling adaptor/Mitochondrial antiviral signalling protein/IFN-β promoter stimulator protein-1). The phosphorylation of the transcriptional factors leads to their translocation into the nucleus in order to induce the production of type 1 interferons (IFNs), IFN-α and IFN-β (Figure 1.7). Translocation occurs when for example the C-terminus of IRF-3 is phosphorylated hence causing its dimerization and exposure of its nuclear localisation signal (NLS), whilst the NLS of

NF-κB is exposed after phosphorylation of its inhibitor molecule (Inhibitor of NF-κB, IκB) that is subsequently degraded by the proteasome. Tank Binding Kinase 1 (TBK1) and IKKε are essential kinases which are also involved in activating IRF-3 and IRF-7. IRF-3 activation can also occur via TLR3 signalling through adaptor molecule Toll-interleukin (IL)-1-resistance (TIR) domain-containing adaptor inducing IFN-β (TRIF) and kinases TBK1 and IKKε (Goodbourn *et al.*, 2000; García-Sastre & Biron, 2006; Randall & Goodbourn, 2008; Schneider *et al.*, 2014; Hoffmann *et al.*, 2015).

IFN-α and IFN-β are cytokines that are expressed widely by a number of cell-types, and are encoded on chromosome 9 along with other type 1 IFNs (IFN-ε, IFN-K and IFN-ω) (Reikine *et al.*, 2014). The produced IFN-α/β use the JAK-STAT signalling pathway to signal the expression of a number of proteins that have antiviral effects and/or are positive or negative regulators of the pathway (IFN-stimulated genes, ISGs) (Goodbourn *et al.*, 2000; Randall & Goodbourn, 2008; Schneider *et al.*, 2014; Hoffmann *et al.*, 2015). The JAK-STAT pathway is activated when IFN-α/β bind to the type 1 IFN heterodimeric receptor complex (IFNAR1 and IFNAR2), both on the cell they were produced in and on adjacent cells. The IFNAR receptors are expressed on almost all cells and when activated lead to a conformational change in the bound IFN receptor chain with Janus activated Kinase 1 (JAK1) and non-receptor tyrosine kinase 2 (TYK2). JAKs are ubiquitously present in cells and activated JAKs lead to phosphorylation of transcriptional activator proteins STAT1 and STAT2 (signal transducer and activator of transcription). STAT1 is phosphorylated by JAK1 on tyrosine 701 and Tyk2 phosphorylates STAT2 on tyrosine 690. This causes the dimerization of STAT1 and STAT2 hence forming a NLS, further STAT1/STAT2 interact with IRF9 to form a heterotrimeric transcription factor complex ISG factor 3 (ISGF3), which translocates to the nucleus and binds to an IFN-stimulated response element (ISRE) in the genome. Activation of ISRE then leads to induction of over 100 ISGs (Figure 1.7) (Goodbourn *et al.*, 2000; García-Sastre & Biron, 2006; Randall & Goodbourn, 2008; Reikine *et al.*, 2014; Schneider *et al.*, 2014; Hoffmann *et al.*, 2015).

This intracellular defence mechanism is part of a highly evolved mammalian innate immune response designed to clear the cell of virus infection. However, several viruses

have evolved to encode proteins that function specifically as antagonists against this system (Goodbourn *et al.*, 2000; Randall & Goodbourn, 2008; Schneider *et al.*, 2014; Hoffmann *et al.*, 2015). Bunyaviruses tend to target the cells' early response stage. New York-1 hantavirus (NY-1) for instance, uses its Gn-CT tail to inhibit RIG-1 as well as TBK1 (Helgason *et al.*; Fitzgerald *et al.*, 2003; Alff *et al.*, 2006). Whilst, NSs-encoding bunyaviruses mainly use the NSs protein to target the transcriptional machinery of the host cell hence inhibiting IFN induction (Weber *et al.*, 2002; Elliott & Weber, 2009; Elliott & Blakqori, 2011). The first evidence of NSs being an IFN antagonist was demonstrated in 2001 when Bridgen *et al*. created a BUNV mutant lacking a functioning NSs ORF (rBUNdelNSs) (Bridgen *et al.*, 2001). This mutant displayed a reduced ability to shut-off host cell protein synthesis, was attenuated in mice and induced high levels of type I IFN in cultured cells. Similar results were soon shown with the phlebovirus RVFV (Bouloy *et al.*, 2001). RVFV mutants Clone-13, with a large in-frame NSs deletion of 549 nucleotides, and MP12 with a single-amino acid substitution at position 513 in NSs are attenuated *in vivo* and *in vitro*. When both these mutant NSs ORFs were replaced with that of wild-type (wt) RVFV the viruses behaved similar to the wt in terms of IFN induction and replication efficiency in IFN-competent mice. The absence of IFN-β mRNA in both the wt RVFV and wt BUNV infected cells demonstrated that NSs was blocking IFN-β production at the transcription level (Bouloy *et al.*, 2001; Weber *et al.*, 2002). Similar results were obtained with other bunyaviruses such as LACV, AKV, SBV and UUKV (Blakqori & Weber, 2005; Ogawa *et al.*, 2007; Elliott *et al.*, 2013; Rezelj *et al.*, 2015) demonstrating that at least in these viruses NSs is non-essential for virus replication, but rather enhances replication by antagonising the host cells response.

We are still in the process of understanding all NSs interactions within a mammalian cell. From work on BUNV and RVFV we know that its ability to inhibit IFN-β activation occurs downstream of transcriptional activation through disruption of the DNA-dependent RNA polymerase II (RNAPII) activity (Weber *et al.*, 2002; Kohl *et al.*, 2003b; Billecocq *et al.*, 2004). RNAPII is an enzyme that transcribes all protein- coding genes of the eukaryotic genome and is regulated by multiprotein complex Mediator (Med) (Allen & Taatjes, 2015). Sub-units of this Mediator complex respond to external

cell stimuli signalling the complex formation, which consists of modules head, middle and tail. The head module is involved in stabilizing the RNAPII initiation complex (Plaschka *et al.*, 2015) and BUNV NSs was found to interact with sub-unit Med8 of this module (Figure 1.8) (Leonard *et al.*, 2006). Med8 is one of the sub-units that interact with the carboxy-terminal domain (CTD) of RNAPII. The CTD is made up of a heptad repeat sequence ($Y_1S_2P_3T_4S_5P_6S_7$), of which there are 52 in the mammalian RNAPII, and its phosphorylation is essential for RNAPII function. Phosphorylation at serine (Ser) 5 is required for initiation and recruitment of capping enzymes, while Ser2 phosphorylation is required for elongation and 3'-end processing of the nascent mRNA transcript, Figure 1.8 (Robinson *et al.*, 2012; Corden, 2013; Eick & Geyer, 2013). Cells infected with BUNV show a significant reduction in RNAPII Ser2 phosphorylation. This was initially thought to be due to an interaction of the BUNV NSs C-terminus (amino acids 83 – 91) with Med8, however a BUNV NSs mutant lacking a N-terminus of 21 amino acids was also unable to degrade RNAPII, indicating that both the C- and the N- terminus are important for NSs function (Thomas *et al.*, 2004; Leonard *et al.*, 2006; van Knippenberg *et al.*, 2010). LACV and SBV NSs target RNAPII for degradation by the proteasome and C-terminal mutations of SBV NSs have been shown to affect the protein's ability to degrade RNAPII (Blakqori *et al.*, 2007; Verbruggen *et al.*, 2011; Barry *et al.*, 2014). The NSs protein of RVFV on the other hand interacts with subunits of the general transcription factor TFIIH (Figure 1.8), which also has a role in RNAPI transcription (Assfalg *et al.*, 2012). With RVFV NSs preventing subunits p44 and XPD from interacting, it presumably affects the activity of Cdk7 (cyclin-dependent kinase) of CAK (Cdk activating kinase), which is responsible for Ser5 phosphorylation on RNAPII, Figure 1.8 (Le May *et al.*, 2004).

RVFV NSs is intriguing as so far it is the only known bunyavirus NSs to form filamentous structures in the nucleus. It is also so far the only bunyavirus NSs shown to directly target the IFN-β promoter by interacting with SAP30 (Sin3A associated protein 30) and transcriptional repressor protein YY1. This interaction maintains the YY1/SAP30/NCor/HDAC/Sin3A co-repressor complex in a silent state on the IFN-β promoter thereby directly inhibiting IFN-β transcription (Le May *et al.*, 2008). With SFTSV it seems that the NSs forms viral inclusion bodies in the cytoplasm which the

virus uses to capture kinases TBK1 and IKKε, and the proteins STAT1 and STAT2 (Ning *et al.*, 2014; Ning *et al.*, 2015). Viruses from the Anopheles A, B and Tete serogroups encompass some of the non-NSs encoding orthobunyaviruses, and as expected show no inhibition of IFN-β production (Mohamed *et al.*, 2009). For rodent viruses TULV and PUUV, only putative NSs ORFs have been predicted, and over-expression of these in reporter assays have shown an inhibition of IFN-β, NF-kB and IRF-3 activity (Jaaskelainen *et al.*, 2007). HTNV, Dobrava (DOBV) and SEOV rodent viruses on the other hand have been shown to use their N protein to inhibit NF-kB activation, by targeting the signalling protein tumor necrosis factor-α (TNF-α) (Taylor *et al.*, 2009). Nairovirus CCHFV however, seems to use its L protein to antagonise the host immune system. For the TNF-α mediated NF-kB pathway to be activated its inhibitor IκB must be ubiquitinated, and with an OTU-domain present on the CCHFV L protein the virus is able to inhibit protein ubiquitination in the cell. OTU-domains have protease activity and these domains are also present in other nairoviruses such as DUGV and Nairobi sheep disease virus (NSDV) (Frias-Staheli *et al.*, 2007).

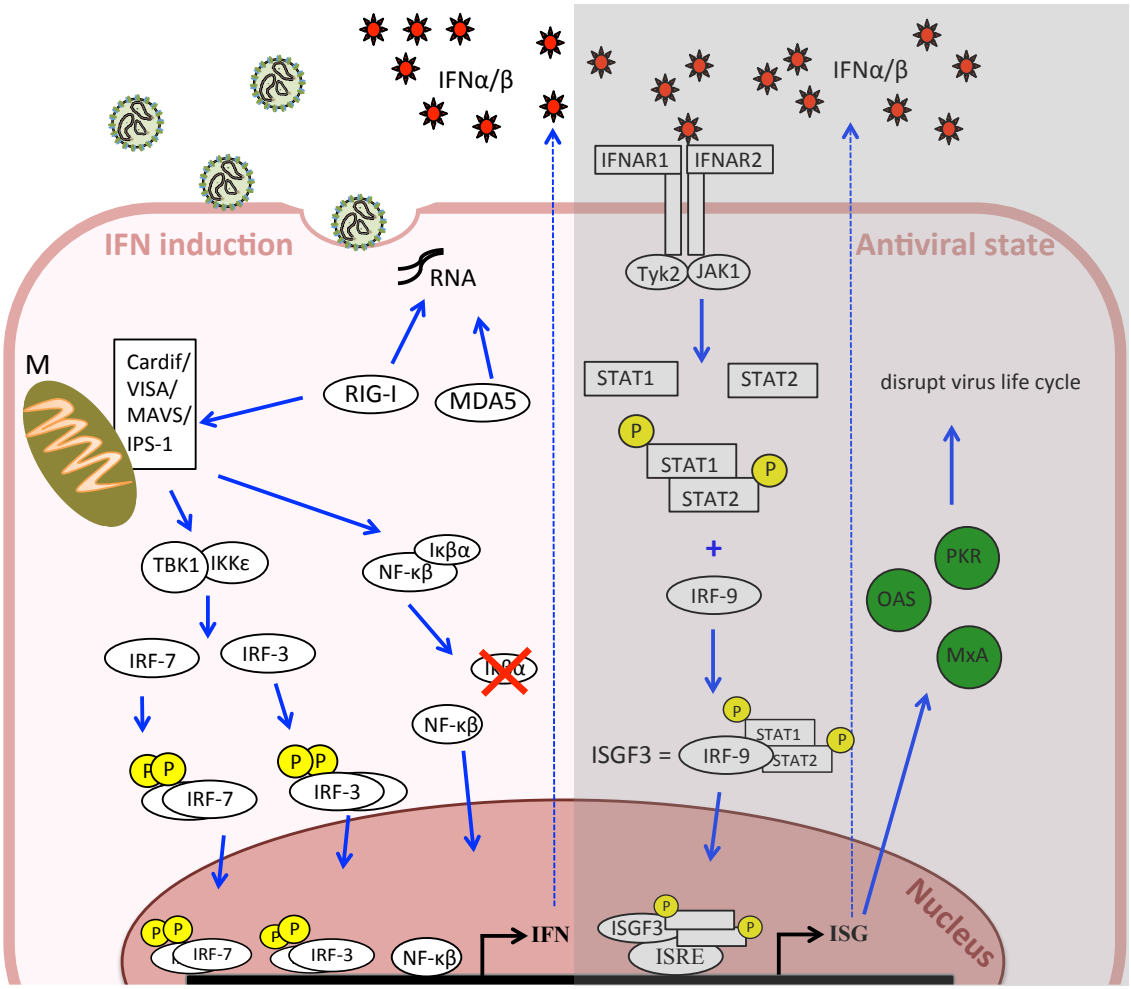

Figure 1. 7. Schematic of the type I IFN pathway.

A simplified schematic of IFN induction and signalling via RIG-1 and MDA5. Recognition of viral nucleic acid eventually leads to phosphorylation of transcription factors causing their translocation into the nucleus to turn on type I IFN transcription. Produced IFNs bind to IFNAR receptors on the cell and in adjacent cells causing phosphorylation of STAT1/2. This in turn leads to the transcription of various ISGs, for example MxA (Myxovirus resistance), OAS (2'5'-oligoadenylate synthase) and PKR (protein kinase R). M, Mitochondria.

Modified version from (Goodbourn *et al.*, 2000; Randall & Goodbourn, 2008).

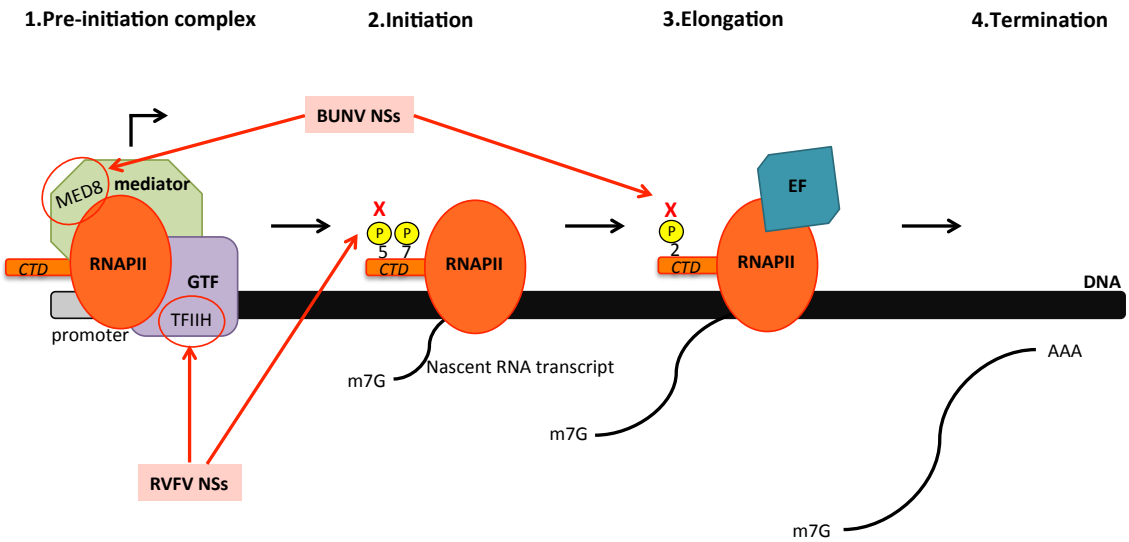

Figure 1. 8. Bunyavirus and the host cell transcriptional machinery.

A simplified version of mammalian-cell transcription (Eick & Geyer, 2013; Allen & Taatjes, 2015). CTD, C-terminal domain of RNAPII; GTF, general transcription factors; EF, elongation factors. The grey box is the promoter. BUNV NSs interacts with MED8 preventing it from assembling with other subunits of the mediator complex. Serine 2 phosphorylation levels are low in BUNV-infected cells and this prevents elongation. RVFV NSs interacts with p44 and p62 subunits of TFIIH of the GTF. RVFV NSs prevents Serine 5 phosphorylation. Phosphorylation of the CTD is important for RNAPII to progress to various stages. The red arrows and crosses indicate disruption.

Bunyaviruses and the antiviral response

Enzymes dsRNA-dependent protein kinase R (PKR) and 2'5'-oligoadenylate synthase (2'5'OAS), along with the Mx (Myxovirus resistance) class of proteins have been studied extensively for their role in the antiviral response. PKR and 2'5' OAS are both activated by dsRNA. PKR phosphorylates the α-subunit of the eukaryotic translational initiation factor 2 (eIF2α), which then prevents its recycling and cuts short initiation. 2'5' OAS on the other hand catalyses ATP binding to RNase L, ultimately degrading all RNA in the infected cell. Both of these enzymes also play a role in IFN signal induction (Goodbourn *et al.*, 2000; Randall & Goodbourn, 2008). BUNV replication upregulates PKR, however its antiviral effects, if any, are only seen *in vivo* (Streitenfeld *et al.*, 2003). With RVFV, the NSs protein specifically targets and degrades PKR (Habjan *et al.*, 2009b). LACV, RVFV, PUUV, HTNV, CCHFV, Tahyna virus (TAHV) and sandfly fever Sicilian virus (SFSV) appear to be sensitive to the antiviral effects of IFN-induced MxA (Frese *et al.*, 1996; Kanerva *et al.*, 1996). MxA belongs to the Mx family, which are large GTPases and from work on LACV it was shown to sequester the viral N protein into perinuclear complexes thereby preventing viral replication (Kochs *et al.*, 2002). Work on CCHFV and RVFV have also shown similar results where MxA targets the N protein to inhibit RNA synthesis (Andersson *et al.*, 2004; Habjan *et al.*, 2009a). Sequencing of the host cell transcriptome has shown that a number of ISGs are upregulated in response to bunyavirus infection, however we are only starting to understand their role in viral clearance. The ISG viperin (virus inhibitory protein, endoplasmic reticulum associated, interferon inducible) for example is expressed in A549 cells infected with a BUNV mutant lacking the NSs protein, and over-expressing viperin in cells can inhibit BUNV replication (Carlton-Smith & Elliott, 2012). Similarly, IFITM- (IFN-induced transmembrane protein) -2 and -3 proteins can reduce RVFV replication (Mudhasani *et al.*, 2013). Bunyaviruses are susceptible to the effects of IFN-α *in vitro*, but only when cells have been pre-treated prior to infection. BUNV and RVFV titres can decrease by a 1000-fold in cells pre-treated with IFN-α, indicating that these viruses are susceptible to the downstream effects of various ISGs (Streitenfeld *et al.*, 2003; Carlton-Smith & Elliott, 2012; Mudhasani *et al.*, 2013).

Programmed death of a bunyavirus-infected cell

External and internal signals can activate programmed death pathways in virus-infected cells as a means to rid infection. Receptors such as TNFR1 or Fas on the cell surface, as well as anti-apoptotic bcl-2 and pro-apoptotic Bax proteins inside the cell, can trigger this death pathway. IFN-inducible proteins such as transcriptional regulator p53, as well as PKR and 2'5' OAS have been implicated in inducing activation of apoptosis. These events ultimately lead to the activation of various caspases with protease activity (Roulston *et al.*, 1999; Kotwal *et al.*, 2012). Viruses either use cell death as a means to spread, or slow, or even inhibit the process altogether. The BUNV NSs protein interacts with IRF-3 and delays apoptosis in cultured cells (Kohl *et al.*, 2003b). Similarly, RVFV uses its NSm protein to inhibit caspase 8 and 9 activation (Terasaki *et al.*, 2013). On the other hand LACV, HTNV, Prospect Hill virus (PHV), OROV, San Angelo virus (SAV), California encephalitis virus (CEV) and SBV induce apoptosis. LACV was shown to induce apoptosis *in vivo* in mouse brain, with regulator protein bcl-2 being an important factor (Pekosz *et al.*, 1996). The C-terminus of LACV, SAV and CEV NSs proteins were shown to share sequence similarities to *Drosophila* Reaper protein (an inhibitor of Inhibitors of Apoptosis [IAP]) (Colon-Ramos *et al.*, 2003). These NSs proteins were also found to function in a manner similar to Reaper, by accelerating cytochrome-C release independent of caspase activation (Colon-Ramos *et al.*, 2003). For LACV and SBV, the NSs protein appears to be important for inducing apoptosis (Blakqori & Weber, 2005; Barry *et al.*, 2014), whether this is the case for pro-apoptotic OROV is currently unknown (Acrani *et al.*, 2010). HTNV can activate caspases 8 and 3 (Li *et al.*, 2004) presumably triggered by the down-regulation of p53 protein levels (Park *et al.*, 2013), bcl-2 protein levels (Kang *et al.*, 1999) and disruption of Fas-signalling (Li *et al.*, 2002). Caspase activation is mainly mediated by the viral N protein.

1.2 Oropouche virus

The following section highlights our current understanding of Oropouche virus - the focus of this PhD project.

1.2.1 Epidemiology

OROV is a midge-borne orthobunyavirus that causes a febrile illness in the South American human population. OROV is currently endemic in Brazil where all major Oropouche fever (OROF) outbreaks have been reported in Amazonian cities (Figure 1.9 A). OROV, however, was first recorded in Trinidad, West Indies, in 1955. The virus was isolated from the acute-phase serum of a 24-year old febrile forest worker from a village called Vega de Oropouche, located near the Oropouche river in Sange Grande town in Trinidad (Anderson *et al.*, 1961). Interestingly, no other febrile cases were reported, however serological surveys found neutralising antibodies in 3/46 humans, 8/26 capuchin monkeys (*Cebus capucinus*) and 9/26 red howler monkeys (*Alouatta seniculus insularis*) indicating that the virus was indeed circulating. In 1960 the virus was again isolated in Trinidad from a pool of *Mansonia venezuelensis* mosquitoes (Anderson *et al.*, 1961; Roberts *et al.*, 1977). That same year the virus was isolated for the first time in Brazil from a dead sloth found near a Belem-Brasilia highway construction site. The following year in 1961 in Belem city 11,000 people were reported ill in what became the first OROF outbreak (Pinheiro, 1962). The largest OROF outbreak to date occurred in 1980 in the state of Para with an estimated 100,000 cases (Pinheiro *et al.*, 1981b; Pinheiro F P, 2004). Between 1978 and 1981 about 220,000 OROF cases were reported in Para, Amazonas and Amapa States (Anderson *et al.*, 1961; Pinheiro, 1962; Pinheiro *et al.*, 1976; Dixon *et al.*, 1981; Epidemiological Bulletin, 1982). In 1988 the virus spread to the states of Maranhao and Goias where about 200 people were reported ill (Vasconcelos *et al.*, 1989). OROF outbreaks were soon being reported in cities all along the Amazon River, and between 1961 to 1996 more that 30 outbreaks were recorded with an estimated 500,000 cases (Table 1.4) (Pinheiro F P, 2004). Outside of Brazil OROF outbreaks were reported for the first time in Panama in 1989 and Peru in 1992. The geographic distribution of OROV today includes Brazil, Panama, Peru and Argentina. Serological evidence suggests that the virus may also be circulating in Ecuador and Bolivia, and in nonhuman primates in

Colombia (Tesh, 1994; Rosa *et al.*, 1996; Watts *et al.*, 1997; Baisley *et al.*, 1998; Pinheiro *et al.*, 1998; Pinheiro F P, 2004; Mercer & Castillo-Pizango, 2005; Azevedo *et al.*, 2007; Bernardes-Terzian *et al.*, 2009; Epidemiological Alert, 2010; Forshey *et al.*, 2010).

Similarity in signs and symptoms of OROF to other endemic viral diseases such as dengue, chikungunya and Mayaro fevers and the lack of a differential surveillance system has resulted in underreporting, and hence the exact epidemiology of OROV in Central and South America remains unclear. It is important to point out that the Belem-Brasilia highway construction that took place between 1958 and 1960 resulted in considerable loss of the Amazon Rain forest. Similarly, the original Trinidad case was from a highly deforested area around Melajo forest. An interesting publication by Vasconcelos *et al*. describes the ecological changes that took place in Brazil in the early 60s and 80s and reports the identification of 187 different viruses that were isolated between 1954 and 1998 (Vasconcelos *et al.*, 2001). OROF is a classical example of how human impact on the environment can contribute to spillover and re/emergence of a new zoonosis. OROV circulates in two cycles; in the urban cycle it is transmitted amongst human populations via the biting midge *Culicoides paraensis* (Pinheiro *et al.*, 1976; Dixon *et al.*, 1981; Pinheiro *et al.*, 1981a; Roberts *et al.*, 1981; Pinheiro *et al.*, 1982a). In contrast, tropical forest cycles involve the pale-throated three-toed sloth, *Bradypus tridactylus* and the black-tufted marmoset, *Callithrix penicillata*, though the vector/s remain largely unknown (Figure 1.9 B) (Nunes *et al.*, 2005). OROF outbreaks typically occur during the rainy season, presumably due to high vector density (Pinheiro F P, 2004). Laboratory experiments and epidemiological surveys have reported that mosquitoes *Aedes serratus, Aedes scapularis, Aedes albopictus, Culex fatigans, Culex quiquefaciatus, Coquilettidia venezuelensis* and *Psorophora ferox* are susceptible to OROV infection (Anderson *et al.*, 1961; Roberts *et al.*, 1977; Pinheiro *et al.*, 1981b; Smith & Francy, 1991). Neutralizing antibodies against OROV have also been detected in both wild and domestic birds (Pinheiro *et al.*, 1976; Roberts *et al.*, 1977; Pinheiro *et al.*, 1981b), leading to speculation that birds could be carriers of the virus (Personal communication, Professor Alan Barrett, University of Texas Medical Branch).

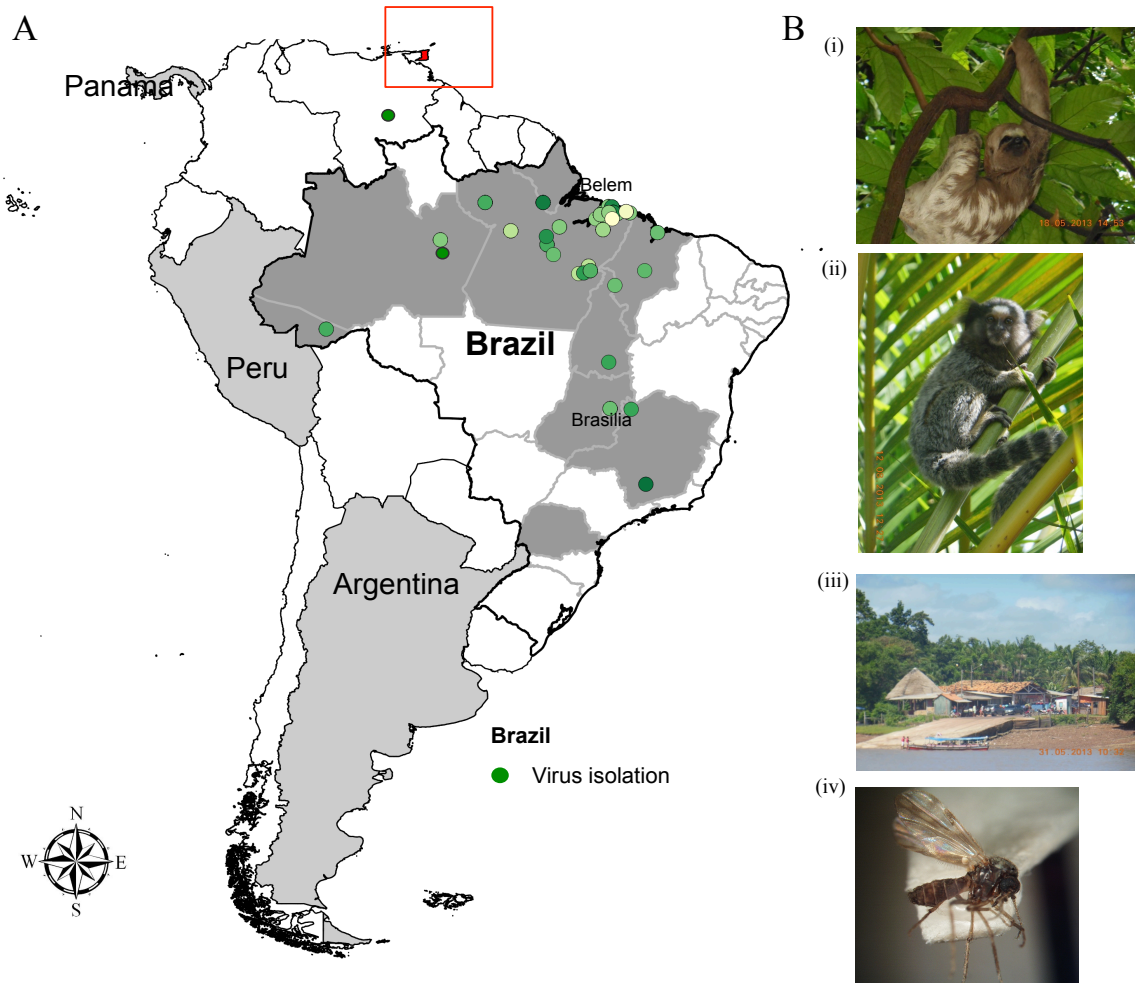

Figure 1. 9. Epidemiology of OROV.

(A) Map showing the geographic distribution of OROV in South America. Data on virus isolation in Brazil (green dots) was obtained from the Evandro Chagas Institute in Belem, Brazil. The red box highlights Trinidad, where OROV was first isolated in 1995. The grey area highlights where OROV has been detected in humans either by serology or virus isolation. The map was created using QGIS Version 2.2.0. (B) OROV transmission cycle. OROV reservoirs; Pale-throated three-toed sloth, *Bradypus tridactylus* (i) and (ii) Black-tufted marmoset, *Callithrix penicillata.* (iii) human settlements along the banks of the Amazon River (iv) OROV vector *Culicoides paraensis*. Image of *Culicoides paraensis* taken from https://cedarcreek.umn.edu/insects/029023n.html. Images (i), (ii) and (iii) were photographed during my stay in Brazil.

Table 1. 4. Recorded Oropouche fever outbreaks in South America

County	State	Location	Year	Month	Estimated cases	Viral Isolation	Reference
Brazil	Para	Belem	1961	Feb - May	11000	15	Pinheiro *et al.* 1981b
Brazil	Para	Caratateua	1967	Feb - Mar	400	2	Pinheiro *et al.* 1981b
Brazil	Para	Braganca	1967	Mar - Jul	6000	8	Pinheiro *et al.* 1981b
Brazil	Para	Belem	1968	Feb - Jul	n/a	101	Pinheiro *et al.* 1981b
Brazil	Para	Baiao	1972	Jun - Sept	85	n/a	Pinheiro *et al.* 1981b
Brazil	Para	Santarem	1974	n/a	n/a	n/a	Pinheiro *et al.* 2003
Brazil	Para	Itupiranga	1975	May - Jun	420	9	Pinheiro *et al.*1981b
Brazil	Para	Santarem	1975	Feb - Apr	14000	65	Pinheiro et al. 1976; Pinheiro *et al.* 1981b
Brazil	Para	Alter do Chao	1975	Jul - Aug	280	16	Pinheiro *et al.* 1981b
Brazil	Para	Mojui dos Campos	1975	Dec - Apr	600	42	Pinheiro *et al.* 1981b
Brazil	Para	Palhal	1975	Feb - Apr	420	22	Pinheiro *et al.* 1981b
Brazil	Para	Belterra	1975	Apr - Jun	1600	n/a	Pinheiro *et al.* 1981b
Brazil	Para	Tome-Aci	1978	Jun - Oct	2000	22	Pinheiro *et al.* 1981b
Brazil	Para	Belem	1979	Apr - Jun	16,000	16	Tesh 1994
Brazil	Para	Several	1979	Mar - Nov	9000	46	Tesh 1994
Brazil	Para	Belem	1980	Feb - Oct	102,000	n/a	Tesh 1994
Brazil	Para	Several	1980	Mar - Aug	37,000	52	Tesh 1994
Brazil	Amapa	Mazagao	1980	n/a	n/a	n/a	Tesh 1994
Brazil	Amazonas	Barcelos	1980	May - June	171	n/a	Tesh 1994
Brazil	Amazonas	Manaus	1980 - 81	Nov - Mar	97,000	9	Epidemiological Bulletin, 1982, Tesh 1994
Brazil	Amapa	Mazagao	1981	n/a	n/a	n/a	Vasconcelos *et al.* 2001
Brazil	Maranhao	Porto Franco	1987 - 88	Dec - Mar	130	75	Tesh 1994, Pinheiro 1998
Brazil	Goias	Tocantinopolis	1988 - 88	Dec - Mar	n/a	10	Vasconcelos *et al*. 1989, Tesh 1994, Pinheiro 1998
Brazil	Rondonia	Ariquemes	1991	Feb - Mar	58,574	n/a	Tesh 1994
Brazil	Rondonia	Quro Preto do Oeste	1991	Feb - Mar	35,413	n/a	Tesh 1994
Brazil	Para	Serra	1994	Nov -	5000	12	Rosa *et al*. 1996,

County	State	Location	Year	Month	Estimated cases	Viral Isolation	Reference
		Pelada		Dec			Pinheiro 1998
Brazil	Para	Oriximina	1996	Apr - May	n/a	33	Pinheiro 1998
Brazil	Para	Altamira	1996	Feb - Jun	n/a	n/a	Vasconcelos *et al*. 2001
Brazil	Para	Brasil Novo	1996	Jan - Feb	n/a	7	Pinheiro 1998
Brazil	Amazonas	Novo Airao	1996	Mar - May	n/a	40	Pinheiro 1998
Brazil	Para	Vitoria do Xingu	1996	n/a	n/a	3	Pinheiro 1998
Brazil	Acre	Xapuri	1996	Mar - Apr	n/a	4	Vasconcelos *et al*. 2001, Pinheiro 1998
Brazil	Para	Paraua-pebas	2003	Apr - May	n/a	n/a	Azevedo *et al*. 2007
Brazil	Para	Porto de Moz	2004	Jul - Aug	n/a	n/a	Azevedo *et al*. 2007
Brazil	Acre	n/a	2004 - 06	n/a	n/a	n/a	Bernardes-Terzian *et al.* 2009
Brazil	Para	Braganca	2006	Apr - Aug	18000	n/a	Vasconcelos *et al.* 2009
Brazil	Manaus	n/a	2007 - 08	Nov - Mar	128	n/a	Mourao *et al*. 2009
Brazil	Amapa	Mazagao	2009	Jun - Oct	-	-	Personal Communication, IEC
Panama	Panama	Chame/San Miguelito	1989	Sept	n/a	n/a	Tesh 1994
Panama	Panama	Chilibre	1990	n/a	n/a	n/a	Tesh 1994
Peru	Loreto	Iquitos	1992	Jan - Apr	n/a	n/a	Tesh 1994
Peru	Loreto	Iquitos	1996 - 97	n/a	n/a	n/a	Watts *et al.* 1997
Peru	Pachiza	Bagazan	n/a	May	282	n/a	Epidemiological Alert: Outbreak of Oropouche Fever, Pan American Health Organization, 2010

1.2.2 Clinical profile

The signs and symptoms of OROF include fever, headache, malaise, myalgia, arthralgia, photophobia, retrobulbar pain, nausea, vomiting, dizziness, skin rash, encephalitis and in some cases meningitis (Figure 1.10). OROV is not known to be fatal in humans. The incubation period of the virus ranges between 4 and 8 days. Symptoms typically last between 2 and 7 days, but can prolong for up to one month. A relapse of symptoms appears to be quite common with OROF, and some patients report a recurrence 10 days after acute-phase symptoms have subsided. Attempts to isolate virus during this period have not been successful (Pinheiro *et al.*, 1976; Pinheiro *et al.*, 1981b; Pinheiro F P, 2004; Bastos Mde *et al.*, 2012).

Three routine diagnostic tests are carried out on all febrile patients in Brazil, and these include hemagglutination inhibition (HI) test, complement fixation text and ELISA. For the HI test samples are screened for 19 different arboviruses, but its low specificity often results in cross-reaction. More specific tests like the ELISA-immunoglobulin M (IgM) are then carried out. OROV-positive samples are taken forward for viral isolation only if the sample was collected within a five-day window, as OROV titres in patients decrease by day 5. Virus is isolated in newborn mice (*Mus musculu*) and cell culture (Personal communication, Department of Arbovirology and Hemorrhagic Fevers, Evandro Chagas Institute in Belem, Brazil).

1.2.3 Molecular Epidemiology

The first genome sequences for OROV were reported almost 15 years ago (Saeed *et al.*, 2000; Wang *et al.*, 2001; Aquino *et al.*, 2003; Aquino & Figueiredo, 2004). Since then the epidemiology and genetic variation of OROV has been widely studied and discussed. In most cases the information is largely based only on partial gene sequences. Saeed *et al*. carried out the first phylogenetic analysis for OROV (Saeed *et al.*, 2000). The author's analysis was based on the N ORF of 28 isolates and they identified that OROV clustered into three distinct genotypes. All subsequent studies confirmed this finding (Nunes *et al.*, 2005; Mourao *et al.*, 2009; Vasconcelos *et al.*, 2009; Ladner *et al.*, 2014). In 2011, Vasconcelos *et al*. attempted to analyse the genetic evolution and

dispersal of OROV in South America (Vasconcelos *et al.*, 2011). Using samples from 1961 to 2009 the authors mapped a dispersal route for OROV and, more interestingly, identified that the OROV N ORF clusters in a novel fourth genotype. However, the information presented has to be treated with caution as the authors again utilised only partial genetic information.

1.2.4 Pathogenesis

The first OROV report in 1961 (Anderson *et al.*, 1961) demonstrated that mice and hamsters are equally susceptibility to OROV infection. The authors also showed that adult mice were resistant to infection via intraperitoneal inoculation (i.p) compared to infant mice. In order to understand OROV pathogenesis, models based on these two animal models have since been established. Subcutaneous inoculation of OROV in adult Syrian golden hamsters (*Mesocricetus auratus*) results in a systemic infection, with symptoms similar to human infection appearing 72 hours post infection (p.i). Using immunohistochemistry the authors demonstrated OROV antigens in the liver and brain at 4 days p.i, indicative of hepatitis and CNS damage (Rodrigues *et al.*, 2011). In contrast to what was seen in hamsters, Santos *et al*. found that in neonatal BALB/c mice OROV could be detected solely in the brain and spinal cord, both at high titres (Santos *et al.*, 2012). Using immunohistochemistry Santos *et al*. subsequently demonstrated that in these mice OROV could be found in the brainstem and in particular the periaqueductal gray about 3 days p.i (Santos *et al.*, 2014). During this period animals did not exhibit any symptoms until infection progressed to the forebrain 5 to 6 days p.i. Infection in neonatal mice lead to death approximately 10 days p.i (Santos *et al.*, 2012). Though disease progression is not as exaggerated in human cases, OROV has been isolated from patient CNS (Pinheiro *et al.*, 1982b; Bastos Mde *et al.*, 2012). The highest number of meningitis cases were reported during a 1980 OROF outbreak in Para, in 22 out of a total 292 patients. OROV was subsequently isolated from the CNS of one of these patients (Pinheiro *et al.*, 1982b; Bastos Mde *et al.*, 2012).

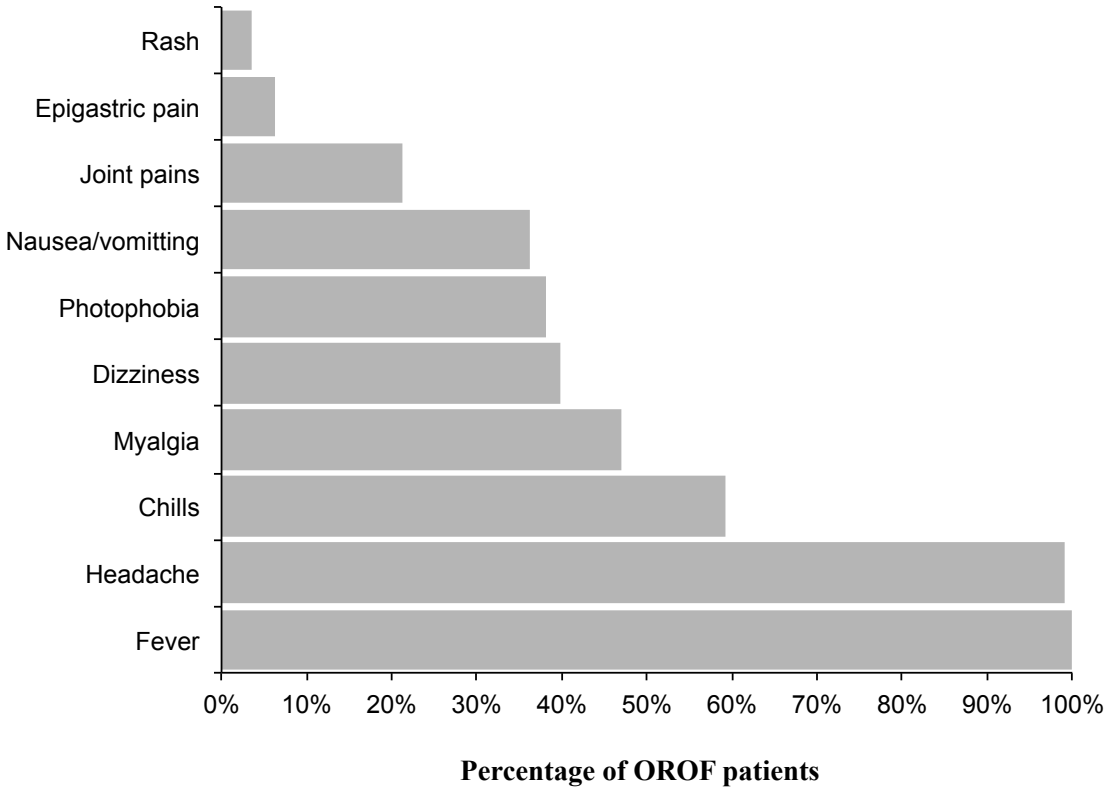

Figure 1. 10. Clinical symptoms of OROV.

Percentage of 113 patients with OROF patients that presented indicated clinical symptoms during a 2006 outbreak in Para, Brazil. Data to produce the graph was taken from (Vasconcelos *et al.*, 2009).

1.2.5 Virus-host interaction

The lack of a reverse genetics system for OROV has limited research on a molecular level. As discussed earlier in this Chapter, Santos *et al*. demonstrated that OROV enters HeLa cells via the CME pathway (Santos *et al.*, 2008). Acrani *et al*. later reported that OROV causes apoptosis in HeLa cells, and that this is triggered by viral protein synthesis, indicating that a particular protein may have a pro-apoptotic role (Acrani *et al.*, 2010). In a recent study comparing 6-week old C57BL/6 mice knockout mutants, it was shown that MAVS activation is crucial for type 1 IFN signalling during OROV infection. The authors demonstrated that MDA5 knockout mice did not show any increased susceptibility to OROV infection, indicating that MAVS activation did not occur via MDA5. The authors also demonstrated that downstream to this both IRF 3 and 7 are required together for transcriptional activation. Similar to an earlier hamster model study, the authors also found extensive hepatic necrosis in the liver of $Mavs^{-/-}$, $Ifnar^{-/-}$ and $Irf3^{-/-} \times Irf7^{-/-}$ knockout mice, while other tissues either had no detectable virus or extremely low viral yields. The authors further demonstrated that, similar to other orthobunyaviruses, in human immunocompetent cell-lines such as 2fTGH and U3A, OROV is capable of inhibiting type 1 IFN production (Proenca-Modena *et al.*, 2015a).

1.2.6 Antivirals and OROV

The antivirals Ribavirin and Mycophenolic acid have been tested against OROV *in vivo* and *in vitro* (Livonesi *et al.*, 2006; Livonesi *et al.*, 2007a). Both these drugs have been proven to exhibit antiviral activity against several RNA viruses and are being used clinically for several viral infections. However, both drugs demonstrated no antiviral effect against OROV. In a comparative study on the effects of IFN-α against several different orthobunyaviruses it was shown that OROV displayed resistance to its antiviral effects both *in vivo* and *in vitro* (Livonesi *et al.*, 2007b). A decrease in OROV titres was only observed at a high dose of IFN-α (10,000 U/ml), and only when cells were either pre-treated for 24 hours or treated 2 hours p.i. Similarly, the survival rate of mice increased only when they were treated prophylactically with IFN-α.

1.3 Reverse genetics

Genetics in the classical sense involves phenotypic observation prior to genetic identification and modification. The establishment of reverse genetics on the other hand allows recombinant DNA technology to be used in order to introduce specific mutations in the genome prior to phenotype observation. This targeted approach allows any phenotypic alteration to be attributed to the introduced mutation and has been a major step forward in virus research (Walpita & Flick, 2005; Elliott & Schmaljohn, 2013; Stobart & Moore, 2014).

Reverse genetics for RNA viruses are complicated due to the lack of stability to the RNA molecule, and hence the genome requires conversion into cDNA before a mutation can be introduced. Negative-sense RNA viruses are further complicated by the fact that its genome in is the opposite orientation to the host cell's mRNA. To overcome this they have evolved to package their own RNA-dependent RNA polymerase (RdRp) in order to initiate viral transcription and replication once inside a host cell. The naked genome of a negative-sense RNA virus is therefore not infectious, but instead it is the RNP complex that forms the minimal infectious unit for these viruses (Walter *et al.*, 2011). DNA and positive-sense RNA viruses on the other hand can use the host cell machinery to initiate their replication cycle, which means they are relatively easier to rescue as infectious virus can be generated directly from DNA plasmids (Elliott & Schmaljohn, 2013).

The ability to generate recombinant viruses has allowed us to understand mechanisms used by viruses to evade the host immune system, and most importantly it has enabled us to target crucial proteins for antiviral and vaccine development (Elliott & Schmaljohn, 2013; Stobart & Moore, 2014). A lot of the work reviewed in this chapter would not have been possible had it not been for the initial work by Bridgen and Elliott in 1996 (Bridgen & Elliott, 1996), who established how segmented negative-sense RNA viruses could be recovered solely from cDNA.

1.3.1 A brief history

The first DNA virus to be rescued was T2 Bacteriophage in 1957 by Fraser *et al.* (Fraser *et al.*, 1957) and the first RNA virus to be rescued was Bacteriophage Qβ in 1978 by Taniguchi *et al.* (Taniguchi *et al.*, 1978). The first mammalian cell-infecting positive-sense RNA virus recovered from DNA plasmids was poliovirus (Racaniello & Baltimore, 1981). In the late 1980s methods were developed to purify vRNP for segmented negative-sense influenza A virus, which allowed viral transcripts to be synthesised *in vitro* and so functional RNPs could then be transfected into cells (Kawaoka & Neumann, 2004). Using this method Luytjes *et al*. (Luytjes *et al.*, 1989) generated influenza viral transcripts encoding chloramphenicol acetyltransferase (CAT), and Enami *et al*. (Enami & Palese, 1991) rescued mutant influenza A viruses by genome reassortment with a helper influenza A virus. In 1994 Schnell *et al*. (Schnell *et al.*, 1994) rescued rabies virus; this was the first time a non-segmented negative-sense virus was recovered entirely from cDNA alone. Here, the authors discovered that it in order to generate infectious negative-sense virus the cDNA plasmids had to contain antigenome (positive-sense) copies of the viral genome. The authors also supplied the system with "helper plasmids" in order to express the viral proteins required to start primary transcription. The first breakthrough for segmented negative-sense RNA viruses however, came when Bridgen and Elliott (Bridgen & Elliott, 1996) rescued BUNV. The authors used a similar system to Schnell *et al*., but due to the amount of plasmids being transfected the system was not very efficient and was later developed to allow virus recovery using three antigenome plasmids alone (Lowen *et al.*, 2004).

Reverse genetics systems for negative-sense RNA viruses are well established today, and the methodology to generate the viral transcripts can be either through use of the bacteriophage T7 RNA polymerase or cellular DNA dependent RNA polymerase I and II (Kawaoka & Neumann, 2004).

1.3.2 Bunyavirus reverse genetics

To date, a number of bunyaviruses have been rescued and these include BUNV (Bridgen & Elliott, 1996), LACV (Blakqori & Weber, 2005), RVFV (Ikegami *et al.*,

2006), AKV (Ogawa *et al.*, 2007), SBV (Elliott *et al.*, 2013; Varela *et al.*, 2013), SFTSV (Brennan *et al.*, 2015), UUKV (Rezelj *et al.*, 2015) and CCHFV (Bergeron *et al.*, 2015). To rescue these viruses mammalian cell lines are transfected with three "transcription plasmids" that contain an antigenomic-sense cDNA copy of the three viral segments (Figure 1.11). Here, RNA transcription is usually under the control of a T7 promoter, and T7 RNA polymerase is delivered to the cells either through a helper vaccinia virus (vTF7-3) or fowlpox virus (FPT7) or it is constitutively expressed, for example, in BSR-T7/5 cells (Buchholz *et al.*, 1999). Support/helper plasmids encoding viral proteins N and L are also transfected in some cases in order to boost initial transcription (Kawaoka & Neumann, 2004; Bouloy & Flick, 2009). Further, transcription efficiency of the T7 promoter in the transcription plasmid is increased with the addition of a G residue (either one, two or three) immediately after the promoter sequence. Billecocq *et al*. (2008) found that infectious RVFV could only be produced when at least two of the transcription plasmids had at least one 'G' after the T7 promoter. The authors found that, without that increased efficiency the number of produced transcripts were too low to initiate replication (Billecocq *et al.*, 2008). Hence, bunyavirus transcription plasmids contain one, two or three G's immediately after the T7 promoter sequence. The newly generated viral RNA transcripts do not function if they contain extra nucleotides at the 3' UTR, and so to prevent this, a self-cleaving hepatitis delta virus (HDV) ribozyme sequence is usually placed just before the T7 terminator (Figure 1.11) (Perrotta & Been, 1990; Schnell *et al.*, 1994; Bouloy & Flick, 2009). A study by Ghanem *et al*., (Ghanem *et al.*, 2012) demonstrated the inability of rabies virus to replicate when the transcripts contained extra nucleotides at their 3'end, whereas 5' UTR overhangs were tolerated. The authors were able though to enhance rescue efficiency by using a hammerhead ribozyme (HHrz) to generate exact 5' ends as well.

Although the T7 system is the preferred method to rescue bunyaviruses the cellular polymerase I/II system has also been used. This system was initially developed for viruses that replicate in the nucleus, such as influenza viruses (Kawaoka & Neumann, 2004; Billecocq *et al.*, 2008). In 2001 Flick *et al*. (Flick & Pettersson, 2001) used the system to rescue UUKV minigenomes (discussed below), and also demonstrated that

pol-I derived CCHFV (Flick *et al.*, 2003b) and HTNV (Flick *et al.*, 2003a) minigenome segments could be packaged. Then in 2007 Ogawa *et al*. (Ogawa *et al.*, 2007) rescued AKAV using this system. In 2008, Billecocq *et al*. (Billecocq *et al.*, 2008) conducted a comparative study of both transcription systems using RVFV. Results from the study demonstrated that both the pol-I system and the T7 system efficiently generated high titres of infectious virus. Results also demonstrated that it was only the T7 system that produced infectious virus in the absence of the N and L helper plasmids. The N and L transcripts that are generated from the transcription plasmids are sufficient to initiate further steps, and hence bunyavirus rescue systems are successful with three plasmids (Bridgen & Elliott, 1996).

Some bunyaviruses are, however proving to be difficult to rescue, for example viruses of the *Hantavirus* genus. Considerable efforts are being made towards understanding the underlying causes preventing virus recovery in cultured cells. With the current advancement in sequencing technology, comparisons between the dynamics of clinical isolates and cell-culture adapted virus populations will become easier, and with our growing understanding of how bunyaviruses function we may be a step closer to creating viruses from this important genus as well. These viruses do prove that although we have come a long way since Dimitrii Ivanovsky first observed tobacco mosaic "disease" in 1892, we still have a long way to go in our understanding of how a virus population functions.

Minigenome and Virus-like Particle (VLP) production assay

Minigenomes and Virus-like Particle (VLP) assays can also be used to study various aspects of the virus life cycle without the need to rescue infectious virus. This can be especially useful when viruses require high containment for their use, like CCHFV, which requires a biosecurity level 4 laboratory. In the minigenome system viral UTRs flank reporter genes such as Green Fluorescent protein (GFP), CAT or luciferase. These genes are placed in a viral genomic sense (negative-sense), so expression can only be derived with the correct viral L and N protein. Hence, the system also serves as a way to test viral UTRs and protein-coding genes for functionality before attempting to rescue the virus (Figure 1.12). The minigenome system has served as a way to study

bunyavirus transcription, encapsidation and promoter strength (Dunn *et al.*, 1995; Weber *et al.*, 2001; Blakqori *et al.*, 2003; Flick *et al.*, 2003a; Kohl *et al.*, 2004b; Ikegami *et al.*, 2005; Bergeron *et al.*, 2010). In 2006 Shi *et al.* demonstrated that by including a glycoprotein expression plasmid in the minigenome system VLPs could be generated, Figure 1.12 (Shi *et al.*, 2006). VLPs are formed because the L and N proteins interact with the reporter segment to form RNPs, and as the authors subsequently demonstrated using this assay, the RNP interacts with the Gn-CT in order to assemble and eventually bud out as a virion (Shi *et al.*, 2006; Shi *et al.*, 2007). Overby *et al.* (Overby *et al.*, 2006) compared UUKV-VLPs to authentic UUKV-virions showing that their morphology in cell culture was identical. Since VLPs do not contain all the elements of an authentic virus they are not capable of further rounds of replication. Recently Devignot *et al*. demonstrated that by transfecting the "VLP-recipient" cells with L, M and N expression plasmids VLP production could be increased, which, as the authors point out, could be highly beneficial for VLP-based vaccine/antiviral development (Devignot *et al.*, 2015).

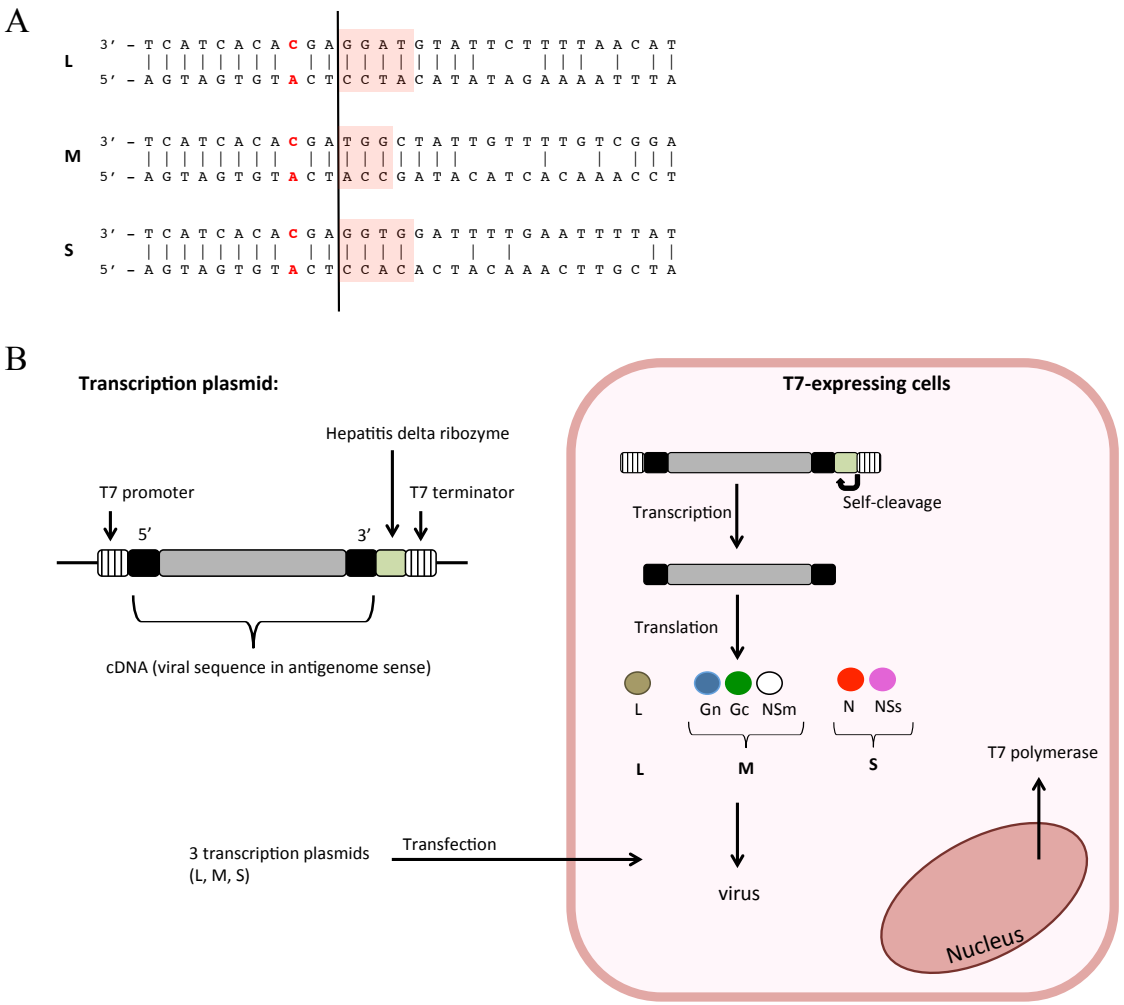

Figure 1. 11. Bunyavirus rescue system.

(A) BUNV UTR sequences. Sequences are presented in the antigenomic sense. Nucleotides in red highlight the mismatch at nucleotide number 9. The black line separates the first 11 nucleotides that are conserved for all three segments and within the *Orthobunyavirus* genus. Positions 8 and 9 vary in some viruses. The red shading shows the nucleotides that are conserved for that particular segment in the *Orthobunyavirus* genus, nucleotides beyond this vary for each virus. (B) Rescue system based on BUNV. The viral sequences shown in (A) need to be accurate in order for them to function (black box in the transcription plasmid). The transcription plasmid contains a T7 promoter and terminator, a hepatitis delta ribozyme and the cDNA copy of the viral segment. These are transfected into cells that express T7 polymerase to allow transcription from the plasmids. Viral proteins expressed are sufficient to initiate replication. Figure B adapted from (Elliott, 2014).

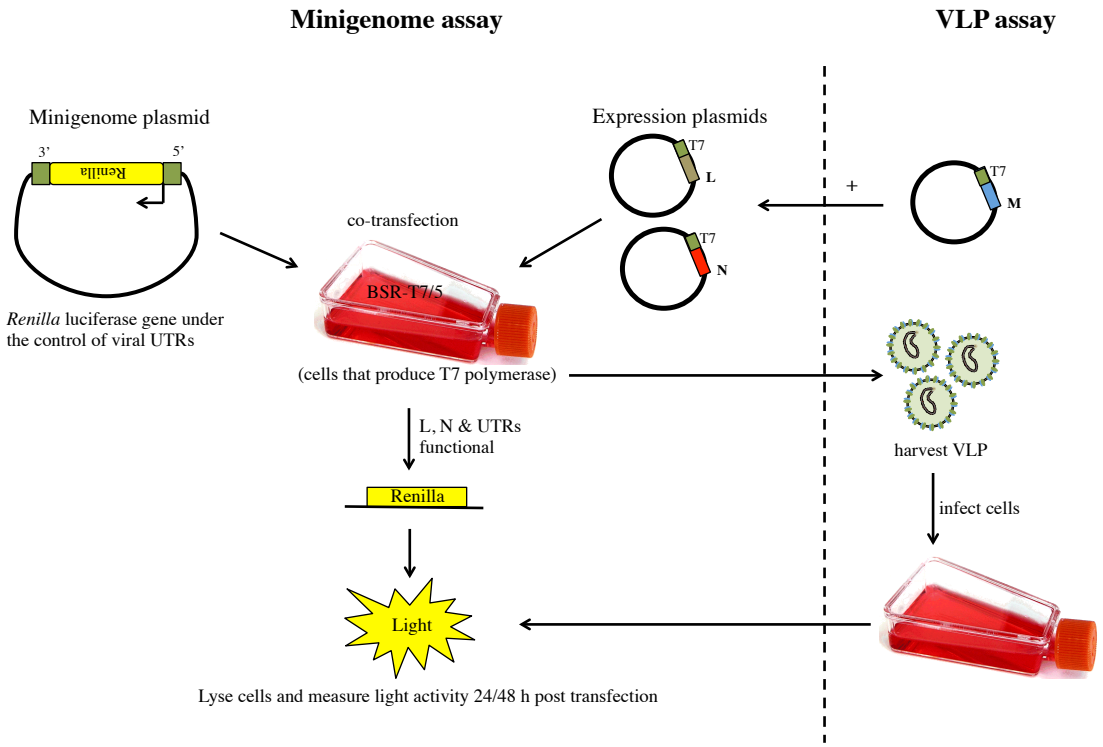

Figure 1. 12. Schematic of a minigenome and VLP assay.

The diagram explains how a minigenome and a VLP (virus-like particle) assay are carried out. The minigenome plasmid contains a reporter gene flanked by viral UTRs in the genomic sense orientation. Expression plasmids encode the viral L (polymerase) and N (nucleocapsid) protein, and in order to produce VLPs an M (glycoprotein) expression plasmid is used as well. If the plasmids are under the control of a T7 promoter, cells must be able to produce T7 RNA polymerase (eg. BSR-T7/5 cells).

1.4 Aims

From the reviewed literature it is evident that we still have a lot to learn about OROV. Being able to genetically modify the virus would be a huge advantage to allow future investigation, and to build on all the important findings that have been discussed above.

The overall aim of my PhD project was to establish a reverse genetics system for OROV and begin initial characterization of the virus in a cell-culture based system.

To achieve my overall aim I developed the following approach:

1. To re-sequence the genome of OROV prototype strain BeAn19991.
2. To deep sequence OROV field isolates.
3. To compare the prototype and field isolates.
4. To establish a minigenome system for OROV.
5. To establish a VLP system for OROV.
6. To rescue OROV strain BeAn19991.
7. To rescue OROV mutants lacking (a) NSm (b) NSs.
8. To compare OROV with BUNV in its ability to inhibit type I IFN production.

Chapter II

Materials and Methods

Chapter II. Materials and Methods

2.1 Materials

2.1.1 Bacterial strains

JM109 *Escherichai coli* strain: endA1, recA1, gyrA96, thi, hsdR17 (rk–, mk+), relA1, supE44, Δ(lac proAB), [F´ traD36, proAB, laqIqZΔM15].

Grown in LB medium.

2.1.2 Eukaryotic cell lines

2fTGH Human Epithelial fibrosarcoma cells.
Maintained in Dulbecco's modified Eagle's medium (DMEM; Invitrogen) supplemented with 10% fetal bovine serum (FBS).

A549 Adenocarcinomic human alveolar basal epithelial cells.
Maintained in DMEM (Life Technologies) with 10% (v/v) FBS (Life Technologies).

A549NPro A cell line derived from A549 cells. These cells express the NPro protein of bovine viral diarrhea virus. The NPro protein antagonises IFN-β production by targeting IRF-3 for proteasomal degradation.
Maintained in DMEM (Life Technologies) with 10% (v/v) FBS (Life Technologies).

A549V A cell line derived from A549 cells. These cells express the V protein of simian virus 5. The V protein blocks type 1 IFN signalling by degradation of STAT1.

Maintained in DMEM (Life Technologies) with 10% (v/v) FBS (Life Technologies).

Aag-2 — Derived from *Aedes aegypti* mosquito neonatal larvae.
Maintained in Schneider's *Drosophila* medium with L-glutamine (Gibco) supplemented with 10% FBS.

BHK-21 — BHK-21 clone 13, derived from baby hamster kidney fibroblast cells.
Maintained in Glasgow modified Eagle's medium (GMEM, Life Technologies) with 10% (v/v) newborn calf serum (NCS, Life Technologies) and 10% (v/v) tryptose phosphate broth (TPB; Invitrogen).

BSR-T7/5 — Derived from BHK-21 cells, these cells stably express the T7 bacteriophage T7 RNA polymerase (T7RNAP) (Buchholz *et al.*, 1999).
Maintained in GMEM (Life Technologies) supplemented with 10% (v/v) FBS, 10% (v/v) TPB and 1 mg/ml G418 (Geneticin; Invitrogen).

CPT-Tert — Sheep choroid plexus cells. These cells have been immortalized with the simian virus 40 T-antigen and human telomerase reverse transcriptase. These cells lack a fully functioning IFN system.
Maintained in DMEM (Life Technologies) and supplemented with 10% (v/v) FBS (Life Technologies).

DF-1 — Chicken embryo fibroblasts.
Maintained in DMEM (Life Technologies) and supplemented with 10% (v/v) FBS (Life Technologies).

HeLa — Human cervix adenocarcinoma epithelial cells.
Maintained in DMEM (Life Technologies) and supplemented with 10% (v/v) FBS (Life Technologies).

LLC-MK2 *Macaca mulatta* kidney epithelial cells.
Maintained in DMEM (Life Technologies) and supplemented with 10% (v/v) FBS (Life Technologies).

MDCK Canine kidney epithelial cells.
Maintained in DMEM (Life Technologies) and supplemented with 10% (v/v) FBS (Life Technologies).

MRK101 Derived from Grey red-backed vole kidney cells (*Myodes rufocanus*).
Maintained in DMEM (Life Technologies) and supplemented with 10% (v/v) FBS (Life Technologies).

QT-35 Japanese quail fibrosarcoma cells.
Maintained in DMEM (Life Technologies) and supplemented with 10% (v/v) FBS (Life Technologies).

U4.4 Derived from *Aedes albopictus* mosquito neonatal larvae.
Maintained in L-15 cell culture medium (Life Technologies) and supplemented with 10% (v/v) FBS and 10% TPB

Vero E6 African green monkey (*Cercopithecus aethiops*) kidney epithelial cells.
Maintained in DMEM (Life Technologies) and supplemented with 10% (v/v) FBS.

2.1.3 Viruses

Encephalomycocarditis virus (EMCV).

Bunyamwera virus (BUNV)

wtBUNV and rBUNVdelNSs2.

rBUNVdelNSs2 is a recombinant virus that does not express the NSs protein.

Oropouche virus (OROV)

OROV strain BeAn 19991 was kindly donated by Professor Luiz Tadeu Moraes Figueiredo, from the Ribeirao Preto School of Medicine, University of Sao Paulo, Brazil.

OROV isolates - BeH 759021, BeH 759022, BeH 759024, BeH 759025, BeH 759040, BeH 759146, BeH 759529, BeH 759620, BeAn 789726 and BeAn 790177 were kindly provided by Professor Pedro Vasconcelos, from the Department of Arboviruses and Hemorrhagic Fever, Evandro Chagas Institute, Ministry of Health, Ananindeua, Brazil.

All experiments with OROV were conducted under Containment Level 3 laboratory conditions.

2.1.4 Oligonucleotides

All synthetic oligonucleotides were purchased from Integrated DNA technologies (IDT) at 25 nM scale with standard desalt purification.

Table 2. 1. Common sequencing Primers

Oligonucleotide	Sequence (5'-3')	Purpose
PCR Anchor Primer	GACCACGCGTATCGATGTCGAC	3’ RACE analysis
Oligo d(T)-Anchor Primer	GACCACGCGTATCGATGTCGAC TTTTTTTTTTTTTTTV	3’ RACE analysis
pTM-R	CAACTCAGCTTCCTTTCGGGC	Reverse sequencing pTM1 plasmids
pTM-up	GGTGCACATGCTTTACATGTG	Forward sequencing pTM1 plasmids
pUC118-F	AGCGCCCAATACGCAAAC	Forward sequencing pTVT7R plasmids

Table 2. 2. List of primers used in chapter 3, section 1

Name	5' - 3'	Segment	Position
Ama460MF	CGGAACAACTTCGACATCAGG	M	460 – 480
Ama1151MF	GCAATCATTTTGGTATTGTTGC	M	1151 – 1172
Ama2737MR	CATTATAGTTTATCTGTCTC	M	2756 – 2737
Ama2795MF	GGATCAGATTTGATGACACAC	M	2795 – 2815
Ama4056MR	GCACTGGAGATCCTCTTCCC	M	4075 – 4056
Ama2470MF	CACTGCGCAACCAGCAGATATG	M	2470 – 2491
H759529 MR	GCTTTATATTTGCTGTCTATC	M	2334 – 2314
H759529 MF	GCAATGATATGGATATATTAG	M	3324 – 3344
H759620 MR	TTCAATATTCCAATCATCTG	M	2105 – 2087
AMA2930LF	GCAAAAATGTGCCTGTACCTTGTC	L	2930 – 2953
AMA3082LR	CTTTATTGTATTACTGATATAC	L	3061 – 3082
Ama4987LF	CAGAGAGAATATGAGAGAG	L	4987 – 5005
Ama4202LF	GCTTAGGTACATATCTCTTG	L	4202 – 4226
Ama5447LF	GAGAGTTAAATTCTTAGGA	L	5446 – 5464
Ama2733LF	CAGATTACACAGACTATATG	L	2733 – 2752
Ama1513LR	GTCCCACATTTCTACACTAC	L	1513 – 1494
Ama267LF	CACCTGATAATTACTTACTG	L	267 – 286
Ama944LF	CCAAGCATGCATTTTATATGG	L	944 – 964
Ama1466LF	GAGCATTTTTCAGCTAAGAT	L	1466 – 1485
Ama2509LR	GTTATTTGCATTTTCTACTCG	L	2509 – 2489
Ama2489LF	CGAGTAGAAAATGCAAATAAC	L	2489 – 2509
Ama794LF	GAGTTTACTAAAGGGCATGC	L	794 - 813
Ama2118F	CAGCATACGAGCAGAGGAAA	L	2118 - 2137
Ama2998LF	GATAAGTGAACCAGGTGATTC	L	2998 - 3018
Ama3508LF	GGAAGCAGCAACATTATTAG	L	3508 - 3527
Ama4089LF	GAAAATTATCATCTCCGATC	L	4089 - 4108
Ama6099LF	TGGATCTGTCAGAGTTAATG	L	6099 - 6118
OROVL_Anti	ACCTCTCCAAAAATCTCATT	L 5' UTR	384 – 365
OROVL_gen	GAACTAGACAATTGTATTCA	L 3' UTR	6494 – 6513
OROVM_Anti	CTAATATCACATGCTGCTCTACATG	M 5' UTR	396 – 372
OROVM_gen	GCACATATCTGTGGGAGAGACAT	M 3' UTR	3959 – 3981
OROSlig1	CTTGCGCCAATTCGGAATTGAC	S UTR	713 – 734
OROSlig2	GGTACATCGTTGAAAATGAAC	S UTR	73 – 53
PRM_Anti	CCTGTATTGGGTTGCACTCG	M 3' UTR	300 – 281
PRM_gen	GGGCTACCCATCCTTAGAC	M 3' UTR	4206 – 4224

Table 2. 3. List of primers used for OROV BeAn19991 genome sequencing and cloning in Chapter 3, section 2.

Oligonucleotide	Sequence (5'-3')	Segment/ gene	Position
OROLFg	GGGGTACCCGTCTCATATAG**AGTAGTGTGCTCCTATTCCG**	L	1 – 19
OROL1	GAAGTTAGTTAGATATGTCT	L	3706 – 3687
OROLRg	GCTCTAGACGTCTCTACCC**AGTAGTGTGCTCCTATTTAG**	L	6833 – 6852
OROL2	CCCTTGTGA ACTCAATGGTA	L	3537 – 3556
OROMFg	GGGGTACCCGTCTCATATAG**AGTAGTGTGCTACCGGCAACAAACA**	M	1 – 25
OROMRg	GCTCTAGACGTCTCTACCC**AGTAGTGTGCTACCGACAACAATTT**	M	4508 – 4484
OROSFg	GGGGTACCCGTCTCATATAG**AGTAGTGTGCTCCACAATTC**	S	1 – 20
OROSRg	GCTCTAGACGTCTCTACCC**AGTAGTGTGCTCCACTATAT**	S	754 – 785 §
OROdelNSsF	GAGTTCATTTTCAACGA**C**GTACCACAACGGACTACATCTACATTTGATCCGGAGGC AGCATA**C**GTA**G**CATTTGAAGC	delNSs	51 – 127
OROdelNSsR	GCTTCAAATGC**T**AC**G**TATGCTGCCTCCGGATCAAATGTAGATGTAGTCCGTTGTGG TAC**G**TCGTTGAAAATGAACTC	delNSs	127 – 51
pTM1-OROVL-F	AAAACACGATAATACC**ATGTCACAACTGTTGCTCAACCAATATCG**	L	44 – 72
pTM1-OROVL-R	TTAATTAGGCCTCTC**TTAGAAGTCAAATTTGGATTTGCCAGT**	L	6802 – 6776
pTM1-OROVM-F	AACACGATAATACC**ATGGCGAATTTAATAATTATTTCAATGGTTC**	Glycoprotein	32 – 62
pTM1-OROVM-R	TTAATTAGGCCTCTC**CTACTTGATTTTCTGCTCCATGGCATATTCTATTTCATGT CTGATT**	Glycoprotein	4294 – 4249
pTM1-OROVS-F	AAACACGATAATACC**ATGTCAGAGTTCATTTTCAACGATGTACCAC**	N	45 – 75
pTM1-OROVS-R	TTAATTAGGCCTCTC**CTATATGTCAATTCCGAATTGGCGCAAGAAGTCTCTTGC TGC**	N	740 – 699
OROVL_Anti	ACCTCTCCAAAAATCTCATT	L 5' UTR	384 – 365
OROVL_gen	GAACTAGACAATTGTATTCA	L 3' UTR	6494 – 6513
OROVM_Anti	CTAATATCACATGCTGCTCTACATG	M 5' UTR	396 – 372
OROVM_gen	GCACATATCTGTGGGAGAGACAT	M 3' UTR	3959 – 3981
OROSlig1	CTTGCGCCAATTCGGAATTGAC	S UTR	713 – 734
OROSlig2	GGTACATCGTTGAAAATGAAC	S UTR	73 – 53

Viral sequences are shown in bold, §Based on GenBank accession number NC_005777.1.

Table 2. 4. List of primers used for cloning in Chapter 3, section 2.

Oligonucleotide	Sequence (5'-3')	Purpose
pTVT7OROVMRen(–)		
OROVMhRen+	**CAACAAACAGTGACA**ATGGCTTCCAAGGTGTACGAC	Amplify Renilla
OROVMhRen-	**GGGAAAAATCGGTTTA**TTACTGCTCGTTCTTCAGCACG	
OROVdelMORF+	**ATTTGGCTAAAAAGGGTAGG**	Delete M ORF
OROVdelMORF-	**ACAGTGACAAACAACGACC**	
OROVMhRenFlip+	GAAATTAATACGACTCACTATAG**AGTAGTGTGCTACCAACAAC**	Invert Renilla
OROVMhRenFlip-	GGAGATGCCATGCCGACCC**AGTAGTGTACTACCAGCAACAAAC**	
pTVT7OROVLRen(–)		
OROVLhRen+	**CAAACAAAAACAATCTCAAA**ATGGCTTCCAAGGTGTACGAC	Amplify Renilla
OROVLhRen-	**CTACTTTTACATGTGTATACC**TTACTGCTCGTTCTTCAGCACG	
OROVdelLORF+	**GGTATACACATGTAAAAGTAGTGTT**	Delete L ORF
OROVdelLORF-	**TTTGAGATTGTTTTTGTTTGTTTCGG**	
OROVLhRenFlip+	TTAATACGACTCACTATAG**AGTAGTGTGCTCCTATTTAGAAAC**	Invert Renilla
OROVLhRenFlip-	GGAGATGCCATGCCGACCC**AGTAGTGTACTCCTATTCCGAAACAAAC**	
pTVT7OROVSRen(–)		
OROVShRen+	**CATAAAAAGAAATTCCAATA**ATGGCTTCCAAGGTGTACGAC	Amplify Renilla
OROVShRen-	**AGTAGTGTGCTCCA**TTACTGCTCGTTCTTCAGCACG	
OROVdelSORF+	**TGGAGCACACTACTGGGTCG**	Delete S ORF
OROVdelSORF-	**TATTGGAATTTCTTTTTATGTTTTGAATTG**	
OROVShRenFlip+	GAAATTAATACGACTCACTATAG**AGTAGTGTGCTCCATTACTGCTCGTTC**	Invert Renilla
OROVShRenFlip-	GGAGATGCCATGCCGACCC**AGTAGTGTACTCCACAATTCAAAAC**	
M -UTR		
OROMRenF9	GTTTGTTGCTGGTAGCACAC	Quick-change
OROMRenR9	GTGTGCTACCAGCAACAAAC	
OROMRenTCF	GTTTGTTGCCGGTAGTACAC	Quick-change
OROMRenTCR	GTGTACTACCGGCAACAAAC	
L -UTR		
OROVLRenGAF	GTTTCGaAATAGGAGTACAC	Quick-change
OROVLhRenGAR	GTGTACTCCTATTtCGAAAC	
S -UTR		
LShRen-	TTATTTGTTTACTGTACTCCA**TTACTGCTCGTTCTTCAGCACG**	Amplifying Renilla
LOROVdelSORF+	TGGAGTACAGTAAACAAATAA	Deleting S ORF
LShRenFlip+	**GAAATTAATACGACTCACTATAG**AGTAGTGTGCTCCCAATTCAA	Invert Renilla

Oligonucleotide	Sequence (5'-3')	Purpose
Tagging OROV NSs		
ONSsV5F	CTGCTAGGTTTAGACAGCACC**TAATAGTGAGAGA GGCCTAATTAATTAAG**	V5 tag
OVNSsV5R	TGGGTTAGGGATGGGCTTGCC**GGTATCCTGACAG ACGGTGCAGGG**	
ONSseGFPF	GAAAAACACGATAATACC**ATGTACCACAACGG**	eGFP tag
ONSseGFPR	GCCCTTGCTCACCATG**GTATCCTGACAGAC**	

Bold, viral sequences

Table 2. 5. Oligonucleotides used to generate plasmids for M-UTR analysis in Chapter 3, section 3.

Oligonucleotide	3'-5'	Purpose
OROVtoSBV3F	CACTATAG**AGTAGTGTTCTACCAACAC**	8A/A 9A/A (point mutation at the 3' UTR)
OROVtoSBV3R	**GTGTTGGTAGAACACTACT**CTATAGTG	
OROVtoSBV5F	**GTTGCTGGTAGTTCACTACT**GGGTCGGC	8A/A 9A/A (point mutation at the 5' UTR)
OROVtoSBV5R	GCCGACCC**AGTAGTGAACTACCAGCAAC**	
SBVtoOROV3F	CACTATAG**AGTAGTGTGCTACCACATGAAA**	8T/A 9C/A (point mutation at the 3' UTR)
SBVtoOROV3R	**TTTCATGTGGTAGCACACTACT**CTATAGTG	
SBVtoOROV5F	**CATTTTGATTGTGGTAGTACACTACT**GGGTC	8T/A 9C/A (point mutation at the 5' UTR)
SBVtoOROV5R	GACCC**AGTAGTGTACTACCACAATCAAAATG**	
OROV13delRenR	**GTAGCACACTACT**CTATAGTGAG	Using pTVT7OROVMRen(-) excise *Renilla* gene along with OROV M UTR, but maintaining 13 conserved nts
OROV13delRenF	**GTAGTACACTACT**GGGTCGGCATG	
OROV13CF	**CTATAG**AGTAGTGTGCTACTTACTGCTCGTTCTTC	Amplify *Renilla* gene along with the terminal 13 nts of OROV UTR as overhangs
OROV13CR	**CCC**AGTAGTGTACTACATGGCTTCCAAGG	

Bold, viral sequences.

Table 2. 6. Oligonucleotides used to create minigenome plasmids in Chapter 3, section 3.

Oligonucleotide	3'-5'	Purpose
TVT7RSBVLhRen(-)		
SBVLhRenF	**CCCCTAATTACAATCACT**ATGGCTTCCAAGGTGTACGACC CCGA	Amplify Renilla
SBVLhRenR	**GTATTATTTAAGATCAAG**TTACTGCTCGTTCTTCAGCACG CGC	
SBVdelLF	**CTTGATCTTAAATAATACATAATCTTTGCCCC**	Delete SBV L ORF
SBVdelLR	**AGTGATTGTAATTAGGGGTACACTACT**	
SBVLhRenFlipF	TTAATACGACTCACTATAG**AGTAGTGTGCCCCTAATTACA TGAAAC**	Invert Renilla
SBVLhRenFlipR	GGAGATGCCATGCCGACCC**AGTAGTGTACCCCTAATTAC AATCAC**	
pTVT7AKVMhRen(-)		
AKVMUTRRLF	**GAACTACCACAACAAA**ATGGCTTCCAAGGTGTACG	Amplify Renilla
AKVMUTRRLR	**GTCTATTTTAATTTGA**TTACTGCTCGTTCTTCAGC	
AKVdelMR	**TTTGTTGTGGTAGTTCACTAC**	Delete AKV M ORF
AKVdelMF	**TCAAATTAAAATAGACATAATGG**	
AKVMhRenFlipF	TACGACTCACTATAG**AGTAGTGTTCTACCAC**	Invert Renilla
AKVMhRenFlipR	ATGCCATGCCGACCC**AGTAGTGAACTACCAC**	
pTVT7LENMhRen(-)		
Leanyer3UTRR1	**TTATATTCTCATTTTAAATTGGAGTGGAGCACACTACT**C TATAGTGAGTCGTA	3' UTR
Leanyer3UTRF1	**GGATTTGTCTTAACCTCACATTCAATTTATTTGATGTA**T TACTGCTCGTTCTTC	3' UTR
Leanyer3UTRR2	**CCCTTCTCGATGATTCTTTTCCCAGCTACTTATATTCTC ATTTT**	3' UTR
Leanyer3UTRF2	**ATTTGTTCTATCTTTTTGTTTTACATTGACTTAATTGGAT TTGTCTTAACC**	3' UTR
Leanyer3UTRR3P	**CCTGCAATGTTCAACTAACAGATTTATATTTATTATCCC TTCTCGATGATTC**	3' UTR
Leanyer3UTRF3P	**TTTTTGTTTTATTTTTTATTTTTATTTTTATTTATTTTATT TGTTCTATCTTT**	3' UTR
Leanyer5UTRFP	**GTAGTGCACTACT**GGGTCGGCATGGCAT	5' UTR
Leanyer5UTRRP	CACTACAAAGTTAAAATGGCTTCCAAGGTG	5' UTR
pTVT7OYAMhRen(-)		
Oya3hRenF1	**AATAAATTTGAATGTTTGTACGTGGTAGCACA**CTACTCT ATAGTGAGTCG	3' UTR
Oya3hRenR1	**GATTTATTCTCACTTGCTATATACACTGCAC**TTACTGCTC GTTCTTCAGC	3' UTR
Oya3hRenF2P	**GAACCGAAAGGTTCTACACAACTGCTAATTAAATAAATT TGAATG**	3' UTR
Oya3hRenR2P	**TATTTTATTTTATTTTATTCGTCTGTATTTATTAGTTGAT TTATTCTC**	3' UTR
OyaMR5PF	**GTATGTGGTAGTACACTACT**GGGTCGGCATGGCATC	5' UTR
OyaMR5PR	**AACAAACTTTTCAGAGAATTAAA**ATGGCTTCCAAGGTGT AC	5' UTR

pTVT7PEDMhRen(-)		
PR48433UTRR1	**TAACATAATATTGTTGGTAGCACACTACT**CTATAGTGAG TCGTA	3' UTR
PR48433UTRF1	**GATAGCACAGATCTATATTAGTCATTCTATTTATT**TTACT GCTCGTTCTT	3' UTR
PR48433UTRF2P	**AGGACTTAGATAATATAATAAAATACAAATATATAAAAT AACATAATATTGTTGG**	3' UTR
PR48433UTRR2P	**GTGATTCTATAATATAATCAACTTGTTAGGTTTATTGAT AGCACAGATCTA**	3' UTR
PR48435UTRFP	**GTAGTACACTACT**GGGTCGGCATGGCATC	5' UTR
PR48435UTRRP	**CAACAACAAG**ATGGCTTCCAAGGTG	5' UTR

Table 2. 7. Oligonucleotides used in Chapter 3, section 4.

Primer	Sequence (5'-3')	Plasmid
delNSmOROVR	TCCTGCAATTGGTGAGATGAATTC	pTVTOROVdelNSm
delNSmOROVF	GATGAAGATTGCTTATCTAAAGAT	pTVTOROVdelNSm
OROV48NSsF	CAGCATATGTAGCATTTGAAGCTAGATACG	pTVTOROV48delNSs
OROV48NSsR	CGTATCTAGCTTCAAATGCTACATATGCTG	pTVTOROV48delNSs
OROV246NSsF	CGGACAACGGTCTAACCCTGCACCGTCTGT	pTVTOROV246NSs
OROV246NSsR	ACAGACGGTGCAGGGTTAGACCGTTGTCCG	pTVTOROV246NSs
OROVdelNSs2F	GAGTTCATTTTCAACGACGTACCACAACGGACTACATCTACATTTGATCCGGAGGCAGCATACGTAGCATTTGAAGC	pTVTOROVdelNSs2
OROVdelNSs2R	GCTTCAAATGCTACGTATGCTGCCTCCGGATCAAATGTAGATGTAGTCCGTTGTGGTACGTCGTTGAAAATGAACTC	pTVTOROVdelNSs2

2.1.5 Plasmids

Expression plasmids

pTM1, contains a bacteriophage T7 promoter followed by an EMCV internal ribosome entry site (IRES) and a T7 terminator sequence (Moss *et al.*, 1990). This plasmid was also used as a backbone in construction of other expression plasmids.

Table 2. 8. Plasmids based on pTM1 backbone

Plasmid	Purpose	Reference
pTM1-FF-Luc	Firefly luciferase	Weber *et al.* 2001
pTM1OROV-L	OROV L ORF	This study
pTM1OROV-M	OROV M ORF	This study
pTM1OROV-N	OROV N ORF	This study
pTM1OROV-NSs	OROV NSs ORF	This study
pTM1SBV-L	SBV L ORF	Prof Elliott
pTM1SBV-M	SBV M ORF	Prof Elliott
pTM1SBV-N	SBV N ORF	This study
pTM1BUNV-L	BUNV L ORF	Prof Elliott
pTM1BUNV-M	BUNV M ORF	Prof Elliott
pTM1BUN-N	BUNV N ORF	Prof Elliott
pTM1eGFP	eGFP	Prof Elliott
pTM1ONSseGFP	OROV NSs tagged with eGFP	This study
pTM1ONSsV5	OROV NSs tagged with V5	This study

Transcription plasmids

pTVT7R(0,0), is a T7 RNA polymerase transcription plasmid (Johnson *et al.*, 2000). Plasmids used in this study contain one 'G' immediately after the T7 promoter sequence in order to aid efficient transcription. The plasmid also contains the hepatitis δ ribozyme sequence followed by the T7 terminator sequence.

Table 2. 9. Plasmids based on pTVT7 backbone

Plasmid	Purpose	Reference
pTVTOROVL	OROV BeAn19991 L segment	This study
pTVTOROVM	OROV BeAn19991 M segment	This study
pTVTOROVS	OROV BeAn19991 S segment	This study
pTVTOROVdelNSs(48NSs)	OROV mutant S segment, refer to Chapter 3, Section 4	This study

Plasmid	Purpose	Reference
pTVTOROVdelNSs2	OROV mutant S segment, refer to Chapter 3, Section 4	This study
pTVT7-246NSsOROV	OROV mutant S segment, refer to Chapter 3, Section 4	This study
pTVT7-159NSsOROV	OROV mutant S segment, refer to Chapter 4	This study
pTVT7-90NSsOROV	OROV mutant S segment, refer to Chapter 4	This study
pTVT7-78NSsOROV	OROV mutant S segment, refer to Chapter 4	This study
pTVTOROV2080S	OROV mutant S segment, refer to Chapter 3, Section 4	This study
pTVTOROVdelNSm	OROV mutant M segment, refer to Chapter 3, Section 4	This study

Reporter plasmids

Minigenome-expressing plasmids contain the pTVT7R(0,0) backbone. The T7 transcripts produced contain *Renilla* luciferase in negative-sense polarity.

phRL-CMV, is a reporter plasmid expressing *Renilla* luciferase under the control of the cytomegalovirus (CMV) promoter. Provided by Professor Richard M. Elliott.

Table 2. 10. Minigenome plasmids

Plasmid	Purpose	Reference
pTVT7OROVMRen(-)	OROV M-minigenome	This study
pTVT7OROVLRen(-)	OROV L-minigenome	This study
pTVT7OROVSRen(-)	OROV S-minigenome	This study
pTVT72080SRen(-)	OROV isolate BeH759025 S-minigenome	This study
T7OROVMRenminus9	M UTR mutant; 9C:G 15U:A; refer to Chapter 3, Section 2	This study
T7-OROV-MRen(-) 9C/A15C:G	M UTR mutant; refer to Chapter 3, Section 2	This study
T7-OROV-MRen(-) 9C/A15C/A	M UTR mutant; refer to Chapter 3, Section 2	This study
T7-OROV-MRen(-) 9C:G15C:G	M UTR mutant; refer to Chapter 3, Section 2	This study
pTVT7OROV-shortSRen(-)	OROV S-minigenome, with 14 nt 3' UTR	This study
T7-OROV-LRen(-)/18	OROV L-minigenome, mutation at nt 18	This study
TVT7-SBVLRen(-)	SBV L-minigenome	This study
pTVT7AKVMRen(-)	AKV M-minigenome	This study
pTVT7LENMRen(-)	LENV M-minigenome	This study

Plasmid	Purpose	Reference
pTVT7OYAMRen(-)	OYAV M-minigenome	This study
pTVT7PEDMRen(-)	Perdoes virus M-minigenome	This study
TVT7-SBVMRen(-)	SBV M-minigenome	Prof Elliott
pTVT7-BUN-M-Renilla	BUNV M-minigenome	Prof Elliott

2.1.6 Reagents

2.1.6.1 Bacterial Culture

- LB-Agar Miller, Formedium
  40 g in 1 L of distilled water. Autoclaved. Stored at 4 °C.
- LB-Broth Miller, Formedium
  25 g in 1 L of distilled water. Autoclaved. Stored at 4 °C.
- Ampicillin Sodium, Sigma-Aldrich
  Stock solution at 100 mg/ml in distilled water, filter sterilised. Stored at -20 °C.

2.1.6.2 Tissue Culture

- 2X MEM
  20% (v/v) 10X Modified Eagle's media (MEM, Invitrogen), 2% (v/v) L-glutamine, 0.435% (v/v) sodium bicarbonate, 4% NCS, diluted in distilled water.
- 1X MEM
  (Minimum Essential Medium), no glutamine, no phenol Red, Life Technologies.
- DMEM
  Dulbeccos modified Eagle's medium, Life Technologies.
- FBS (Fetal Bovine Serum), Life Technologies.
- GMEM
  Glasgow modified Eagle's medium, Life Technologies.
- G418 sulphate, Invitrogen.
- Leibovitz 15 medium (Life Technologies).
- NCS (Newborn Calf Serum), Life Technologies.
- Opti-MEM (Opti-Minimum Essential Medium), Life Technologies.

- Phosphate buffered saline (PBS)
  137 mM NaCl, 15 mM KCL, 10 mM Na_2HPO_4/KH_2PO_4, pH 7.4.
- TPB (Tryptose Phosphate Broth), Life Technologies
  Trypsin (10X), 2.5%, no Phenol Red, Invitrogen.

2.1.6.3 Fixing and staining solutions

- 8% formaldehyde (v/v) in PBS.
- Crystal violet stain
  20% (v/v) ethanol, 1% (v/v) methanol, 0.1% (w/v) crystal violet, diluted in H_2O.
- Neutral Red, Sigma-Aldrich
  Stock made at 10X in PBS and filtered. Used at 0.6% (w/v).

2.1.6.4 Virus plaque assay overlay

Agarose overlay 0.6% (w/v)

3% (w/v) of Agarose type HSA (Park Scientific Ltd.) in 100 ml of distilled water. Autoclaved and stored at room temperature (RT) until use. Diluted in 1XMEM (no phenol Red) prior to use in plaque assay.

Avicel overlay 0.6% (w/v)

1.2% (w/v) of Avicell (Avicell RC/CL, Microcrystalline cellulose & Sodium carboxymethylcellulose) in 100 ml of distilled water. Autoclaved and stored at room temperature (RT) until use. Prior to use in plaque assay diluted 50:50 with 2X MEM.

2.1.6.5 Transfection reagents

- Lipofectamine 2000, Invitrogen.
- TransIT-LT1 Transfection Reagent, Mirus.

2.1.6.6 DNA analysis

- Agarose, Molecular Grade, BIOLINE.
- Blue/Orange 6X Loading Dye, Promega.
- Ethidium bromide, 10 mg/ml, Biotechnology grade, AMRESCO.
- KOD Hot Start DNA polymerase, 1000u, Novagen, Cat No: 71086-4, Lot No:

D00144074.

- 1Kb DNA ladder, Promega.
- 10X TAE buffer

  0.4 M Tris, 1.142% (v/v) acetic acid, 0.01 M EDTA, diluted in H_2O. Diluted to 1X in H_2O prior to use.
- 10X TBE buffer

  1 M Tris, 0.9 M boric acid, 0.01 M EDTA, diluted in H_2O. Diluted to 1X in H_2O prior to use.

2.1.6.7 RNA analysis

- TRizol Reagent, Invitrogen.

2.1.6.8 Protein analysis

- Acrylamide:bis-acrylamide

  37.5:1 solution, Fisher Scientific.
- Benzonase, Novagen.
- Blotting Pad, 707, VWR International

  Hybond ECL nitrocellulose membrane (GE Healthcare Life Sciences).
- Permeabilisation buffer

  0.1% (v/v) Triton X-100 diluted in PBS.
- PBS 0.1% (v/v) Tween-20.
- Protein Disruption Buffer (PDB)

  0.125 M Tris-HCl (pH 6.8), 4% (w/v) SDS, 25% (v/v) glycerol, 0.02% (w/v) bromophenol blue. Prior to use mix DTT 1M in a ratio of 4:1 (v/v), with 5 µl benzonase (≥ 250 units/µl) per 1 ml PDB.
- Membrane transfer buffer

  20X NuPAGE Transfer Buffer (Novex, Life technologies) diluted in H_2O.
- MES SDS running buffer

  20X NuPAGE MES SDS Running Buffer (Invitrogen, Cat no. NP0002-02), diluted in H_2O.
- NuPAGE 4 – 12% Bis-Tris protein gel, 1.0 mm 10 or 12 or 15 wells, novex, life technologies, LOT 14030571.

- SuperSignal West Pico Chemiluminescent Substrate, Thermo Scientific, Prod ♯ 34080, Lot ♯ OA183286.
- TEMED (Fisher Scientific).
- VECTASHIELD antifade mounting medium with DAPI (Vector Laboratories).
- Western Blot blocking buffer
  5% skimmed milk powder (Marvel Original Dried Skimmed Milk) diluted in PBS 0.1% Tween-20.

2.1.7 Antibodies

Primary antibodies

- Anti-OROV, ascetic fluid from mice infected with OROV. This was a gift from Dr. Eurico Arruda (University of Sao Paulo, Brazil). Used at dilutions 1:500 (Western Blot) and 1:400 (IF).
- OROV anti-N polyclonal rabbit antibody (1:1000; GenScript) was a kind gift from Professor Massimo Palmarini (MRC-University of Glasgow Centre for Virus Research).
- BUNV anti-N-Rb (1:5000; (Shi & Elliott, 2009)).
- anti-MxA (1:500; catalogue no. sc-50509, Santa Cruz Biotech).
- anti-pSTAT1 (1:750; catalogue no. 9167S; Cell signaling).
- anti-STAT1 (1:750; catalogue no. 9172, Cell signaling).
- anti-tubulin monoclonal antibody (1:5000; catalogue no. T5168, Sigma).
- Anti-V5 mouse. This was a gift from Professor Richard E. Randall (University of St. Andrews). Used at dilutions 1:1000 (Western Blot) and 1:400 (IF).

Secondary antibodies

- HRP-coupled secondary anti-rabbit (catalogue no. A0545; Sigma) and anti-mouse (catalogue no. A4416; Sigma) were used at 1:5000.

2.1.8 Enzymes

Restriction enzymes

Bbs1 (New England BioLabs).

Bsg1 (Promega).

BsmB1 (Promega).

Modifying enzymes

Dpn1 (Promega).

In-Fusion® HD Cloning Plus Kit (Clonetech, Takara Bio).

KOD Hot Start DNA Polymerase (Novagen, Merck Millipore International).

Moloney murine leukemia virus (MMLV) reverse transcriptase (Promega).

Poly-A tailing kit (Ambion).

T4 RNA ligase (New England Biolabs).

RNaseOUT^{TM} Recombinant Ribonuclease Inhibitor (Life Technologies).

Shrimp Alkaline Phosphatase (rSAP) (New England BioLabs).

T4 DNA ligase (Roche).

2.2 Methods

2.2.1 Cell culture

2.2.1.1 Cell maintenance

Mammalian cells

Cell monolayers were cultured and maintained in 25, 75 or 225 cm^2 tissue culture flasks. At 90% confluency cell monolayers were washed three times with PBS and then detached in 1X trypsin EDTA (Gibco) at 37°C. Detached cells were re-suspended in appropriate media and cell numbers determined using an automated cell counter (TC20, BioRad). For general maintenance cells were split at a ratio of 1:10 in fresh media. All mammalian cells were incubated at 37°C in 5% CO_2 in a humidified atmosphere.

Insect cells

Mosquito cell lines were cultured and maintained in non-vented 25 or 75 cm^2 tissue culture flasks. At 90% confluency cell monolayers were washed once with PBS and then detached using a cell scraper. Cells were then counted and re-suspended in appropriate media as described above. Insect cells were incubated at 28°C in a non-humidified atmosphere.

2.2.1.2 Transfection of mammalian cells

Transfection

Cells were seeded 24 hour (h) prior to transfection in 6-, 12- or 24-well cell culture dishes. Cells were transfected at 60 – 70 % confluency. For a 6-well vessel (surface area of one well 9 cm^2), calculated amount of DNA was aliquoted into polystyrene tubes with 125 µl of serum-free Opti-MEM (Gibco). In separate tubes 125 µl Opti-MEM was mixed with 3 µl transfection reagent per µg of DNA. After 5 minutes (min) at room temperature (RT), the DNA and Opti-MEM mix was added to the Opti-MEM and transfection reagent mix. This was incubated for 20 min at RT. Cell culture media was then removed from monolayers and the transfection mix added drop-wise. Cells were

then incubated for 2 h at 37°C, before removing the transfection mix and replacing with fresh cell culture media.

The volumes used were scaled up or down depending on the cell culture vessel.

Minigenome assay

1.5×10^5 BSR-T7/5 cells/ml in 24-well plates were transfected with the desired amount of protein-expressing plasmids, 0.5 µg of a minigenome-expressing plasmid and 100 ng pTM1-FF-Luc (Weber et al., 2001) using 5 µl of Lipofectamine 2000 (Invitrogen), as per manufacturers instructions. The amount of DNA in each well was kept constant by addition of empty vector, pTM1. To normalize transfection efficiencies cells were co-transfected with the firefly luciferase expression plasmid pTM1-FF allowing induction levels of *Renilla* luciferase to be calculated. At 24 h post-transfection (p.t), cells were washed with 0.5 ml PBS and then lysed using 100 µl Passive lysis buffer from the Promega Dual-Luciferase Reporter Assay kit (Promega) and the rest of the assay carried out as per manufacturer's recommendations. Readings were measured on a GloMax 20/20 luminometer (Promega).

Virus-like particle production assay

1.5×10^5 BSR-T7/5 cells/ml in 12-well plates were transfected with desired amount of protein-expressing plasmids, 0.5 µg of a minigenome-expressing plasmid and 100 ng pTM1-FF-Luc (Weber et al., 2001) using 5 µl of Lipofectamine 2000 (Invitrogen), as per manufacturers instructions. At 24 h p.t *Renilla* and firefly luciferase activities were measured using Dual-Luciferase Reporter Assay kit (Promega). To generate VLPs, the transfection mix was supplemented with 0.5 µg of glycoprotein-expressing plasmid. At 24 and 48 h p.t supernatants were harvested, clarified by centrifugation (4,000 rpm for 5 min), digested with benzonase (≥ 250 units/µl, Novagen), and then used to infect naive BHK-21 cells or BSR-T7/5 cells that were pre-transfected with protein-expressing plasmids 24 h prior to infection. *Renilla* activity was measured after 24 h using the Promega Dual-Luciferase Reporter Assay kit (Promega).

To neutralise VLPs, samples were incubated with hyperimmune mouse ascetic fluid to

OROV or with anti-BUNV rabbit antiserum for 1 h at RT before infecting cells.

2.2.1.3 Oropouche virus rescue

Recombinant OROV viruses were generated by transfecting BSR-T7/5 cells (1.5×10^5 cells/ml) in 6-well cell culture dishes with 1 µg of pTVTOROVL, pTVTOROVM (or pTVTOROVdelNSm) and pTVTOROVS (or pTVTOROV2080S) using 3 µl transfection reagent TransIT-LT1 (Mirus Bio LLC) per µg of DNA. Replacing the wild-type (wt) S segment (pTVTOROVS) with 1.5 µg of pTVTOROVdelNSs, pTVTORO246NSs, or pTVTOROVdelNSs2, mutant NSs viruses were generated.

7 days p.t. cell culture media was removed and centrifuged at 4,000 rpm for 5 min at 4°C to pellet cell debris. The clarified supernatant was then separated into 1 ml aliquots and stored at -80°C. Rescue outcome and virus titre were determined by plaque assay on BHK-21 cells. These viral stocks were termed passage-0 (p0).

2.2.1.4 Preparation of working viral stocks

All viruses used in this study were grown in Vero E6 cell lines. Cells were infected at MOI 0.001 PFU/cell in PBS 2% (v/v) FBS. Cells were incubated at 37°C for 1 h and then topped up with appropriate cell media and incubated at 37°C/5% CO_2. When cytopathic effect (CPE) was evident the supernatant from the flasks were removed and centrifuged at 4,000 rpm for 5 min at 4°C to pellet any cell debris. The clarified supernatant was then stored in 0.5 ml aliquots at -80°C.

2.2.1.5 Virus titration by plaque assay

BHK-21 cells were seeded at a density of 3.5×10^5 cells/ml in 6 (or 12) well cell culture plates. 12 – 18 hours later cells were infected with 150 µl (12-well plate) or 200 µl (6-well plate) of a 10-fold serial dilution of the virus stock prepared in PBS 2% (v/v) NCS. After 1 h incubation at 37°C the cell monolayer was overlaid with 0.6% Avicell (FMC) in 2X MEM/2% NCS and incubated at 37°C for 72 h. The cell monolayers were then fixed by immersion of the plates in 8% formaldehyde fixing solution. After a period of

4 h (sufficient time to ensure complete inactivation of the pathogen), the plates were removed and rinsed with dH_2O. Plaques were visualised by staining the monolayers with crystal violet staining solution. Plaques were counted and titres estimated as PFU/ml.

PFU/ml = P/D x V

P = Plaque number
D = Dilution factor of the well counted
V = Volume of diluted virus added to the well

2.2.1.6 Plaque purification

A plaque assay similar to the one described above was carried out on BHK-21 cells using only the dilution that produced individual plaques. A 0.6% Agarose overlay diluted in 1XMEM without phenol red was used to overlay the cells and incubated for 96 h at 37°C. 1 ml of 0.06% neutral red diluted in PBS was added onto the overlay and incubated for 1 h at 37°C to stain for plaques. Using a 1000 µl pipette tip plaques were picked through the agarose and rinsed in 0.5 ml DMEM. Confluent Vero E6 monolayers were then infected with this inoculum and incubated at 37°C until CPE was visible. Supernatant was then harvested and clarified by centrifugation for 5 min at 4,000 rpm to remove any cell debris. Samples were stored as 0.5 ml aliquots at -80°C and titrated on BHK-21 cells to determine viral titre.

2.2.1.7 Virus yield assay

Cells were seeded at a density of 2.5×10^5 cells/ml in 12-well cell culture plates. 12 – 18 h later cells were infected with 150 µl virus inoculum calculated at the desired viral MOI and diluted in PBS 2% (v/v) FBS. After an adsorption period of 1 h at 37°C, virus inoculum was removed and cells washed three times with PBS. Cells were then topped up with complete medium and incubated at the 37°C/ 5% CO_2. At 48 h post infection (p.i) supernatant was harvested and cells collected for analysis by western blot. Viral titres were then determined by plaque assay on BHK-21 cells as described above.

2.2.1.8 Virus growth curve

To study viral growth kinetics, cells were seeded in 12-well plates at 2.5×10^5 cells/ml. 12 – 18 h later cells were infected with 150 µl virus inoculum calculated at the desired viral MOI and diluted in PBS 2% (v/v) FBS. After an adsorption period of 1 h at 37°C, virus inoculum was removed and cells washed three times with PBS. At desired time points supernatant was harvested and cells collected for analysis by western blot. Viral titres were determined by plaque assay on BHK-21 cells.

2.2.1.9 Interferon-based assays

Biological IFN production assay

IFN-competent A549 cells were seeded at 3×10^5 cells per ml in a 6-well plate. 12 – 18 h later cell monolayers were infected with an MOI of 1 PFU/cell in PBS 2% (v/v) FBS. After an adsorption period of 1 h at 37°C virus inoculum was removed and cells washed three times in PBS. Cells were then topped up with complete medium and incubated at 37°C for 24 h. Supernatant was clarified by centrifugation and residual virus was inactivated by UV irradiation (8W, 254nm at a distance of 2 cm for 4 min with occasional shaking). A two-fold serial dilution of the UV-inactivated supernatant was added onto fresh IFN-incompetent A549/BVDV-Npro cells grown in 96-well plates for 24 h. The cells were then infected with encephalomyocarditis virus (EMCV; a virus that is sensitive to IFN) at 0.03 PFU/cell in DMEM 2% (v/v) FBS. Cells were incubated at 37°C for 72 h and fixed by immersion of the 96-well plate in 8% formaldehyde fixing solution. After a period of 4 h, the plates were removed and rinsed with dH_2O. Cells were stained with crystal violet staining solution to monitor EMCV-induced CPE. The relative amount of IFN produced was calculated as Relative IFN units (RIU) = 2^N, where N is the dilution affording protection against EMCV infection.

IFN sensitivity assay

IFN-deficient Vero E6 cells were seeded at 1.5×10^5 cells per ml in a 12-well plate. At desired time points either pre- or post- viral infection cell monolayers were treated with universal type-1 IFN-α (0, 10, 100, 1000 or 10,000 IFN units/ml). Cells were infected with virus at a desired MOI in PBS 2% (v/v) FBS. After an adsorption period of 1 h at

37°C virus inoculum was removed and cells washed three times in PBS. Cells were then topped up with complete medium with or without universal IFN-α. Cells were incubated at 37°C for 48 h before harvesting and determining virus yield by plaque assay. Cell extracts were also collected for analysis by western blot.

2.2.2 Protein analysis

2.2.2.1 Sodium Dodecyl Sulfate Poly-Acrylamide Gel Electrophoresis (SDS-PAGE)

NuPAGE Novex 4-12% Bis-Tris polyacrylamide gels (Invitrogen) for SDS-PAGE were placed in BioRad electrophoresis chambers filled with MES SDS running buffer (Invitrogen) and run 180 V for 50 min. When resolving smaller proteins a higher percentage gel (15%) was prepared by first setting the separating gel (0.375 M Tris-HCl, pH 8.8 (Sigma-Aldrich); 40% Acrylamide:bis-acrylamide 37.5:1 solution (Fisher Scientific), 0.1% ammonium persulfate (APS), 0.1% SDS, 0.1% TEMED (Fisher Scientific)), and then the stacking gel (0.125 M Tris-HCl, pH 6.8; 40% Acrylamide:bis-acrylamide 37.5:1 solution (Fisher Scientific), 0.1% APS, 0.1% SDS; 0.1% TEMED).

Cell lysates were denatured for 5 min at 95ºC before being loaded into wells. All gels were run with an appropriate marker.

2.2.2.2 Western blotting

Cell lysates were prepared in lysis buffer (100 mM Tris-HCl [pH 6.8], 4% SDS, 20% glycerol, 200 mM DTT, 0.2% bromophenol blue, and 25 U/ml Benzonase [Novagen]), about 30 μl/cm^2 cell monolayer area. Samples were then boiled at 100 °C for 5 min and centrifuged at top speed for 1 min. Proteins were then separated on a 4-12% gradient NuPAGE Bis-Tris gel (Invitrogen) along with a PageRule pre-stained protein ladder (Fermentas), at 180 V for 50 min in MES SDS running buffer (Invitrogen). Proteins were transferred to a nitrocellulose membrane (Amersham) using membrane transfer buffer. Semi-dry transfers were performed using the Trans-Blot® Turbo™ Transfer System (Bio-Rad) at 10 V for 50 min. Membranes were then blocked for 1 h in 5%

milk/PBS 0.1% (v/v) Tween-20 under constant agitation. Membranes were then incubated in primary antibody overnight at 4°C and secondary antibody for 1 h at 37 °C. Between each incubation step membranes were washed with PBS 0.1% (v/v) Tween-20 for 30 min with 2X 15 min washes. Proteins were then visualized using SuperSignal WestPico chemiluminescent substrate (Pierce) followed by exposure on a Bio-Rad ChemiDoc imager.

2.2.2.3 Immunofluorescence

Cells were seeded at a density of 1.5×10^5 cells per well of a 12-well cell culture vessel containing 30 mm glass coverslips. At 12 – 18 h cells were infected with virus at desired MOI as in 2.2.1.7. At appropriate time points cells were fixed for 30 min in 5% formaldehyde + 2% sucrose in PBS. Cells were then incubated for 10 min in permeabilising buffer (0.5% NP-40 + 10% sucrose in PBS). Cells were then incubated in the dark for 1 h with primary antibody at the required dilution and then washed three times in PBS to get rid of any unbound antibody. Cells were incubated for 1 h again in dark with conjugated secondary antibody and washed again using PBS. The coverslips were then mounted onto slides using VECTASHIELD mounting solution (Vector Laboratories). Slides were stored at - 20°C until use. Antibodies were diluted in PBS 2% (v/v) NCS.

2.2.2.4 Metabolic labelling of mammalian cells

Vero E6 cells were grown in 12-well plates and infected at an MOI of 3 of each virus and at indicated time points supernatant was removed and cells starved in methionine/cysteine-free DMEM at 37 °C for 30 min. Cells were then washed and labeled with 10μCi per well of [35 S]-EasyTag™ EXPRESS mixed in methionine/cysteine-free DMEM for 2 h at 37 °C. Cell were then lysed in 150 μl of lysis buffer (100 mM Tris-HCl [pH 6.8], 4% SDS, 20% glycerol, 200 mM DTT, 0.2% bromophenol blue, and 25 U/ml Benzonase [Novagen]) and proteins separated by SDS-PAGE. Gels were fixed and dried and then labeled proteins were visualized by phosphorimaging (Storm840 Phosphorimager [Molecular Dynamics]).

2.2.2.5 Luciferase assay

Luciferase assays was performed using the Dual-Luciferase® Reporter System (Promega) according to manufacturer's recommendations. Assays were performed in triplicate in 6-, 12- or 24-well culture plates, with two or three repeats. Luciferase readings were measured on a GloMax® 20/20 Single Tube-Luminometer (Promega), using manufacturers recommended protocol, with a 10 second integration period.

2.2.3 Viral RNA Extraction

Total cellular RNA

Total cellular RNA was extracted using TRIzol reagent (Invitrogen) according to manufacturers recommendations. As OROV is a Containment Level 3 pathogen, cells were left in TRIzol for 30 minutes to ensure complete inactivation of the virus before removal from the laboratory. Samples were stored at -80°C until extraction. To extract RNA 0.2 volumes of chloroform was added to the samples and mixed by inverting 5 – 10 times. The samples were centrifuged at >13,000 rpm (>15,000 g) for 10 min before the aqueous phase was removed to a fresh tube containing 500 µl of isopropanol. After mixing, samples were incubated at RT for 15 min before centrifugation at >13,000 rpm for 20 min at 4°C. Supernatant was carefully removed and the pellet washed in 1000 µl of ice-cold ethanol before further centrifugation at >13,000 rpm (>15,000 g) for 10 min at 4°C. Supernatant was removed and the pellet allowed to air-dry before being re-suspended in 50 µl nuclease-free water. The concentration of RNA was determined using a NanoDrop spectrophotometer (Thermo Scientific).

Virion RNA

For virion RNA extraction the QIAamp Viral RNA mini kit (Qiagen) was used, following manufacturers recommendations. RNA was eluted in 50 µl nuclease-free water and the concentration determined using a NanoDrop spectrophotometer (Thermo Scientific).

2.2.4 Nucleic acid manipulation

2.2.4.1 Polymerase Chain Reaction (PCR)

PCR reactions were carried out in 50 µl volumes containing 2.5 µl of each primer (10 µM), 5 µl 10X PCR reaction buffer, 5 µl dNTP mix (2 mM each), 3.5 µl $MgSO_4$ solution (25 mM), I U of KOD Hot Start DNA polymerase (Merck) and 1 µl of template DNA (1-10 ng/µl). Reaction conditions were - initial denaturation of 5 min at 95°C followed by 30 cycles of denaturing at 95°C for 30 seconds, primer annealing at 45 – 60°C for 30 seconds, extension at 70 °C and final extension of 70 °C for 5 min. Samples were then held at 4°C. Primer annealing temperature was determined by primer Tm and extension time was determined by the length of the amplicon, using an amplification speed of KOD polymerase set at 25 seconds per 1 Kb of amplicon size.

Quick-change and excision PCRs

For introducing specific mutations into a plasmid a quick-change (site-directed mutagenesis) PCR was carried out. Here, complementary 30 – 35 nucleotide primers were designed targeting the region where the change was to be made. The specific mutation to be introduced was designed in the centre of the primer sequence.

Excision PCR was used to delete specific nucleotides. Here, 18 – 25 nucleotides long primers flanking each side of the deletion were designed in outward directions.

The PCR cycle number was reduced to 18 cycles. PCR reactions were then treated with 1 U DpnI and incubated for 1 h at 37°C. 1 in 10 dilution of this reaction in nuclease-free water was then used to transform competent JM109 bacteria.

Reverse transcription polymerase chain reaction (RT-PCR)

2 ng/µl RNA with 1.5 µl of RT primer (10 µM/ml) was added to DNase/RNase-free water making up a total reaction of 25 µl. The reaction was then heated to 74°C for 5 min before rapidly cooling on ice for 5 min. To this 200 U Moloney murine leukemia virus (MMLV) reverse transcriptase (Promega), 10 µl 5X buffer, 1 µl 10 mM 4xdNTPs and 40 U (1 µl) of RNaseOUT (Life Technologies) were added and the reaction

incubated at 42°C for 2 h. Samples were then heated to 90°C for 10 min to inactivate the enzyme before being stored at -20°C until use in a PCR reaction. PCRs were performed using 5 µl of the synthesised cDNA in a 50 µl reaction containing 2.5 µl of each primer (10 µM/ml), 5 µl 10X PCR reaction buffer, 5 µl dNTP mix (2 mM each), 3.5 µl $MgSO_4$ solution (25 mM) and I U of KOD Hot Start DNA polymerase (Merck). PCR conditions were followed as described above.

2.2.4.2 Cloning

Restriction digestion

Restriction digests were performed in a reaction volume of 50 µl containing 1 U of restriction enzyme per 1 µg of DNA and 1X final concentration of appropriate enzyme buffer. Nuclease-free water was used to make up final reaction volume. Reactions were incubated at 37 °C for between 1 to 4 h. Digested DNA was then analysed using agarose electrophoresis gels and extracted and purified using a gel extraction kit (Promega).

Ligation

Prior to ligation the vector was linearised either using PCR or restriction digestion methodology. Samples were then dephosphorylated with CIAP (calf intestinal alkaline phosphatase; Promega) by addition of CIAP Reaction buffer and 0.1 U CIAP per µl (final volume). Reactions were incubated at 37 °C for 1 h before being purified using a gel purification kit (Promega). Ligations were performed using T4 DNA ligase (Promega) overnight at RT, using a 1:3 and 1:5 molar ratio of vector to insert. The amount of insert DNA to be added was calculated using the equation below.

$$\left(\frac{\text{ng of vector X size of insert in bp}}{\text{size of vector in bp}}\right) \text{X molar ratio of } \left(\frac{\text{insert}}{\text{vector}}\right) = \text{ng of insert}$$

bp = total number of base pairs.

Infusion reaction

Infusion cloning was used as an alternative to restriction enzyme based cloning. Plasmids were linearised using restriction enzymes or by excision PCR. Excision PCR primers for linearising the plasmid (vector) were designed to incorporate the terminal 15

nt of the insert. Primers for the insert sequence were then designed to include 15 nts of the linearised plasmid boundaries. PCR products thus contain 15 nt complementary sequences at each end. 100 ng of insert, 50 ng of vector and 2 µl 5X InFusion enzyme pre-mix (InFusion HD Cloning Kit; Clonetech Laboratories Inc.) along with nuclease-free water made up to a volume of 10 µl was incubated at 50°C for 15 min. The reaction mix was then placed on ice for 5 min before using the entire 10 µl to transform competent JM109 bacteria. Bacterial cells were plated on LB-agar with appropriate antibiotic, and incubated at 37°C.

Colony PCR

Bacterial colonies were screened for insert using colony PCR. Individual colonies were resuspended in 13.5 µl of DNase free water and heat shocked at 95 °C for 5 min before cooling on ice. PCR was carried out using 4 µl 5X PCR buffer, 0.4 µl dNTP mix (10 mM), 1 µl forward primer (10 mM), 1µl reverse primer (10 mM) and 0.1 µl GoTaq polymerase (Promega). PCR conditions were - initial denaturation at 95°C for 5 min; 30 cycles of denaturation at 95°C for 30 seconds, primer anneal for 30 seconds, extension at 72°C final extension at 72°C for 10 min; followed by cooling and storage at 4°C. Bacterial colonies that were positive for the insert were then used to inoculate 5 ml LB-broth cultures for DNA preparation using Qiagen QIAprep Spin Miniprep kit (Qiagen, Germany). Plasmids were then sequenced via Sanger sequencing (Source BioScience).

Agarose gel electrophoresis

DNA fragments were visualised using agarose gel electrophoresis. Agarose gels were prepared by melting agarose (Bioline) in 1X TBE buffer (89 mM Tris-Borate, 2 mM EDTA, pH 8.3; Sigma-Aldrich) or 1X TAE buffer (40 mM Tris-acetate and 1 mM EDTA, pH 8.3; Sigma-Aldrich) with ethidium bromide (10 mg/ml, Biotechnology grade; AMRESCO). The solution was microwaved in order to melt the agarose and left to cool at RT. The solution was then poured into a horizontal gel chamber with a comb and left at RT until set. DNA samples were prepared by adding an appropriate amount of Gel Loading Dye (in a ratio of 1:6 of dye to sample). A maximum sample volume of 50 µl was then loaded onto the agarose gel. DNA bands were separated at 75 – 100V for at least 30 min in running buffer. DNA fragments were then visualized using a UV transilluminator (Bio-Rad). If required DNA bands were cut using sterile blades and

transferred into eppendorfs and then purified from the gel using Wizard® SV Gel and PCR Clean-Up System (Promega), according to manufacturer's recommendations. If required, DNA bands were sequenced via Sanger sequencing (Source BioScience).

Preparation and maintenance of plasmid stocks

JM109 cells were made chemically competent using the Mix & Go *E. coli* Transformation Kit & Buffer Set (Zymo Research).

All plasmids used in this project contained Ampicillin selection genes and so transformation of these plasmids in competent cells involved only 5 mins on ice. 5 ml LB-broth cultures (starter culture) were inoculated with the transformation mix for 18 h at 37°C with constant agitation. For large-scale plasmid preparation, 150 ml cultures were inoculated with 1.5 ml of the starter culture for another 18 h. Cultures were centrifuged at 4,000 rpm for 30 min at 4°C. Supernatant was discarded and the bacterial pellet re-suspended in re-suspension buffer for either small-scale DNA preparation (Qiagen QIAprep Spin Miniprep Kit; Qiagen; Germany) or large-scale DNA preparation (NucleoBond Xtra midiprep kit; Macherey-Nagel; Germany). Protocols for DNA extraction were according to manufacturers recommendations. DNA concentration was determined on a NanoDrop spectrophotometer (Thermo Scientific). DNA preparations were stored at -20°C.

Cultures containing cDNA plasmids for viral M-segments or the glycoprotein were grown at RT with constant agitation for 36 h.

Generation of bacterial glycerol stocks

500 µl from bacterial cultures containing sequence-validated plasmids were mixed with 500 µl of sterile 50% glycerol. Glycerol stocks generated were stored at -80°C for long-term storage.

The sequences of all plasmids generated in this study have been confirmed by Sanger sequencing (Source BioScience).

2.2.5 Viral genome sequencing

2.2.5.1 Amplification of viral sequences for Sanger sequencing

Virus was first grown in cell culture and both cells and supernatant were harvested, and both total cellular RNA and virion RNA was extracted. cDNAs to each segment were synthesized separately, using segment-specific primers, and random primers (Promega), together with MMLV reverse transcriptase (Promega). Each cDNA preparation was used in a segment-specific PCR using the appropriate primer pairs and KOD Hot Start DNA polymerase (Merck), according to the manufacturer's protocol. The full-length PCR products were cloned into pGEM-T Easy cloning vector (Promega) and nucleotide sequences determined (SourceBioscience) using the T7F and SP6 primers in the first genome walking reaction.

2.2.5.2 RACE analysis

As total infected cell RNA contains both genomic and antigenomic segments, 3' RACE analysis was capable of generating both the 5' and 3' terminal sequences using strand-specific primers. RNA was first polyadenylated (Ambion) for 1 h at 37°C and then purified using an RNeasy Mini kit (Qiagen), as per manufacturer's protocol. The polyadenylated RNA was then used in a reverse transcription reaction with MMLV reverse transcriptase (Promega) and oligo-d(T) primer, followed by PCR using 3' PCR anchor primer (Roche) and the appropriate segment specific primer with KOD Hot Start DNA polymerase (Merck). Amplified products were purified on an agarose gel and their nucleotide sequence determined (Sanger sequencing at SourceBioscience).

2.2.5.3 RNA ligation

Total infected cell RNA was first denatured at 90°C for 3 min and then ligated using T4 RNA ligase (New England Biolabs) for 2 h at 37°C. The reaction was heat inactivated at 65°C and purified using an RNeasy Mini kit (Qiagen). cDNA was synthesized using MMLV reverse transcriptase (Promega) and segment specific oligonucleotide. PCR was then performed with KOD Hot Start DNA polymerase (Merck). The PCR product was purified on an agarose gel and its nucleotide sequence determined.

2.2.5.4 Deep sequencing

Virus was harvested and filtered through a 0.2 µm sterile filter and then concentrated using polyethylene glycol (PEG) 8000. The virus aggregate was resuspended in 500 µl PBS and treated with 25 U/µl of benzonase (Novagen) for 30 min at 37°C. RNA was extracted using TRIzol reagent (Invitrogen) according to manufacturer's protocol and quantified on a Qubit 2.0 Flurometer (Invitrogen). The genomes were obtained using the following basic steps: i) cDNA synthesis using random primers (cDNA synthesis kit, Roche Life Science); ii) library preparation (second strand cDNA synthesis and emulsion PCR); and iii) nucleotide sequencing using both GS FLX 454 (Roche Life Science) and Ion Torrent (Life Technologies) as previously described (Margulies *et al.*, 2005; Rothberg *et al.*, 2011). The SSF (Standard Flowgram Format) files generated by both GS FLX 454 and Ion Torrent machines containing the sequencing trace data were transferred onto a Linux-based computer for analysis. *De novo* DNA sequence assemblers Newbler v.2.6 (GS Assembler, 454 sequencing, Roche) and Celera were used to assemble reads. Adaptors were first trimmed from generated reads and then assembled to generate contigs. These contigs were then compared against sequences in Genbank (NCBI) by performing a BLASTx search. Using the top hit generated by BLASTx as a reference sequence, reads were assembled against it to generate more contigs using GS Reference Mapper Software (Roche). Parameters were left to default. Sequences were evaluated for homopolymers before attempting to fill gaps in the genome by the mapping reference method in CLC Genomics Workbench 6 (CLC bio). Scaffold sequences from a consensus of reads and contigs were generated and evaluated before generating the final genome sequence.

2.2.6 Genetic analysis

2.2.6.1 Phylogenetic analysis

Bunyavirus sequences to be included in the analysis were downloaded from Genbank (NCBI) and compiled to include a single sequence for each strain. The L, M and S segment coding regions were aligned using the MUSCLE algorithm in MEGA6.06 (Tamura *et al.*, 2013). A model test was then performed on this alignment and the best

DNA substitution model was used to generate the phylogenetic trees for the L, glycoprotein and N ORFs using a Maximum Likelihood method in MEGA6.06 (Tamura *et al.*, 2013), with 1000 bootstrap replicates. Final trees were created using FigTreev1.4.2. Each gene segment was aligned according to the protein alignment using Clustal Omega (Sievers *et al.*, 2011) and PAL2NAL (Suyama *et al.*, 2006). Phylogenetic analyses were reconstructed using the GTR+GAMMA+I substitution model as selected by the Bayesian Information Criterion (BIC) in jModeltest (Darriba *et al.*, 2012). Maximum likelihood phylogenies were generated in Phyml (Guindon *et al.*, 2010) using 1000 bootstrap replicates and Bayesian tree reconstruction was carried out using MrBayes (Ronquist & Huelsenbeck, 2003) across 4 chains for 2 million generations sampling every 100 generations, and stationarity was determined from examination of the log likelihoods and the convergence diagnostics. Trees recovered prior to stationarity being reached were discarded and Bayesian posterior probabilities of each bipartition, representing the percentage of times each node was recovered, were calculated from a 50% majority rule consensus of the remaining trees.

2.2.6.2 Reassortant and genetic divergence analysis

To examine reassortment, all genes were concatenated for isolates that had complete genomes and the concatenated alignment was analyzed in RDP3 (Martin *et al.*, 2010) using the various built-in recombination analysis methods. Genetic distances were calculated at the amino acid level using a pairwise p-distance method with complete deletion in MEGA6.06 (Tamura *et al.*, 2013). Pairwise sliding-window analysis at the amino acid level was performed using SimPlot V3.5.1 (Lole *et al.*, 1999). With a 200 bp window, step 20 bp, Kimura (2-parameter) and 1000 bootstrap replications, results were plotted in Prism 6.2.

2.2.7 Data analysis

CLC Genomic Workbench 6 (CLC bio, www.clcbio.com) was used to carry out sequence analysis, primer and plasmid design.

All statistical analysis were performed using GraphPad Prism version 6.2 for Mac OS X (GraphPad software, La Jolla California USA, www.graphpad.com)

Maps in this study were created using QGIS version 2.2.0 (www.qgis.org)

Chapter III

Results

(Sections 1 – 4)

Note:

Sections 1, 2 and 4 are published and describe the sequencing of Oropouche virus (OROV) and the development of a reverse genetics system. Section 1 re-determines OROV phylogeny and reports the identification of a new Simbu serogroup virus M segment.

Section 3 describes an application for OROV minigenome system in reassortment studies with Schmallenberg virus.

Chapter III. Results

Section 1: Genetic analysis of members of the species Oropouche virus and identification of a novel M segment sequence

In 2013 I was awarded the MRC Centenary Award for Early Career Researchers which enabled me to spend four months at the Evandro Chagas Institute (IEC) in Belem, Brazil. In collaboration with Dr. Marcio Roberto Teixeira Nunes at the Center for Technological Innovation, IEC, I cultured and deep sequenced OROV field isolates. The results of that work are discussed in this section.

3.1.1 Introduction and Aims

The first attempt to determine a phylogenetic relationship among OROV isolates was in 2000 by Saeed *et al*. (Saeed *et al.*, 2000). Using the N gene of 28 isolates the authors found that OROV formed three distinct lineages or genotypes. Genotype 1 consisted mainly of isolates from Brazil, whilst genotype 2 consisted of isolates from Peru and genotype 3 from Panama. In 2011 Vasconcelos *et al*. (Vasconcelos *et al.*, 2011) carried out a more extensive genetic analysis using the N gene of 66 isolates covering a 49-year period from 1960 to 2009. Here, the authors found that OROV N gene formed an additional lineage, indicating that there were now 4 genotypes based on the N gene, 3 genotypes based on the Gn gene and 2 genotypes based on the L gene.

Although the molecular epidemiology of OROV has been extensively studied these analysis are solely based on partial genetic information. There are just over a hundred complete N gene sequences for OROV available in GenBank, and even less for the L and M genes. The aim of this study was to therefore use deep sequencing technology to determine the complete genome sequences of OROV field isolates, and additionally identify variations, in the NSs protein, in comparison to our laboratory strain OROV

BeAn19991.

This is the first time deep sequencing and Sanger sequencing have been used together to obtain complete genome sequence for OROV isolates.

3.1.2 A brief look at deep sequencing technology

Deep sequencing is carried out on a set of "Next" generation sequencers, each varying slightly in the underlying technology. The various platforms include 454 [(Roche), 454 LifeSciences/Roche], Illumina (illumina), SOLiD [(Solid) Applied Biosystems/ThermoFisher Scientific] and Ion torrent [(IonTorrent) Life Technologies/ThermoFisher Scientific]. Originally developed to sequence large eukaryotic genomes we now have modified protocols to allow these platforms to also sequence the small genomes of viruses. "Genome" walking has traditionally been used to sequence unknown viral genomes, and consensus primers used to amplify unknown viruses, such as with bunyaviruses (Pringle *et al.*, 1984; Elliott, 1989). However, sequences obtained this way are prone to errors due to mutations generated during genome amplification, cloning and/or Sanger sequencing. To obtain a reference sequence several clones are then usually sequenced and a consensus generated from this (Grada & Weinbrecht, 2013; Marston *et al.*, 2013). This method is time-consuming and now with our increasing appreciation of the extent of genomic diversity within a virus population, deep sequencing is preferable in order to obtain a "true" consensus sequence. Deep sequencing has also gained wide-use in clinical and diagnostic virology (Barzon *et al.*, 2011; Quinones-Mateu *et al.*, 2014), and with the continuous advancement in technology we can now carry sequencers out onto field sites and perform "real-time" sequencing of an on-going outbreak (Carroll *et al.*, 2015).

In order to sequence OROV isolates in this study, we used the Roche 454 FLX+ platform. The system sequences fragments of approximately 600 - 1000 bp long with approximately 1,000,000 reads per run. The 454 platform works by using pyrosequencing technology. It is also known as "sequencing by synthesis" method, whereby chemiluminescent enzymatic reactions allow detection of nucleotide

incorporation. Sequencing reactions are carried out on fibre optic plates. A charged-coupled device (CCD) camera is placed in front of the optic plate to detect light emitted from the reaction. These are then recorded as peaks in an output graph called a pyrogram. Data files are then transferred to computers and nucleotide reads analysed to detect regions of overlap within the sequence. These overlaps allow sequences to be stitched together forming longer sequences, hence removing the need to use a reference sequence. This method of assembly is known as *De novo* sequencing. Another advantage of using next-generation sequencers is the use of random primers instead of "consensus" primers, this is important as will be discussed in detail in section 2 of this chapter. Though deep sequencing is still PCR-based a large number of reads are generated for the entire genome allowing one to visualise the consensus sequence. Genomes can also be "barcoded" with small sequence tags allowing multiple samples to be sequenced in a single run (Center for Genome Innovation; Roche). A flow-chart of the various stages involved in the sequencing protocol for 454 is presented in Figure 3.1.1.

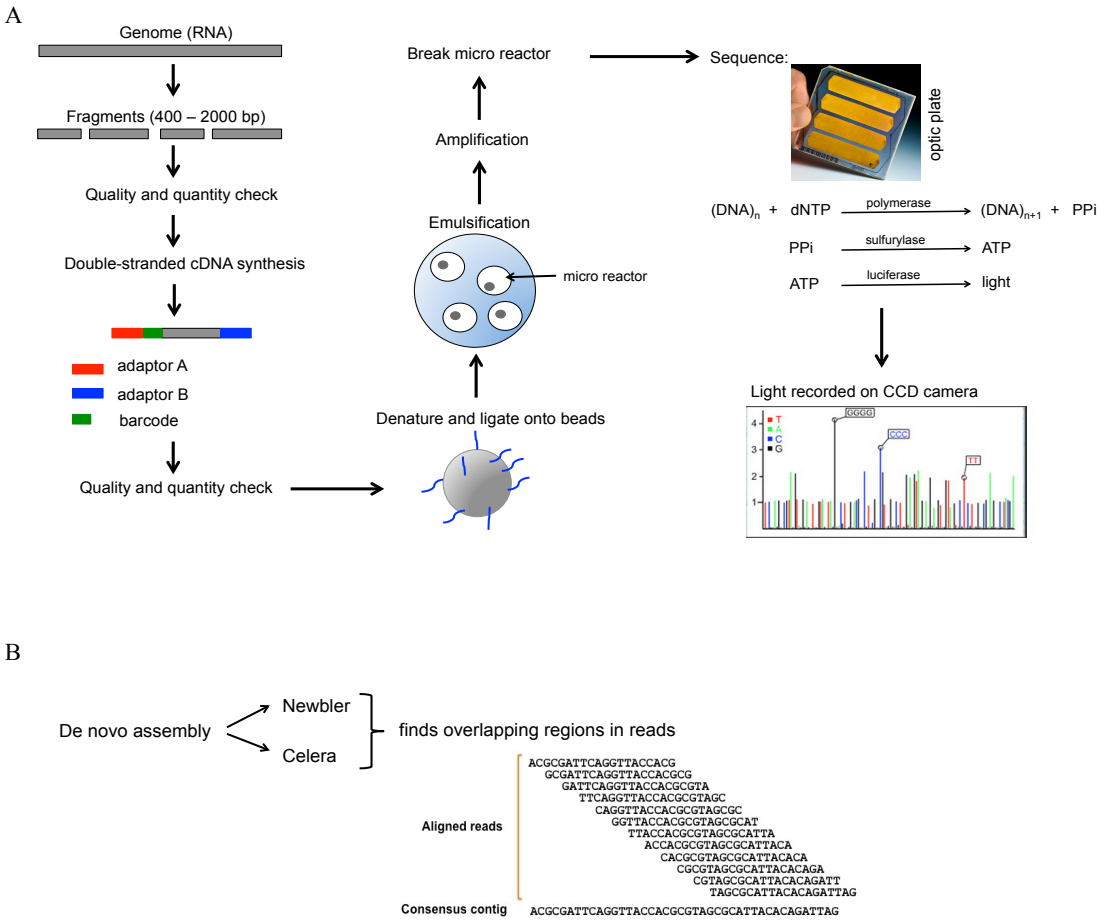

Figure 3.1. 1. Stages involved in 454 sequencing.

(A) Sequencing. OROV RNA was fragmented using $ZnCl_2$. Samples are analysed using a bioanalyzer before proceeding to cDNA synthesis. Adaptors and a barcode are then ligated onto DNA sequences and checked for quality and concentration before ligation onto beads. An emulsion is then created into which the beads are added so that each bead is held in a micro-reactor of its own, allowing a clonal amplification of the sequence. The fibre optic plate is known as a Picotitre plate and contains about 1,600,00 wells of about 44 µM in size. Enzymes (polymerase, sulfurylase and luciferase) are added along with the samples. dNTPs are added in a timed manner. Apyrase is also added to degrade any un-incorporated dNTP. Light signals are proportional to the number of incorporated nucleotides. PPi, pyrophosphate. (B) *De novo* assembly. Softwares Newbler and Celera were used in this study to assemble OROV sequence reads. Newbler is designed by Roche specifically for 454. Reads are aligned, assembled and merged at overlapping regions to form a longer sequence, which is known as a contig. Figures modified from online literature available on Roche's website (Roche).

3.1.3 Sample information

Samples used in this study were obtained from the World Health Organization Reference Centre for Arboviruses at the Department of Arbovirology and Hemorrhagic Fevers, Instituto Evandro Chagas (Belem, Brazil). OROV isolates BeH759021, BeH759022, BeH759024, BeH759025, BeH759040, BeH759146, BeH759529 and BeH759620 represent a small portion of OROV isolates that were obtained from febrile humans between June and August 2009 in the town of Mazagao, Amapa state, Brazil (Table 3.1.1, Figure. 3.1.2). The mean age of the patients was 26.5 years and all had presented a similar clinical picture characterized by fever, headache, arthralgia, myalgia and ocular pain. Viral isolates BeAN790177 and BeAN789726 were isolated from liver samples collected from two separate black-tufted marmosets (*Callithrix penicillata*) found dead in the municipality of Perdoes, Minas Gerais state, in 2012. A suspension of monkey viscera prepared with PBS (pH 7.4) and antibiotics (penicillin and streptomycin) was used to inject suckling mice (*Mus musculus*) via the intracranial route. Animals were observed daily and collected immediately when disease was evident.

OROV clinical isolates BeH759021, BeH759022, BeH759024, BeH759025, BeH759040, BeH759146, BeH759529 and BeH759620 had previously been passaged three times in Vero E6 cells. This stock was used to inoculate cultures for sequencing. Suckling mice inoculated with OROV isolates BeAN790177 and BeAN789726 were previously stored at -80°C. A suspension of these mice brain in PBS (pH 7.4) was used to infect Vero E6 cells. Virus was harvested 72 h p.i. when CPE was evident.

Table 3.1.1 and Figure. 3.1.2 describe the viral isolates used in the study and the geographical locations.

Table 3.1. 1. Information about samples sequenced in this study

NA, not applicable

Sample	ID	Isolation date	Host	Country	State	Town	Age	Gender	Source	GenBank accession nos
BeH759021	AMA 2076	23/07/2009	Human	Brazil	Amapa	Mazagao	18	M	Serum	KP691606–8
BeH759022	AMA 2077	24/07/2009	Human	Brazil	Amapa	Mazagao	39	M	Serum	KP691609–11
BeH759024	AMA 2079	24/07/2009	Human	Brazil	Amapa	Mazagao	24	M	Serum	KP691603–5
BeH759025	AMA 2080	24/07/2009	Human	Brazil	Amapa	Mazagao	23	F	Serum	KP691612–14
BeH759040	AMA 2095	23/07/2009	Human	Brazil	Amapa	Mazagao	48	M	Serum	KP691615–17
BeH759146	AMA 2337	20/08/2009	Human	Brazil	Amapa	Mazagao	31	M	Serum	KP691630–32
BeH759529	AMA 2238	17/06/2009	Human	Brazil	Amapa	Mazagao	13	F	Serum	KP691618–20
BeH759620	AMA 2329	23/06/2009	Human	Brazil	Amapa	Mazagao	16	M	Serum	KP691621–23
BeAn789726	PR 4837	2012	*Callitrhix penicillata*	Brazil	Minas Gerais	Perdoes	NA	NA	Viscera	KP691624–26
BeAn790177	PR 4843	2012	*Callitrhix penicillata*	Brazil	Minas Gerais	Perdoes	NA	NA	Viscera	KP691627–29

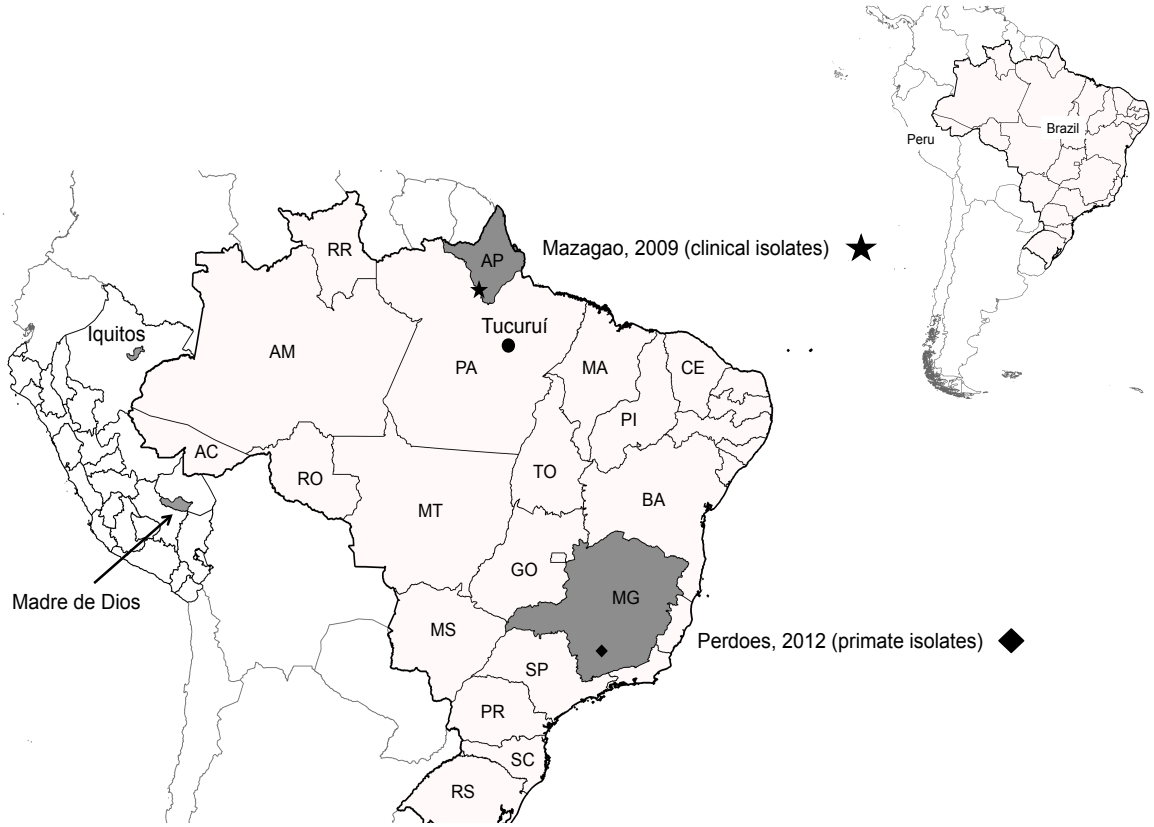

Figure 3.1. 2. Location of samples sequenced in this study.

The map also shows Iquitos and Madre de Dios in Peru where OROV M segment reassortants were isolated, and Tucuruı´, a municipality in Para, Brazil, where JATV was isolated. AC, Acre; AM, Amazonas; AP, Amapa; BA, Bahia; CE, Ceara; GO, Goias; MA, Maranhao; MG, Minas Gerais; MS,Mato Grosso do Sul; MT, Mato Grosso; PA, Para; PI, Piaui; PR, Parana; RO, Rondonia; RR, Roraima; SC, Santa Catarina; SP, Sao Paulo; RS, Rio Grande do Sul; TO, Tocantins. The map was created using QGIS Version 2.2.0.

3.1.4 Complete genome sequences of OROV clinical isolates S segment

For samples BeH759021, BeH759022, BeH759024, BeH759025, BeH759040, BeH759146, BeH759529 and BeH759620 a *De Novo* assembly generated an average S segment contig length of 867 nt. This is 113 nt longer than the published S segment sequence for OROV prototype strain BeAn19991 (GenBank Accession number NC_005777.1). Simultaneously, while attempting to establish a rescue system for OROV BeAn19991 it was found that the published S segment (NC_005777.1) lacked approximately 200 nts at the 3' UTR. Details of this work will be discussed in Section 2 of the results chapter. Using our re-determined BeAn19991 S segment (GenBank accession no. KP052852) as a reference sequence a complete S segment of 947 nt was obtained for clinical isolate BeH759022. This is 11 nt shorter than that of BeAn19991 (KP052852). Due to poor read converge at the 3' UTR it was not possible to complete the sequences for the remaining seven isolates. The 3' UTR of OROV S segment is poly-A rich and sequencing of this region can be problematic. Using a 3' RACE analysis and RNA ligation methods the complete 3' and 5' UTRs for all isolates were sequenced via Sanger sequencing (Source BioScience) with primers OROSlig1 and OROSlig2 (Table 2.2).

The S segment of these isolates lack nt 781–791 compared to the S segment of BeAn19991 (Chapter 3, Section 2). Differences are also observed at positions G750A, A754G, C771T, T820C and T888C, resulting in 92.6% 3' UTR similarity with BeAn19991 (Figure.3.1.3.A). The encoded N gene is 95% similar to BeAn19991, with a 100% conservation of the translated protein sequence. The NSs coding region contains a tandem AUG translational start codon, formed by C/U variation at nt 56. Additionally, position 332 (A to G) results in a Gln to Arg change in the NSs protein at position 89, in comparison to BeAn19991.

M and L segments

Sufficient reads could not be generated to complete the L and M segments of samples BeH759024, BeH759529, BeH759620 and BeH759146. These genomes were therefore cloned into pGEM-T Easy cloning vector and nucleotide sequences were determined using the T7 F and SP6 primers in the first genome walking reaction. Primers used to

complete the remaining pieces of the genome are listed in Table 3.1.2. Terminal UTR sequences were confirmed using 3' RACE analysis (Table 2.2). The clinical isolates displayed a 99% similarity among each other across the complete L and M segments, and all had identical UTR sequences that showed 90 and 96% similarity to the L and M segment UTRs respectively, of BeAn19991. The amino acid sequences of the M and L segment encoded proteins were 98.5 and 98.0% similar to the M and L segment proteins of BeAn19991, respectively.

3.1.5 Complete sequence of a novel Simbu virus M segment

The L and S segments of isolates BeAn789726 and BeAn790177 showed 99 and 100% similarity, respectively, to those of the eight clinical isolates described above. The S segment of both BeAn789726 and BeAn790177 similar to the clinical isolates lacked 11 nt at the 3' UTR in comparison to BeAn19991 (GenBank accession no. KP052852). The 3' and 5' UTRs of both the L and S segments were confirmed by 3' RACE and RNA ligation methods, respectively (Table 2.2).

De Novo assembly of the M segments on the other hand generated a sequence with only 56% identity at the nucleotide level to other OROV M segment sequences (about 48% at the amino acid level). A BLASTx search of the translated protein sequence resulted in a 76.5% similarity to JATV polyprotein (BeAn423380, GenBank accession number: AFI24667). To confirm if this was indeed a new sequence, the genomes were re-sequenced on the Ion Torrent (Life Technologies) platform (Technical assistance for this was provided by Clayton Lima, Janaina M. Vasconcelos and Layanna Oliveria, at the Institue Evandro Chaga, Brazil). The 3' and 5' UTRs were then completed using 3' RACE analysis (Table 2.2). Figure.3.1.3A shows an alignment of the UTRs of this novel sequence. The 11 nt terminal consensus sequence with the conserved C/A mismatch at position 9/-9 is present. Similar to JATV, BeAn790177 and BeAn789726 contain shorter 5' UTRs of about 23 nt in comparison to 31 nt in OROV.

The complete M segment of BeAn790177 and BeAn789726 is 4418 nt in length and encodes a 1417 aa polyprotein. There are two nucleotide differences between the two M

segments. A silent mutation at position 1676 (U in BeAn790177, C in BeAn789726), and a second at position 1856 (G in BeAn790177, U in BeAn789726) that caused an amino acid change in the translated protein sequence of K or N at position 611 in the polyprotein.

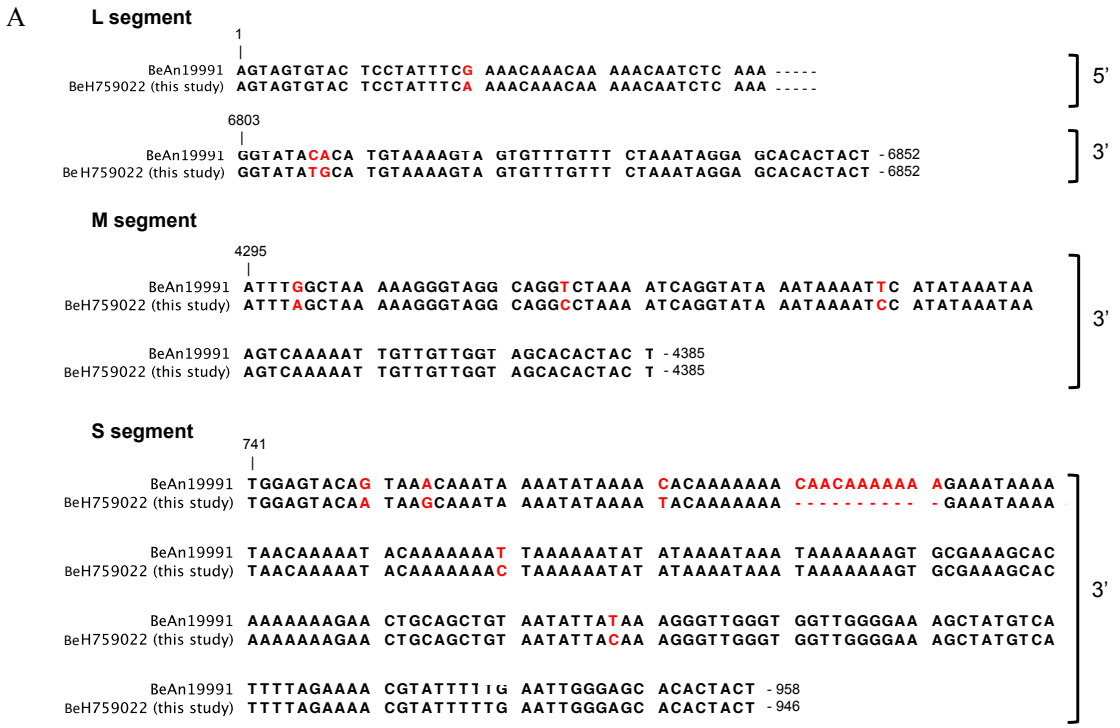

Figure 3.1. 3. Comparison of UTR sequences.

(A) Comparison of the UTRs of BeH759022 isolate (chosen as a representative of the clinical isolates) with OROV strain BeAn19991*. The bases in red highlight differences between BeAn19991 and BeH759022. Sequences are given in the anti-genome sense.

*Sequence information from Chapter 3-Section 2.

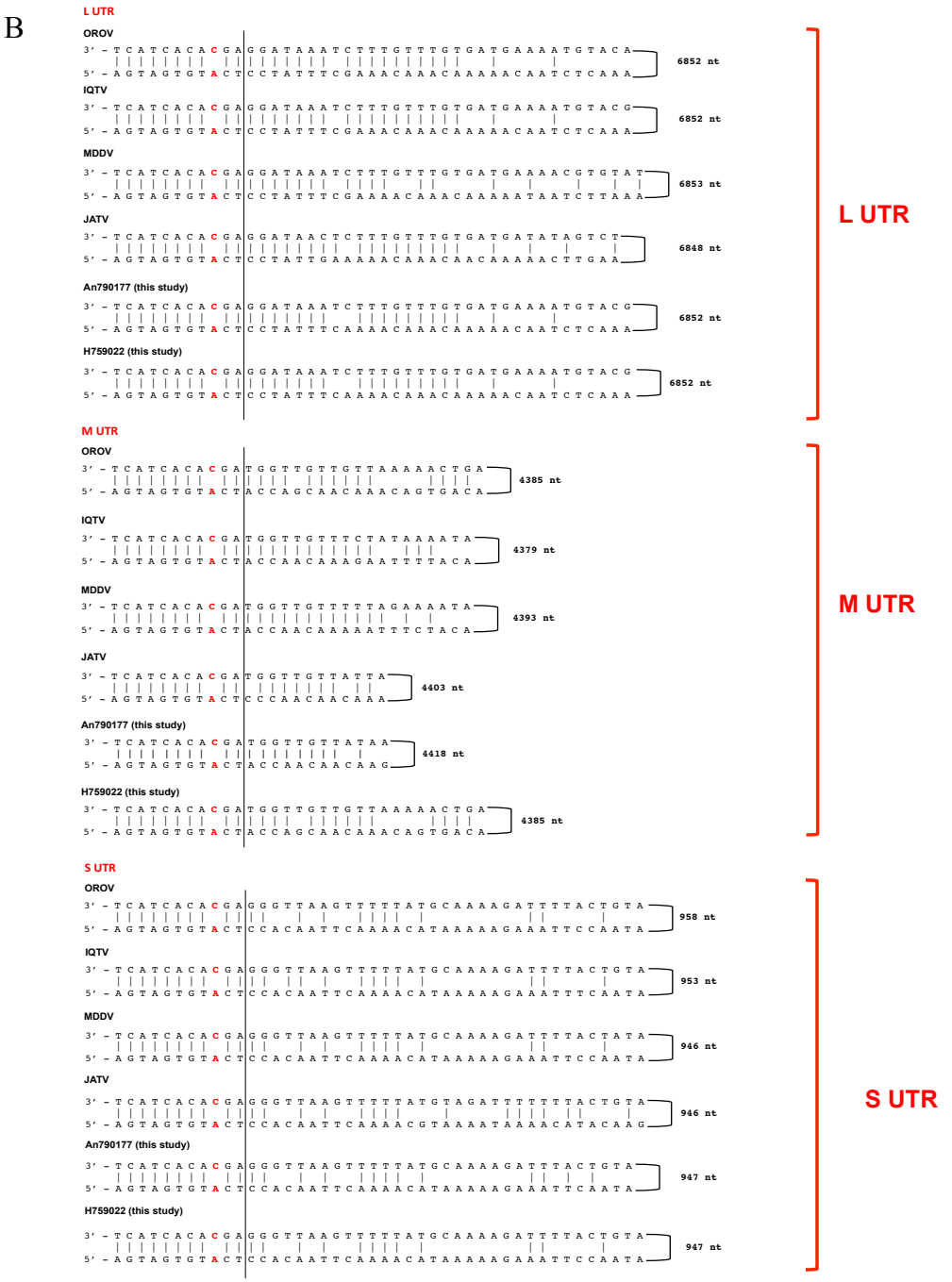

Figure 3.1.3 (B) Comparison of the M segment UTRs of the novel M segment (BeAn790177) with those of OROV, Iquitos virus (IQTV), Madre de Dios virus (MDDV) and JATV. The C/A mismatch is highlighted in red. The line indicates the extent of the conserved terminal sequence. New information on OROV BeAn19991 is presented in Chapter 3-Section 2 of this thesis.

3.1.6 Phylogenetic analysis

The newly sequenced isolates were compared to other Simbu serogroup viruses in order to determine a phylogenetic relationship. Information about the Simbu sequences used in this analysis are provided in Table 3.1.2. First, the complete L, M and S segment coding regions were aligned using the MUSCLE algorithm in MEGA6.06 (Tamura *et al.*, 2013). A model test was then performed on this alignment, and the best DNA substitution model was used to generate the phylogenetic trees for the L, M and S ORFs using a maximum-likelihood method in MEGA6.06 (Tamura *et al.*, 2013), with 1000 bootstrap replicates. The results demonstrate that the L, M and N genes of all eight clinical isolates cluster with that of OROV (Figure 3.1.4. A, B and C). However, with primate-derived isolates BeAn790177 and BeAn789726 only the L and N genes cluster with OROV (Figure 3.1.4. A and C), whilst the M gene displays a closer relationship to JATV (Figure 3.1.4. B).

Pairwise comparisons of the polymerase amino acid sequence for all 10 isolates revealed a pairwise p-distance of 2% towards BeAn19991 and an even closer relationship with Iquitos virus (IQTV) L protein (Figure 3.1.5.A). The glycoprotein precursor of the eight clinical isolates displayed a pairwise p-distance value of 1% towards BeAn19991 (Figure 3.1.5.A). Whilst, BeAn790177 and BeAn789726 had a pairwise p-distance value of 21% with JATV and a much higher value of 48 – 49% with IQTV, OROV and Madre de Dios virus (MDDV) (Figure 3.1.5.A), indicating a closer relationship to JATV. A pairwise sliding-window analysis of BeAn790177, IQTV (strain IQT9924), MDDV (strain FMD1303) and JATV (strain BeAn423380) was then performed to analyse the level of similarity in the M polyprotein in comparison with OROV (strain BeAn19991). The highest level of similarity between OROV and BeAn790177 occurred between amino acid positions 1141 and 1341 (Figure 3.1.5.B).

Table 3.1. 2. Information and accession numbers of all the Simbu serogroup viruses that were used in the phylogenetic analysis

L, large; M, medium; S, small; NA, not available

*, isolate K0098, location Australia; §, isolate CSIRO153, host biting midges (*Culicoides* sps.)

Virus	Strain	Accession number (L, M, S)			Source	Location	Reference
Aino	38K	HE795087	HE795088	HE795089	NA	NA	GenBank
Akabane	OBE-1	-	-	-	Bovine fetus	Japan	Personal communication
Oropouche	BeAn19991	-	-	-	Three-toed slot	Brazil	This PhD
Bunyamwera	-	NC_001925	NC_001926	NC_001927	NA	NA	GenBank
Buttonwillow	BFS 5002	KF697160	KF697161	KF697162	Biting midges (*Culicoides* sps.)	USA	GenBank
Cat Que	VN04-2108	JQ675598	JQ675599	JQ675600	Mosquitoes (*Culex* sps.)	Vietnam	Ladner *et al.* 2014
Douglas	isolate 93-6	HE795090	HE795091	HE795092	NA	NA	GenBank
Facey's Paddock	Aus Ch 16129	KF697138	KF697137	KF697136	Mosquito	Australia	Ladner *et al.* 2014
Ingwavuma	SA An 4165	KF697139	KF697140	KF697141	Spectacled weaver	S. Africa	Ladner *et al.* 2014
Iquitos	IQT9924	KF697142	KF697143	KF697144	Humans	Peru	Ladner *et al.* 2014
Jatobal	BeAn 423380	JQ675603	JQ675602	JQ675601	Ring-tailed coati	Brazil	Ladner *et al.* 2014
Leanyer	AusN16701	HM627178	HM627176	HM627177	Mosquito	Australia	GenBank
Madre de Dios	FMD 1303	KF697147	KF697145	KF697146	Humans	Peru	Ladner *et al.* 2014
Manzanilla	TRVL 3586	KF697150	KF697149	KF697148	Red howler monkeys	Trinidad	Ladner *et al.* 2014
Mermet	AV 782	KF697153	KF697151	KF697152	Purple martin	USA	Ladner *et al.* 2014
Oya	SC0806	JX983194	JX983193	JX983192	Mosquito	China	GenBank
Peaton	CSIRO 110	HE795093	HE795094	HE795095	Biting midges (*Culicoides* sps.)	Australia	GenBank
Sabo	IB AN 9398	HE795096	HE795097	HE795098	Goat	Nigeria	GenBank
Sathuperi	-	HE795102	HE795103	HE795104	NA	NA	GenBank
Shamonda	IB An 5550	HE795105	HE795106	HE795107	Adult cattle	Nigeria	GenBank
Shmallenberg	BH80/11-4	HE649912	HE649913	HE649914	Cow	Germany	Elliott *et al.* 2013

Virus	Strain	Accession number (L, M, S)			Source	Location	Reference
Shuni	Ib An 10107	HE800141	HE800142	HE800143	NA	NA	GenBank
Simbu	SA Ar 53	HE795108	HE795109	HE795110	Mosquito (*Aedes* sps.)	S. Africa	GenBank
Tinaroo	-	incomplete	*AB208700	[§]AB000819	-	-	GenBank
Utinga	Be An 84785	KF697154	KF697155	KF697156	Pale-throated sloth	Brazil	Ladner *et al.* 2014
Utive	Pan An 48878	KF697157	KF697159	KF697158	Brown-throated sloth	Brazil	Ladner *et al.* 2014

(Table 3.1.3. Cont'd)

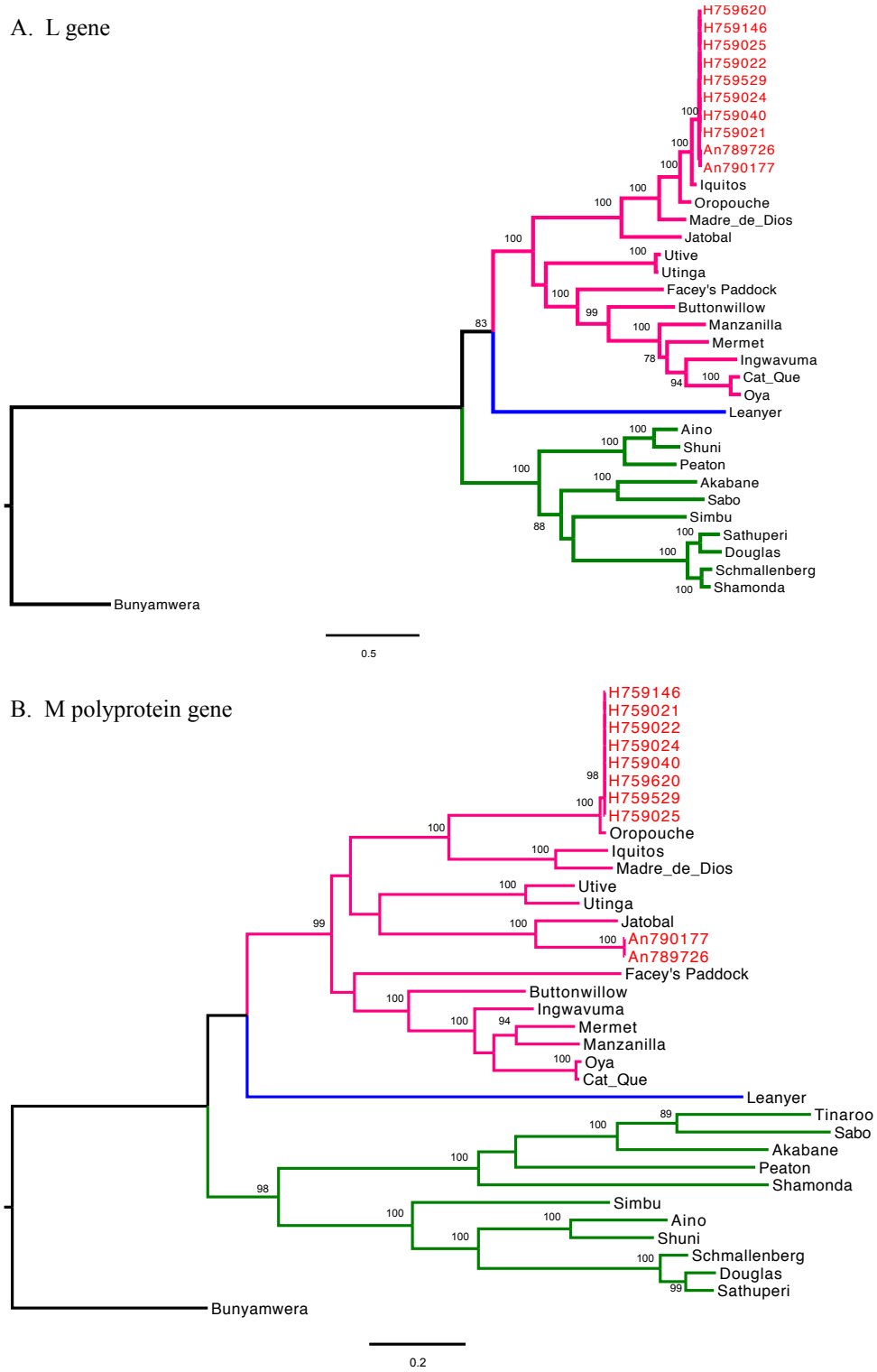

Figure 3.1. 4. Phylogenetic trees of the Simbu serogroup viruses.

(A) and (B). (Explanation on the next page)

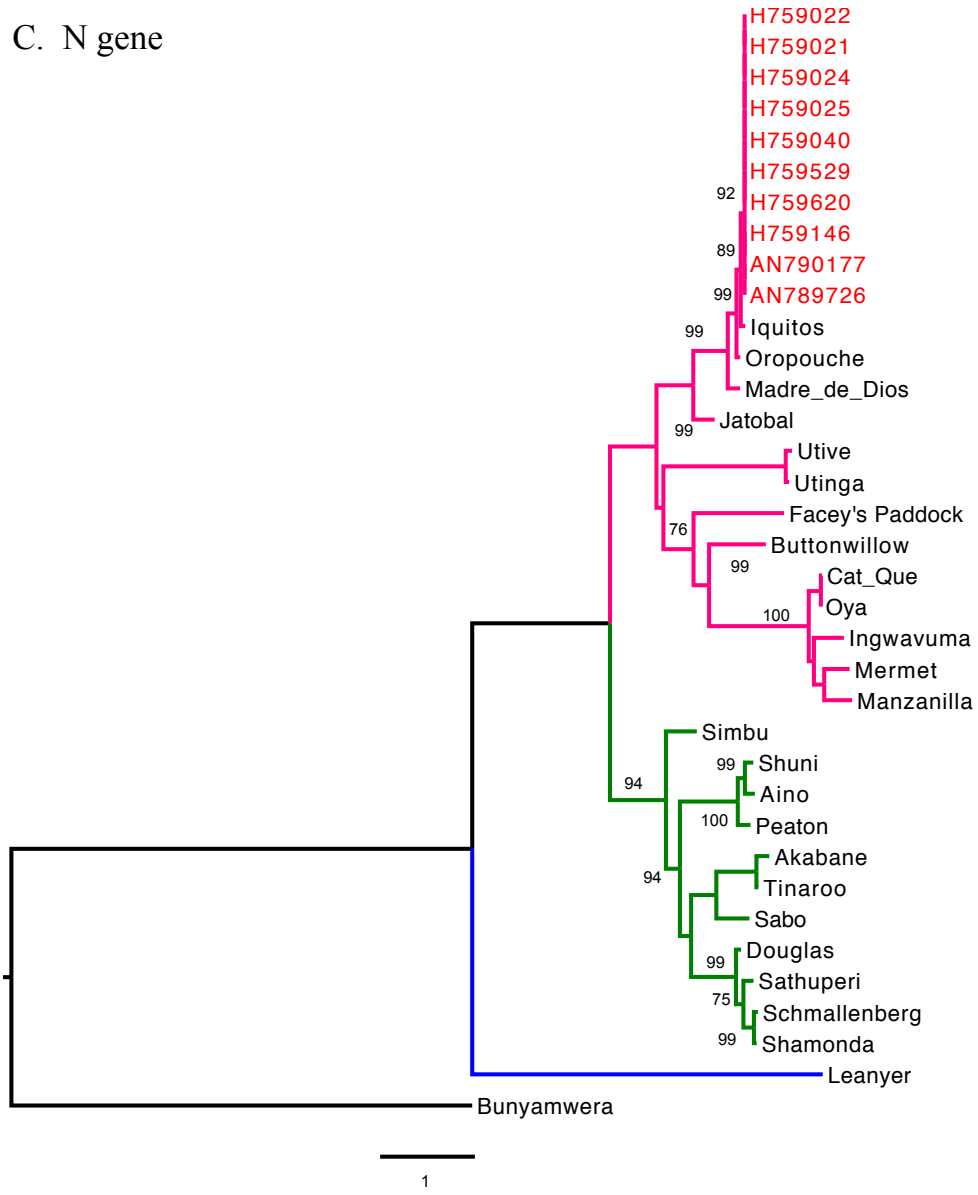

Figure 3.1.4. Phylogenetic trees of the Simbu serogroup viruses. The trees were recreated using a maximum-likelihood method based on the general time reversible model (GTR) with five rate categories and assuming sites are evolutionary invariable, for the L gene (A) the GTR model with discrete gamma distribution for the M polyprotein gene (B) and the Tamura three-parameter model with discrete gamma distribution for the N gene (C) Bars, number of nucleotide substitutions per site. Positions with lower than 95% site coverage were eliminated. Alignment and analysis were conducted in MEGA6 (Tamura *et al.*, 2013) and final trees were created using FigTree v.1.4.2. Samples sequenced in this study are highlighted in red.

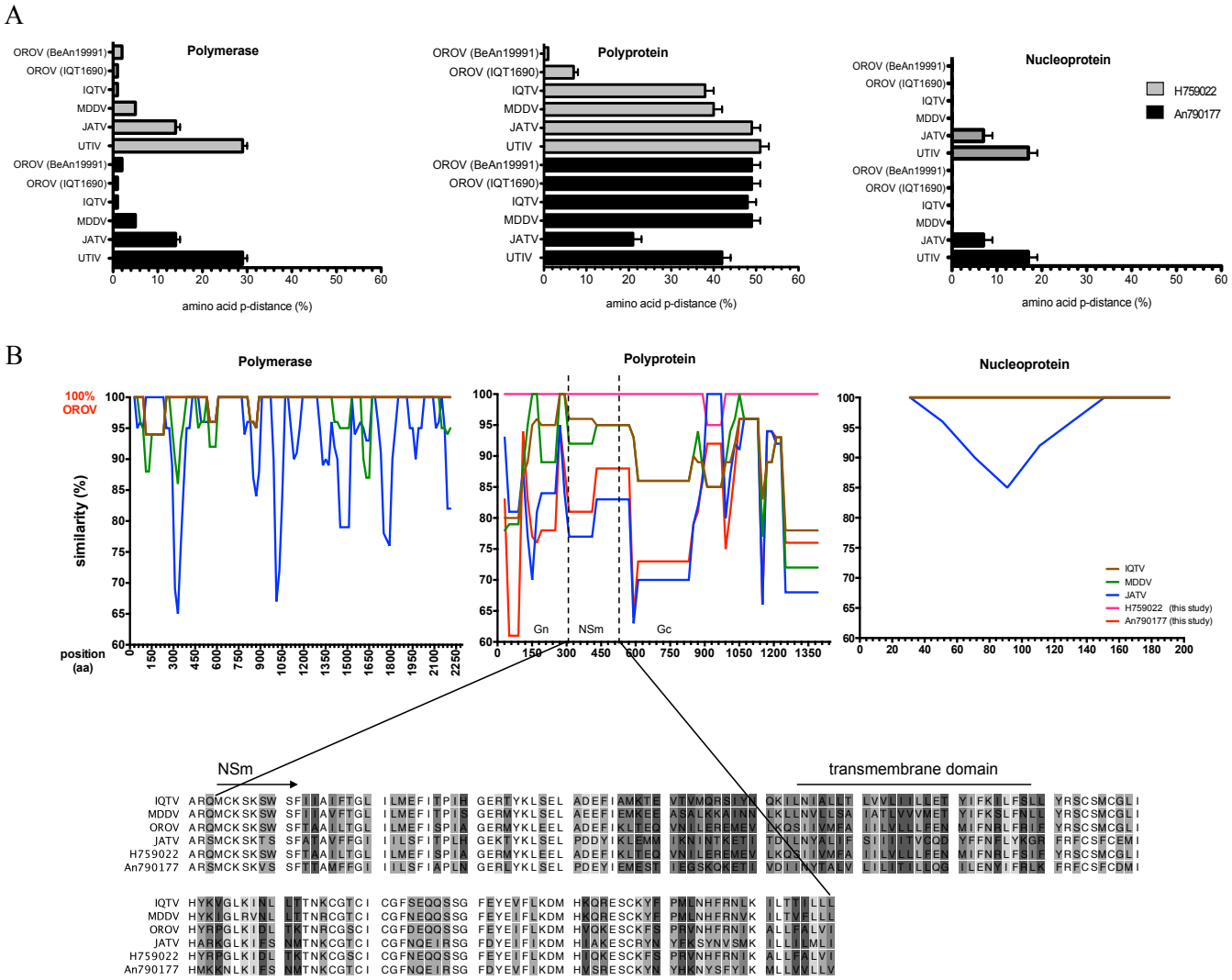
A
Polymerase
Polyprotein
Nucleoprotein
OROV (BeAn19991)
OROV (IQT1690)
IQTV
MDDV
JATV
UTIV
H759022
An790177
amino acid p-distance (%)
B
Polymerase
Polyprotein
Nucleoprotein
100% OROV
similarity (%)
position (aa)
Gn
NSm
Gc
IQTV
MDDV
JATV
H759022 (this study)
An790177 (this study)
NSm
transmembrane domain

Figure 3.1.5

Figure 3.1. 5. Amino acid comparisons among viruses comprising the species Oropouche virus.

(A) Pairwise amino acid p-distance scores of BeH759022 and BeAn790177 with *Oropouche virus* species and Utinga virus (UTIV). (B) Amino acid similarity plots using OROV as a query sequence and IQTV, MDDV, JATV and BeAn790177 as reference sequences. The degree of conservation in the NSm region of the M polyprotein is shown below, with white being 100% conserved.

3.1.7 Genetic relationships among members of the species Oropouche virus

All 10 isolates sequenced in this study were analysed against all available OROV sequences in GenBank (Appendix, Supplementary Table). This work was done in collaboration with Dr. Joseph Hughes (MRC-University of Glasgow Centre for Virus Research).

First, all OROV sequences were downloaded from GenBank and compiled to include a single sequence for each isolate. Only sequences with complete ORFs were included. Each gene segment was aligned according to the protein alignment using CLUSTAL Omega (Sievers *et al.*, 2011) and PAL2NAL (Suyama *et al.*, 2006). Phylogenetic analyses were reconstructed using the general time reversible (GTR)+GAMMA+I substitution model as selected by the Bayesian Information Criterion (BIC) in jModeltest (Darriba *et al.*, 2012). Maximum-likelihood phylogenies were generated in Phyml (Guindon *et al.*, 2010) using 1000 bootstrap replicates and Bayesian tree reconstruction was carried out using MrBayes (Ronquist & Huelsenbeck, 2003). Bootstrapping and Bayesian posterior probabilities are statistical tests that are performed in order to evaluate the reliability of a generated phylogenetic tree from a given dataset (Baldauf, 2003; Erixon *et al.*, 2003). In this study these values have been presented as percentages on tree branches, with 100 demonstrating high support for a produced clade.

Results produced two clearly identifiable clades for the L and M genes of OROV. This is supported by high bootstrap and posterior probabilities (Figure 3.1.6.A and B). The trees were topologically different especially with respect to the M gene of isolates BeAn790177 and BeAn789726, which clustered with high support with JATV (BeAn423380) (Figure 3.1.6. B). Interestingly, the Amapa clinical isolates in the L gene tree clustered with IQTV (IQT9924) and the Peruvian OROV isolate (IQT1690) with high bootstrap support and posterior probability (100 and 1, respectively) (Figure 3.1.6. A). The N gene phylogeny on the other hand was less resolved, with most isolates belonging to a single clade and all being closely related (Figure 3.1.6. C).

Next, in order to analyse reassortment within *Oropouche species* a dataset of concatenated genes for each isolate was created and analyzed with the Recombination Detection Program (RDP). This recognized four reassortment events with breakpoints close to the gene boundaries, and a total of 33 isolates were identified as reassortants. Three of these reassortment events were well supported by the gene phylogenies and formed three different mosaic patterns: (i) IQT1690, BeH759021, BeH759022, BeH759024, BeH759025, BeH759040, BeH759146, BeH759529 and BeH759620; (ii) IQT9924; and (iii) BeAn790177 and BeAn789726. These isolates represented inter-clade reassortants (Figure 3.1.7.). The fourth reassortment event suggested an intra-clade (D) reassortment, for which there was less phylogenetic support.

A. L gene

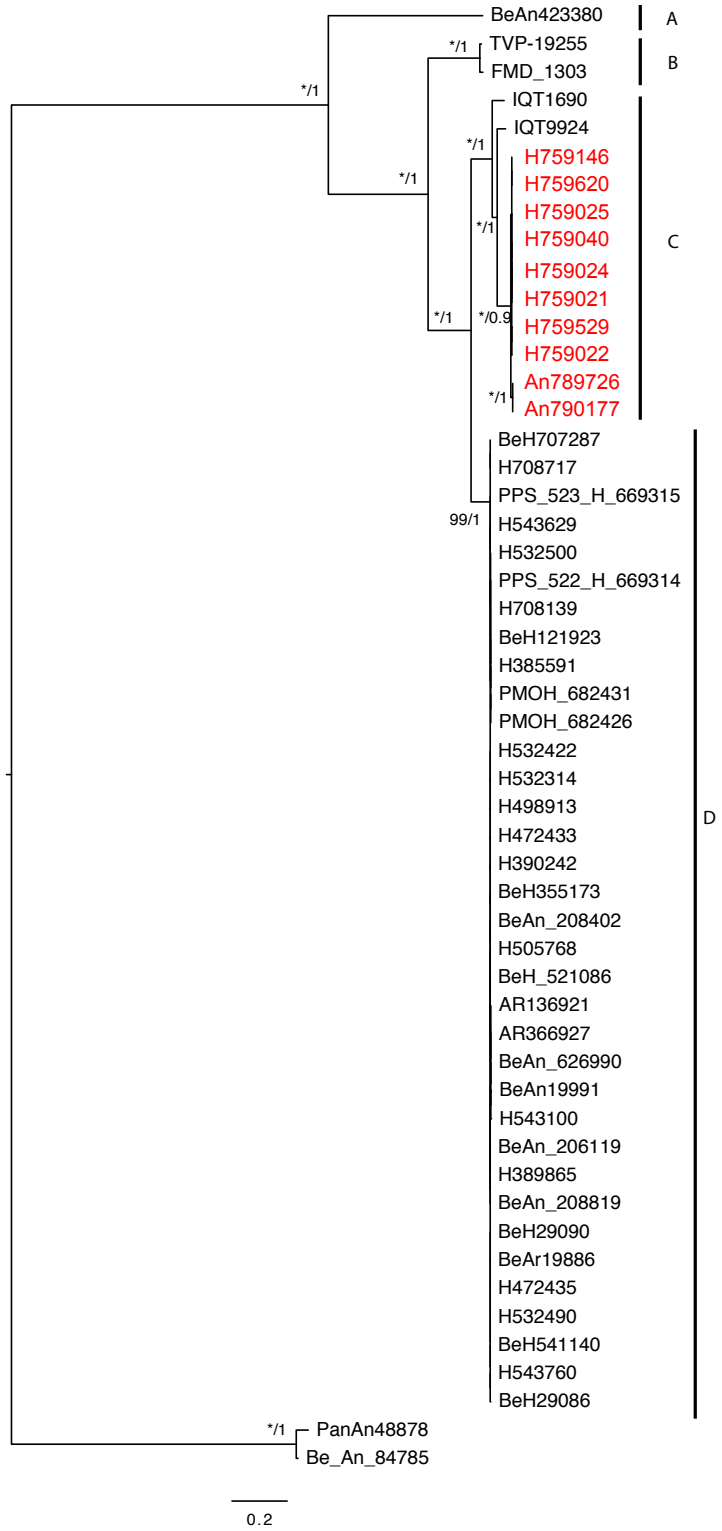

Figure 3.1. 6. Phylogenetic trees of viruses comprising members of the species Oropouche virus.

(A). (Explanation on page 112).

B. M gene

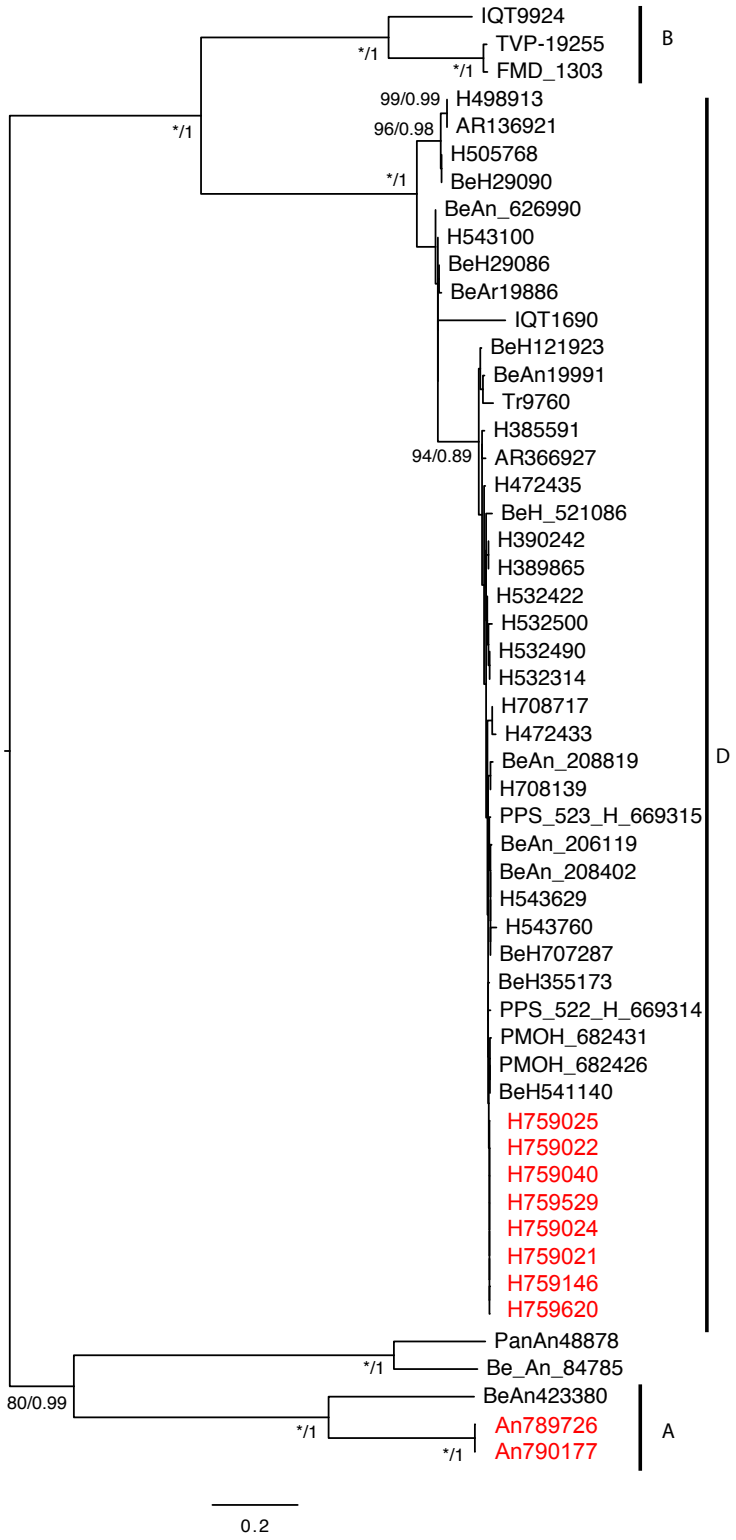

Figure 3.1.6. Phylogenetic trees of viruses comprising members of the species Oropouche virus. (B)
(Explanation on page 112).

C. N gene

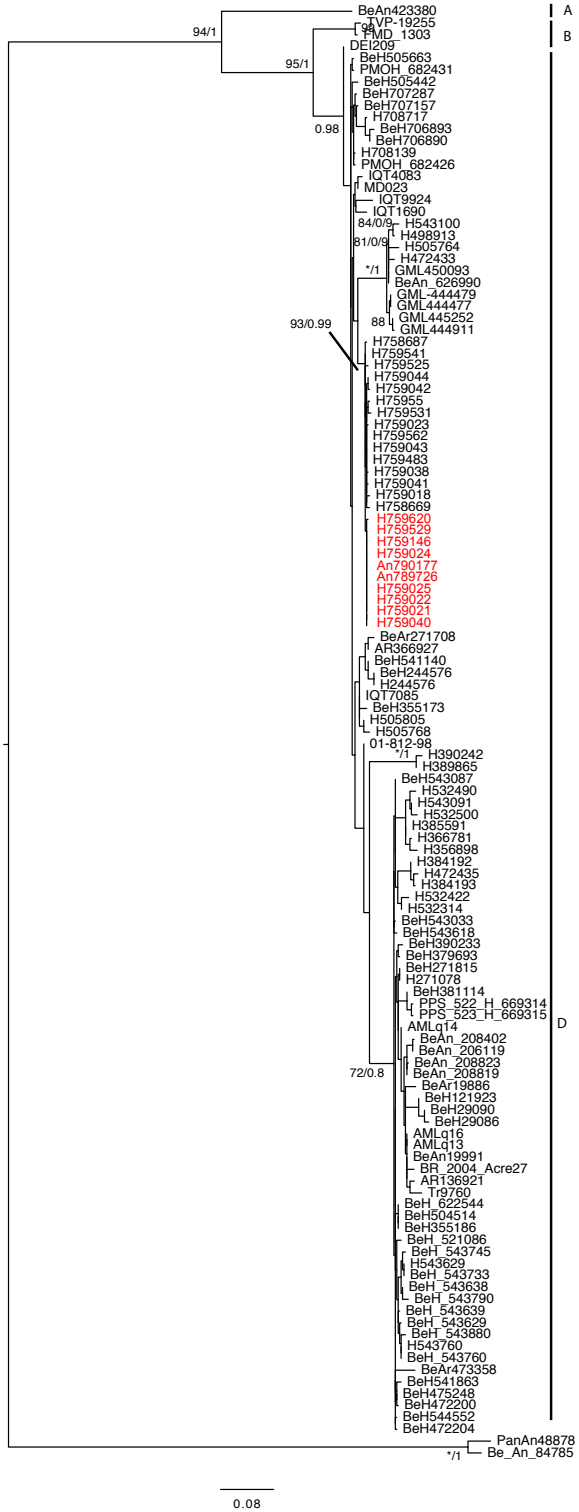

Figure 3.1.6. Phylogenetic trees of viruses comprising members of the species Oropouche virus. (C)
(Explanation on page 112).

Figure 3.1.6. Phylogenetic trees of viruses comprising members of the species Oropouche virus. (A) Maximum-likelihood phylogeny of the L gene with bootstrap support/Bayesian posterior probability shown on the branch. (B) Maximum-likelihood phylogeny of the M polyprotein gene with bootstrap support/Bayesian posterior probability shown on the branch. (C) Maximum-likelihood phylogeny of the N gene with bootstrap supports/Bayesian posterior probability shown on the branch. In (A) (C), * represents 100% bootstrap support. Isolates sequenced in this study are highlighted in red. Full details of the strains used in this analysis are presented in Table S2. Bars, number of nucleotide substitutions per site. Clades A–D are indicated.

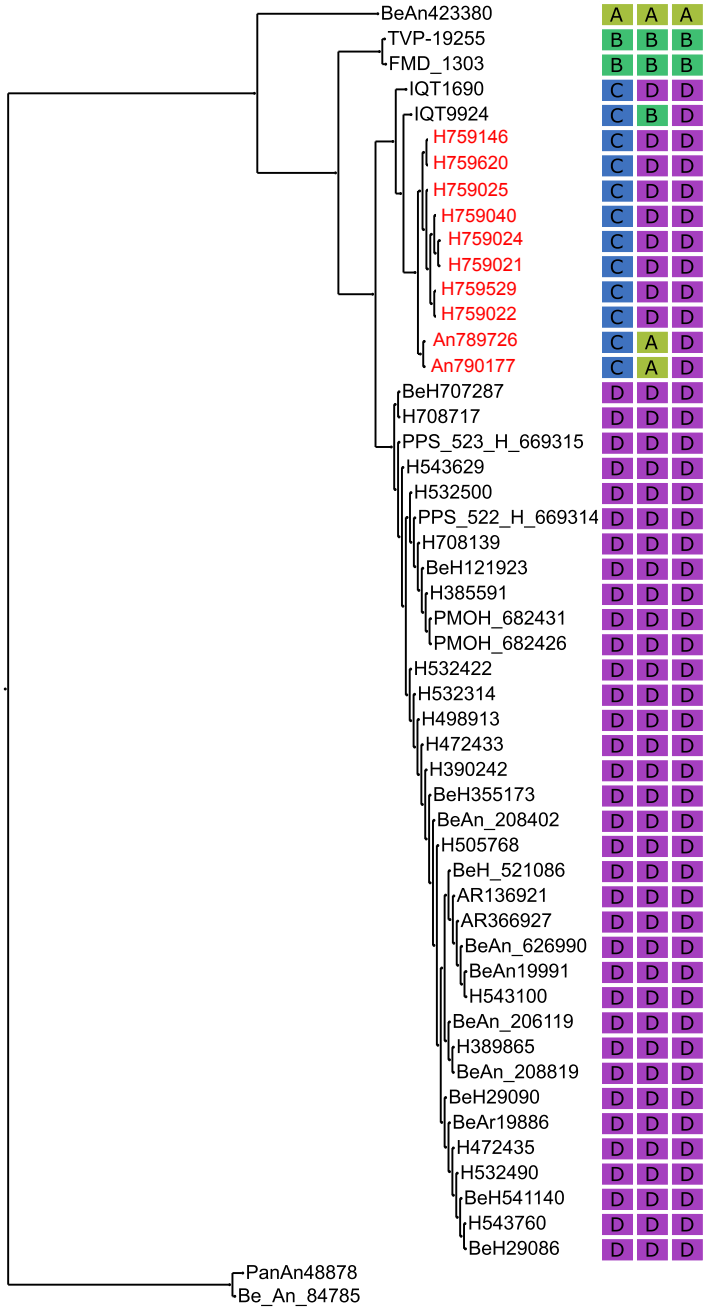

Figure 3.1. 7. Reassortment among viruses comprising the species Oropouche virus.

Maximum-likelihood phylogeny of the L segment with each isolate annotated with their clade assignment (A–D) according to the L-, M- and S segment phylogenies. The different patterns represent the different interclade reassortments: pattern 1, C-D-D; pattern 2, C-B-D; pattern 3, C-A-D; pattern 4, D. Isolates sequenced in this study are highlighted in red.

3.1.8 Discussion

Recent phylogenetic analysis of the OROV N gene had re-classified OROV into four genotypes (Nunes *et al.*, 2005; Azevedo *et al.*, 2007; Vasconcelos *et al.*, 2009; Aguilar *et al.*, 2011; Vasconcelos *et al.*, 2011). However, the bootstrap values for this classification into four distinct genotypes did not give strong support, prompting the current study to re-analyse all available OROV sequences in GenBank, along with the newly sequenced field isolates. This analysis revealed that OROV N gene tree lacks structure and that the recently classified genotypes are in fact not clearly distinguishable. It appears that OROV N gene is much more conserved compared to its L and M genes, where two distinct clades are distinguishable. Based on this finding OROV N gene does not form four genotypes.

In 2011 Vasconcelos *et al*., analyzed the genetic evolution and dispersal of OROV in South America using samples from 1961 to 2009 (Vasconcelos *et al.*, 2011). This is the first study aimed at understanding the molecular epidemiology of OROV in South America, however the authors only used partial genetic information from each segment, and not complete sequences. The S segment 3' UTR for all field isolates sequenced in the present study differs from that of the prototype BeAn19991 quite significantly with the loss of 11 nucleotides between position 781 – 791 in the 3' UTR. Interestingly these isolates are separated temporally and spatially as well as the host from which they were derived (Table 3.1.1 and Figure 3.1.2). For the M segment UTRs, the field isolates differed from BeAn19991 at positions G4299A, T4319C and T4343C, whilst for the L segment the differences were G20A, C6809T and A6810G. These highlight the need to consider complete sequence information as they can reveal important information when trying to understand the evolutionary history of a virus. Current advancement in nucleotide sequencing technology means that full-genome determination is now feasible on a routine basis. The loss of 11 nt in the S segment is intriguing, and the effect of this, if any, on the virus will be discussed in Section 2 and 3.

Another important finding of this study was the identification of a novel Simbu serogroup virus M segment (in samples BeAn790177 and BeAn789726). These samples

were obtained from the primate *Callithrix penicillata* in the Minas Gerais state, south-east Brazil, seven years after OROV was first isolated there (Nunes *et al.*, 2005). Interestingly the OROV isolate (BeAn626990, GenBank accession number AY117135) described by Nunes *et al*. (Nunes *et al.*, 2005) was also isolated from *Callithrix penicillata*. The S segment of BeAn626990 had a 92% pairwise sequence identity compared to the S segments of BeAn790177 and BeAn789726, and they clustered separately in the phylogenetic tree (Figure 3.1.6. C). The L and M sequence information for sample BeAn626990 is currently unavailable, but this virus was identified as OROV based on complement fixation tests that measure antibody responses against the N protein, similar to the way in which the viruses in this study were initially identified as OROV isolates (Personal communication, Dr. Marcio Nunes, IEC). The fact that OROV has been detected in the area twice is of concern, as it would suggest that the virus is stabely circulating in the marmoset population in a region where currently OROV or other Simbu virus outbreaks have not yet been reported. For epidemiological and phylogenetic research purposes, sequencing of all three segments is crucial so that reassortants, such as the one described in this study, are detected.

Genetic reassortment is common among segmented viruses such as bunyaviruses (Briese *et al.*, 2013). IQTV and MDDV, both isolated from febrile patients in Peru in 1999 and 2007, respectively, contain L and S segments highly similar to those of OROV, but with M segments that cluster further away from OROV in a sister clade (Aguilar *et al.*, 2011; Briese *et al.*, 2013; Ladner *et al.*, 2014). The L and S segments of the primate-derived virus in this report revealed a similar level of nucleotide identity to that of OROV and IQTV, whilst the M segment was unique and clustered close to JATV. JATV was originally isolated in 1985 from a ring-tailed coati (Nasua nasua) in Para, Brazil (Figueiredo & Da Rosa, 1988). In 2001, the S and M segments of JATV were sequenced, classifying this virus as a potential OROV reassortant based on the fact that its N and NSs proteins encoded by the S segment were highly similar to OROV isolates from Peru and that its M segment was unique (Saeed *et al.*, 2001). Recent deep sequencing on the same JATV virus stock now suggests that the S, M and L segments of JATV are more divergent from OROV than initially thought (Ladner *et al.*, 2014). Based on our genetic analysis of the BeAn790177 and BeAn789726 M segments and

the significant distance to OROV, IQTV, MDDV and JATV, we propose naming this isolate Perdoes virus, after the municipality in which it was isolated.

In this study, the viruses currently comprising the species Oropouche virus were classified into clades A, B and D. IQTV fell into its own clade C for the L gene; however, it clustered in clades B and D for the M and N genes, respectively (Figure 3.1.7). In a recent analysis of the species Manzanilla and Oropouche virus, Ladner *et al.* (2014) suggested that Manzanilla and Utinga viruses could be thought of as distinct strains of a single virus owing to the level of genetic similarity among current members. The authors suggest that this may not be applicable to the Oropouche virus species due to the level of M segment differences. However, it is possible that these viruses also represent different strains of the same virus, but with a higher degree of M segment divergence. Unlike the L and S segment encoded proteins that function together in RNA synthesis and hence potentially co-evolve together, the M segment codes for the Gc and Gn envelope glycoproteins that are entry binding proteins as well as being major antigenic targets. Selective pressure to produce viable virus in different host species and in different geographical settings could potentially result in higher levels of variation in the M segment. If this were true, we would assume that the non-structural NSm ORF would remain more conserved, and would expect a higher level of variation in the Gn and Gc proteins.

Pairwise, sliding-window distance analysis of OROV (BeAn19991) and the possible reassortants IQTV, MDDV, JATV and Perdoes virus (BeAn790177) indicated an almost equidistant position between IQTV and MDDV, and between the more distant JATV and BeAn790177, with the lowest similarity scores in the N-terminus of Gn protein (positions 1–200, Figure 3.1.5.B). The similarity pattern for the NSm and Gc ORFs was constant, maintaining the distance between IQTV/MDDV and JATV/BeAn790177 almost unchanged until residue 950, where a sudden variation of sequence divergence could suggest possible recombination. From residues 950 to 1200, we observed a higher degree of variation within a single viral genome for each virus, with a higher percentage of divergence when compared with the rest of the protein. However, this was the region with the highest degree of similarity among all four viral

sequences (except OROV), in contrast to what is observed in the rest of the protein, which could suggest that this particular region is subjected to more selective pressure and prone to a higher degree of conservation. It could also suggest that at some point during evolution they all shared the same sequence with a common ancestor, and the distribution to different geographical regions, such as Brazil (Para, Amazonas, Acre, Rondonia, Amapa, Maranhao, Tocantins, Minas Gerais), Peru and Venezuela, to different hosts (humans, *Bradypus trydactulus*, *Callithrix sp*. and wild birds) and to different invertebrate vectors (*Culicoides paraensis, Culex quinquefasciatus, Coquillettidia venezuelensis* and *Ochlerotatus serratus*) allowed a higher degree of variation through natural selection in the whole M segment, but not in this region, nor in the S and L segments (Pinheiro *et al.*, 1982b; Baisley *et al.*, 1998; Nunes *et al.*, 2005; Vasconcelos *et al.*, 2009). This analysis of the amino acid sequences could suggest that these five viruses are all variants of a single species, contrary to the proposal of Ladner *et al.* (2014) based on the nucleotide sequence.

It is interesting that the two viruses closer to OROV (IQTV and MDDV) are human isolates, whilst the ones more distant in this analysis were isolated from animals (JATV and An790177), potentially explaining the different selective pressure and the degree of similarity among these viruses

3.1.9 Summary

1. OROV N gene is highly conserved across all available isolates in GenBank, based on this it is therefore not possible to classify the virus into four genotypes/lineages
2. S segments of recently isolated field isolates sequenced in this study display a loss of 11 nucleotides in the 3' UTR compared to OROV strain BeAn19991 that was isolated in 1960.
3. A novel Simbu serogroup M segment was identified. This virus contains S and L segments similar to OROV. This novel virus has been named Perdoes virus, after its location.

Complete nucleotide sequences for the L, M and S segments of samples BeH759021, BeH759022, BeH759024, BeH759025, BeH759040, BeH759146, BeH759529, BeH759620, BeAN790177 and BeAN789726 were deposited into GenBank. Accession numbers for these sequences are listed in Table 3.1.1.

Chapter III. Results

Section 2: Establishment of a minigenome system for Oropouche virus reveals the S genome segment to be significantly longer than reported previously

3.2.1 Introduction and Aims

Minigenome systems have been established for bunyaviruses BUNV (Weber *et al.*, 2001), LACV (Blakqori *et al.*, 2003), UUKV (Flick *et al.*, 2004), RVFV (Ikegami *et al.*, 2005), SBV (Dong *et al.*, 2013a; Elliott *et al.*, 2013), SFTSV (Brennan *et al.*, 2015) and CCHFV (Devignot *et al.*, 2015). It is a robust tool in virus research, allowing various aspects of the virus life-cycle to be studied without the need to use infectious virus. The minigenome system comprises of a negative-sense genome analogue encoding a reporter gene, which gets packaged into RNP to be transcribed and replicated by co-expressed viral N and L proteins, leading to measurable reporter activity. Further, by expressing the glycoprotein gene, the minigenome can also be packaged into virus-like-particles (VLP), analogous to virus rescue (Shi *et al.*, 2006; Elliott & Schmaljohn, 2013). By generating a minigenome construct for each viral segment, the promoter activity, encapsidation and packaging ability of each segment can be studied and compared. The system therefore also serves as a test for sequence accuracy, before attempting to rescue infectious virus (Dunn *et al.*, 1995; Weber *et al.*, 2001; Blakqori *et al.*, 2003; Flick *et al.*, 2003a; Kohl *et al.*, 2004b; Ikegami *et al.*, 2005; Bergeron *et al.*, 2010). Recent examples illustrating the importance of a minigenome system include work on the evolutionary relationship between the viral polymerase and the UTRs in BUNV (Mazel-Sanchez & Elliott, 2015), and the identification of the endonuclease domain in CCHFV polymerase (Devignot *et al.*, 2015). The aim of this section was to develop such a minigenome system for OROV.

The main step in establishing reverse genetics systems involves obtaining accurate sequence information for the virus in order to generate functional cDNA plasmids. Minigenome constructs can either be under the control of T7-RNA polymerase (T7RNAP) or RNA-polymerase I promoters. Reverse genetics systems for bunyaviruses have typically used the T7RNAP method, which requires the polymerase to be supplied *in trans* (Elliott & Schmaljohn, 2013). The approach chosen for OROV was to develop cDNA clones based on a T7RNAP-driven plasmid system as described for SBV (Elliott *et al.*, 2013), another closely related Simbu virus. BSR-T7/5 cells that have been engineered to constitutively express T7RNAP were used here (Buchholz *et al.*, 1999). The sequences generated in this study are based on OROV strain BeAn19991. This virus was originally isolated from a sloth (*Bradypus tridactylus*) in 1960, in Brazil.

3.2.2 Cloning and sequence determination of the genome of Oropouche virus strain BeAn19991

OROV strain BeAn19991 was cultured in BHK-21 cells at 37°C. Both cells and supernatant were harvested 30 h p.i and RNA extracted using TRIzol reagent (Invitrogen). Extracted RNA was then reverse transcribed using random primers before amplifying each segment using segment-specific primers (Table 3.2.1). Oligonucleotides were designed based on available complete sequences in GenBank [L, accession number NC_005776.1 (Aquino *et al.*, 2003); M, NC_005775.1 (Wang *et al.*, 2001); and S, NC_005777.1; V. H. Aquino and others, unpublished]. PCR products were first cloned into pGEM-T Easy (Promega). After selection of positive clones, the inserts were excised by digestion with BsmBI and ligated into BbsI-linearized T7 RNA polymerase transcription plasmid TVT7R(0,0) (Johnson *et al.*, 2000), Figure 3.2.1. The L segment cDNA was amplified in two fragments using primer pairs OROFLg/OROL1 and OROL2/OROLRg (Table 2.2, Figure 3.2.1). The first primer pair amplified nt 1–3706 and the second pair amplified nt 3537–6852, resulting in two PCR products with a 170 bp overlapping region containing a unique BsgI restriction site (nt 3590 in the full-length segment). The inserts from pGEM-T Easy were then excised by digestion with restriction enzymes BsgI and BsmBI, and the full-length L segment was assembled by

ligating both fragments into TVT7R(0,0). L and M segments were initially cloned by Dr. Gustavo Olszanski Acrani (University of Sao Paulo School of Medicine) and differences in the L ORF determined prior to the start of my Ph.D. OROV cDNAs were cloned such that T7 polymerase would transcribe antigenome sense RNAs. An extra G residue was also included at the 5' end of the cDNA for efficient T7 transcription. These OROV plasmids were designated pTVTOROVL, pTVTOROVM and pTVTOROVS. All sequences presented in this work are in the antigenome sense orientation, i.e. 5'-3'.

L segment

The complete L segment sequence obtained was 6852 nt in length which is 6 nt longer than the published complete L segment sequence for OROV BeAn19991 (GenBank accession number NC_005776.1). Alignment of this sequence with that of GenBank accession number NC_005776.1 revealed a number of differences in the regions from nt 2405 to 2450 and from nt 2592 to 2617, resulting in amino acid changes in the region from aa 798 to 812 and from aa 860 to 867 (Figure. 3.2.2). The sequence of this region was verified by reverse transcription (RT)-PCR amplification of a fragment from nt 2130 to 2980 using specific primers and viral RNA as template. Alignment of this sequence with partial sequences of the L segments of OROV strains TRVL-9760, GML-444479 and IQT-1690 (GenBank accession numbers KC759122.1, KC759128.1 and KC759125.1, respectively) revealed that, apart from a few variations at the nucleotide level, the translated amino acid sequence for this region was conserved (Figure. 3.2.2). Based on this finding it appears that the published sequence for the BeAn19991 L segment contains errors in this region. Additionally, two other amino acid differences were noted, L to F at position 415 and N to D at position 1021. These differences have also been confirmed by re-sequencing. The F residue at position 415 is also found in the L protein of other strains of OROV (TRVL-9760, GML-444479 and IQT-1690).

The terminal sequences of the L segment UTRs were determined by 3' RACE procedure on total infected cell RNA, using oligonucleotides designed to anneal to either the genomic or antigenomic strands (Table 2.2). Position 9 of the 5' UTR was

determined as a A residue and the corresponding – 9 position in the 3' UTR was determined as an C residue, resulting in the characteristic mismatch that has been observed in the predicted panhandle structure of other orthobunyavirus genome segments (Kohl *et al.*, 2004a). This mismatch is not present in the published sequence. Additional to this, position 18 at the 5' end was determined to be a T rather than a C residue, as in the published sequence (Figure 3.2.3.A).

M segment

The complete M segment sequence obtained in this study was 4385 nt in length, in agreement with the published sequence (GenBank accession number NC_005775.1). A small number of nucleotide variations were found, six of which resulted in amino acid differences: I274F, F587L, K614N, D750G, K981Q and G982S. These differences were confirmed in independent cDNA clones of the M segment cDNA and also by specific RT-PCR amplification of appropriate regions of the viral RNA.

RACE analysis was then used to confirm the 3' and 5' UTR sequences (Table 3.2.1). Compared to the published sequence two single nucleotide differences were found in the 5' UTR (A at position 9 and at position 15), Figure 3.2.3.B, and one nucleotide difference was found at the 3' UTR (U at position 15; or T at position 4371 of the cDNA sequence). The predicted panhandle therefore has a C/A mismatch at position 9/–9 and a U/A pairing at position 15/–15 (Figure. 3.2.3).

S segment

Amplification of the S segment surprisingly generated two products of ~750 and 1000 nt (Figure 3.2.1). After cloning, the sequences of both products were determined. The nucleotide sequence of the smaller fragment was identical to GenBank accession number NC_005777 (V. H. Aquino and others, unpublished) that is described as 'Oropouche virus segment S, complete genome', but no strain designation is given. Saeed *et al.* (Saeed *et al.*, 2000) reported the complete sequence of the TRVL-9760 strain of OROV also to be 754 nt, although GenBank accession number AF164531 only gives the coding sequence for this strain. The larger 1000 nt fragment contained an

additional 204 nt after the apparent consensus 3' terminal sequence in the GenBank entry. To confirm these additional sequences an RNA ligation method was carried out. Here, total cell RNA was first ligated and then reverse transcribed using oligonucleotide OROSlig1 (Table 2.2). PCR was then performed using primers OROSlig1 and OROSlig2 (Table 2.2) generating a PCR product of 319 bp (Figure 3.2.4.A). Sequencing this product confirmed that OROV S segment is indeed longer than the published sequence (Figure 3.2.4.B).

To investigate further, the two bands from amplification of the S segment (Figure 3.2.5.A) were gel extracted and used as a template in another PCR reaction. The smaller fragment resulted in a single band, which when sequenced was exactly the same as the published S segment. The larger fragment results in two products again of sizes ~750 and 1000 nt (Figure 3.2.5.B). The same results were obtained when these S segment primers were used to amplify the S segment from one of the clinical isolates described in Chapter 3, Section 1 (BeH759025 AMA2080). Sequence inspection of the longer S segment revealed that the primer used to amplify OROV S segment could potentially anneal at nt 735 – 752. Binding of the primer to this "internal binding site" would result in a cDNA product with a 3' termini matching that of the orthobunyavirus consensus sequence making it appear complete (Figure 3.2.5.C and D).

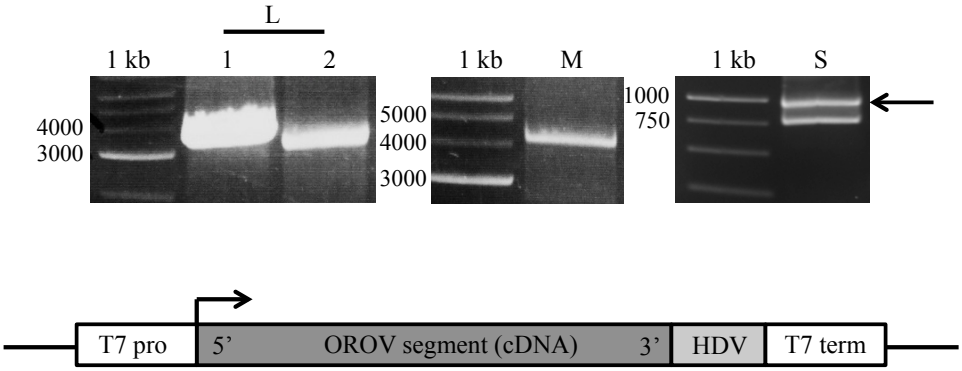

Figure 3.2. 1. Cloning OROV BeAn19991.

RT-PCR products derived from the L, M and S segments of OROV BeAn19991. Amplified products were separated on a 1% agarose gel along with a 1 kb marker (Promega). Products were cloned into a plasmid containing a T7 RNA polymerase promoter and a hepatitis delta ribozyme (TVT7R(0,0)) as shown in the schematic below.

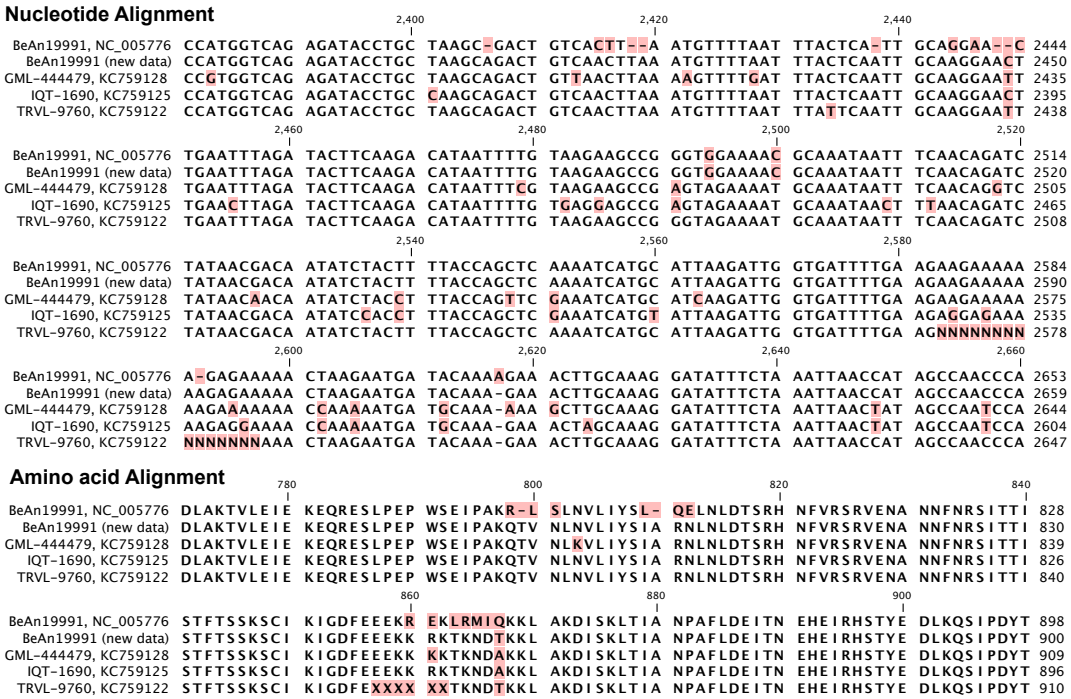

Figure 3.2. 2. Alignment of newly sequenced OROV L segment with published sequences.

Alignment of part of the OROV L segment highlighting the differences between the published sequence for the BeAn19991 strain (GenBank accession number NC_005776) and the sequence obtained in this study (new data), along with three published OROV sequences from different genotypes GML-444479, IQT-1690 and TRVL-9760 (GenBank accession numbers KC759128.1, KC759125.1 and KC759122.1, respectively). The nucleotide alignment is shown in the top panel and the amino acid alignment is shown in the bottom panel. The highlights show differences in the sequences. Alignments were performed using CLC Genomics Workbench 6.5.

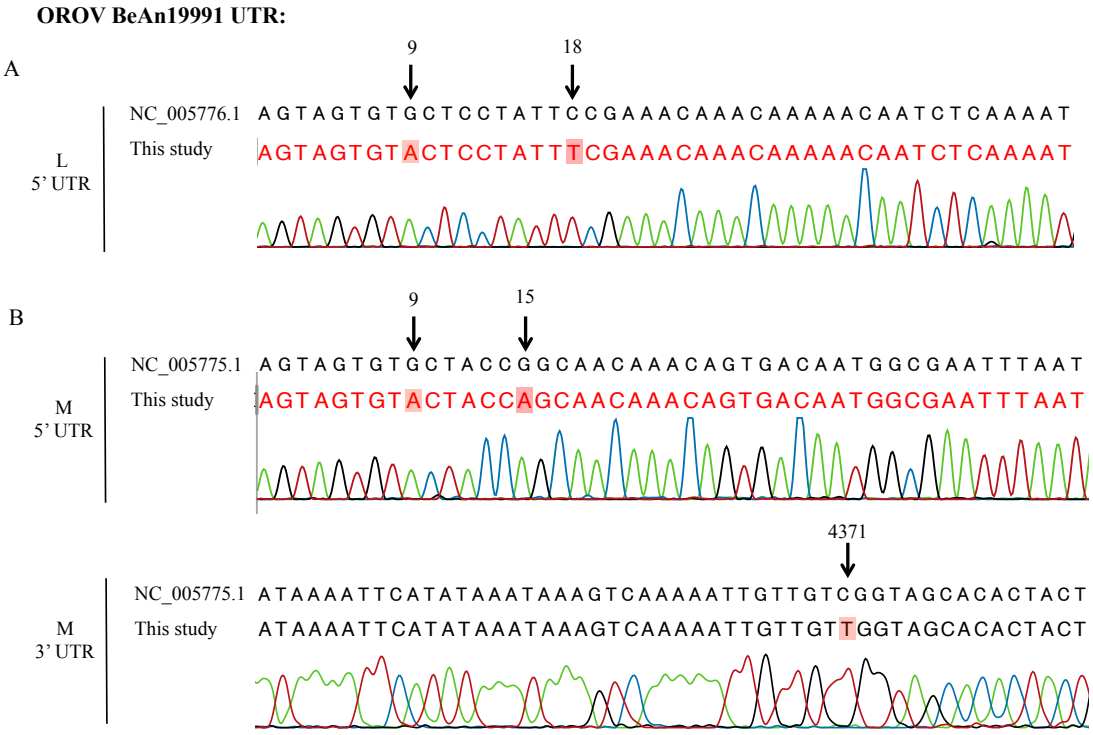

Figure 3.2. 3. Sequencing results of OROV L and M segment UTRs.

Chromatograph from RACE analysis shows the differences between 5' UTR sequences of L and M, and the 3' UTR of M, obtained in this study compared to the published sequences (L, NC_005776.1 and M, NC_005775.1). The numbers above the arrows denotes the nucleotide position, for L (A) and M (B). A, Green; T, Red; G, Black; C, Blue.

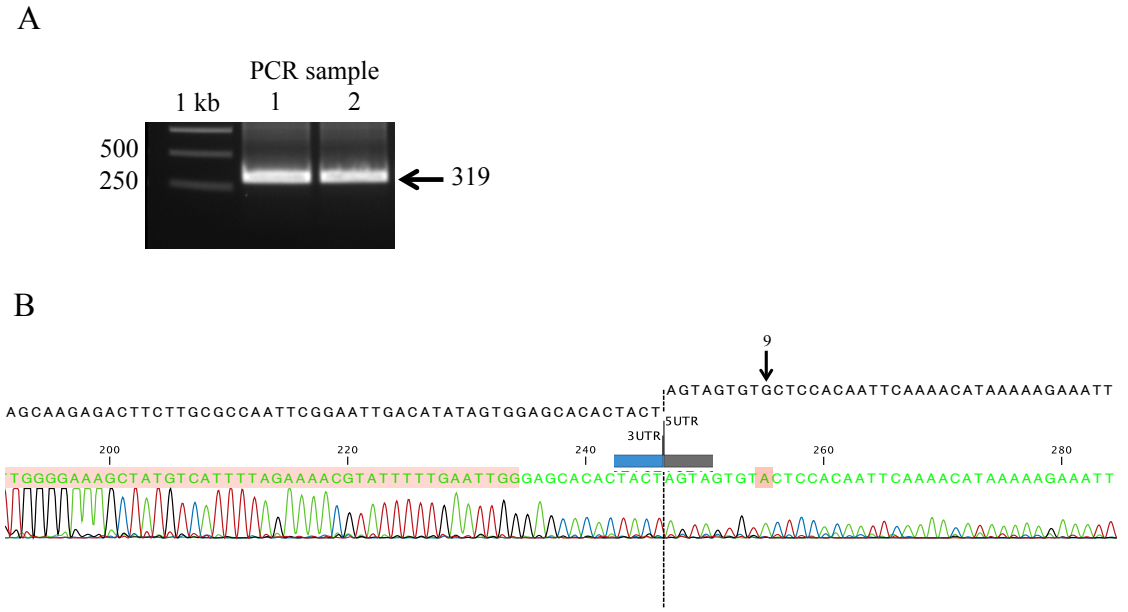

Figure 3.2. 4. Sequencing results of OROV S segment UTRs.

(A) Agarose gel electrophoresis of RNA-ligation products for the S segment. 1 and 2 are duplicate samples. (B) Chromatograph from sequencing (A). Only the terminal ends of the UTRs are shown. The dotted line highlights where the 3' and 5' ends are ligated. Nucleotides highlighted in red show differences between the sequences generated in this study to the publish sequence on top (in black). Arrow shows the 9th position is A, as seen with the L and M segment 5' UTRs (Figure 3.2.3). A, Green; T, Red; G, Black; C, Blue.

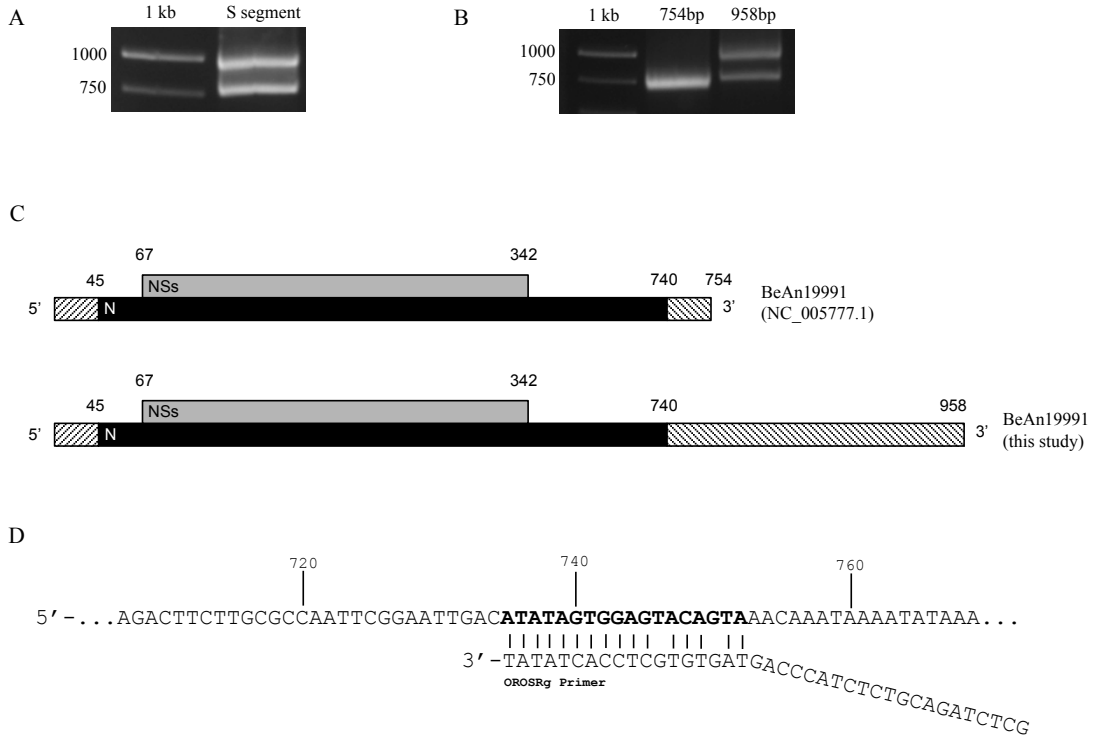

Figure 3.2. 5. Analysis of the OROV S segment.

(A) Agarose gel electrophoresis of OROV S segment (B) Reamplified DNA products using the 754 and 958 nt PCR products (A) as template. (C) Schematic drawing of the OROV S segment, comparing the published sequence of 754 nt (upper drawing) with the newly determined 958 nt sequence (lower drawing). Black boxes, N ORF; grey boxes, NSs ORF; hatched boxes, UTRs. The sequence is presented in the antigenomic 5' to 3' sense. Numbers indicate nucleotide positions in the sequence. (D) Diagram showing the potential internal binding site (bold) in the OROV S segment. Numbers represent nucleotide positions. OROSRg primer represents the primer sequence that was used in this paper to amplify the S segment.

3.2.3 Establishment of an OROV minigenome system

Using plasmids pTVTOROVL, pTVTOROVM and pTVTOROVS the ORFs of each segment were amplified and sub-cloned into pTM1 expression vector (Moss *et al.*, 1990) (Table 3.2.1), under the control of T7 promoter and EMCV internal ribosome entry site sequence (IRES). The constructs were designated pTM1OROV-L and pTM1OROV-M. To generate a plasmid expressing only the N protein, three point mutations (T68C, T113C and G116A) were introduced into pTVTOROVS using primers OROdelNSsF and OROdelNSsR (Table 3.2.1), by site-directed mutagenesis, prior to PCR amplification of the N ORF. These mutations changed the first and second methionine codons in the NSs ORF into threonine codons, and introduced an in-frame translation stop codon at codon 17 (Figure 3.2.6). The coding sequence of the overlapping N ORF was unaffected. This plasmid was designated pTM1OROV-N. A plasmid expressing only NSs was also generated and this was designated pTM1OROV-NSs (Table 3.2.1). pTM1OROV-L and pTM1OROV-NSs cloning was carried out by Dr. Daisy da Silva (Institute Evandro Chagas, Brazil).

Minigenome constructs were created for all three viral segments. This was done by first replacing the viral ORF in each cDNA plasmid (pTVTOROVL, pTVTOROVM and pTVTOROVS) with the sequence for *Renilla* luciferase. The region containing *Renilla* luciferase flanked by the viral UTRs was then amplified and inverted into plasmid TVT7R(0,0) (Johnson *et al.*, 2000) so that T7 transcripts would be in the genomic sense (Weber *et al.*, 2001). A schematic of the cloning strategy used is in Figure 3.2.7. The primers used are listed in Table 2.4. These constructs were designated pTVT7OROVMRen(–), pTVT7OROVLRen(–) and pTVT7OROVSRen(-).

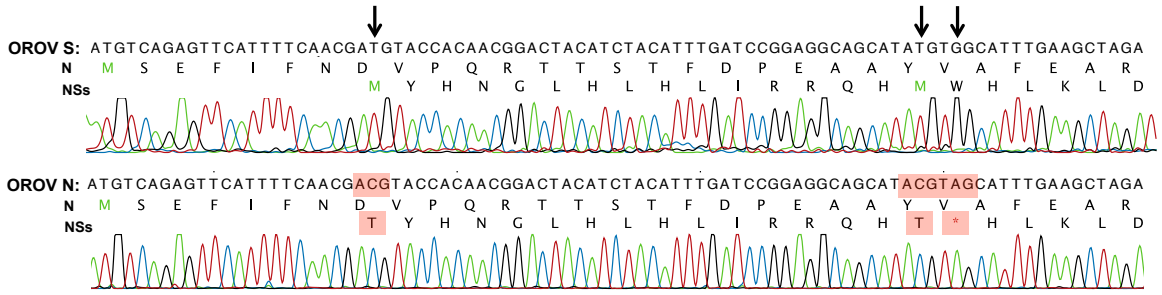

Figure 3.2. 6. pTM1OROV-N.

Chromatograph from Sanger-sequencing demonstrating where mutations were made in the S segment in order to generate a plasmid that would express only the N protein. A, Green; T, Red; G, Black; C, Blue.

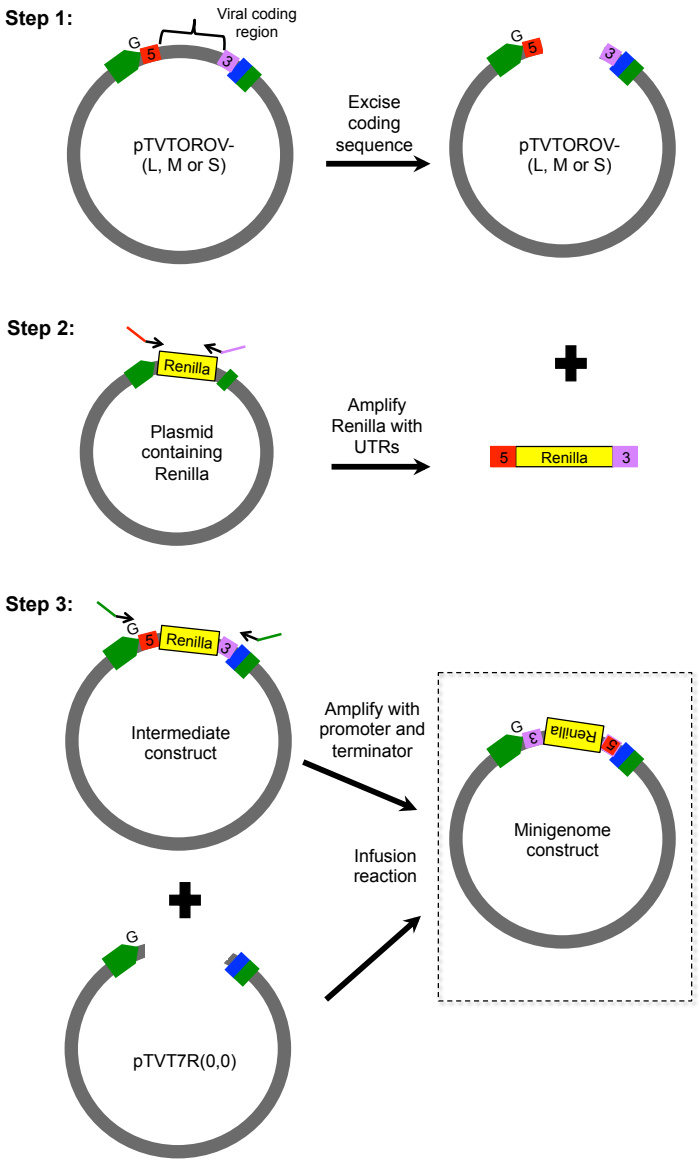

Figure 3.2. 7. Schematic representation for cloning OROV minigenome plasmids.

First, the coding sequence in each pTVT7 clone was deleted by excision PCR, leaving the UTRs intact. These linearized DNAs were then used in an In-Fusion reaction (In-Fusion HD Cloning; Clontech) with amplified luciferase ORF containing 15 nt extensions homologous to the UTR sequences in the linearized pTVT7 construct. The UTR–luciferase–UTR sequence was then amplified by PCR using primers containing 15 nt extensions homologous to the T7 terminator (5' end) and T7 promoter (3'end). This amplified products were combined with TVT7R(0,0) DNA in an In-Fusion reaction to generate minigenome-expressing plasmids such that in T7 transcripts the *Renilla* luciferase was in the negative sense.

Optimisation of OROV minigenome activity

An initial minigenome was created based on the OROV M segment, as studies with BUNV demonstrated that the M-minigenome was the most active (Barr *et al.*, 2003). However, initial attempts using the M segment UTR sequences as reported in GenBank gave low activity over background. Subsequently re-designing the construct to contain UTR sequences generated in this study, with the C/A mismatch at position 9/–9 and U/A at position 15/-15 resulted in high levels of luciferase activity, indicating that (i) both N- and L-expressing constructs were functional and (ii) that the M segment UTR sequences determined herein were active promoters.

The amounts of L- and N- cDNA expressing plasmids required to efficiently transcribe and replicate the minigenome in order to obtain maximum reporter activity was then determined. Briefly, BSR-T7/5 cells (Buchholz *et al.*, 1999) were transfected with various concentrations of pTM1OROV-L, pTM1OROV-N and minigenome pTVT7OROVMRen(–). Cells were also co-transfected with a plasmid expressing firefly luciferase (pTM1-FF-luc). At 24 h p.t cells were lysed and luciferase activity measured using a Dual-Luciferase Reporter Assay kit (Promega). *Renilla* luciferase values were normalised to firefly luciferase values, and minigenome activity expressed as a fold induction over the background control. Control wells did not contain pTM1OROV-L (No L).

High levels of luciferase activity from OROV M-minigenome was obtained when L and N were at a concentration of 1 μg each (1:1 ratio), in a 6-well culture dish (Figure 3.2.8). Increasing concentrations of L decreased minigenome activity. This has been seen with other bunyaviruses as well and has been attributed to the cap-snatching ability of the viral polymerase (Blakqori *et al.*, 2003; Elliott & Schmaljohn, 2013). These optimized amounts were used in all further experiments.

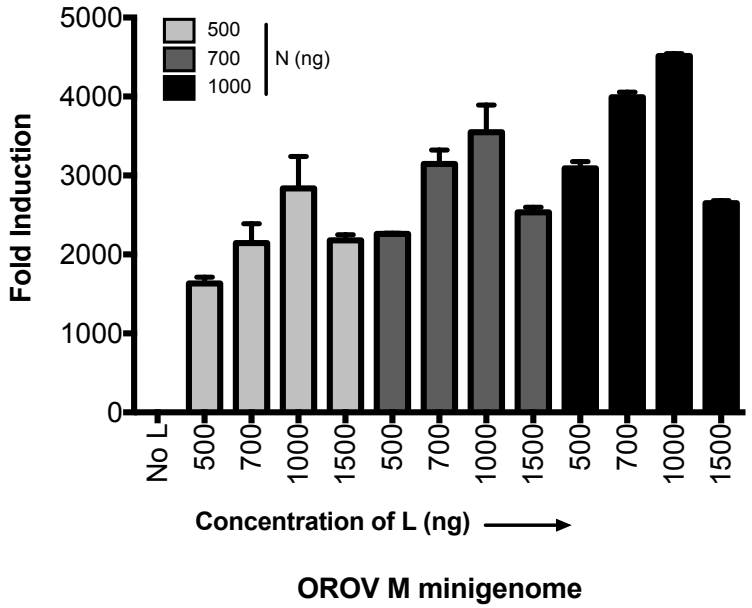

Figure 3.2. 8. Optimisation of OROV minigenome activity.

BSR-T7/5 cells in 6-well plates were co-transfected with 500 ng of OROV M-minigenome expressing plasmid (pTVT7OROVMRen(–)), varying concentration of pTM1OROV-L and pTM1OROV-N, and 100 ng pTM1-FF-Luc. The background control lacked pTM1OROV-L (No L). At 24 h p.t luciferase was measured using a Dual-luciferase Assay kit (Promega). Minigenome activity is expressed as fold induction over the No L control. Error bars indicate SD (n=3).

Functionality analysis of published OROV UTRs and UTRs from this study

To confirm that all the sequence discrepancies generated in this study were not sequencing artifacts, they were compared to the published sequences for minigenome activity. Plasmids reflecting discrepancies were generated using pTVT7OROVMRen(–), pTVT7OROVLRen(–) and pTVT7OROVSRen(-) as templates (Table 2.4; M-UTR, L-UTR, S-UTR). Mutations were confirmed by nucleotide sequencing (Source BioScience). As described above BSR-T7/5 cells were transfected with the optimized amounts of L- and N- along with the indicated OROV minigenome. At 24 h p.t cells were lysed and luciferase activity measured. The M segment UTR as previously published (9C:G, 15C:G) showed low activity, whereas the minigenome with UTR sequences as determined here (9C:A, 15U:A) showed a 2000-fold increased activity over background (cells where no L-expressing plasmid was transfected), Figure 3.2.9A. However, it was not just the mismatch at position 9/–9 that was critical for maximal activity, but also the base-pairing at position 15/–15, as the minigenome with the position 9 C/A mismatch, but C/G at position 15/–15 showed only 500-fold increase in activity. Introduction of the U/A pairing was notable to rescue activity when position 9/–9 was C/G and other nucleotide combinations at position 15 were less active than U/A. Taken together, these results highlight the importance of certain residues within the M segment promoter. Next, the L-minigenomes with either a C or U residue at position 18 in the 5' UTR, resulted in similar high levels of luciferase activity (Figure 3.2.9.B). The minigenome assay was also used to compare the short and long S segment UTR sequences (Figure. 3.2.9 C). Minigenome constructs contained the same 5' UTR and either the 14 nt (published) or 218 nt (as determined herein) long 3' UTR. The minigenome with the short UTR did not result in any activity, whereas the minigenome with the 218 nt 3' UTR resulted in high luciferase activity.

Together, these results confirmed that the UTR sequences as determined for the L, M and S segments were functional promoters, and that a base mismatch at position 9/–9 was critical for promoter activity. A comparison of the published OROV UTR sequences and the UTR sequences determined in this study are presented in Figure 3.2.10.

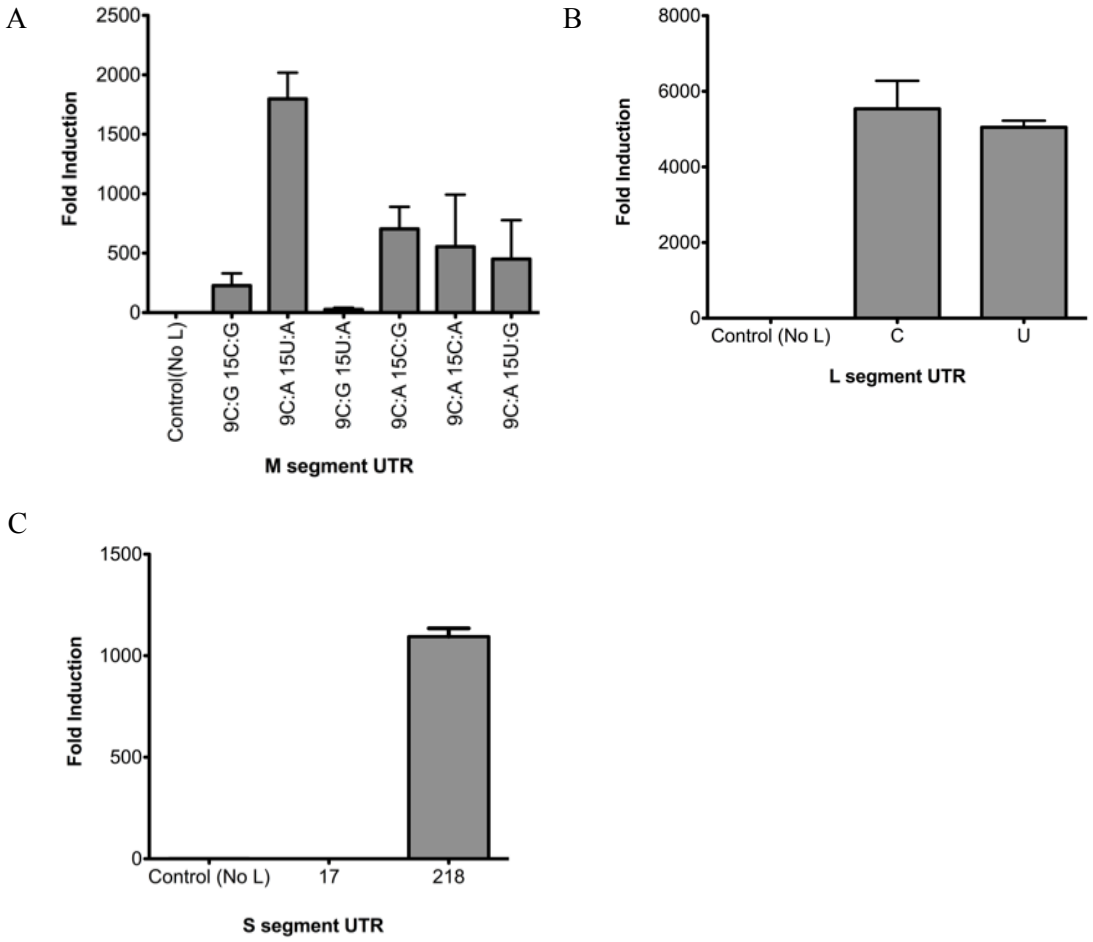

Figure 3.2. 9. Minigenome assay.

(A) Comparison of M-minigenomes. BSR-T7/5 cells were transfected with 1 µg each pTM1OROV-L and pTM1OROV-N, 0.5 µg M-minigenome plasmid, and 100 ng pTM1-FF-Luc; the background control lacked pTM1OROV-L. M-minigenomes contained different nucleotides at position 9/–9 and 15/-15 as indicated. Minigenome activity is expressed as fold induction over the background control. (B) Comparison of L-minigenomes containing a C or U at position 18 in the 3' UTR. (C) Comparison of S-minigenomes containing the published (17 nt) or newly defined long (218 nt) 5' UTR. Error bars indicate SD (n=3).

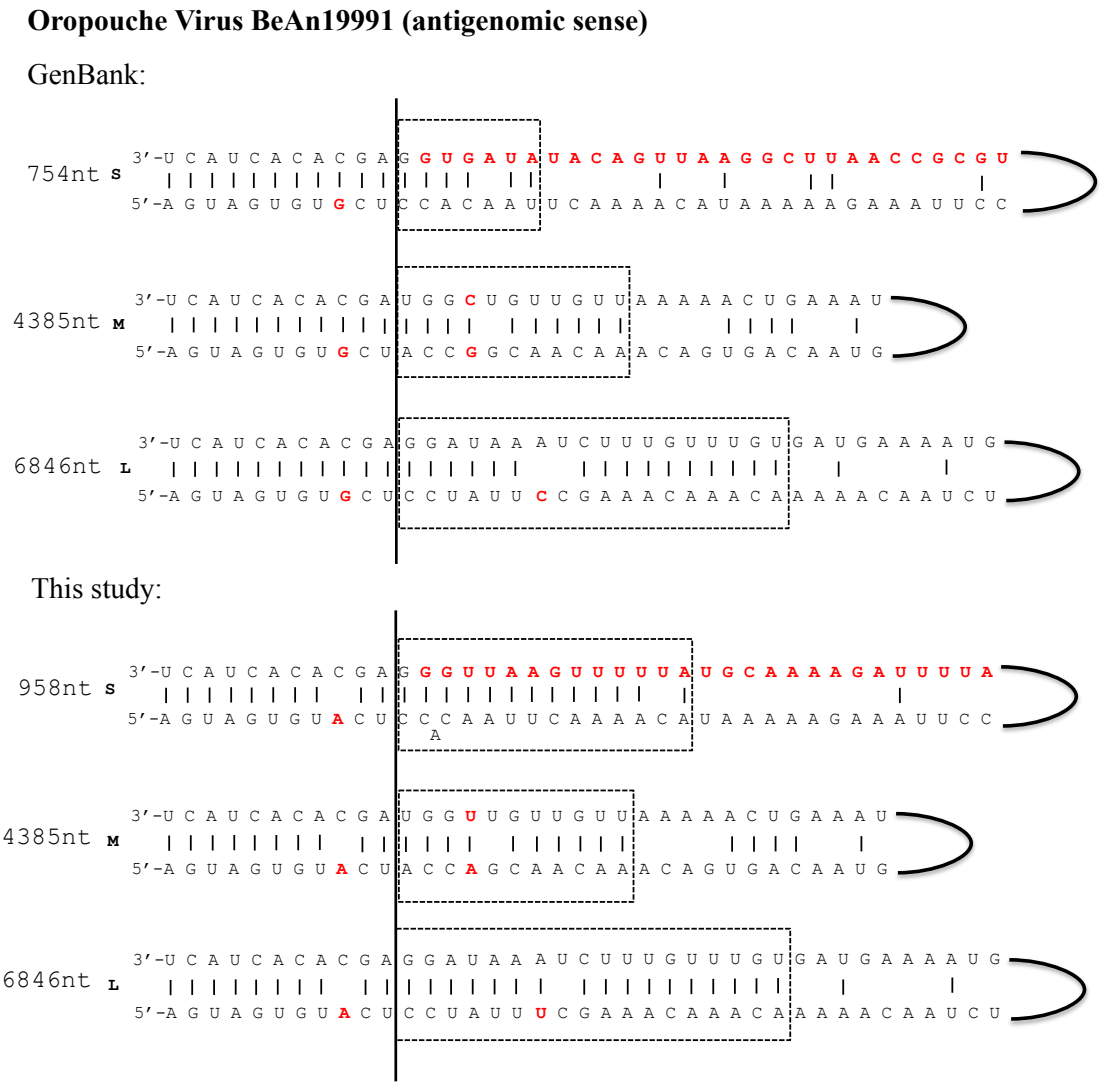

Figure 3.2. 10. Comparison of the published and the revised OROV BeAn19991 UTR sequences shown as a panhandle structure (antigenomic sense).

Differences between the published and revised sequences are shown in red. The length of each segment is also given. nt, nucleotide. The terminal 11 conserved residues are separated by a vertical line. The box highlights nucleotides that are conserved for that particular segment within the *Orthobunyavirus* genus, nucleotides beyond this vary for each virus.

3.2.4 A comparison of two different OROV S segment UTRs

In Chapter 3, Section 1, OROV field isolates were deep sequenced. Results from that study revealed that the recently isolated viruses (from 2009 and 2012) contained significant differences in the S segment 3' UTR, in comparison to the prototype strain used in this study. The complete S segment length of the OROV isolates was determined as 947 nt, in contrast to the S segment length determined in this study for strain BeAn19991 (958 nt). Our collaborators (Dr Martin Spiegel and Prof Manfred Weidmann, University Medical Center Göttingen) have subsequently re-sequenced OROV strain TRVL9760 that was originally isolated in Trinidad in 1955. Similar to strain BeAn19991, this S segment length is also 958 nt (GenBank accession number, KP026181). The UTR sequences for the field isolates were confirmed using the RNA ligation method as described for BeAn19991 in this study. Nucleotide sequencing confirmed the absence of 11 nt between position 781 – 791 (Figure 3.2.11.A). Additional differences have been discussed in Chapter 3, Section 1 of this thesis.

To test if the UTR variations also resulted in variation in promoter activity a minigenome construct based on one of the isolates (OROV Ama2080 BeH759025) was generated, as described in section 3.2.3. This construct was designated as pTVT72080SRen(–). A minigenome assay in BSR-T7/5 cells was carried out as described above. Despite the sequence differences, promoter activity of BeH759025 was similar to that of BeAn19991 (Figure 3.2.11.B), in a minigenome assay. It is probable that the loss of these nucleotides offers an *in vivo* advantage to the virus.

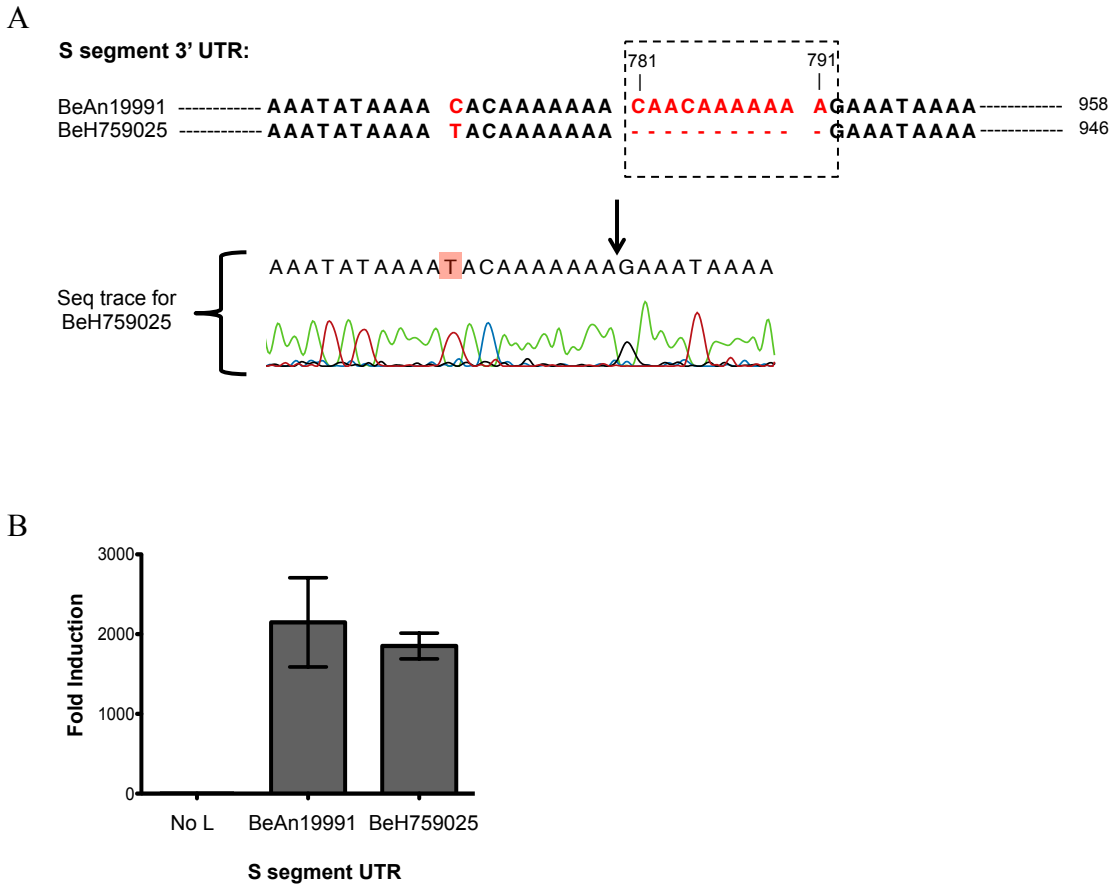

Figure 3.2. 11. Comparison of OROV S segment UTRs.

(A) Sanger-sequencing results demonstrating that the S segment 3' UTR of clinical isolate BeH759025 lacks nts between 781 to 791 of prototype strain BeAn19991. A, Green; T, Red; G, Black; C, Blue. (B) Minigenome activity of the clinical isolate and the prototype S UTRs. BSR-T7/5 cells in 24-well plates were transfected with 250 ng of pTM1OROV-L and pTM1OROV-N, 125 ng of S-minigenome expressing plasmid pTVT72080SRen(–) or pTVT7OROVSRen(–) and 100 ng pTM1-FF-Luc. Control transfection mix lacked pTM1OROV-L (No L). At 24 h p.t cells were lysed and luciferase values determined. Error bars indicate SD (n=3).

3.2.5 Establishment of a virus-like particle assay for OROV

To investigate whether the glycoprotein gene was also functional, a VLP assay was developed. In this system a plasmid expressing the glycoprotein precursor was added to the minigenome system, allowing the minigenome-based RNP to be packaged into virus-like particles. Gn and Gc are co-translational products from the viral glycoprotein precursor and are responsible for virus assembly and budding (Shi *et al.*, 2007). As described above, BSR-T7/5 were transfected with pTM1OROV-L, pTM1OROV-N and pTVT7OROVMRen(–), along with a glycoprotein expressing cDNA plasmid (pTM1OROV-M). At 24 and 48 h p.t cells were lysed and luciferase activity measured, using Dual-luciferase Reporter kit (Promega). Supernatants from these samples were clarified and used to treat naive BHK-21 cells. At 24 h p.t cells were lysed and luciferase activity measured as before.

Renilla values were normalised to firefly values, and minigenome activity expressed as fold-induction over the background control (No L). A significant increase in luciferase activity in cells that were transfected with the glycoprotein cDNA at 48 h was observed (Figure 3.2.12.A), suggesting spread of VLPs within the culture. Transfer of this supernatant to BHK-21 cells had resulted in high levels of luciferase activity (Figure 3.2.12.B, L+M) compared with those exposed to supernatants from cells not transfected with the glycoprotein cDNA (Figure 3.2.12.B, +L). This confirmed that VLPs were produced and were capable of infecting cells. This is a stringent assay relying only on transcription of the packaged minigenome in the VLP without the need for exogenously supplied viral N and L proteins. Incubation of the supernatant with antibodies to OROV (antibody neutralisation test) before infection markedly reduced luciferase expression, whereas incubation with an irrelevant antiserum (anti-BUNV serum), had no effect (Figure 3.2.12.B).

Taken together, these results indicated that the OROV glycoprotein gene cDNA was functional in this VLP assay.

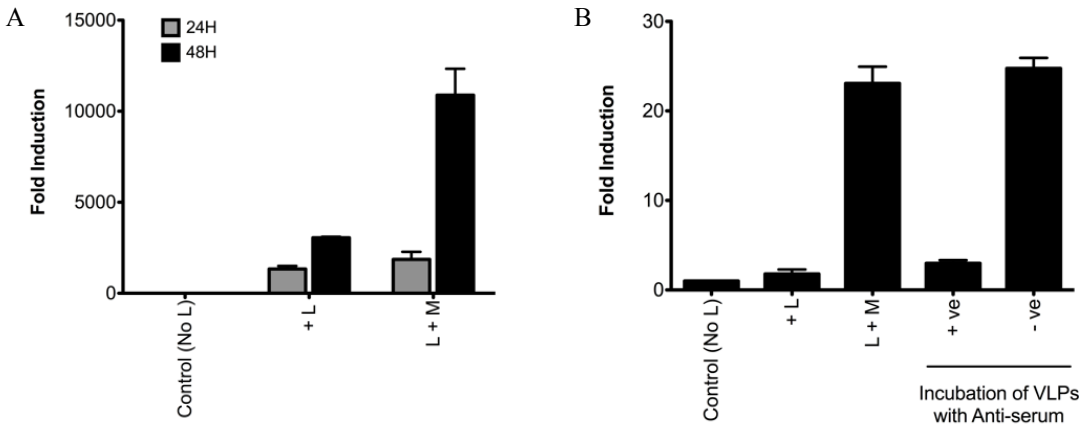

Figure 3.2. 12. VLP production assay.

BSR-T7/5 cells in 6-well plates were transfected with 1 µg each of pTM1OROV-L and pTM1OROV-N, 0.5 µg pTM1OROV-M, 0.5 µg M-minigenome expressing plasmid (pTVT7OROVMRen(–)) and 100 ng pTM1-FF-Luc; control transfection mixes lacked pTM1OROV-L (No L) or pTM1OROV-M (+L). At 24 or 48 h post-transfection, clarified supernatants were used to infect naive BHK-21 cells, and luciferase activity measured 24 h later. (A) Minigenome activity in transfected BSR-T7/5 cells at 24 or 48 h post-transfection. (B) Minigenome activity in BHK-21 cells infected with supernatants from cells in (A). VLPs were also incubated with anti-OROV antibodies (+ve) or irrelevant antibodies (–ve) before infection of cells as indicated. Error bars indicate SD (n=3).

3.2.6 Analysis of OROV promoter strength

Bunyaviral UTRs contain signals for genome replication, packaging and encapsidation. The promoter strength of these UTRs varies for each segment allowing a differential regulation of each gene (Elliott & Schmaljohn, 2013). In mammalian cells the relative levels of promoter activity for BUNV (Barr *et al.*, 2003; Kohl *et al.*, 2004b) and UUKV (Flick *et al.*, 2004) was found to be the highest in M, followed by L and then S (M > L > S). For RVFV this was found to be in the order of L > S > M (Gauliard *et al.*, 2006). In mosquito cells for BUNV, M was again found to be the highest, whilst the activities of the L and S promoters appeared similar (Kohl *et al.*, 2004b). To test the difference between OROV UTRs both minigenome and VLP assays were used. The assays were performed as previously described. At 48 h p.t luciferase activity from BSR-T7/5 cells transfected with L+M was significantly higher using the S-minigenome (Figure 3.2.13.A, L+M), in comparison to cells without M (Figure 3.2.13A, +L) where luciferase activity is higher with the L-minigenome. BHK-21 cells exposed to the supernatants from these samples for 24 h show high levels of luciferase activity from the S-minigenome based assay (Figure 3.2.13.B). Based on these results it would appear that in a minigenome assay that measures transcription and replication, the promoter strength of OROV UTRs follows an order of L > M > S, whereas in a VLP assay which also measures packaging ability, the UTRs are in a S > L > M order.

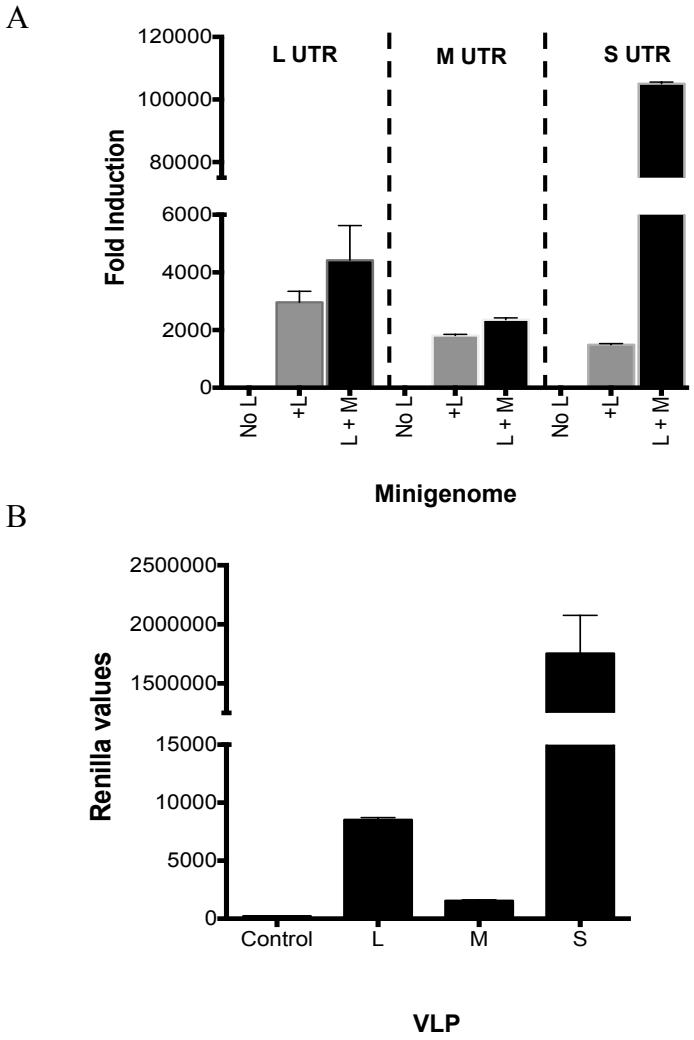

Figure 3.2. 13. OROV promoter strength.

BSR-T7/5 cells in 12-well plates were transfected with 0.5 µg each of pTM1OROV-L and pTM1OROV-N, 0.25 µg pTM1OROV-M, 0.25 µg L, M or S-minigenome expressing plasmid, and 100 ng pTM1-FF-Luc; control transfection mixes lacked pTM1OROV-L (No L) or pTM1OROV-M (+L). At 48 h post-transfection, clarified supernatants were used to infect naive BHK-21 cells, and luciferase activity measured 24 h later. (A) Minigenome activity in transfected BSR-T7/5 cells at 48 h post-transfection. (B) Minigenome activity in BHK-21 cells infected with supernatants from cells in (A). Error bars indicate SD (n=3).

3.2.7 Analysis of OROV NSs

Effect of OROV NSs on minigenome activity

Bunyavirus NSs proteins have a regulatory role on the L protein and this is seen when NSs-expressing cDNA is added to a minigenome assay (Weber *et al.*, 2001; Kohl *et al.*, 2004b; Brennan *et al.*, 2011; Brennan *et al.*, 2015). To determine if OROV NSs has similar dose-dependent effects, BSR-T7/5 cells were transfected as previously described. In addition, cells were also transfected with increasing concentrations of pTM1OROV-NSs (1, 10, 100, 1000 ng). The minigenome assay was carried out using pTVT7OROVMRen(–). At 24 h p.t cells were lysed and luciferase activity measured. Renilla values were normalized to firefly values. Cells that did not contain OROV NSs resulted in high levels Renilla readings (Figure 3.2.14, No NSs). OROV NSs appears to drastically decrease minigenome activity even at low concentrations (1 ng) (Figure 3.2.14).

Effect of OROV NSs on CMV promoter

BUNV and RVFV NSs proteins have been demonstrated to reduce gene expression from CMV driven plasmids (Billecocq *et al.*, 2004; Leonard *et al.*, 2006). To determine if a similar effect occurs with OROV NSs, BSR-T7/5 cells were transfected with pTM1OROV-NSs, phRL-CMV and pTM1-FF-luc. phRL-CMV contains *Renilla* luciferase gene under the control of CMV immediate-early promoter. pTM1-FF-luc (T7RNAP-driven) was included as a control to determine whether any effect observed was CMV specific. At 24 h p.t cells were lysed and luciferase activity determined. Cells without NSs resulted in high luciferase readings. Addition of OROV or BUN NSs decreased Renilla values significantly (Figure 3.2.15). NSs had no effects on firefly values indicating NSs specificity for CMV-driven expression and not T7-driven expression.

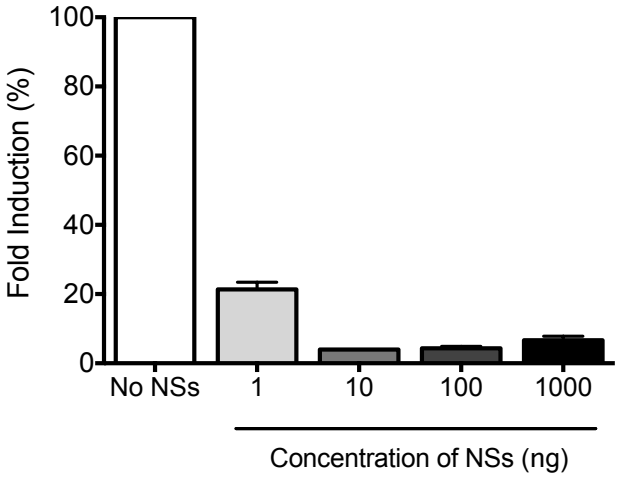

Figure 3.2. 14. Effect of NSs on minigenome activity.

BSR-T7/5 cells were co-transfected with pTM1OROV-N (1 μg), pTM1OROV-L (1 μg), pTM1-FF-luc (100 ng) and pTVT7OROVMRen(–) (0.5 μg), along with indicated amounts of NSs-expressing pTM1OROV-NSs. Luciferase values were measured 24 h p.t using a Dual-luciferase Reporter Assay kit (Promega). Values for NSs samples are plotted as fold-induction over control (No NSs), set at 100% activity. The experiment was carried out in triplicate.

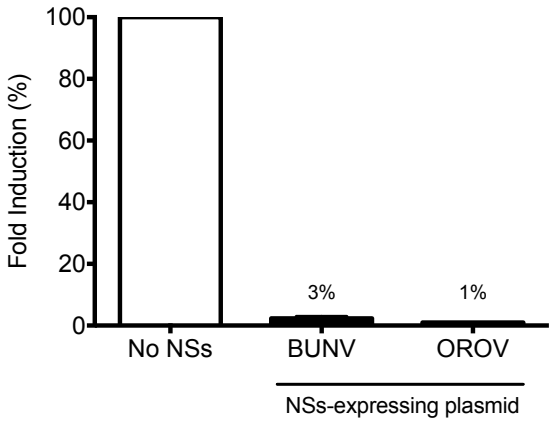

Figure 3.2. 15. Effect of NSs on CMV-driven reporter gene expression.

BSR-T7/5 were co-transfected with 0.5 μg of phRL-CMV, pTM1-FF-luc and pTM1BUNVNSs or pTM1OROVNSs. Luciferase values were measured 24 h p.t using a Dual-luciferase Reporter Assay kit (Promega). Values for BUNV and OROV NSs samples are plotted as fold-induction over Control (No NSs), set at 100% activity. The experiment was carried out in triplicate.

Cellular localization of OROV NSs

To determine the intracellular localization of OROV NSs, the protein was tagged with eGFP or V5. Both tags were C-terminally placed using pTM1 plasmid as a backbone. Briefly, to tag OROV NSs with eGFP, a pTM1 plasmid expressing eGFP was first linearized. OROV NSs was then amplified with eGFP overhangs at the 5' and 3' ends, and ligated to the linearized eGFP plasmid by In-Fusion reaction (Clonetech Laboratories Inc.). With the V5 tag, pTM1OROV-NSs was PCR-linearised using primers containing the V5 sequence, such that the PCR amplified product could then be ligated back together (T4 DNA ligase, Promega). Primers used are in Table 2.4. Plasmids were confirmed by nucleotide sequencing (Source BioScience), and designated as pTM1ONSsV5 and pTM1ONSseGFP.

Intracellular localisation was determined by immunofluorescence. BSR-T7/5 cells on coverslips were transfected with pTM1ONSseGFP or pTM1ONSsV5. At indicated time-points cells were fixed, and pTM1ONSsV5 samples were stained using anti-V5 antibody. Both fusion proteins were detected in the cytoplasm of the cells (Figure 3.2.16.A, B; Figure 3.2.17.A, B). However, the eGFP version at later time points was also detected in the nucleus (Figure 3.2.16.A, B; 24 h). eGFP is a larger protein tag (26.9 KDa) and over-expression is known to cause fused-proteins to translocate into the nucleus. Expression and functionality of pTM1ONSseGFP and pTM1ONSsV5 were tested by Western blotting, minigenome and CMV-driven assays. In a Western-blot samples were stained using anti-GFP (Figure 3.2.16.C) and anti-V5 (Figure 3.2.17.C) confirming appropriate proteins sizes. Both fusion protein were active in reducing minigenome activity ((Figure 3.2.16.D; Figure 3.2.17.D), however pTM1ONSseGFP was unable to efficiently reduce CMV-driven *Renilla* luciferase expression (Figure 3.2.16.E) in comparison to pTM1ONSsV5 (Figure 3.2.17.E).

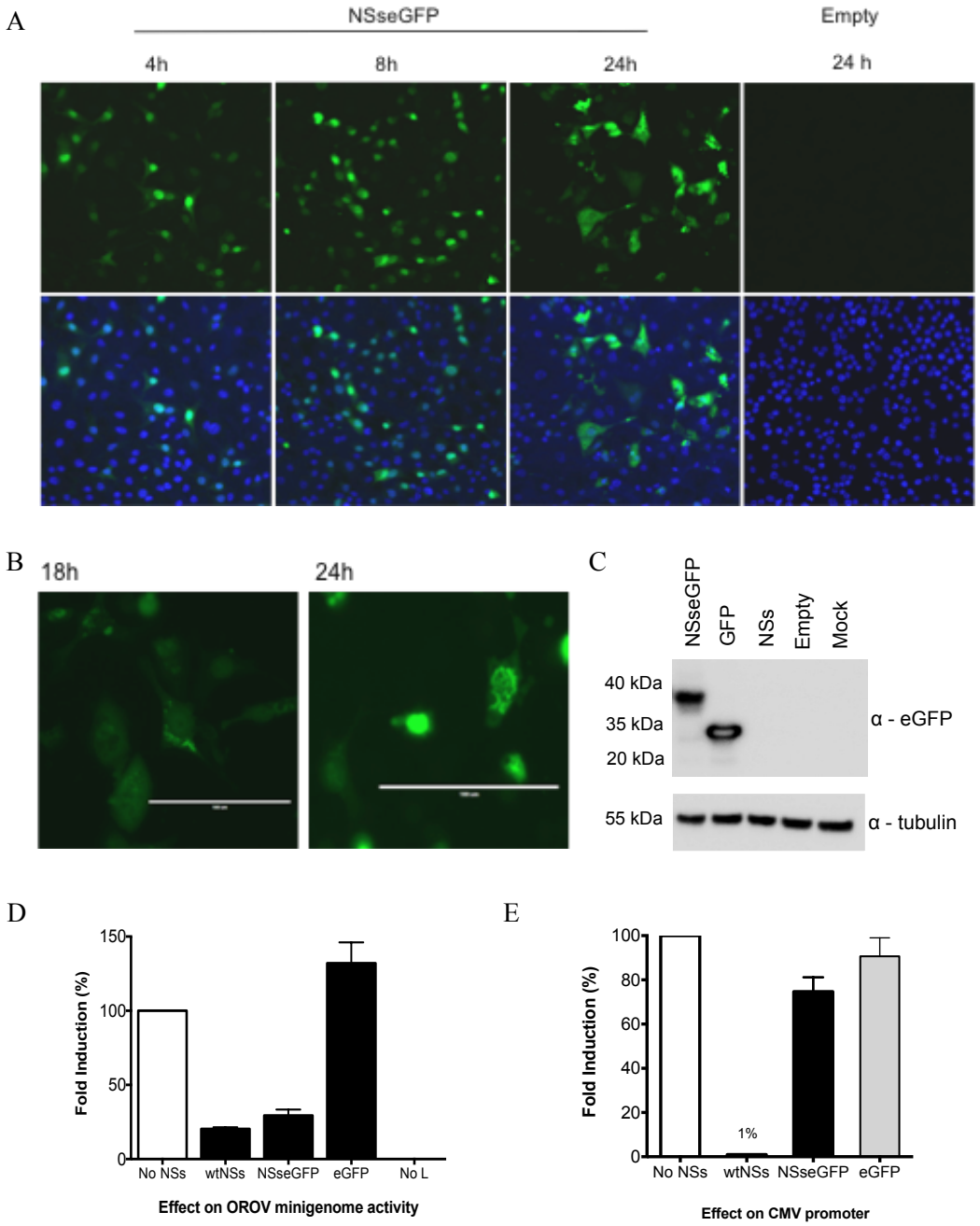

Figure 3.2. 16. eGFP-tagged OROV NSs protein.

(A), (B) Intracellular localization of eGFP-tagged OROV NSs in BSR-T7/5 cells. Cells were transfected with 500 ng of pTM1OROVNSseGFP in a 6-well culture dish, and fixed and stained at indicated time points. (C) Western blotting demonstrated that pTM1OROVNSseGFP expresses a protein of appropriate size (NSseGFP, 37.61 kDa). The size of eGFP is 32.7 kDa. (D) Minigenome assay, and (E) CMV-driven *Renilla* expression. BSR-T7/5 cells were transfected as described in section 3.2.7.

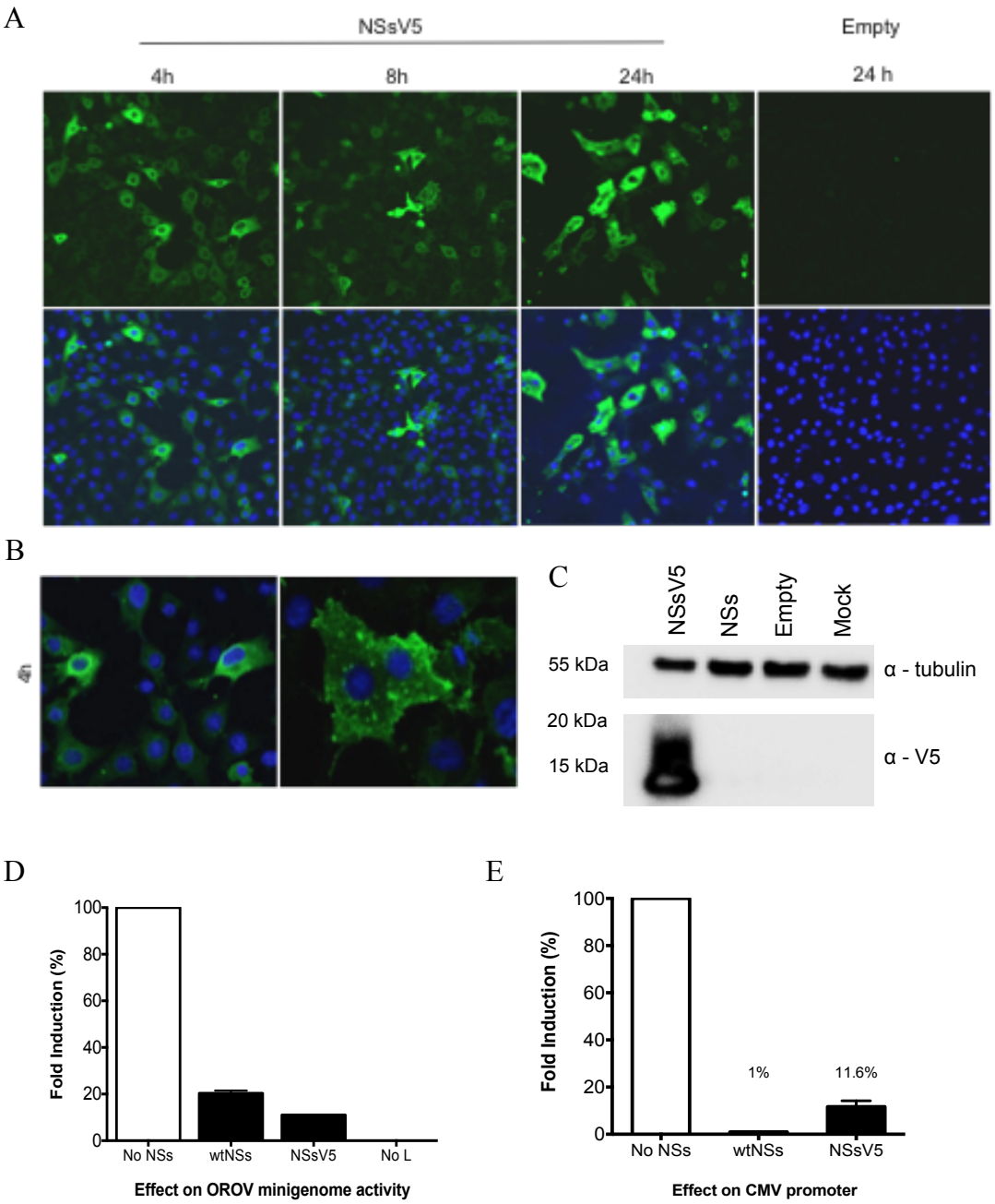

Figure 3.2. 17. V5-tagged OROV NSs protein.

(A), (B) Intracellular localization of V5-tagged OROV NSs in BSR-T7/5 cells. Cells were transfected with 500 ng of pTM1OROVNSsV5 in a 6-well culture dish, and fixed and stained at indicated time points. (C) Western blotting demonstrated that pTM1OROVNSsV5 expresses a protein of appropriate size (NSsV5, 12.11 kDa). (D) Minigenome assay, and (E) CMV-driven *Renilla* expression. BSR-T7/5 cells were transfected as described in section 3.2.7.

3.2.8 Discussion

A crucial step in developing reverse genetic systems for RNA viruses is obtaining cDNA clones that are representative of the authentic viral genome sequence. As described above, a number of sequence differences were found in the clones derived from the BeAn19991 strain in this study compared with sequences in the database. These included an additional ~200 nt at the 3' end of the S genome segment, an apparent frame shift in the L segment coding sequence and a critical mismatched nucleotide pair in the terminal panhandle sequence on each segment. These significant differences were confirmed when the complete sequence of the Trinidadian prototype strain TRVL-9760 was also determined by our collaborators (Dr Martin Spiegel and Prof Manfred Weidmann, University Medical Center Göttingen; GenBank accession nos. KP026179 – KP026181). Early studies comparing orthobunyavirus genome sequences indicated that the terminal 11 nt of each segment exhibited a high degree of conservation, and hence consensus primers based on sequences of Bunyamwera and California serogroup viruses (Elliott, 1989; Elliott & McGregor, 1989; Elliott *et al.*, 1991; Dunn *et al.*, 1994) have traditionally been used to amplify unknown bunyavirus genomes. However, the actual terminal sequences for the majority of sequences currently available in GenBank have not been verified directly, e.g. by RACE techniques. With regard to the orthobunyavirus 'consensus sequence', there is a single nucleotide difference between the 3' and 5' complementary ends such that, using total infected cell RNA as template, mispriming by either primer could occur or a single primer could bind to both genomic and antigenomic RNAs. Indeed, a single primer was used to amplify the OROV M segment (Aquino & Figueiredo, 2004) or the S segments of a range of orthobunyaviruses (Lambert & Lanciotti, 2008). The importance of the terminal sequence has been investigated by minigenome assays for BUNV (Dunn *et al.*, 1995; Barr *et al.*, 2003; Kohl *et al.*, 2003a; Barr & Wertz, 2004; Kohl *et al.*, 2004a) and the mismatch at position 9/–9 was shown to be crucial for promoter activity (Barr & Wertz, 2005). As more diverse orthobunyavirus genomes have been sequenced, particularly using next-generation sequencing methods (deep sequencing) that are not reliant on specific primers to amplify cDNA, it has become clear that there is more variation in the 'bunyavirus consensus' than observed between Bunyamwera and California serogroup viruses (e.g. (Ladner *et al.*, 2014)), highlighting the requirement

for direct determination of the terminal sequences. In a similar vein, as the genomes of more members of the genus Phlebovirus (another genus in the family Bunyaviridae) have been sequenced, it is apparent that the termini also diverge from the 'phlebovirus consensus' (Dilcher *et al.*, 2012; Matsuno *et al.*, 2013; Elliott & Brennan, 2014). A recent paper (Ladner *et al.*, 2014) suggested the standards that should be applied to viral genome sequence determination and we strongly support the recommendations proposed therein. Saeed *et al*. (Saeed *et al.*, 2000) reported the first nucleocapsid gene sequences of 28 strains of OROV, including the prototypic Trinidadian OROV isolate TRVL-9760 and the Brazilian isolate BeAn19991. They determined the complete S segment to be 754 nts and noted the unusually short length of the 3' UTR, just 14 nts after the translational stop codon, compared with other orthobunyavirus S segments. They employed various experimental procedures to verify the 3' UTR, including chemical denaturation of the purified viral RNA with methylmercury hydroxide before RT-PCR (in case there was a secondary structure that impeded reverse transcription), and a 5' RACE procedure using both purified viral RNA and total cellular RNA as starting material (Saeed *et al.*, 2000). All approaches yielded that same short 3' UTR. Results in the current study indicate that the true length of the S segment is actually 958 nt. Examination of the correct sequence reveals an internal region highly similar to the terminal sequence that could hybridize with the primer and in this study resulted in two PCR products. The functionality of the longer 3' UTR determined in this study was demonstrated in the minigenome assay. We further confirmed that the sequences of the BeAn19991 N and L proteins were functional in driving reporter gene expression from minigenomes, and similarly that the determined UTR sequence for all three segments could be used to construct functional minigenomes. Lastly, by co-transfecting a cDNA that expressed the glycoprotein gene, VLPs capable of packaging a minigenome and infecting naive cells were produced. Taken together, these data provide strong evidence that the cDNA clones reported in this study are fully functional.

In addition, the study has used the established minigenome system to analyse OROV promoter strength, and found that in a minigenome assay OROV promoters are in a L > M > S order, whilst in a VLP assay follow S > L > M. This is in contrast to other bunyaviruses in which the M promoter is the most active (Barr *et al.*, 2003; Flick *et al.*,

2004; Kohl *et al.*, 2004b). OROV NSs does however, behave similar to other tested bunyavirus NSs proteins in its function to reduce minigenome activity and CMV-driven gene expression. Lastly, the loss of 11 nts in the S segment of OROV field isolates was investigated, although it appeared to have no effect on the UTR function when analysed using the minigenome system. Previous work has demonstrated that internal deletions in the S-segment UTRs of BUNV do not affect virus viability, but do interfere with replication causing growth attenuation in cell culture (Lowen & Elliott, 2005). Similar results have also been shown for the BUNV M- and L-segment UTRs (Mazel-Sanchez & Elliott, 2012). The apparent natural deletion of these 11 nts could be important for virus replication efficiency and virus fitness, both *in vitro* and *in vivo*, and are worth pursuing further.

3.2.9 Summary

1. The genome sequences of OROV BeAn19991 have been re-determined.
2. OROV S segment is 958 nt long and not 754 nt as published.
3. OROV field isolates demonstrate a loss of nucleotides at the 3' UTR.
4. A minigenome and a VLP assay for OROV have been established.

The corrected sequences of the OROV strain BeAn19991 genome were deposited in GenBank with accession numbers KP052850 (L), KP052851 (M) and KP052852 (S).

Chapter III. Results

Section 3: Minigenome analysis suggests that Oropouche and Schmallenberg orthobunyaviruses would be capable of reassortment

3.3.1 Introduction and Aims

Chapter 3, Section 2 described the establishment of a minigenome and (VLP) system for OROV. The present study utilised that system to test protein-protein and protein-RNA interactions between OROV and SBV. OROV and SBV are both midge-borne pathogenic orthobunyaviruses, occupying separate clades of the Simbu serogroup (Ladner *et al.*, 2014). OROV causes a febrile illness in humans in South America, whilst SBV is responsible for ruminant fetal malformations in Europe (Anderson *et al.*, 1961; Hoffmann *et al.*, 2012). Separated by host and geographic distance these viruses are ideal for studying determinants of cross-species transmission. The aim of this section was to take advantage of the new reverse genetics tools for OROV that were developed in this PhD project and combine it with that of SBV (Dong *et al.*, 2013a; Elliott *et al.*, 2013; Varela *et al.*, 2013), in order to assess if these viruses are capable of reassortment.

Reassortment is a well-documented phenomenon for viruses with segmented-genomes and can occur when two genetically related viruses co-infect the same cell. Thomas Briese recently hypothesized that all bunyaviruses may have arisen due to reassortment (Briese *et al.*, 2013). Examples of orthobunyavirus reassortants include Apeu virus (de Brito Magalhaes *et al.*, 2011), Aino virus (Yanase *et al.*, 2010), Ngari virus (Gerrard *et al.*, 2004) and Perdoes virus. As described in Chapter 3, Section 1, Perdoes virus consists of L and S segments similar to OROV and an M segment of unknown Simbu origin. Similarly, IQTV and MDDV are also OROV reassortants with unique M segments (Aguilar *et al.*, 2011; Ladner *et al.*, 2014). Bunyavirus reassortants tend to contain L and S segments from the same parental virus, whilst the M segment donor

remains in most cases unknown. The L and S segments encode the viral polymerase (L) and nucleocapsid (N) proteins, which together replicate the viral genome, so it is likely that they coevolve together (Iroegbu & Pringle, 1981; Elliott, 2014). The M segment, on the other hand, encodes a non-structural protein (NSm) and the viral surface proteins Gn and Gc. The Gn/Gc proteins enable the virus to bind to the receptor and enter the host-cell, so they function as the major antigenic targets. Progeny viruses that arise from an M segment reassortant would hence contain new genetic information with the potential of increased infectivity and a new host-range (Briese *et al.*, 2013; Elliott, 2014).

3.3.2 SBV L and N are capable of replicating and transcribing OROV minigenomes

SBV minigenome assay

First, a plasmid expressing SBV N protein was generated since previously the entire S ORF that encodes for both N and the overlapping NSs was cloned into a pTM1 expression vector (Moss *et al.*, 1990) to be used in the minigenome assay (Dong *et al.*, 2013a; Elliott *et al.*, 2013; Varela *et al.*, 2013). NSs is known to decrease minigenome activity (Chapter 3, Section 2), hence to silence the NSs ORF primers previously used to generate SBV mutant lacking the NSs protein (rSBVdelNSs; (Elliott *et al.*, 2013)) were used. This plasmid was designated as pTM1SBV-N, where SBV N is under the control of T7 promoter and EMCV IRES. cDNA expressing plasmid for SBV L protein was previously cloned by Dr Xiaohong Shi (MRC-University of Glasgow, Centre for Virus Research) and SBV M-minigenome (pTVT7R-SBVMRen(–)) has previously been described (Dong *et al.*, 2013a).

Next, the SBV minigenome system was optimised to determine the amounts of L- and N- cDNA expressing plasmids required to obtain maximum reporter activity. Briefly, BSR-T7/5 cells (Buchholz *et al.*, 1999) were transfected with indicated concentrations of pTM1SBV-L, pTM1SBV-N and minigenome pTVT7R-SBVMRen(–)(Dong *et al.*, 2013a). Cells were also co-transfected with a firefly luciferase expressing plasmid (pTM1-FF-luc), control wells did not contain pTM1OROV-L (No L), but was

substituted with an empty pTM1 plasmid to equalize the total amount of DNA added to each well. At 24 h p.t cells were lysed and luciferase activity measured using a Dual-Luciferase Reporter Assay kit (Promega). *Renilla* values were normalised to firefly values, and the minigenome activity calculated as fold induction over the background control (No L). Minigenome activity was the highest when L and N were at a ratio of 1:2 (Figure 3.3.1). This is in contrast to OROV, where equal amounts of L and N were required. As observed with OROV, activity of SBV minigenome decreases with higher concentrations of L protein (Chapter 3, Section 2).

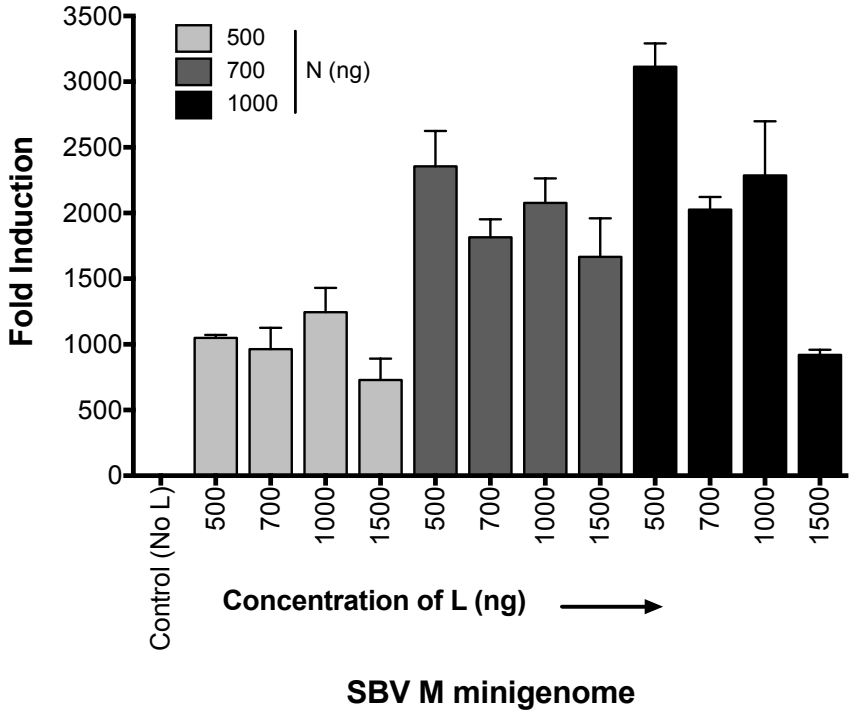

Figure 3.3 1. SBV minigenome optimisation.

BSR-T7/5 cells (6-well plate) were transfected with pTM1SBV-N and/or pTM1SBV-L and minigenome-expressing TVT7R-SBVMRen(–). Firefly luciferase-expressing pTM1-FF-Luc (100 ng) served as a transfection control. At 24 h p.t *Renilla* and firefly luciferase were measured using a Dual-Luciferase Reporter Assay kit (Promega). Luciferase values were normalized. Minigenome activity is expressed as fold-induction over background control (No L). Error bars indicate SD (n = 3).

Protein-protein and protein-RNA interactions between OROV and SBV

To assess protein-protein and protein-RNA interactions between OROV and SBV, BSR-T7/5 cells were transfected with OROV or SBV minigenomes, as previously described (OROV: Chapter 3, Section 2; SBV: 3.3.2), along with the L and N protein-expressing plasmids of the respective virus or with a combination of OROV and SBV L and N (Figure 3.3.2). In the minigenome plasmid the reporter gene *Renilla* Luciferase is placed in the viral genomic sense and is flanked by the viral UTRs. Hence it served as a genomic segment analogue. Expression from the minigenome plasmid is derived only when the L and N proteins can recognize the viral UTR as a functional promoter. Transcription and replication of the viral minigenome then leads to measurable activity. The presence of luciferase activity was chosen as an indication that a potential genomic rearrangement between the tested viruses would be feasible. At 24 h p.t cells were lysed and luciferase activity measured using a Dual-luciferase Assay Reporter Kit (Promega). As expected, minigenome activity was detected with OROV L-N using OROV M-minigenome, and with SBV L-N using SBV M-minigenome (Figure 3.3.2). Interestingly, a greater than 50-fold increase in minigenome activity was also detected with SBV L-N using OROV M-minigenome, contrasting a less than 10-fold increase over background with OROV L-N using SBV M-minigenome (Figure 3.3.2). To test if the low reporter activity with OROV L-N on SBV M-minigenome was due to optimisation efficiency, the assay was repeated by titrating various concentrations of OROV L-N. No increase in reporter activity was detected (Figure 3.3.3).

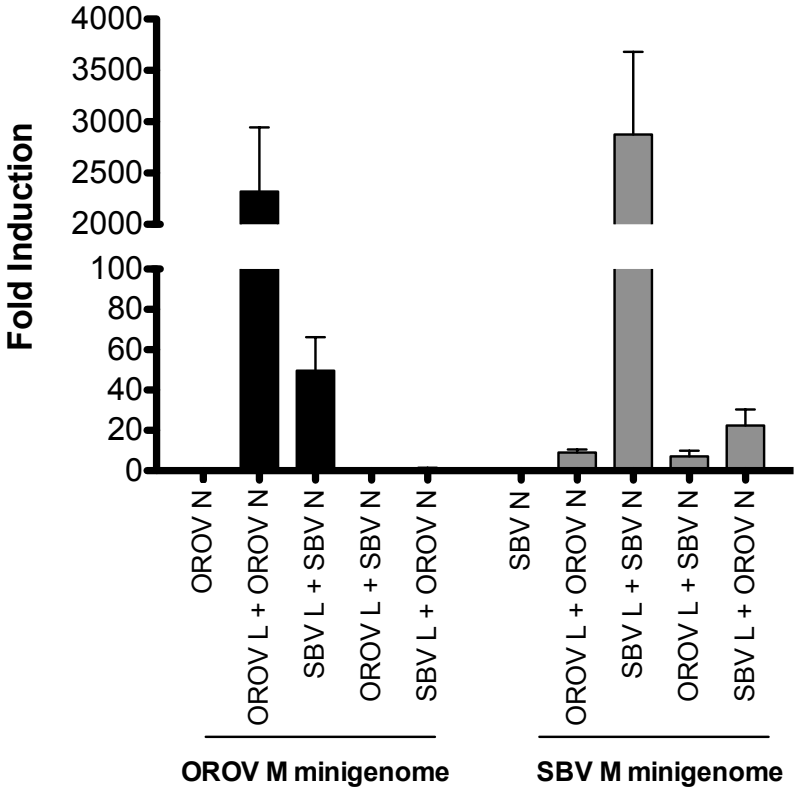

Figure 3.3 2. Minigenome activity.

BSR-T7/5 cells (24-well plate) were transfected with pTM1-N and/or pTM1-L (250 ng) and M-minigenome (125 ng) plasmids, pTVT7R-SBVMRen(–) or pTVT7OROVMRen(-). Firefly luciferase-expressing pTM1-FF-Luc (25 ng) served as a transfection control. At 24 h.p.t *Renilla* and firefly luciferase were measured using a Dual-Luciferase Reporter Assay kit (Promega). Luciferase values were normalized and minigenome-activity expressed as fold-induction over background control (no pTM1-L). Error bars indicate SD (n=3).

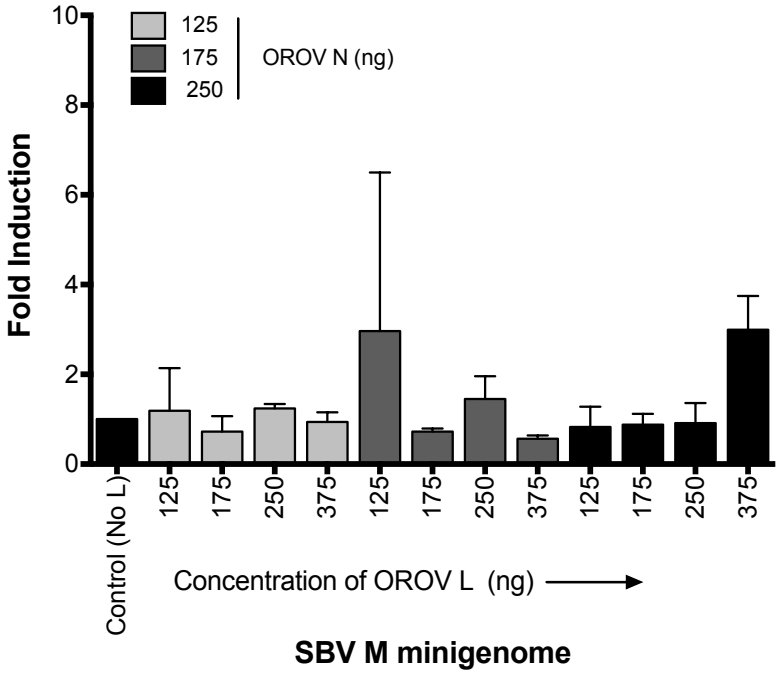

Figure 3.3 3. Titration of OROV L-N on SBV M-minigenome.

BSR-T7/5 cells (24-well plate) were transfected as described above. Indicated amounts of pTM1OROV-N and/or pTM1OROV-L were transfected along with TVT7R-SBVMRen(–) (125 ng) and pTM1-FF-Luc (25 ng). At 24 h.p.t *Renilla* and firefly luciferase were measured using a Dual-Luciferase Reporter Assay kit (Promega). Luciferase values were normalized and minigenome-activity expressed as fold-induction over background control (no pTM1-L). Error bars indicate SD (n = 3).

SBV L and N functionality with OROV UTRs

SBV L and N were tested for their ability to also utilise OROV L and S UTRs. BSR-T7/5 cells were transfected with SBV L and N cDNA expressing plasmids, along with OROV L- (pTVT7OROVLRen(–)), OROV M- (pTVT7OROVMRen(–)), or OROV S- (pTVT7OROVSRen(-)) minigenome expressing plasmids. The minigenome assay was performed as described above. At 24 h p.t luciferase activity was measured and calculated. SBV L-N proteins were able to recognize the UTRs of all OROV segments (Figure 3.3.4). In an OROV-minigenome assay the promoter strength of OROV UTRs follows an order of L > M > S (Chapter 3, Section 2; Figure 3.2.13), however using SBV L-N it appears that the promoter strengths of L and M are similar in activity (Figure 3.3.4).

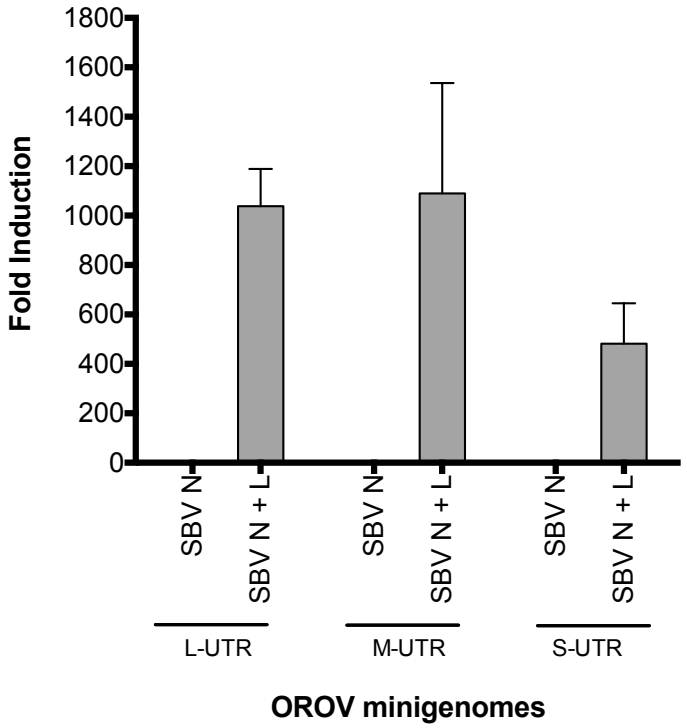

Figure 3.3 4. OROV UTRs.

BSR-T7/5 cells (24-well plate) were transfected as previously described. 250 ng of pTM1SBV-N and/or pTM1SBV-L were transfected with 125 ng of pTVT7OROVLRen(–), pTVT7OROVMRen(–), or pTVT7OROVSRen(-), and pTM1-FF-Luc (25 ng). At 24 h.p.t *Renilla* and firefly-luciferase were measured using a Dual-Luciferase Reporter Assay kit (Promega). Luciferase values were normalized and minigenome-activity expressed as fold-induction over background control (no pTM1-L). Error bars indicate SD (n = 3).

3.3.3 Viral Like Particles (VLPs) confirm minigenome results

Next, a VLP production assay was performed in order to further assess whether OROV and SBV can reassort as the minigenome data suggests. Briefly, BSR-T7/5 cells were transfected with SBV or OROV L and N protein expression plasmids and SBV or OROV M-minigenome, along with SBV or OROV glycoprotein-expressing plasmid (concentration as indicated in the graph, Figure 3.3.5). BUNV glycoprotein was also included as a control. At 48 h p.t the supernatant was harvested, clarified and used to infect fresh BSR-T7/5 cells that were transfected with L, N and M plasmids for 24 h in order to boost transcription, as previously described (Devignot *et al.*, 2015). VLP-infected BSR-T7/5 cells were lysed 24 h p.i and luciferase activity measured as described above. *Renilla* luciferase was detected with OROV glycoproteins in combination with SBV N-L in both OROV and SBV M-minigenomes (Figure 3.3.5.A and B; SBVN + SBVL + OROVM). This suggests that VLP reassortants containing OROV glycoproteins and SBV L and N proteins could be formed, indicating that a viable virus could potentially also form. In contrast, the combination of OROV L-N proteins and SBV M glycoproteins did not produce measurable reporter activity with SBV M-minigenome (Figure 3.3.5.B; OROVN + OROVL + SBVM) and relatively low activity with OROV M-minigenome (Figure 3.3.5.A). Similarly, low activity was observed with SBV N + SBV L + BUNV M protein combination (Figure 3.3.5; SBVN + SBVL + BUNVM). These results indicate that OROV glycoproteins can interact with heterologous SBV RNPs and assemble viral particles that are capable of infecting new cells.

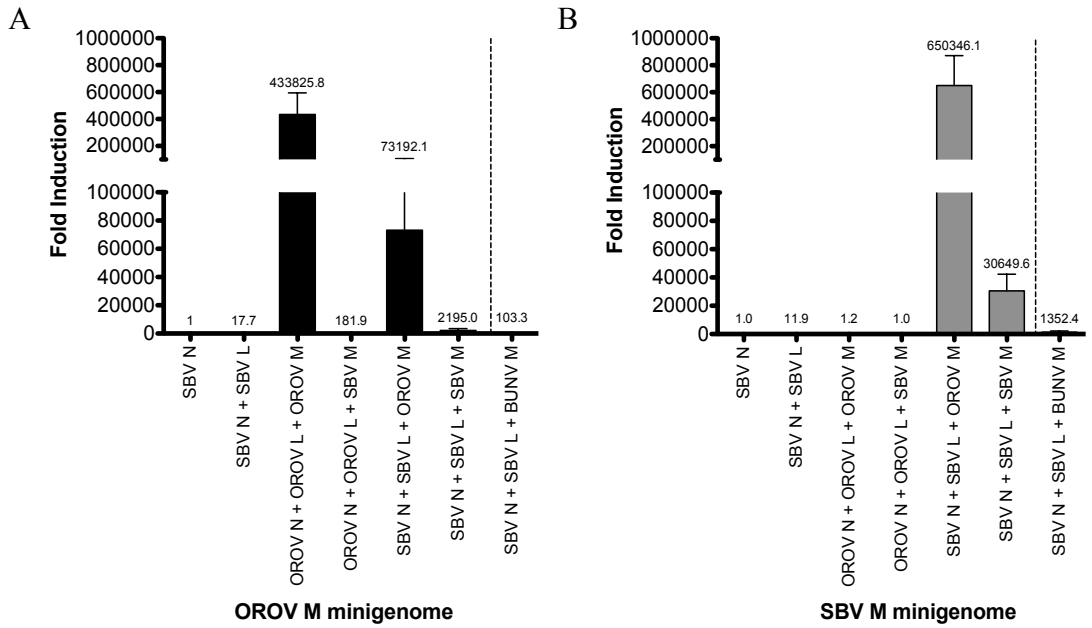

Figure 3.3 5. VLP assay.

BSR-T7/5 cells (12-well plate) were transfected with pTM1SBV-L (200 ng) and pTM1SBV-N (400 ng) or pTM1OROV-L and pTM1OROV-N (400 ng), along with pTM1-M (200 ng), and M-minigenome (200 ng) and pTM1-FF-Luc (40ng). At 48 h.p.t clarified supernatant was used to infect cells pre-transfected with proteins only, as indicated. At 24 h.p.i luciferase readings were measured as described above. *Renilla* activity is expressed as fold induction over control pTM1-N. Error bars indicate SD (n = 3).

3.3.5 The importance of UTR positions 8 and 9

In contrast to OROV L and N, which are unable to function using SBV M UTR, the L and N proteins of SBV can recognise OROV M UTR. To investigate the sequence difference that contributes to UTR recognition a nucleotide alignment of OROV and SBV M segment UTRs along with that of other Simbu viruses Akabane virus (AKV), Oya virus (OYAV), Leanyer virus (LENV), Perdoes virus and the family prototype BUNV were carried out (Figure 3.3.6.A). Interestingly, SBV and AKV (another ruminant pathogen) contain 8A/A-9A/A "double-mismatch" at positions 8 and 9 of the M UTR, and LENV consists of 8A/C-9C/A "double-mismatch". These are variations from the "typical" 8A/T-9C/A "pairing/mismatch" as present in OROV, BUNV, OYAV and Perdoes virus. These positions have previously been shown to be important for orthobunyavirus promoter activity (Barr *et al.*, 2005; Chapter 3, Section 2). To investigate if these residues contributed to promoter recognition by the viral N and L proteins, point mutations were inserted in the minigenome plasmids by site-directed mutagenesis (Table 2.5). The 8th and 9th nucleotides of OROV M-minigenome (8A/T-9C/A) were altered to mimic the residues of SBV M-UTR (8A/A-9A/A), resulting in the first 11 residues of OROV M-UTR being changed to those of SBV (Figure 3.3.6.A). A minigenome assay using this plasmid resulted in loss of UTR functionality with OROV L-N proteins and a decreased efficiency of UTR functionality with SBV L-N proteins (Figure 3.3.6.B; 8A/A 9A/A). A similar approach using the SBV M-minigenome was then carried out, where the first 11 residues of SBV M-UTR were altered to mimic OROV M-UTR (8A/T-9C/A), however this did not result in rescue of luciferase activity for OROV L-N (Figure 3.3.6.B; 8T/A 9C/A). To test whether the terminal 11 nucleotides are sufficient for promoter activity, an OROV M-minigenome containing only the terminal 5' and 3' 13-nucleotides was generated (Table 2.5; plasmid generated using In-Fusion HD Cloning, Clontech). This new minigenome was not functional with either OROV or SBV L-N (Figure 3.3.7.A). The length of the 3' UTR of orthobunyaviruses vary considerably (Dunn *et al.*, 1994; Elliott & Blakqori, 2011), and amongst the viruses focused on in this study AKV has the shortest 5' UTR, only 22 nucleotides (Figure 3.3.7.B). Previous work has demonstrated that the minimum requirement for a viable BUNV S segment mutant is a 22 nucleotide 5' UTR, with at least 112 nucleotides at the 3' terminus (Lowen & Elliott, 2005).

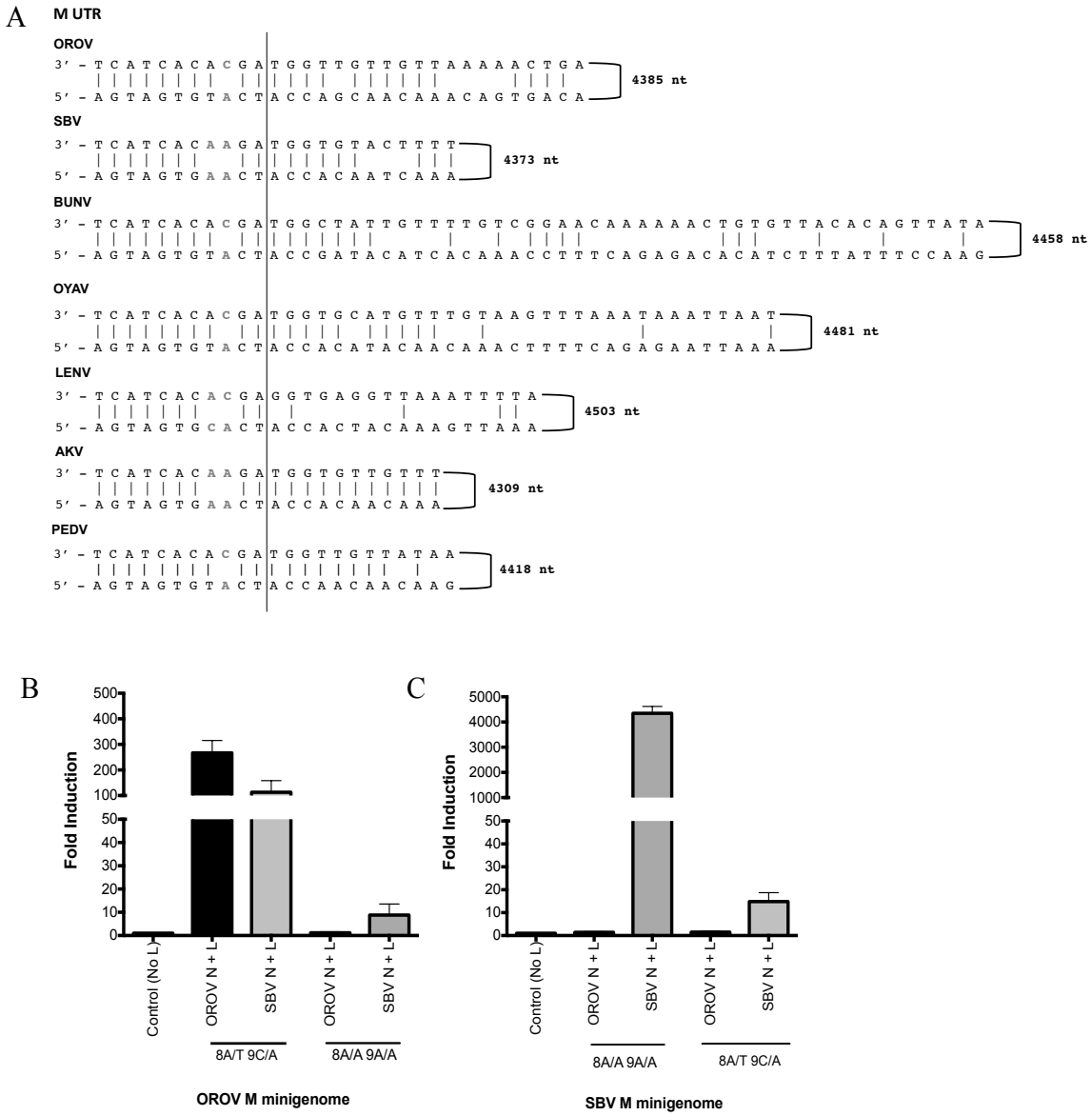

Figure 3.3 6. Analysis of the Simbu M UTR.

(A) Sequence comparison of the 3' and 5' panhandle nucleotides of the M segments of viruses OROV (GenBank accession no, KP052851, this PhD), SBV (Elliott *et al.*, 2013), BUNV (GenBank accession no, NC_001926), OYAV (GenBank accession no, JX983193), LENV (GenBank accession number, HM627176), AKV (GenBank accession no, NC_009895) and Perdoes virus (GenBank accession no, KP691628, this PhD). (B) and (C) Minigenome assays. Performed as described above. Error bars indicate SD (n = 3).

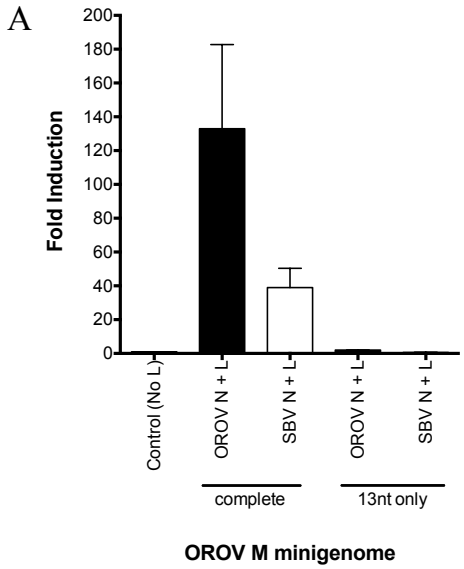

B

```
                                        20                                  40
AKV 5' UTR      AGTAGTGAAC TACCACAACA AA--------  ----------  ----------  ------ 22
SBV 5' UTR      AGTAGTGAAC TACCACAATC AAA-------  ----------  ----------  ------ 23
Perdoes 5' UTR  AGTAGTGTAC TACCAACAAC AAG-------  ----------  ----------  ------ 23
LENV 5' UTR     AGTAGTGCAC TACCACTACA AAGTTAAA--  ----------  ----------  ------ 28
OROV 5' UTR     AGTAGTGTAC TACCAGCAAC AAACAGTGAC A---------  ----------  ------ 31
OYAV 5' UTR     AGTAGTGTAC TACCACATAC AACAAACTTT TCAGAGAATT AAA-------  ------ 43
BUNV 5' UTR     AGTAGTGTAC TACCGATACA TCACAAACCT TTCAGAGACA CATCTTTATT TCCAAG 56
```

Figure 3.3 7. Analysis of the terminal UTR nucleotides.

(A) OROV M-minigenome activity with complete or only 13 terminal-nucleotides. Performed as previously described. Error bars represent SD (n=3). (B) Conservation and diversity of the 5' terminus of Simbu viruses: AKV, SBV, Perdoes virus, LENV, OROV, OYAV and BUNV.

3.3.6 Analysis of SBV L UTR

Next, the L segment UTR sequences were analysed. Interestingly, the L UTRs of viruses OROV, SBV, BUNV, AKV, OYAV, LENV and Perdoes virus in contrast to their M UTRs contain identical nucleotides in the first 11 positions (Figure 3.3.8.A). The L UTR of SBV and AKV do not contain the 8A/A-9A/A "double-mismatch" at positions 8 and 9 that are present in their M UTR (Figure 3.3.6.A). This double mismatch is also present in the S segment of these viruses (Figure 3.3.9). The L UTR of SBV and AKV consist of the "typical" 8A/T 9C/A "pairing/mismatch" similar to OROV, BUNV, OYAV and Perdoes virus (Figure 3.3.8.A). Hence, the SBV L segment promoter was tested for its functionality with OROV or BUN L-N proteins. First, an SBV L-minigenome plasmid was generated using a similar approach as described in Chapter 3, Section 2 (Table 2.5). The previously described SBV L segment plasmid was used as a template (Elliott *et al.*, 2013). SBV L-minigenome (designated as TVT7RSBVLRen(-)) was then tested for functionality in a minigenome assay as previously described. Interestingly, OROV and BUNV L-N proteins were able to transcribe and replicate SBV L-minigenome (Figure 3.3.8.B). These results demonstrate that, in contrast to SBV M UTR (Figure 3.3.2), the L and N proteins of OROV are capable of recognising and using SBV L UTR as a promoter.

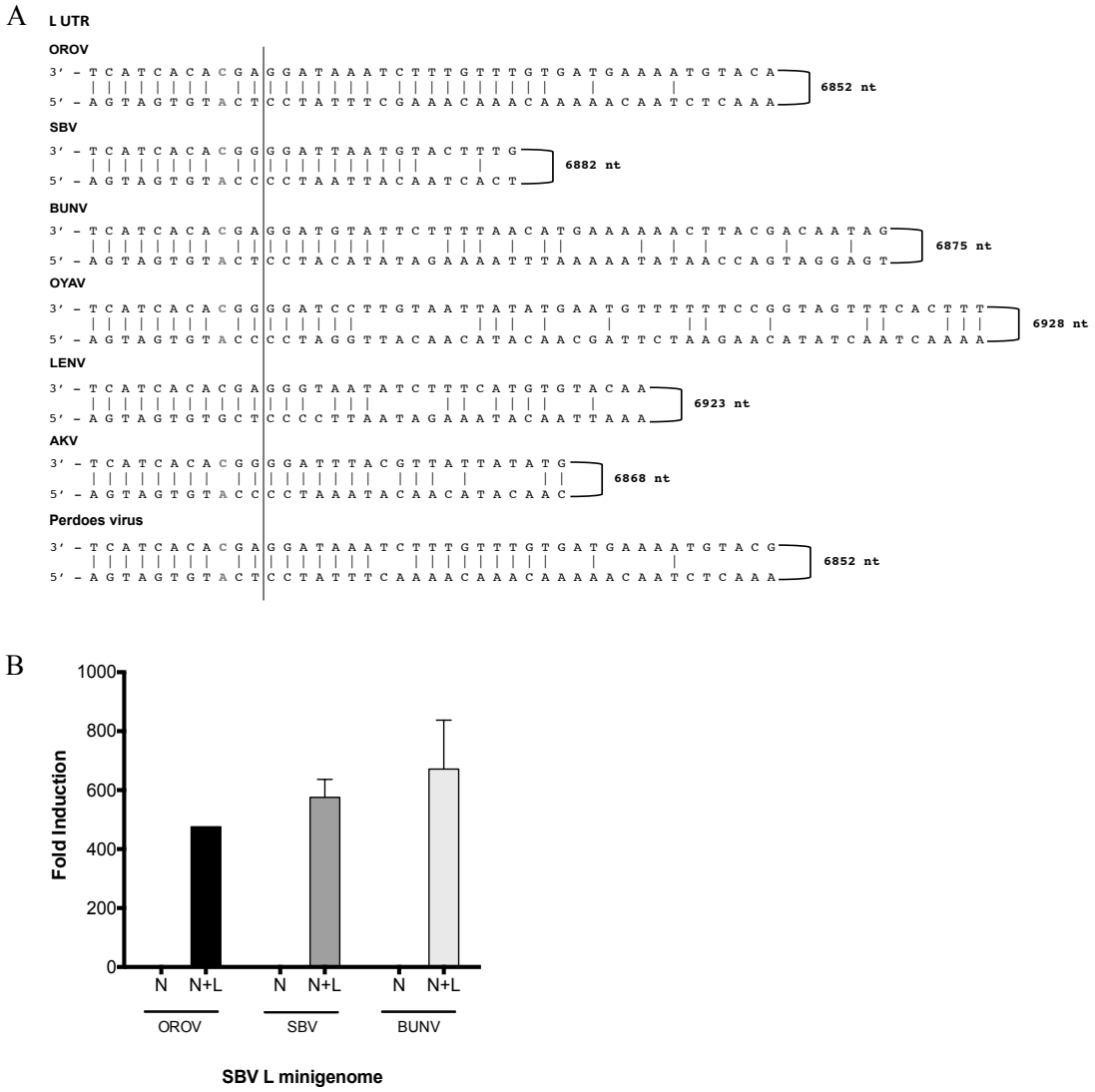

Figure 3.3 8. Analysis of Simbu L segment UTRs.

(A) Sequence comparison of the 3' and 5' panhandle nucleotides of the L segments from viruses OROV (GenBank Accession no. KP052850; this study), SBV (Elliott *et al.*, 2013), BUNV (GenBank Accession no. NC_001925), OYAV (GenBank Accession no. JX983194), LENV (GenBank Accession no. HM627178) and Perdoes virus (GenBank Accession no. KP691627). (B) Minigenome assays. BSR-T7/5 cells (24-well plate) were transfected with OROV N-L, or SBV N-L, or BUN N-L (250 ng), and TVT7RSBVLRen(-) (125 ng) and pTM1-FF-Luc (40ng). At 24 h p.t luciferase activity was measured and calculated as described above. Error bars indicate SD (n = 3).

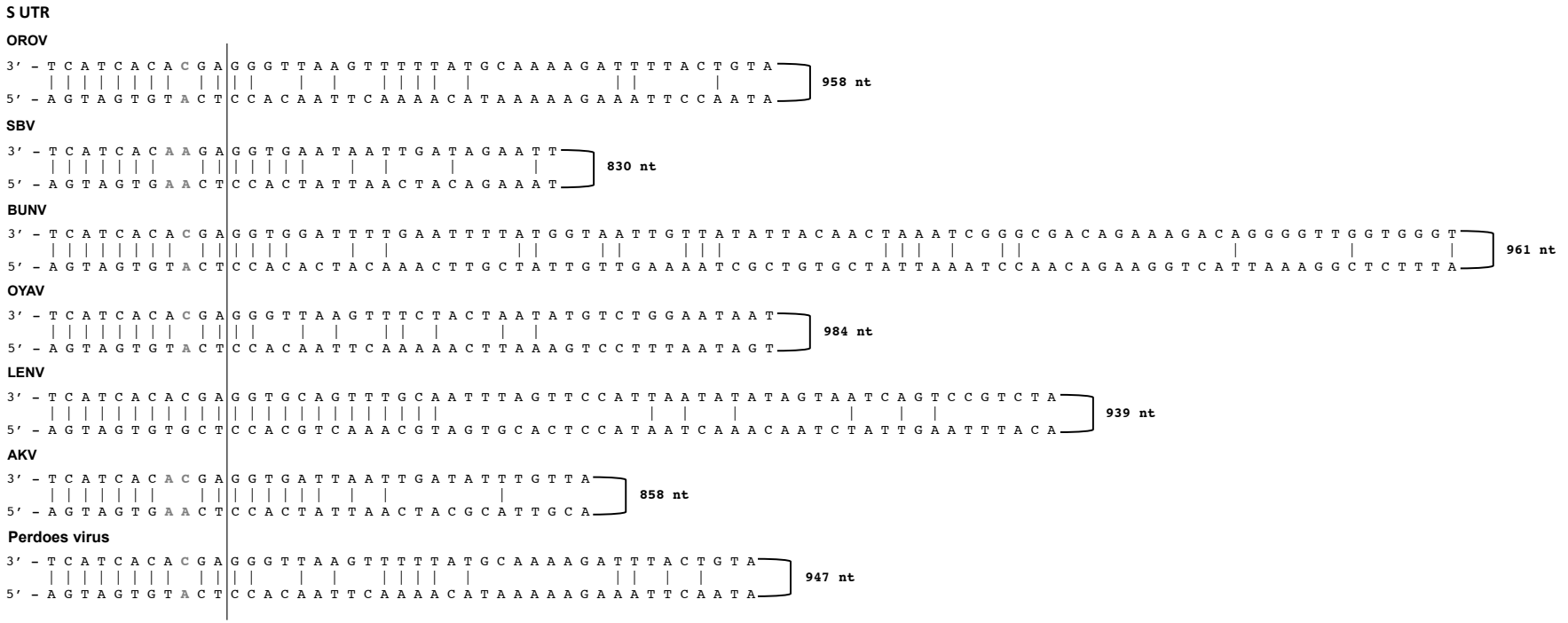

Figure 3.3 9. Analysis of Simbu S segment UTRs.

(A) Sequence comparison of the 3’ and 5’ panhandle nucleotides of the S segments from viruses OROV (GenBank Accession no. KP052852; this study), SBV (Elliott *et al.*, 2013), BUNV (GenBank Accession no. NC_001927), OYAV (GenBank Accession no. JX983192), LENV (GenBank Accession no. HM627177) and Perdoes virus (GenBank Accession no. KP691629).

3.3.7 Analysis of minigenome activity within the Simbu serogroup

In order to further investigate the importance of the M segment UTRs in genomic reassortment, M-minigenomes for Simbu viruses AKV, LENV, OYAV and Perdoes virus were generated. The activity of these minigenome plasmids were then assessed using SBV, OROV or BUNV L and N proteins.

AKV minigenome (pTVT7AKVMRen(-)) was generated as previously described in Chapter 3, Section 2, using a plasmid containing the entire AKV M segment (a gift from Professor Massimo Palmarini, MRC-University of Glasgow, Centre for Virus Research; Table 2.6). Due to the unavailability of viral stocks or plasmids containing genomic sequences for LENV, OYAV and Perdoes virus, an alternate approach to generating minigenome plasmids for these viruses was adopted. To facilitate this, the 3' M UTR of LENV, OYAV or Perdoes virus were added to the 3' end of a negative-sense oriented *Renilla* ORF by PCR amplification. As the 3' UTRs of these viruses are considerably long, at least two PCR reactions were required in order to anneal all viral sequences. The successfully amplified PCR product was circularized and confirmed by sequencing. The resulting plasmid was then used as a template in order to insert the 5' UTR sequences at the other end of *Renilla* ORF in a similar approach (Figure 3.3.10). Oligonucleotides were based on sequences in GenBank (Figure 3.3.6.A; Table 2.6). These plasmid were designated as pTVT7LENMRen(-), pTVT7OYAMRen(-) and pTVT7PEDMRen(-).

Minigenome assays for AKV, LENV, OYAV, Perdoes virus, as well as BUNV were carried out using the L and N proteins of OROV, SBV and BUN. BSR-T7/5 cells were transfected as previously described, and reporter activity detected at 24 h p.t. OYAV and Perdoes virus M-minigenomes were functional with OROV, SBV and BUN L-N (Figure 3.3.11), however reporter activity from AKV M-minigenome could only be detected with SBV L-N (Figure 3.3.11.B). The results also demonstrate that OROV and SBV L-N can transcribe and replicate BUNV M-minigenome (Figure 3.3.11.A and B), whilst BUNV L-N can transcribe and replicate OROV and SBV M-minigenomes (Figure 3.3.11.C). Interestingly, no reporter activity was detected from the LENV M-

minigenome (Figure 3.3.11). The M UTRs of LENV varies from OROV and SBV at positions 8 and 9, as described above (Figure 3.3.6) and determining the activity of this promoter and its relationship to other orthobunyaviruses is beyond the scope of this study.

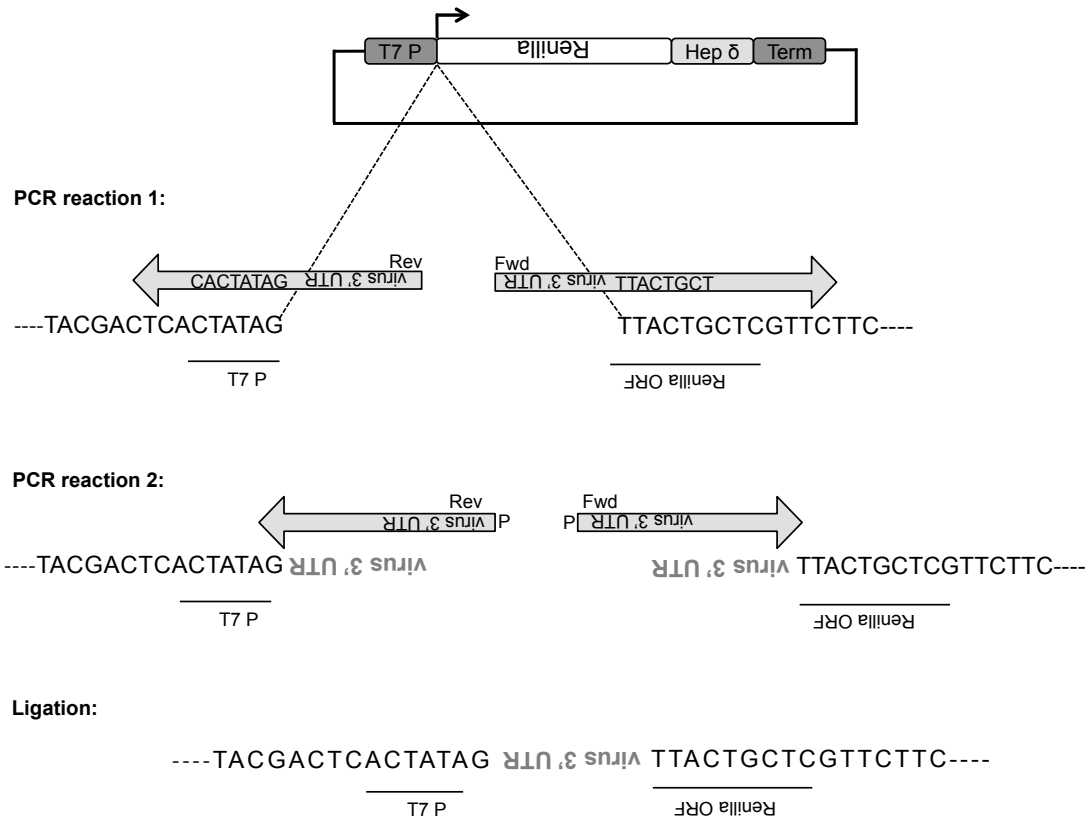

Figure 3.3 10. Schematic representation of cloning strategy used for LENV, OYAV and Perdoes virus M-minigenomes.

Plasmid template contained *Renilla* luciferase gene in a negative-sense orientation. PCR reaction 1, linearised this plasmid annealing viral UTR sequences, which was then used as a template in PCR reaction 2. The ends of the linearised plasmid were then ligated and confirmed by sequencing. This circularised plasmid now containing the 3' viral UTR sequences at the 5' end of the complementary *Renilla* ORF was then used as a template in order to insert the 5' viral UTR sequences, in a similar manner. P, promoter; Hep δ, hepatitis delta ribozyme; Term, T7 terminator; Rev, reverse primer; Fwd, forward primer; seq, sequence; P, phosphorylation.

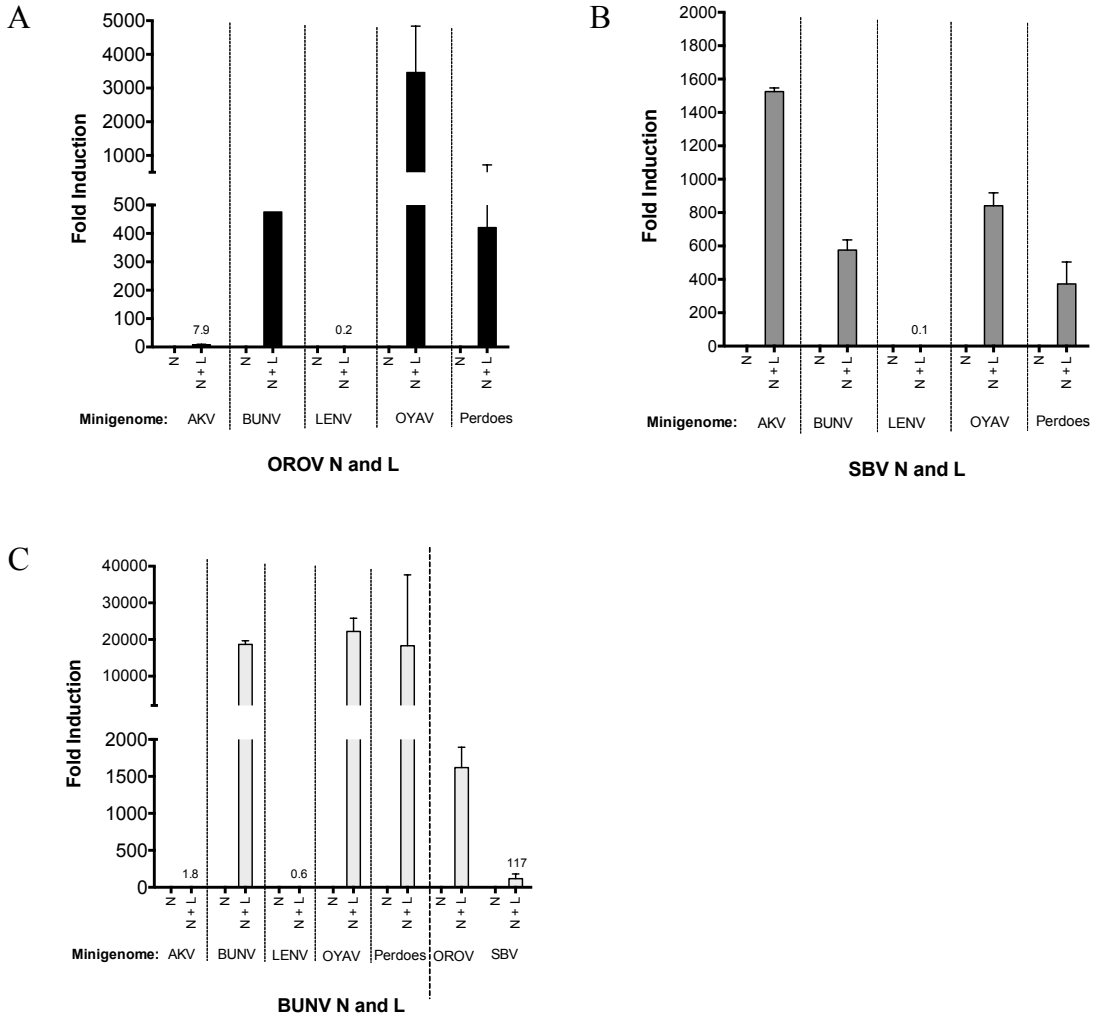

Figure 3.3 11. Simbu M-Minigenome comparison

(A), (B) and (C) BSR-T7/5 cells (24-well plate) were transfected with pTM1-N and/or pTM1-L (250 ng) and M-minigenome (125 ng) plasmids. Firefly luciferase-expressing pTM1-FF-Luc (25 ng) served as a transfection control. *Renilla* and firefly luciferase were measured using a Dual-Luciferase Reporter Assay kit (Promega) 24 h.p.t. Luciferase values were normalized. Minigenome-activity expressed as fold-induction over background control (no pTM1-L). Error bars indicate SD (n = 3).

3.3.8 Discussion

Segmented viruses carry the potential for genomic reassortment, an intriguing characteristic as this allows these viruses to generate new strains and new virus species. This phenomenon on occasions can result in acquisition of new or increased pathogenic characteristics, and hence understanding molecular determinants driving reassortment can be beneficial for predicting the emergence of a new virus. Additionally, the information gathered from studying reassortment may be applied to vaccine development. There are currently no vaccines available for any member of the *Orthobunyavirus* genus, and vaccines based on attenuated viruses carry the risk of reverting back to pathogenicity due to genetic exchange with naturally circulating wild-type strains. Hence, understanding factors that drive reassortment will allow such vaccines to be implemented effectively.

Using a minigenome system the current study focussed on SBV and OROV, two important Simbu viruses of veterinary and public health importance. As expected *Renilla* luciferase activity was detected when OROV L-N were used in combination with OROV M-minigenome, and similarly SBV L-N with SBV M-minigenome, demonstrating the specificity of the assay (Figure 3.3.2). Surprisingly, *Renilla* activity was also detected when SBV L-N were used with OROV M-minigenome, but not the contrary (Figure 3.3.2). To confirm the minigenome results a VLP assay was then carried out. Bunyavirus assembly and budding occurs via interactions between the Gn cytoplasmic tail (CT) and the RNP (Shi *et al.*, 2007; Strandin *et al.*, 2013), hence this forms another important restricting factor for the emergence of new reassortant viruses. The VLP data demonstrated that OROV glycoproteins and SBV-based RNPs are capable of forming infectious VLPs, whilst SBV glycoproteins were unable to form transmissible/entry-competent VLPs with OROV-based RNPs (Figure 3.3.5.A, OROVN+OROVL+SBVN). These results are important as (i) they can be taken as a confirmation that the minigenome assay results are valid (ii) supports the hypothesis that reassortant SBV-OROV viruses could potentially be generated, and (iii) indicates that the possible reassortant virus arising from a co-infection with OROV and SBV would comprise of OROV M segment and SBV S and L segments, and no other combination. The L and S segments encode the L and N proteins, and these function

together to replicate the viral genome and form RNPs (Elliott, 2014; Gerlach *et al.*, 2015; Iroegbu & Pringle, 1981). This reinforces the hypothesis that reassortant viruses containing an L and an S segment from different viruses are not viable, and reassortants are only possible between orthobunyavirus species encoding highly conserved L and N proteins which allow recognition of the genome segment UTR sequences.

Interestingly, the results from this work also revealed that AKV M UTR was only functional with SBV L and N. AKV and SBV are both ruminant viruses and contain 8A/A-9A/A "double-mismatch" at positions 8 and 9, in contrast to 8A/T-9C/A "pairing/mismatch" present in OROV, BUNV, OYAV and Perdoes virus. It is also interesting that the L and N proteins from SBV exhibited a broader range of UTR recognition by successfully transcribing and replicating AKV, OROV, BUNV, OYAV and Perdoes virus minigenome segments, unlike OROV or BUNV (Figure 3.3.2 and Figure 3.3.11). This indicates that even though closely related viruses may share a degree of conservation in their L and N proteins, it is the secondary structure of the M UTR that drives their interaction. This is further proved by the fact that the L and N proteins from the distantly related Bunyamwera serogroup BUNV can recognize OYAV, Perdoes virus and OROV M UTRs (Figure 3.3.11C). The terminal 11 nucleotides of the SBV and AKV L segment UTRs are identical to the other viruses, and surprisingly unlike the M UTR it is functional with OROV and BUNV L and N. By mutating the 8^{th} and 9^{th} nucleotides of OROV M-minigenome (8A/T-9C/A) to mimic the residues of SBV M-UTR (8A/A-9A/A) OROV L-N proteins lost their ability to recognize and transcribe their own OROV M-promoter, whilst the efficiency of SBV L-N also decreased (Figure 3.3.6B). This is interesting because the downstream sequences in the OROV M-minigenome were unchanged, proving that residues 8 and 9 are important for specific interaction between the viral polymerase and nucleocapsid, as previously seen (Dunn *et al.*, 1995; Kohl *et al.*, 2004a; Acrani *et al.*, 2014). Further, changing SBV M-minigenome (8A/A-9A/A) to mimic OROV M-UTR (8A/T-9C/A), with the rationale that if positions 8 and 9 of the M UTRs are determinants for promoter activity, then maybe changing the SBV M-minigenome at these positions would allow OROV L-N proteins to transcribe and replicate this minigenome. However, this was not the case (Figure 3.3.6C; OROV N+L, 8T/A 9C/A), and interestingly reporter activity

also decreased with SBV L-N (Figure 3.3.6C, SBV N+L, 8T/A 9C/A). These results further indicate that although these two residues are essential for the UTR panhandle sequence to function as a promoter, sequences beyond these residues are specific for promoter activity. Previous work on BUNV has shown that mutant viruses lacking large portions of the UTR close to the coding-regions are highly attenuated due to diminished gene regulation (Lowen *et al.*, 2005; Lowen & Elliott, 2005; Mazel-Sanchez & Elliott, 2012). The difference between M UTR nucleotide positions 8 and 9 of the Clade A and Clade B Simbu viruses is intriguing, and it is tempting to speculate that these two residues may play a part in determining reassortment. The availability of complete orthobunyavirus sequences would be beneficial to allow a comprehensive analysis of this region and determine if there is any relevance towards the virus host species.

During bunyavirus co-infections there are theoretically eight potential genome combinations: AAA, ABA, BAA, AAB, BBA, ABB, BAB, BBB (where AAA and BBB are parental viruses and the combination arranged as SML segments). The results from this study demonstrate that OROV L and N proteins are unable to use SBV M promoter, but they can use SBV L promoter. This would suggest that OROV L and N could replicate and transcribe SBV L -, but not SBV M -segment. However, this activity is inconsequential in the viral life-cycle as SBV L protein is functionally incompatible with OROV N protein, and thus any reassortant containing OROV M and S segment with SBV L would be non-viable. Therefore, while there is a degree of plasticity between different orthobunyavirus species in recognition of the L UTR, it plays no role in driving generation of novel species through genomic reassortment. This means that the sole determinant of whether two orthobunyavirus species are capable of generating a novel reassortant virus is based on recognition of the M UTRs in virus A by the L and N proteins of virus B. Using OROV and SBV as an example, it is likely that any reassortant progeny virions would contain SBV S - and L -segments with either SBV M - or OROV M - segment, since SBV L and N proteins can use both OROV and SBV promoters to replicate. However, if the reassortant contains OROV S and L segments, the only possible M segment in this case would be from OROV, because OROV cannot use SBV M UTR as a promoter. Based on these findings, out of the eight possible reassortants between OROV and SBV there may in fact be only one potential viable

progeny, i.e. a virus with S and L from OROV and M from SBV. All the other possibilities are lost, due to the compatibility restrictions between heterologous L and N proteins and the RNA-template. Therefore, even though OROV L and N can use SBV L UTR, this would not make a difference. These results imply that the number of possible reassortants in nature may not be as vast as thought, and that reassortment may in fact be restricted to the M segment alone.

Both OROV and SBV are transmitted by *Culicoides* midges, which have a wide geographic distribution (Carpenter *et al.*, 2013). The spread of SBV outside of Europe is a threat to the cattle farming industry, and in a setting such as Brazil, if geographic boundaries are broken, the possibility of OROV and SBV replicating in the same vector population could arise, with the risk of reassortment. Arboviral reassortants have been reported to arise in arthropod vectors, and it has been suggested that these insects could have played a major role in the evolution and emergence of RNA viruses (Dudas & Obbard, 2015; Li *et al.*, 2015). The emergence of a new reassortant virus containing SBV L and S segments and OROV M segment could potentially be a cause for SBV spillover into the human population.

In 1995 Dunn *et al.* demonstrated by a similar minigenome-based assay that BUNV and Batai virus proteins could interact with each other (Dunn *et al.*, 1995). In 1997 a large outbreak of hemorrhagic fever was reported, a result of a reassortant called Ngari virus, a progeny of viruses BUNV and Batai (Briese *et al.*, 2006). Minigenome and VLP based assays serve as important tools to study various aspects of the bunyavirus life cycle, without the need to rescue the virus. However, such work is only possible when complete and correct sequences are available. There are currently only a handful of complete 3’ and 5’ terminal sequences for bunyaviruses publically available and several others contain errors. This work reinforces the need to review these sequences prior to use in molecular virology assays, as discussed previously in Chapter 3, Section 2.

3.3.9 Summary

1. OROV and SBV may be capable of reassortment, with a potential progeny consisting of OROV M segment and SBV L and S segments.
2. Heterologous L and N proteins are unable to efficiently function together.
3. The M UTR may be a contributing factor for genomic reassortment amongst orthobunyaviruses.

Chapter III. Results

Section 4: Generation of recombinant Oropouche viruses lacking the non-structural proteins NSm or NSs

3.4.1 Introduction and Aims

The lack of a reverse genetics system for OROV has, until now, limited research on this virus at a molecular level, and hence the focus of my PhD has been on addressing this issue. Chapter 3, Section 2, of this thesis describes the establishment of a minigenome and VLP system for OROV. In this Section I report the recovery of infectious OROV, entirely from cDNA plasmids made in Section 2.

To date, a number of bunyaviruses have been rescued and these include BUNV (Bridgen & Elliott, 1996), LACV (Blakqori & Weber, 2005), RVFV (Ikegami *et al.*, 2006), AKV (Ogawa *et al.*, 2007), SBV (Elliott *et al.*, 2013; Varela *et al.*, 2013), SFTSV (Brennan *et al.*, 2015), UUKV (Rezelj *et al.*, 2015) and CCHFV (Bergeron *et al.*, 2015). The work presented in this section is a step forward towards understanding another important yet neglected bunyavirus.

3.4.2 Recovery of wild-type OROV strain BeAn 19991

Chapter 3, Section 2 described the cloning of full-length antigenomic sense cDNA copies of OROV L, M and S segments into the T7 RNA polymerase-driven plasmid backbone pTVT7R(0,0) (Johnson *et al.*, 2000). This plasmid contains a single G residue immediately downstream of the T7 promoter sequence to aid efficient transcription. cDNA copies of the virus genome segments were cloned into pTVT7R in the antigenomic sense. To recover infectious OROV BSR-T7/5 cells (Buchholz *et al.*, 1999) were transfected with 1 μg of the pTVTOROVL, pTVTOROVM and pTVTOROVS plasmid. Supernatant was harvested 7 days p.t. when CPE was visible and success of the rescue attempt was determined by titration of infectious virus by

plaque assay. The rescue of OROV was easily reproducible, yielding titres of 2.0×10^7, 4.5×10^6 and 2.3×10^7 PFU/ml in three independent experiments. Control cells transfected with only pTVTOROVM and pTVTOROVS did not give rise to infectious virus. To test the authenticity of the recombinant OROV (rOROV), permissive Vero E6 cells were infected with the rescue supernatant (Figure 3.4.1.A) and cell extracts used for Western-blotting (Figure 3.4.1.B). Furthermore, rOROV infected Vero E6 cells were fixed and stained at 24 h p.i. using a polyclonal anti-OROV antibody (a kind gift from Professor Luiz Tadeu Moraes Figueiredo, University of Sao Paulo School, Brazil). Substantial amounts of cytoplasmic OROV protein were detectable in the infected cells (Figure 3.4.1.C) further confirming the successful recovery of infectious OROV.

The growth kinetics and plaque phenotype of rOROV was similar to that of the authentic wild-type (wt) virus (Figure 3.4.2). All experiments from this point on were carried out with rOROV.

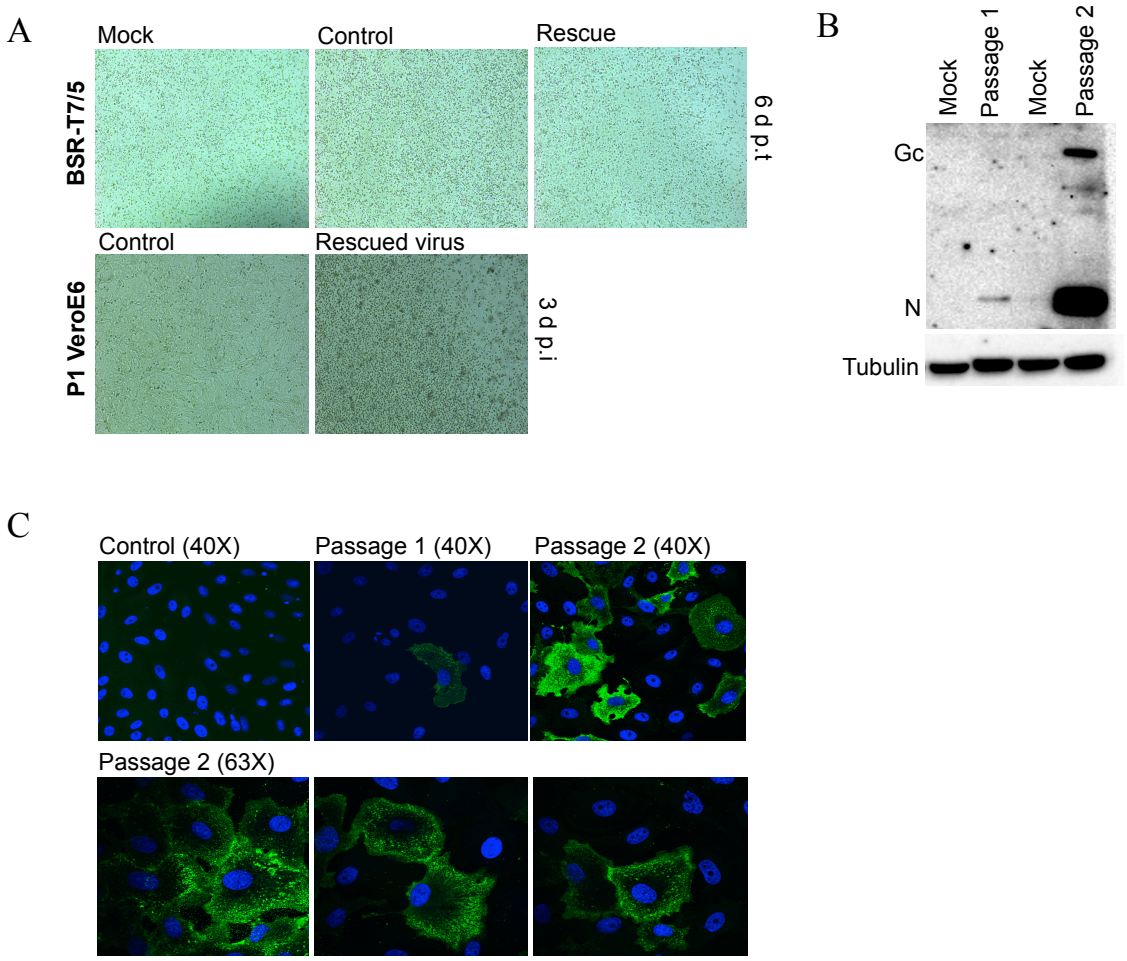

Figure 3.4. 1. Rescue of recombinant OROV strain BeAn19991.

(A) Bright-field microscopy of cell monolayers (10X magnification). Top panels show BSR-T7/5 cells mock-transfected, or transfected with pTVTOROVM and pTVTOROVS (Control) or pTVTOROVL, pTVTOROVM and pTVTOROVS (Rescue). The bottom panel shows cells infected with either the Control or Rescue supernatants from the top panel. (B) Western-blotting. Cell extracts from rOROV-infected or mock-infected Vero E6 cells at passage 1 and 2 were probed for viral proteins using polyclonal anti-OROV. (C) Immunofluorescent detection of OROV proteins. Vero E6 cells grown on glass cover slips were infected with either passage 1 or 2 of rOROV. Control was from the rescue experiment that lacked the L segment. At 24 h p.i cells were fixed and stained with polyclonal anti-OROV (green). Coverslips were mounted with Movial containing DAPI (Vector Laboratories).

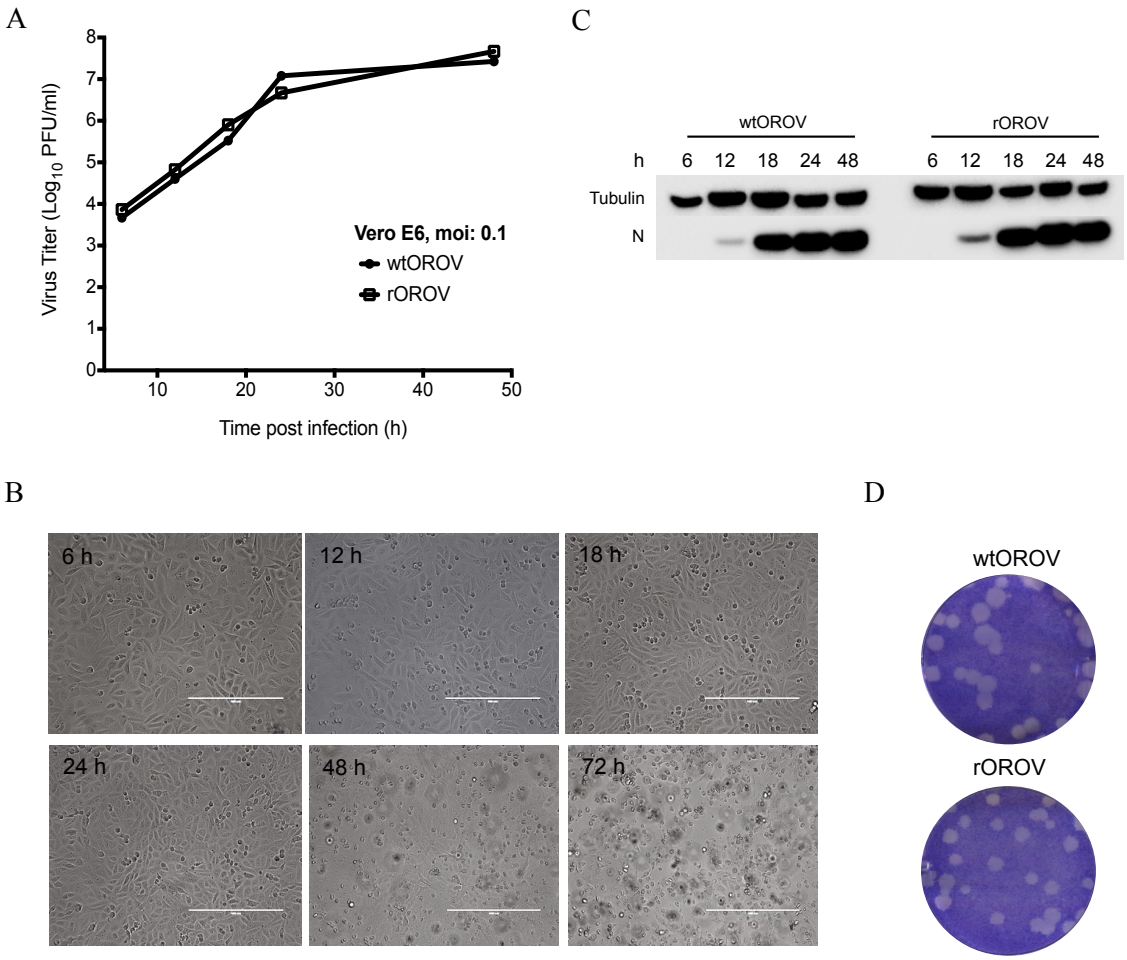

Figure 3.4. 2. Growth comparison of recombinant OROV with the wild-type virus.

(A) Growth properties of wild-type (wt) and recombinant (r) OROV in Vero E6 cells. Cells were infected at MOI 0.1. At indicated time points samples were harvested and titres determined by plaque assay on BHK-21 cells. Graph is a representative experiment. (B) Bright-field microscopy (10X magnification) of Vero E6 cell monolayers infected with OROV (only rOROV shown). (C) Western blot showing N protein synthesis from the growth curve (A). Tubulin was probed as a loading control. (D) Comparison of plaque phenotypes of wtOROV and rOROV. A plaque assay was carried out on BHK-21 cells and at 3 days p.i cells were fixed and stained with crystal violet.

3.4.3 Growth of recombinant OROV in mammalian cell lines

The growth properties of rOROV were tested in Vero E6 cells at MOIs ranging from 0.0001 to 1 PFU/cell. Previous work from our group has demonstrated that some viruses show a better fitness in certain cell types and at different MOIs possibly due to the efficiency at which defective-interfering particles are generated (Elliott *et al.*, 2013; Brennan *et al.*, 2014). rOROV grows to similar titres by 48 h p.i at all MOIs tested (Figure 3.4.3.A), and in a wide range of cell-lines derived from several species (MOI 0.001; Figure 3.4.3.B), similar to other bunyaviruses (Elliott *et al.*, 2013; Brennan *et al.*, 2014). Lower titres were obtained in human cell-lines 2fTGH and HeLa compared to A549 cells, as well as in CPT-tert, QT-35 and MRK101 cell-lines, however due to the specific aims of the current study this was not investigated further. rOROV forms plaques on rodent, monkey, human and sheep cell-lines that were investigated (Figure 3.4.3.C). At 3 days p.i in BHK-21 cells rOROV plaques were larger than in the other cell-lines, and on A549 cells the plaques were harder to visualise (Figure 3.4.3.C). Based on these results, BHK-21 cells were chosen for virus titration. rOROV also produces clear plaques on BHK-21 cells as early as 2 days p.i when titrated in a 12-well culture dish (Figure 3.4.3.D). Based on these findings of rOROV, Vero E6 and A549 cell-lines were chosen for the purpose of initial characterisation of all recombinant viruses in this study. Vero E6 and BHK-21 cells both lack fully functional IFN systems (Desmyter *et al.*, 1968; Emeny & Morgan, 1979; Chinsangaram *et al.*, 1999), whilst A549 cells are IFN competent (Spann *et al.*, 2004).

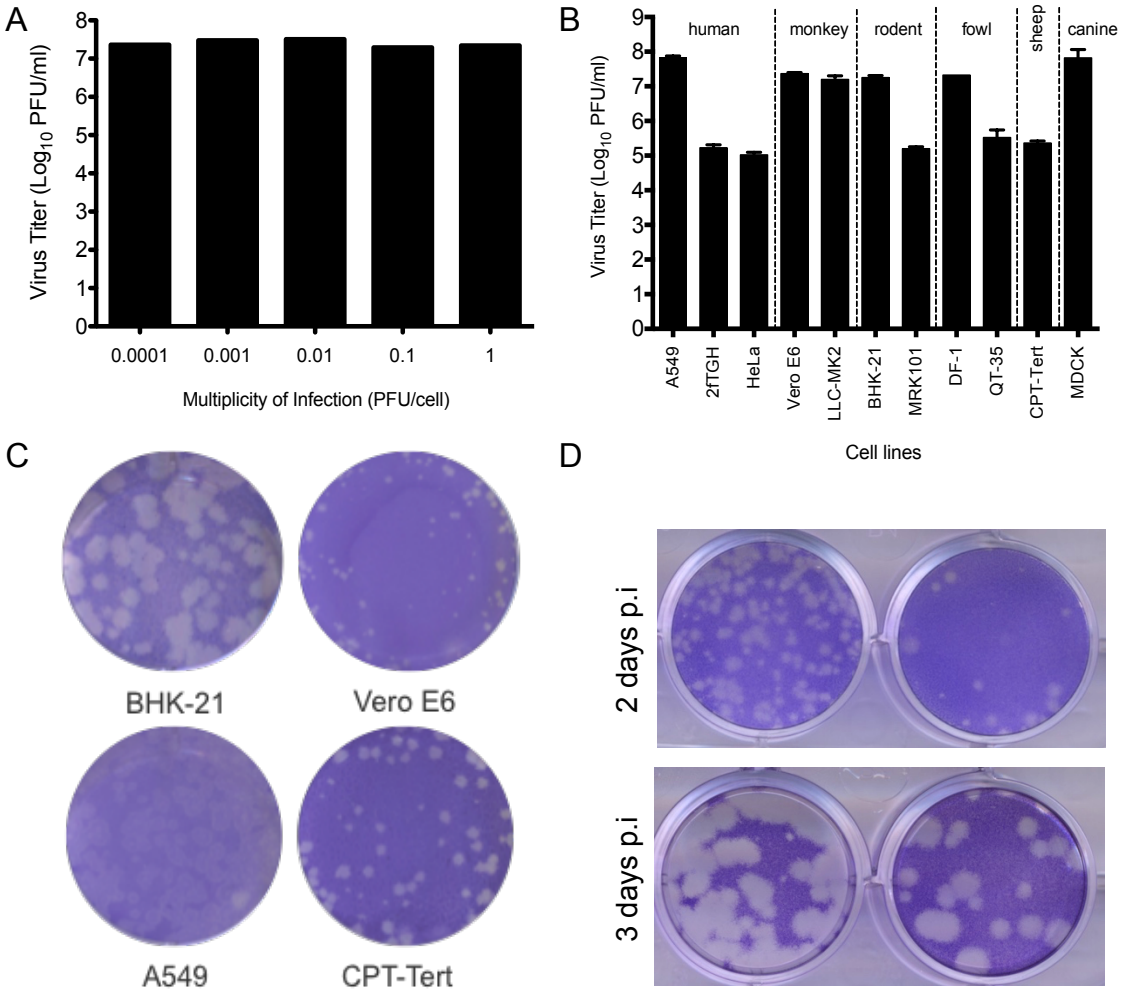

Figure 3.4. 3. Characterization of recombinant OROV.

(A) Effect of different MOI on rOROV yields in Vero E6 cells. Infected cells were harvested 48 h p.i and titrated on BHK-21 cells. Graph is presented for a representative experiment. (B) Comparison of rOROV growth in various cell-lines. Indicated cells were infected at an MOI of 0.001 and at 48 h p.i supernatants were harvested and titrated on BHK-21 cells. Bars represent range from two experiments. (C) Comparison of rOROV plaque phenotypes on BHK-21, Vero E6, A549 and CPT-Tert cells. Infected cells were fixed and stained with crystal violet at 3 days p.i. (D) Comparison of rOROV plaques phenotypes on BHK-21 cells 2 or 3 days p.i. in 12-well plates. Cells are stained with crystal violet.

3.4.4 Generation of OROV mutants

Generation of mutant NSm and NSs plasmids were in collaboration with Dr. Gustavo Olszanski Acrani, University of Sao Paulo.

NSm deletion

A mutant OROV lacking the entire NSm ORF from the M segment was generated. This was done by deleting the entire NSm coding region immediately after the first NSm transmembrane domain (TMD) and predicted cleavage site up to the third TMD, leaving the predicted cleavage site of the Gc protein intact (Figure 3.4.4.A). These sites were predicted using the TMHMM Server v. 2.0 and SignalP 4.1 Server algorithms (www.cbs.dtu.dk) based on work done by Dr. Xiaohong Shi (MRC-University of Glasgow, Centre for Virus Research) for the characterization of orthobunyavirus M segments (Xiaohong Shi and Richard M. Elliott, manuscript submitted). Primers delNSmOROVF/delNSmOROVR (Table 2.7) were designed to bind to positions 1475 – 1498 and 1036 – 1013 of the M segment respectively. This allowed an excision PCR to be performed thereby deleting the entire NSm region, but leaving the first TMD site, so as not to alter the position of the Gc protein in the endoplasmic reticulum and Golgi, during folding. To rescue rOROVdelNSm virus BSR-T7/5 cells were transfected with 1 µg of pTVTOROVL, pTVTOROVS and pTVTOROVdelNSm plasmids. At 7 days p.t when CPE was visible, infectious virus particles were recovered, titrated and sequenced (Source Bioscience) to confirm the mutation (Figure 3.4.4.B and C).

NSs mutants

The following step was the creation of the NSs mutant viruses. As NSs lies in an over-lapping reading frame within the N ORF, the positions at which mutations could be introduced were limited. The NSs ORF of OROV has four in-frame methionines, therefore, in an attempt to abrogate NSs transcription the NSs start codon was left in place and instead a translational stop codon was inserted in-frame immediately after the second methionine at amino acid 17 (Figure.3.4.5.A; 2. rOROVdelNSs). At the nt level this is at position 115 and changes TGG (W) to TAG (stop), resulting in a 48 nt NSs ORF. The reason for this approach was because previous work done on BUNV revealed that when the start codon of NSs was removed the virus was still capable of producing

an NSs protein from a downstream methionine (van Knippenberg *et al.*, 2010). The strategy used in this study for OROV is similar to the one used to create a SBV mutant lacking NSs (Elliott *et al.*, 2013). In addition to this, a C-terminal truncated NSs was also engineered. This was generated by introducing a stop codon at nt position 313 changing TTA (L) to TAA (stop). This results in a 246 nt NSs ORF and a protein sequence of 82 aa compared to wt NSs which is 92 aa (Figure.3.4.5.A; 1. rOROV246NSs). Primers used in generating the plasmids are in Table 2.7. In order to rescue the NSs mutants (named, rOROVdelNSs and rOROV246NSs) BSR-T7/5 cells were transfected with 1 µg of pTVTOROVL, pTVTOROVM and 1.5 µg of the mutant S segment (pTVTOROVdelNSs or pTVTORO246NSs). At 7 days p.t CPE was visible, and infectious virus particles were recovered, titrated and sequenced (Source Bioscience) to confirm mutations, Figure 3.4.5.B.

S-segment mutant

Chapter 3, Sections 1 and 2, report the isolation and sequencing of OROV clinical isolates that differ from the prototype strain (BeAn19991) in the S segment, as they lack 11 nts at position 781 to 791 in the 3' UTR. The encoded NSs ORF of these viruses also contain a tandem AUG translation start codon created by a C-U variation at position 332, and a Gln to Arg change in the NSs ORF at position 89 (Figure.3.4.6.A). To test whether these variations altered the *in vitro* growth properties of the rescued virus, a cDNA plasmid (designated as pTVTOROV2080S) containing the S segment of clinical isolate BeH759025 (Chapter 3, Sections 1; GenBank accession number KP691614) was generated using the same cloning strategy as pTVTOROVS (Chapter 3, Section 2). In order to rescue this S-segment mutant (named rOROV2080S) BSR-T7/5 cells were transfected with plasmids pTVTOROVL, pTVTOROVM and pTVTOROV2080S (1 µg each). At 7 days p.t infectious when CPE was visible virus particles were recovered, titrated and the entire S segment sequenced (Source Bioscience), Figure 3.4.6.B.

All mutant viruses in this study were passaged three times at low MOI in Vero E6 cells and sequenced. Introduced mutations were maintained confirming the stability of these viruses. Subsequent experiments utilised viruses from passage two.

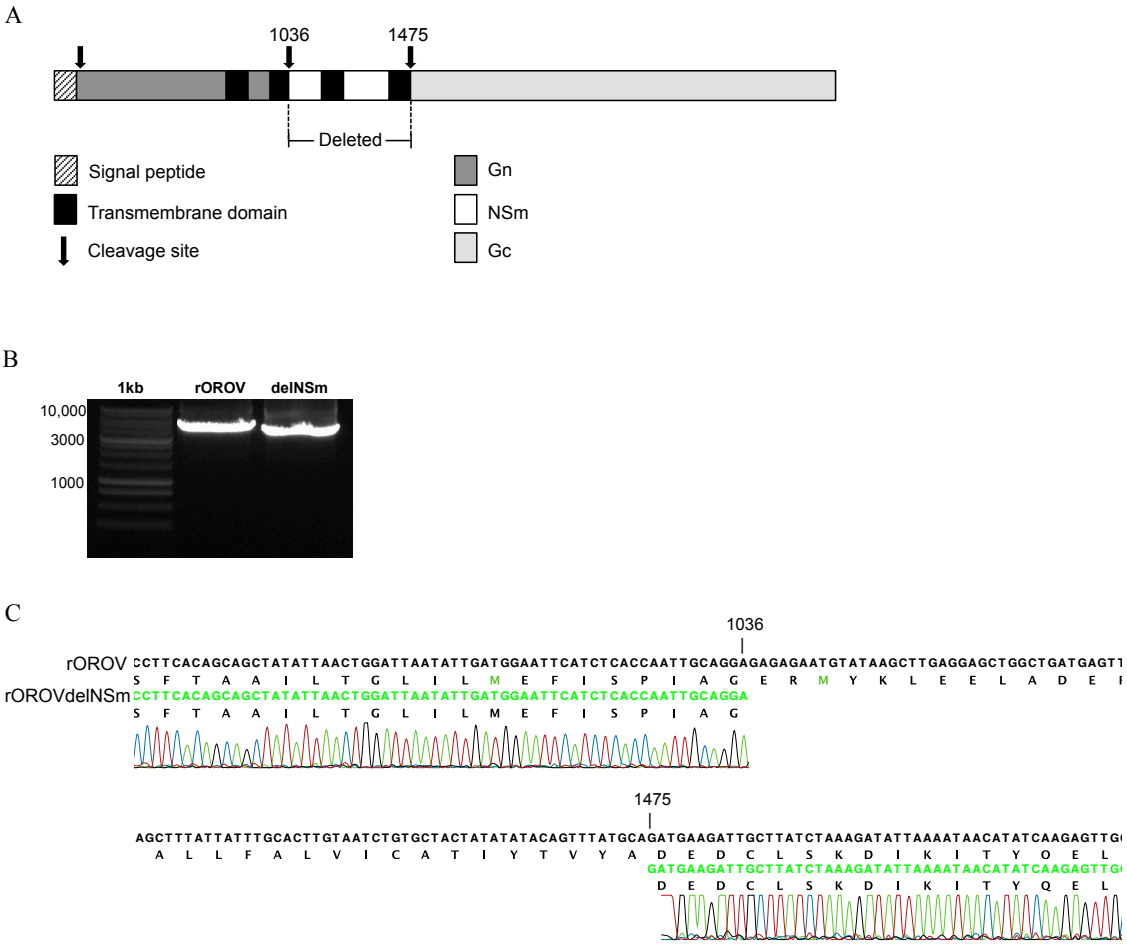

Figure 3.4. 4. Creation of OROV mutant lacking NSm.

(A) Schematic of the M segment showing Gn, NSm and Gc regions. The arrows depict where cleavage occurs. The patterned box indicates the signal peptide and the black boxes represent transmembrane domains. Nucleotides 1036 to 1475 were deleted in order to generate delNSm M segment. (B) RT-PCR of the M segments from rOROV and delNSm viruses grown in Vero E6 cells (passage 2). PCR products were separated on a 1% agarose gel. (C) Chromatograph showing the sequencing results from (B). The nts in black are from rOROV and in green is rOROVdelNSm. Numbers indicate nt position. A, Green; T, Red; G, Black; C, Blue.

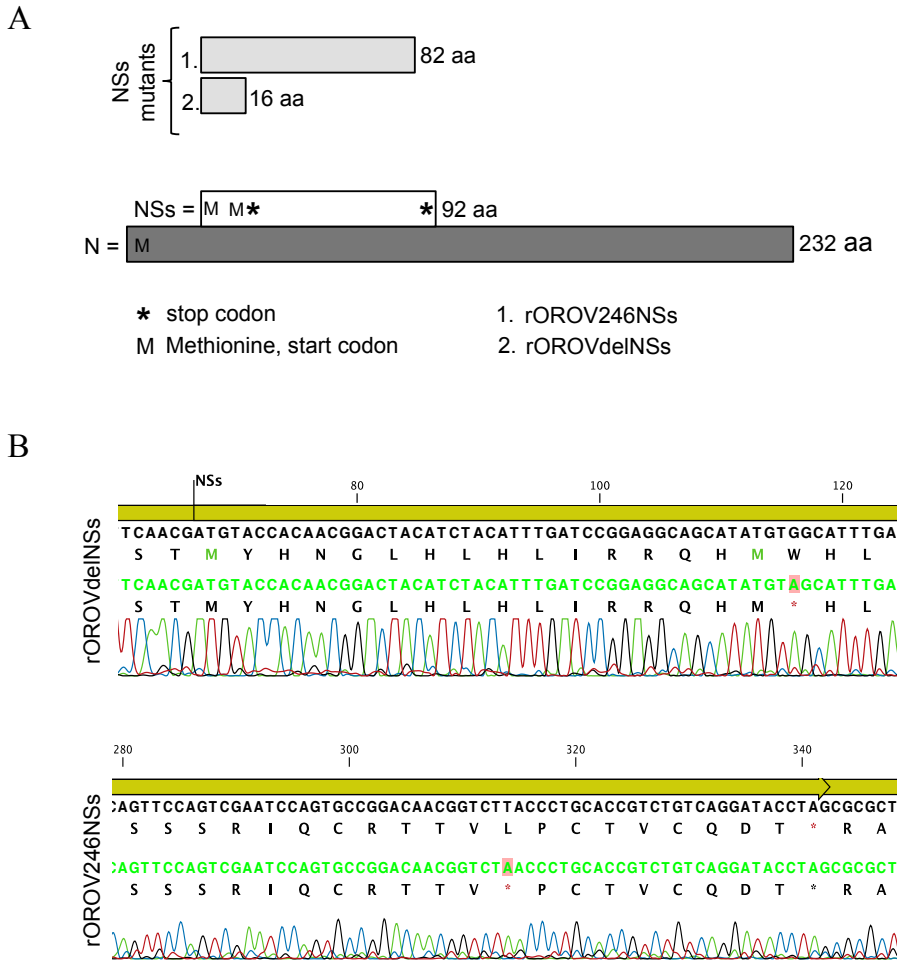

Figure 3.4. 5. Creation of OROV NSs mutants.

(A) S segment products N and NSs. NSs is coded from an overlapping reading frame with N. Schematic shows how NSs mutants differ from wt. rOROV246NSs has a stop codon (asterisk) placed at nt position 314 of S segment cDNA changing TTA to TAA thereby deleting the last nine amino acids. rOROVdelNSs has a stop codon at cDNA nt position 116 changing TGG to TAG so that a stop codon is generated immediately after the second start codon (methionine, M). Numbers are amino acid (aa) lengths. (B) Chromatograph of sequencing results for rOROVdelNSs and rOROV246NSs that were grown in Vero E6 cells (passage 2). The red boxes highlight where mutations were made. A, Green; T, Red; G, Black; C, Blue.

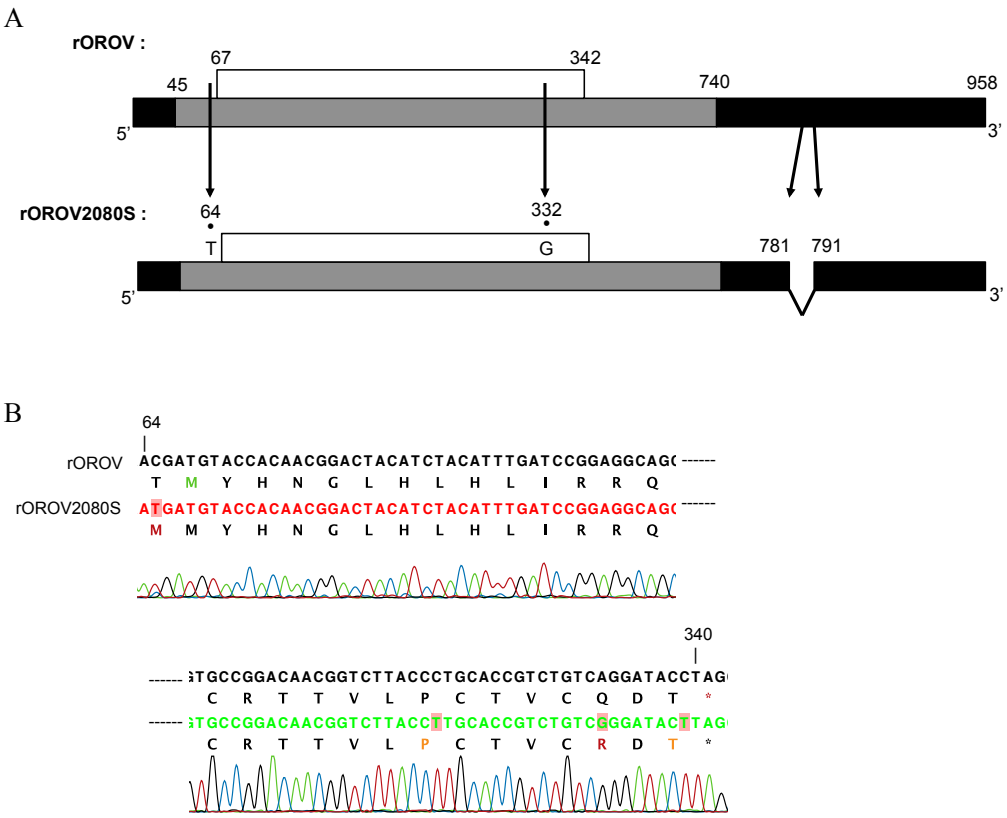

Figure 3.4. 6. Creation of OROV BeAn19991 S-segment mutant.

(A) Schematic showing rOROV2080S S segment in comparison to wt/rOROV S segment. Numbers are nt positions. The grey and white boxes highlight the N and NSs OROF, respectively. The black box highlights the UTR regions. Arrows show where changes occur. First two positions generate a variation in the NSs ORF. (B) Chromatograph showing the NSs region of rOROV2080S. This virus was grown in Vero E6 cells (passage 2). A, Green; T, Red; G, Black; C, Blue.

3.4.5 Growth properties of recombinant viruses in mammalian cell-lines and their effect on host-protein synthesis

Growth kinetics of rOROV, rOROVdelNSm, rOROVdelNSs, rOROV246NSs and rOROV2080S were compared in Vero E6 cells at MOI 0.1. Viruses rOROV, rOROVdelNSm and rOROV2080S replicate with similar efficiency, however mutants rOROVdelNSs and rOROV246NSs appear attenuated and reach titres that are one log lower than rOROV (Figure 3.4.7.A). Western blotting analysis revealed higher amounts of N protein from rOROVdelNSs at earlier time-points, suggesting a possible increased efficiency of the virus to translate N (Figure 3.4.7.B). Plaque morphology of the recombinant viruses was then compared on BHK-21 cells. rOROV, rOROVdelNSm and rOROV2080S produce plaques with a round morphology and are clear and similar to each other. The plaques of viruses rOROVdelNSs and rOROV246NSs on the other hand are smaller with corrugated and ill defined borders (Figure 3.4.7.C).

To investigate whether the recombinant viruses caused inhibition of host-cell protein synthesis Vero E6 cells were infected at MOI 3 and at 12, 24 and 48 h p.i cells were radiolabelled with [^{35}S]methionine. Cell extracts were analysed by SDS-PAGE. rOROV, rOROVdelNSm, rOROV2080S, as well as the rOROVdelNSs and rOROV246NSs demonstrated an ability to cause a shut-off of host translation by 24 h p.i (Figure 3.4.8). It was also observed that the latter two viruses compared to the others produced noticeably more N protein at this time point (Figure 3.4.8). This result also confirmed that the mutant viruses rOROVdelNSm and rOROVdelNSs do not express NSm and NSs proteins respectively, and that the rOROV246NSs virus expresses a truncated version of NSs (Figure 3.4.8).

As rOROV2080S behaves similar to rOROV and rOROV246NSs similar to rOROVdelNSs in terms of *in vitro* replication kinetics, only viruses rOROV, rOROVdelNSm and rOROVdelNSs were focussed on for growth comparison in IFN-competent A549 cells. rOROV and rOROVdelNSm grew with similar kinetics reaching comparable titres, whereas rOROVdelNSs growth appeared more restrictive and at 48 h the viral titres were almost two logs lower than that of rOROV and rOROVdelNSm viruses (Figure 3.4.9.A). Western blot analysis of N expression showed lower amounts

of protein in the rOROVdelNSs-infected cells (Figure 3.4.9.B). Next, the growth of rOROV, rOROVdelNSm and rOROVdelNSs were compared in A549 cells to their growth in IFN-incompetent A549/V cells. These cells express the V protein of parainfluenza type-5 virus thereby blocking type I IFN signalling via STAT1 degradation (Killip *et al.*, 2013). Cells were infected at an MOI of 0.001 and titres measured at 48 h p.i. Cells were also infected with BUNV or a BUNV mutant lacking the NSs protein (rBUNVdelNSs2) for comparison (Bridgen *et al.*, 2001; Hart *et al.*, 2009). All viruses grew to higher titres in the IFN-incompetent cell-line, similar to BUNV. rOROVdelNSs titres were over one log higher in A549/V cells compared to A549 cells, although this difference was not as high as with the rBUNVdelNSs2 virus (Figure 3.4.9.C). Western blot for N confirmed lower levels of expression in A549 cells infected with rOROVdelNSs and rBUNVdelNSs2, corresponding with the yield assay (Figure 3.4.9.D).

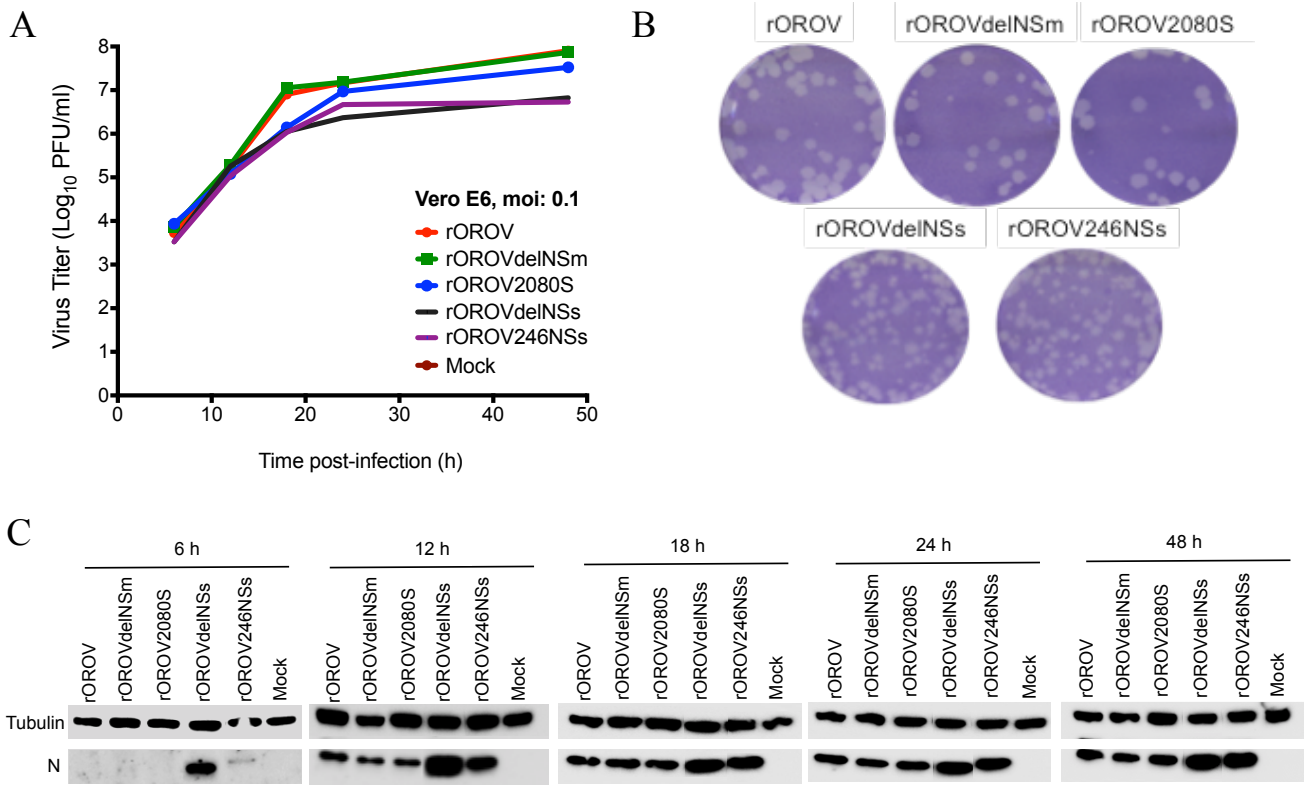

Figure 3.4. 7. Growth properties of recombinant viruses.

(A) Cells were infected at an MOI of 0.1. Samples were harvested at indicated time points and titrated on BHK-21 cells. Representative experiment. (B) N production in recombinant viruses. Cell lysates from growth curve (A) were probed for OROV-N and Tubulin. (C) Plaque phenotype of recombinant viruses in BHK-21 cells. A plaque assay was carried out and at 3 days p.i cells were fixed and stained with crystal violet.

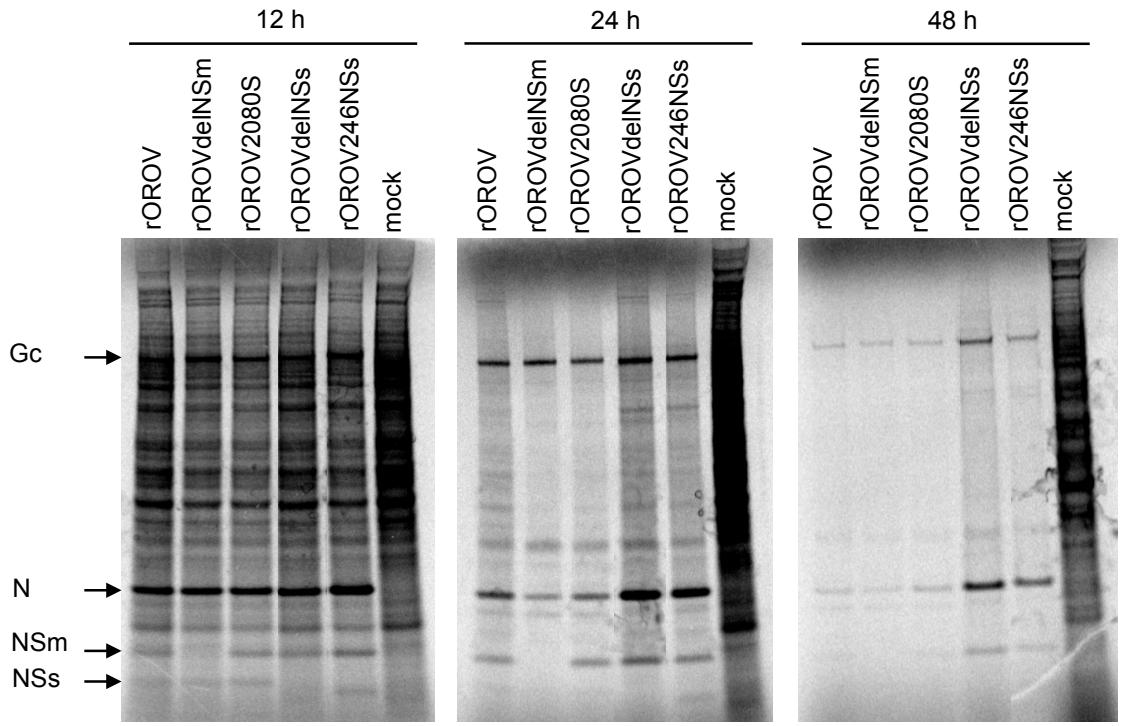

Figure 3.4. 8. Host-cell protein shut-off.

Vero E6 cells were infected with recombinant viruses rOROV, rOROVdelNSm, rOROV2080S, rOROVdelNSs, rOROV246NSs or mock infected. Cells were infected at an MOI of 3 and incubated at 37 °C. At indicated time-points the cells were labelled with [^{35}S]methionine for 2 h. Cells lysates were then separated by SDS-PAGE. Arrows indicate the position of viral proteins Gc, N, NSm and NSs.

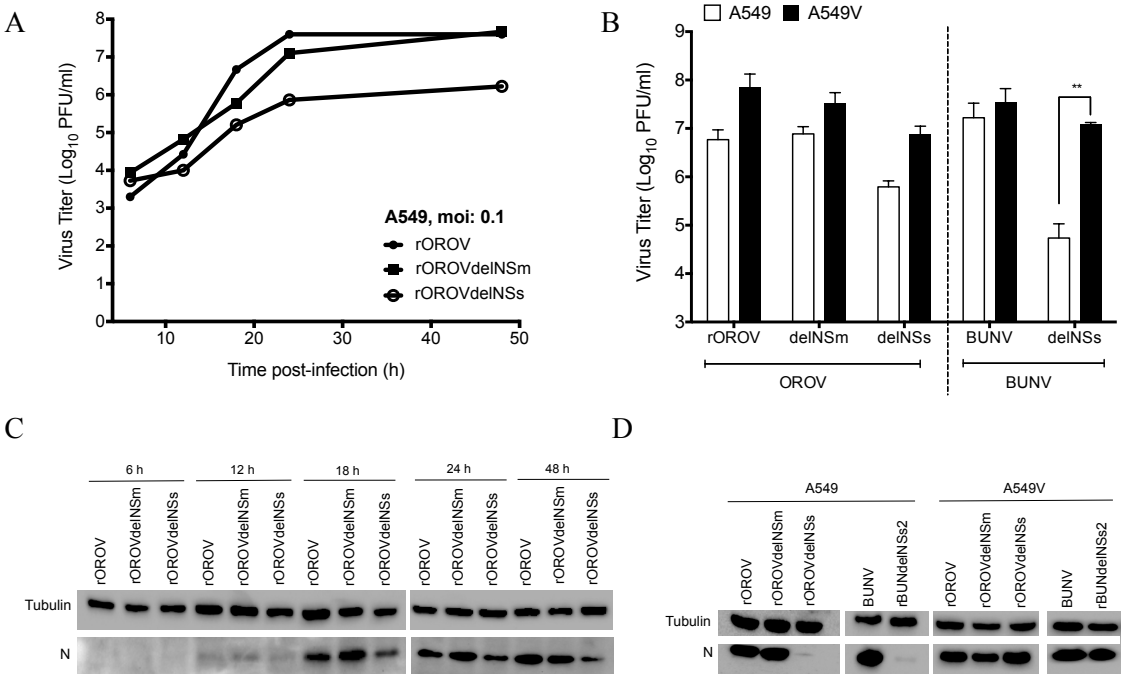

Figure 3.4. 9. Growth properties of recombinant viruses in A549 cells.

(A) Growth kinetics of rOROV, rOROVdelNSm and rOROVdelNSs in A549 cells at an MOI of 0.1. At indicated time-points samples were harvested and viral titres determined by plaque assay on BHK-21 cells. The graph presents results for one representative experiment. (B) Comparison of growth properties in A549 and A549/V cells. Cells were infected at an MOI of 0.001 with indicated viruses. 48 h p.i viral titres were determined by plaque assay. BUNV was used for comparison. Bars indicate SDs (n = 3; **, P< 0.01 by Student's *t* test). (C) Western-blot for cell lysates from growth curve (A). Lysates were separated by SDS-PAGE and probed for OROV N and Tubulin. (D) Western-blot analysis for (B). Cells lysates were probed for viral N protein. Tubulin was probed as loading control.

3.4.6 OROV NSs protein inhibits type I IFN production in A549 cells

IFN production in A549 cells in response to infection with rOROV, rOROVdelNSm, rOROV2080S, rOROVdelNSs or rOROV246NSs viruses at MOI 1 was measured. For comparison cells were also infected with BUNV or rBUNVdelNSs2. At 24 h p.i UV-inactivated virus (4 mins with occasional shaking, 8W, 254 nm) from the supernatant was used to treat A549/BVDV-NPro cells for 24 h. The amount of protection offered to these cells from encephalomyocarditis virus (EMCV) infection was then measured via observation of cytopathic effect (CPE). A549/BVDV-NPro cells cannot produce IFN as they express the IFN antagonist NPro protein from bovine viral diarrhea virus (BVDV), but are still capable of responding to exogenous IFN (Hale *et al.*, 2009). As expected, no IFN was produced from mock or BUNV infected cells, and rBUNVdelNSs2-infected cells produced considerable amounts of IFN. Whilst rOROV, rOROVdelNSm and rOROV2080S induced small amounts of IFN, rOROVdelNSs induced high amounts (Figure 3.4.10.A and B). rOROV246NSs virus that lacks only nine aa at the NSs protein C-terminus, induced IFN to the same extent as rOROVdelNSs (Figure 3.4.10.A and B). Next, we used Western-blotting to probe the A549 cell extracts for STAT1, phosphorylated STAT1 (pSTAT1) and the Interferon Stimulated Gene (ISG) protein MxA. pSTAT1 and MxA expression were detected in cells infected with rOROVdelNSs and rOROV246NSs, but not in cells infected with, rOROV, rOROV2080S and rOROVdelNSm (Figure 3.4.10.C.), confirming that that OROV NSs is an IFN antagonist.

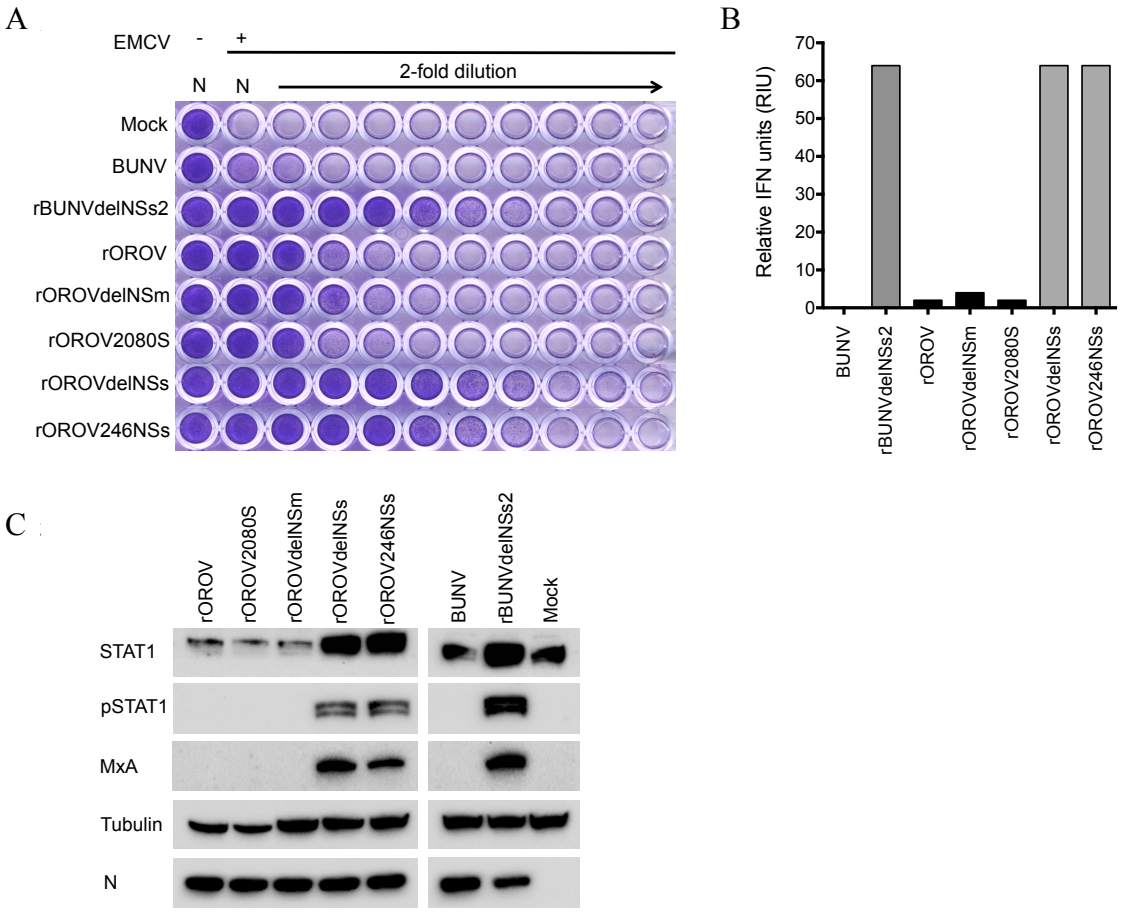

Figure 3.4. 10. Biological interferon production assay.

A549 cells were infected at MOI 1 with BUNV, rBUNdelNSs2, rOROV, rOROVdelNSm, rOROV2080S, rOROVdelNSs, rOROV246NSs or mock infected. Supernatant was harvested at 24 h p.i and cell extracts separated by SDS-PAGE. (A) UV-inactivated supernatant was used to pre-treat A549-N pro cells prior to infection with EMCV. At 3 days p.i cells were fixed and stained with crystal violet. Representative experiment. (B) Graph calculated from (A) and represents relative IFN units (RIU) expressed as 2N where N is the number of 2-fold dilution that offered protection. (C) Cell extracts were probed for OROV N, STAT1, pSTAT1 and MxA. Tubulin was probed as a loading control.

3.4.7 Creation of an additional OROV delNSs mutant

To generate an OROV mutant lacking the NSs ORF a stop codon was inserted immediately after the second in-frame methionine, with the reasoning that ribosomal translation would result in a highly truncated and non-functional peptide without further scanning to produce a protein from a downstream methionine. In addition to this however, another delNSs OROV was also generated. Here, NSs start codon and the second methionine were both mutated and a stop codon inserted at aa 17 (Figure 3.4.11; rOROVdelNSs2) (Table 2.7). This version of OROV delNSs (named rOROVdelNSs2) behaved similar to the original rOROVdelNSs in its growth kinetics and inability to antagonise the IFN system (Figure 3.4.11.B-F). However, at early time points the amount of N protein produced is similar to rOROV and not to rOROVdelNSs. Knippenberg *et al.* previously identified a spontaneous mutant from a stock of recombinant BUNV that was generated to lack the NSs protein. This spontaneous mutant appeared to have introduced a downstream start codon and produce an N-terminally truncated form of NSs (van Knippenberg *et al.*, 2010). If OROV were to produce such an N-terminal truncated NSs it could do so using the third in-frame methionine highlighted in Figure 3.4.11.A. Using SDS-PAGE (18% gel; data not shown) a band corresponding to this truncated NSs protein was not detectable, however it is possible that a potentially unstable protein is translated. This virus was not carried forward for further experimental analysis in this study.

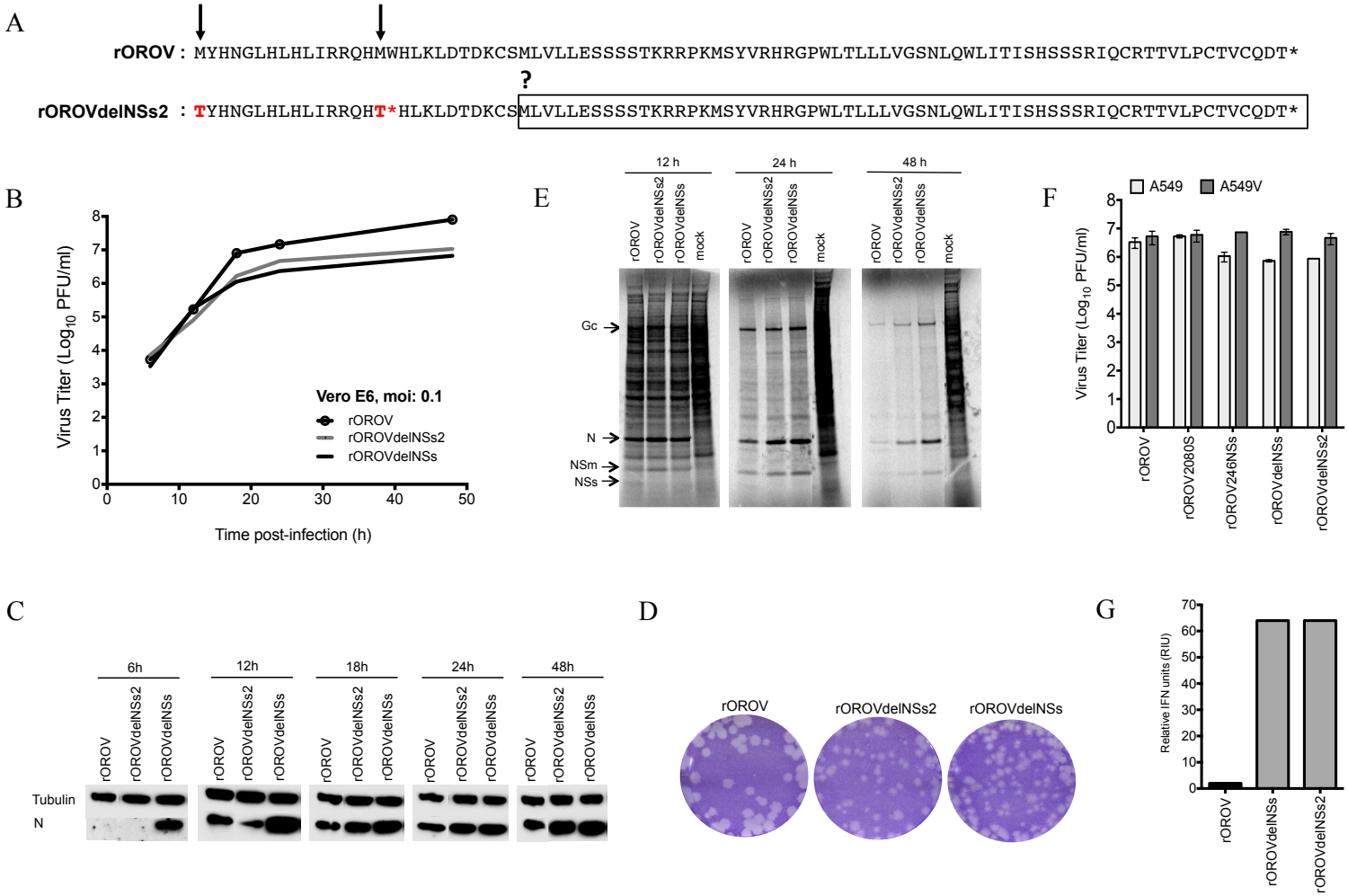
A
rOROV : MYHNGLHLHLIRRQHMWHLKLDTDKCSMLVLLESSSSTKRRPKMSYVRHRGPWLTLLLVGSNLQWLITISHSSSRIQCRTTVLPCTVCQDT*
?
rOROVdelNSs2 : TYHNGLHLHLIRRQHT*HLKLDTDKCSMLVLLESSSSTKRRPKMSYVRHRGPWLTLLLVGSNLQWLITISHSSSRIQCRTTVLPCTVCQDT*
B
Virus Titer (Log10 PFU/ml)
Time post-infection (h)
Vero E6, moi: 0.1
rOROV
rOROVdelNSs2
rOROVdelNSs
E
12 h
24 h
48 h
rOROV
rOROVdelNSs2
rOROVdelNSs
mock
Gc
N
NSm
NSs
F
A549
A549V
Virus Titer (Log10 PFU/ml)
rOROV
rOROV2080S
rOROV246NSs
rOROVdelNSs
rOROVdelNSs2
C
6h
12h
18h
24h
48h
rOROV
rOROVdelNSs2
rOROVdelNSs
Tubulin
N
D
rOROV
rOROVdelNSs2
rOROVdelNSs
G
Relative IFN units (RIU)
rOROV
rOROVdelNSs
rOROVdelNSs2

Figure 3.4.11.

Figure 3.4. 11. Generation and characterization of rOROVdelNSs2 virus.

(A) NSs protein sequence. The arrows show where changes were made to generate rOROVdelNSs2. A stop codon (asterisk) was also inserted after the second start codon (methionine, M). The box and question mark highlight a potential ORF that could be used. (B) Growth kinetics of rOROVdelNSs2 virus in comparison to rOROV and rOROVdelNSs. Vero E6 cells were infected at MOI 0.1. Samples were harvested at indicated time-points and viral titres determined by plaque assay. (C) N production for growth curve (B), where cell extracts were separated by SDS-PAGE and probed for OROV N and Tubulin. (D) Plaque phenotype in BHK-21 cells. Plaque assays were performed and 3 days p.i fixed and stained with crystal violet. (E). Host-protein shut-off in Vero E6 cells. Cells were infected at MOI 3 and at indicated time-points labelled for 2 h with [^{35}S]methionine. Proteins in cells lysates were separated by SDS-PAGE. Gc, N, NSm and NSs proteins are indicated using arrows. (F) Growth comparison in A549 and A549/V cells. Cells were infected with rOROV, rOROV2080S, rOROV246NSs, rOROVdelNSs and rOROVdelNSs2 at MO1 0.001 and harvested at 3 days p.i. Bars indicate range from two experiments. (G) IFN bioassay. A549 cells were infected with indicated viruses at MOI 1 and harvested at 24 h p.i. UV-inactivated media was used to pre-treat A549-NPro in a serial-dilution manner before infecting them with EMCV. Graph represents relative IFN units (RIU) expressed as 2N where N is the number of 2-fold dilution that offered protection.

3.4.8 OROV is less sensitive to IFN-α treatment than BUNV

BUNV replication was previously shown to be highly sensitivity to IFN-α (Streitenfeld *et al.*, 2003). To test if OROV was equally sensitive to INF-α treatment, Vero E6 cells (which cannot produce but can respond to IFN (Desmyter *et al.*, 1968)) were treated with increasing doses of universal type-1 IFN-α (0, 10, 100, 1000 and 10,000U/ml), either pre (-24 or -2 h) or post (+2 or +24 h) infection. Cells were infected with BUNV or rOROV at MOI 0.01 and IFN-α was maintained in the media throughout the infection period. At 48 h p.i the amount of infectious virus in the culture media was determined by plaque assays. Whilst both viruses showed sensitivity to IFN-α, OROV was clearly less sensitive than BUNV (Figure 3.4.12.). For example, pre-treating cells with 10,000 units of IFN-α either 2 or 24 h p.i completely inhibited BUNV replication, as did treating cells with 1000 units at 24 h p.i. In contrast, there was only a 1 to 2 log reduction in the titres of OROV in cells pre-treated for 2 h with 10,000 units of IFN-α prior to infection, and a 3 log reduction in cells pre-treated for 24 h (Figure 3.4.12; rOROV). Whilst pre-treating cells with 1000 units of IFN-α for 24 h pre-infection completely inhibited BUNV (Figure 3.4.12; BUNV), there was only a 2 log reduction in cells infected with OROV (Figure 3.4.12; OROV). Repeating the experiment with rOROV using 10,000 U/ml of IFN-α and at MOIs 0.001 and 0.01 demonstrated that at 24 or 48 h p.i at both MOIs rOROV replication was not completely inhibited, as observed with BUNV, with titres decreased by 2 to 3 logs compared to untreated cells (Figure 3.4.13). rBUNVdelNSs virus displayed similar levels of sensitivity to IFN-α as wt BUNV (Figure 3.4.12; rBUNVdelNSs), and this confirmed previous work (Streitenfeld *et al.*, 2003; Carlton-Smith & Elliott, 2012). Addition of 1000 U/ml of IFN-β to cells 6 h or 12 h post-infection was previously shown to have no effect on BUNV or rBUNVdelNSs titres (Carlton-Smith & Elliott, 2012), however results from this study shown that 1000 U/ml of IFN-α 2 h post-infection and 10,000 U/ml 24 h post-infection appears to completely inhibit rBUNVdelNSs growth (Figure 3.4.12; rBUNVdelNSs). In contrast, rOROVdelNSs virus is not as sensitive as rBUNVdelNSs and is still capable of replicating even at high concentrations of IFN-α (Figure 3.4.12; rOROVdelNSs). As seen in Figure 3.4.7, rOROVdelNSs is attenuated compared to rOROV in Vero E6 cells and by addition of 10,000 IU/ml of IFN-α to these cells prior

to infection further decreases rOROVdelNSs growth by a log (Figure 3.4.12; rOROVdelNSs; -24h), demonstrating that rOROVdelNSs virus is sensitive to the effects of IFN-α similar to the wt virus. However, it appears that the inherent resistance of OROV to IFN-α means that even removing the IFN antagonist does not alter this resistance. Furthermore, these results also demonstrate that the increased resistance of OROV to IFN-α compared to BUNV is not due to expression of a functionally NSs protein. Viruses rOROVdelNSm, rOROV2080S and rOROV246NSs also demonstrate a similar sensitivity to IFN-α as rOROV (Figure 3.4.14.A). Next, pre-treated (1000 U/ml) Vero E6 cells were infected at an MOI of 1 with rOROV or rOROVdelNSs and at various time-points cell extracts were collected. These results further confirm that OROV is sensitive to IFN-α (Figure 3.4.14.B). The plaque morphology on pre-treated Vero E6 cells was also investigated for rOROV and rOROVdelNSs in comparison to BUNV. 1000 U/ml of IFN-α was maintained in the overlay during the infection period. No BUNV or rBUNVdelNSs plaques were observed when the plaques assays were performed in the presence of IFN-α. In contrast, rOROV and rOROVdelNSs plaques were observed in the presence of IFN-α, although they were considerably smaller than those on untreated cells (Figure 3.4.15). Taken together, these results demonstrate that although OROV is sensitive to IFN-α in a dose-dependent manner, it is significantly more resistant than BUNV to IFN-α. Furthermore, the NSs protein is not responsible for this increased resistance.

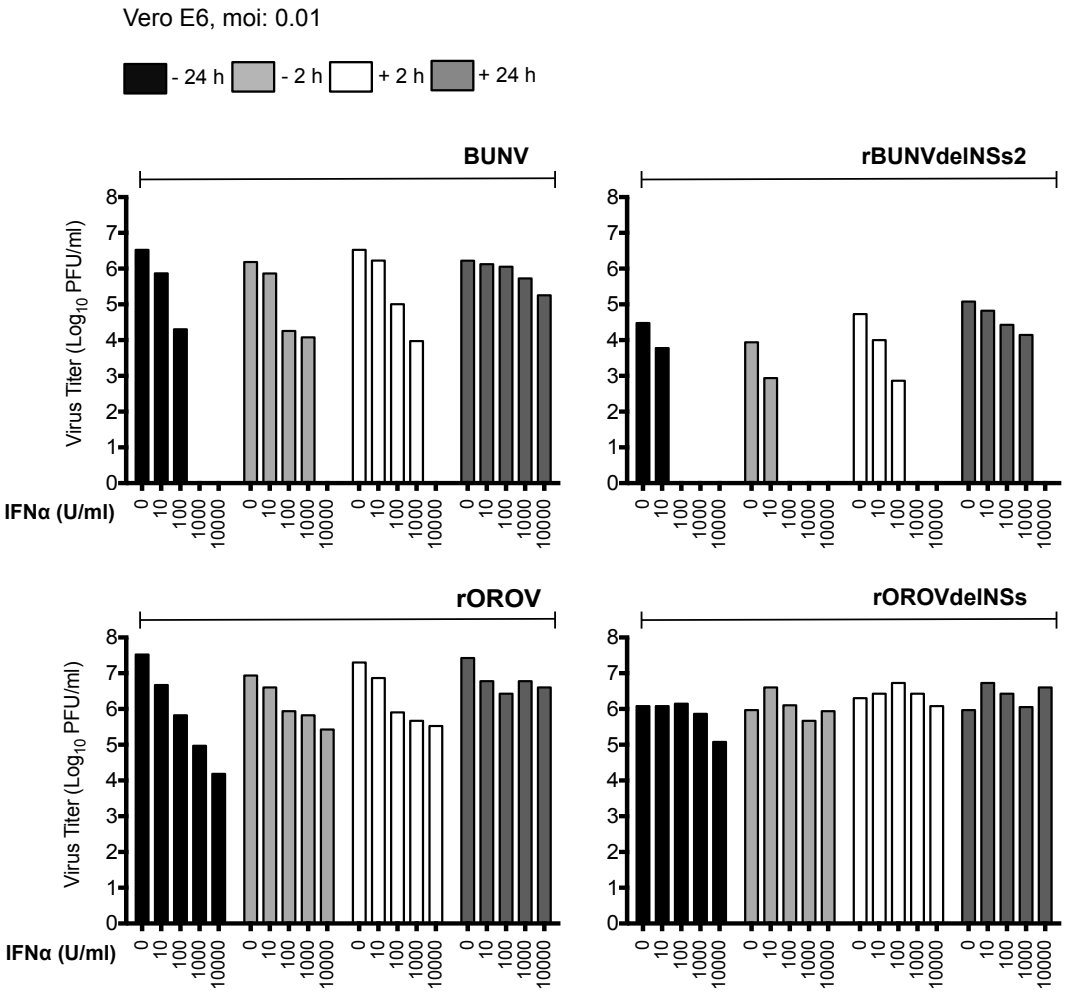

Figure 3.4. 12. Sensitivity of OROV to IFN-α treatment.

Vero E6 cells were treated with an increasing concentration of IFN-α (0, 10, 100, 1000, 10000) either before (-) or after (+) infection. Cells were infected with BUNV, rBUNVdelNSs2, rOROV or rOROVdelNSs at an MOI 0.01. 48 h p.i supernatant was harvested and viral titres determined by plaque assay on BHK-21 cells. Graph shows results of a representative experiment.

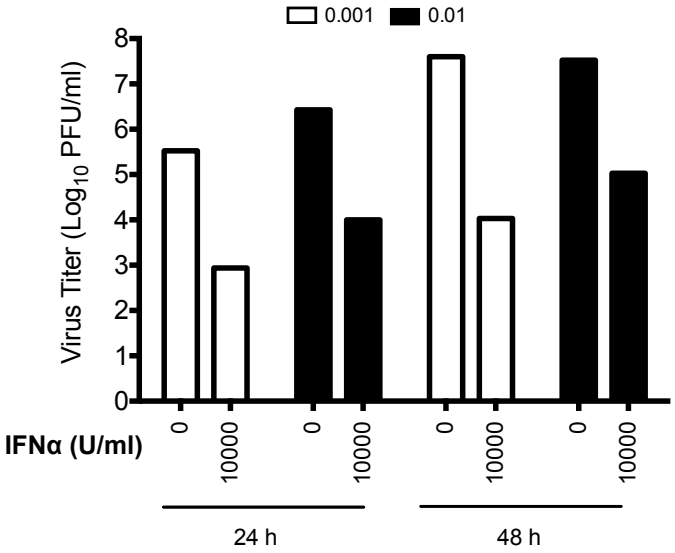

Figure 3.4. 13. Sensitivity of rOROV to IFN-α treatment pre-treatment.

Vero E6 cells were pre-treated for 24 h with 10,000 U/ml of universal type-I IFN-α. Cells were infected with rOROV at an MOI of 0.001 or 0.01, and harvested either at 24 h or 48 h p.i. Viral titres were determined by plaque assay on BHK-21 cells. Graph is a representative experiment.

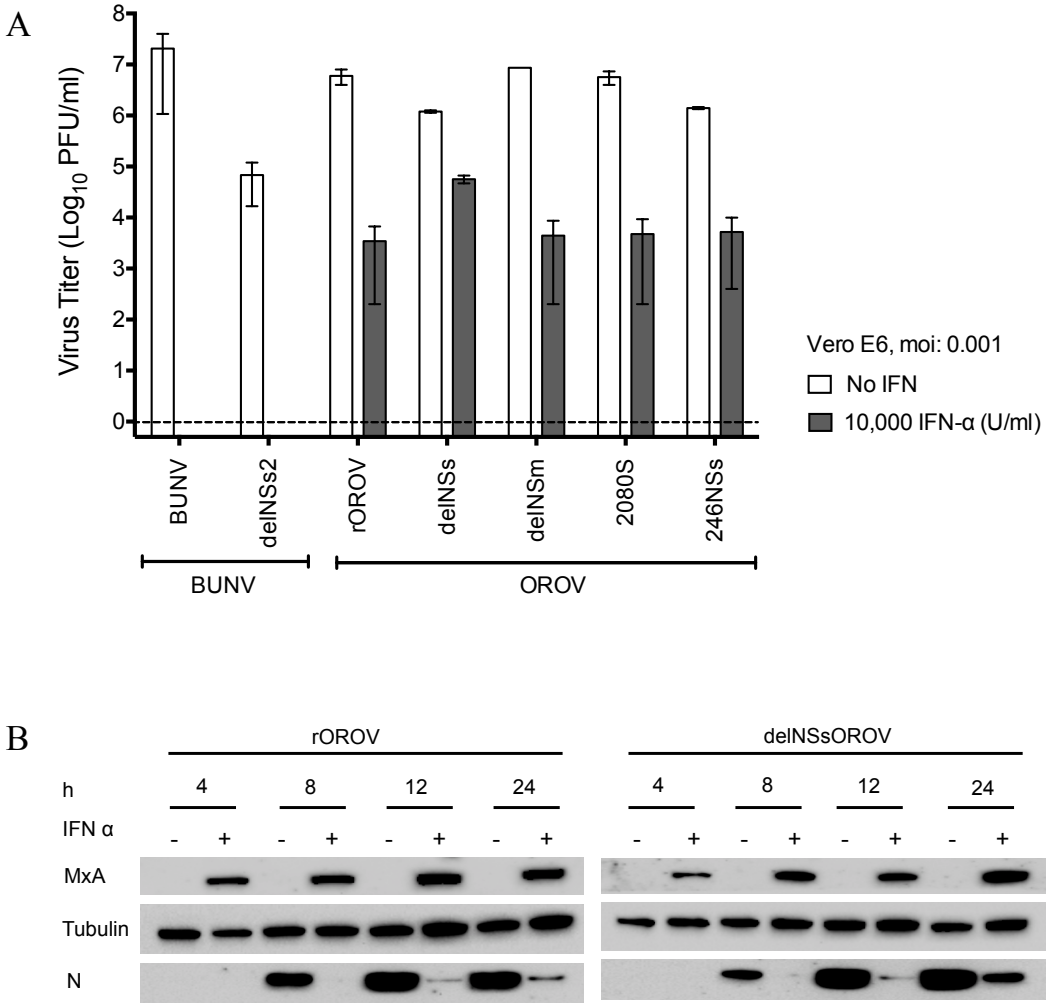

Figure 3.4. 14. OROV recombinants and IFN-α.

(A) Vero E6 cells were treated with 10,000 U/ml of IFN-α 24 h prior to infection with indicated viruses; at an MOI of 0.001. Samples were harvested at 48 h p.i and viral titres determined by plaque assay on BHK-21 cells. Bars represent range from two experiments. (B) N production in IFN-α treated cells. Vero E6 cells were pre-treated (+) 24 h prior to infection with 1000 U/ml of IFN-α, or left untreated (-). Cells were infected with rOROV or delNSsOROV at MOI 1. At indicated time points lysates were extracted and a western blot performed. Samples were probed for OROV N, MxA and Tubulin.

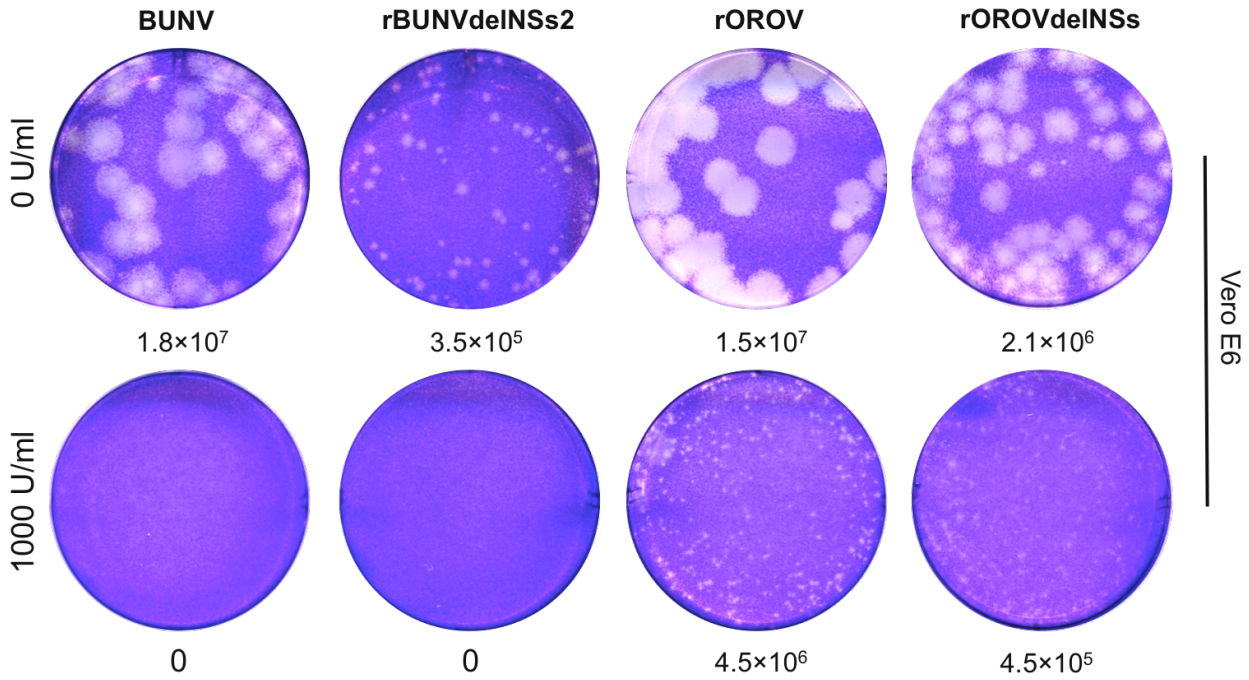

Figure 3.4. 15. Plaque phenotype in IFN-α treated cells.

Vero E6 cells were treated (1000 U/ml) or untreated (0 U/ml) with IFN-α 24 h prior to infection. A plaque assay for BUNV, BUNVdelNSs2, OROV or delNSsOROV viruses was performed. 4 days p.i cells were fixed and stained with crystal violet.

3.4.9 Replication of rOROV in ISG-expressing cell-lines

Vero E6 derived cell-lines constitutively expressing ISGs of human (EDH4, HK2, IFITM3, ISG20, IRF1, NOS2A, SCO2) or macaque (ISG20, LGAS59, RHO3) origin along with an empty control vector (Empty) were supplied by Mr. Jungie Feng (MRC-University of Glasgow, Centre for Virus Research) as part of a collaboration into investigating the effects of various ISGs on different bunyaviruses. To test OROV replication each cell-line was infected with rOROV at MOI 0.001 and at 48 h p.i samples were harvested and titres determined by plaque assay on BHK-21 cells. On control cells rOROV grew to a titre of 3.3 x10^6 PFU/ml (Figure 3.4.16.A; Empty), titres were over two logs lower in ISG20 expressing cells of human origin and two log lower in the ISG20 cell-line of macaque origin (Figure 3.4.16.A; ISG20Hs and ISG20Mm). EDH4 and IRF1 expressing cells demonstrated over one log reduction in viral titres (Figure 3.4.16.a; ED4Hs and IRF1Hs). Western-blotting for presence of N confirmed viral replication (Figure 3.4.16.B). Next, the plaque morphologies of rOROV on these ISG-expressing cell-lines were investigated. At 4 days p.i rOROV plaques on the control cells were clear, round and distinct (Figure 3.4.17; Empty). In comparison the ISG20 expressing cell-lines, in particular of human origin produced smaller, but clear plaques, whilst EHD4 and IFITM3 cells produced very indistinct rOROV plaques (Figure 3.4.17).

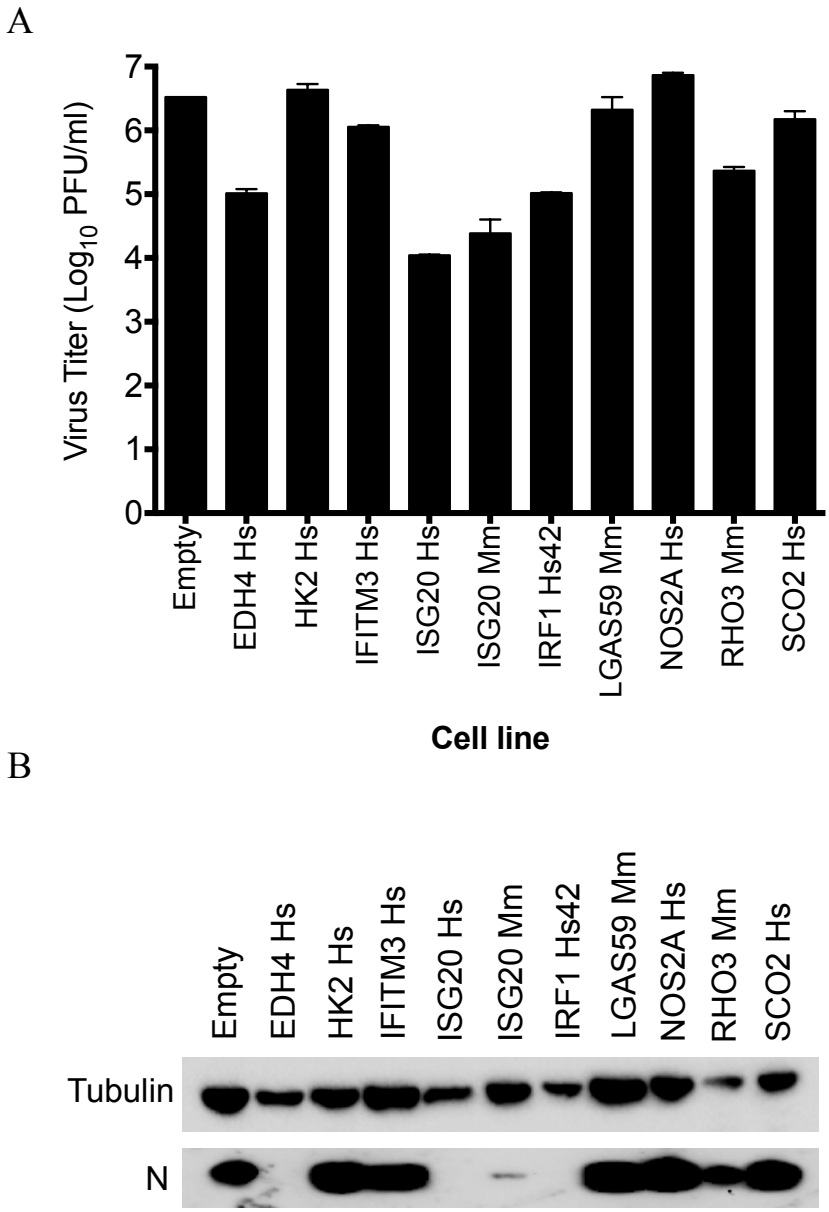

Figure 3.4. 16. OROV growth in ISG-expressing cell-lines.

(A) Viral yield assay. ISG-expressing cell-lines were infected with rOROV at moi 0.001. At 48 h p.i samples were harvested and titrated. Bars represent range from two repeats. (B) N production in samples from (A) Tubulin was probed as a loading control. Empty, control cells transduced with empty plasmid. Hs, *Homo sapiens*; Mm, *Macaca mulatta*.

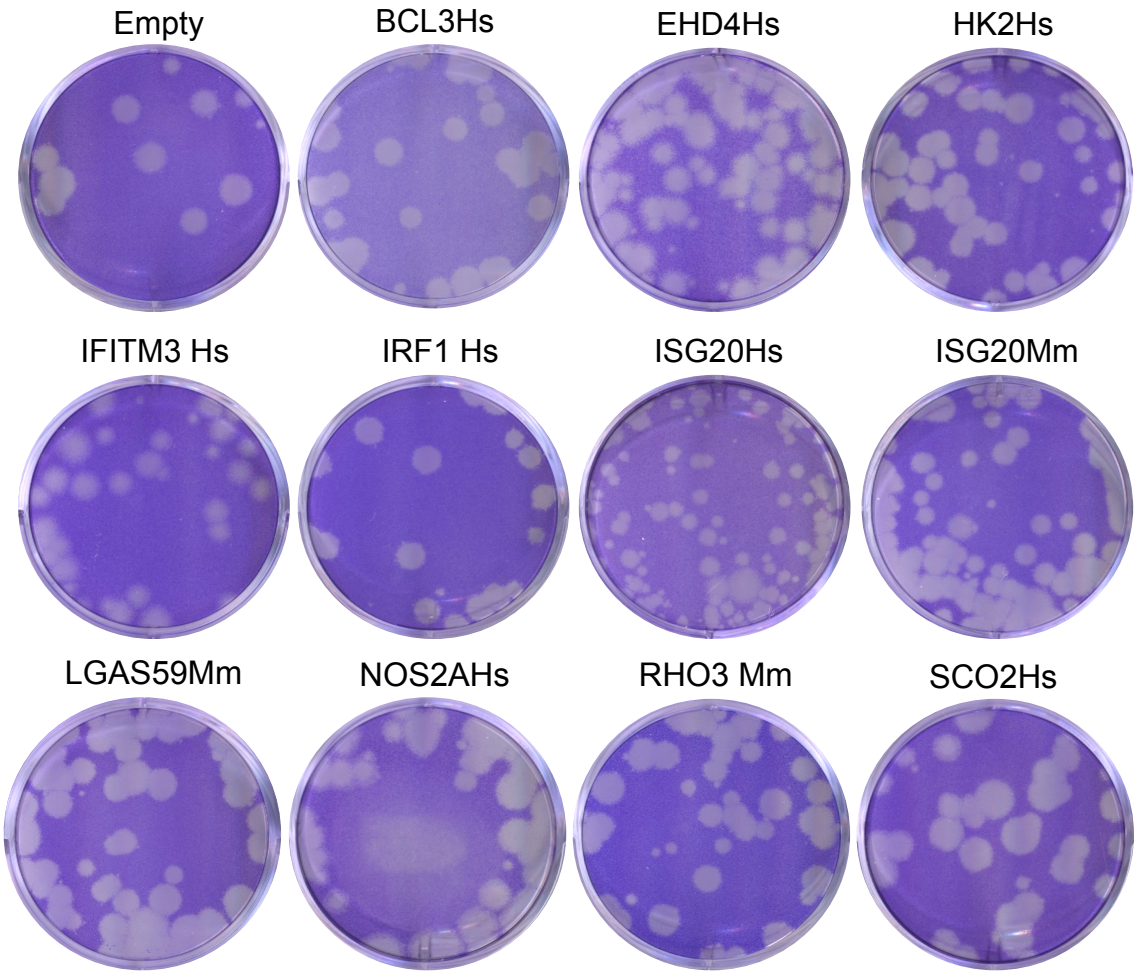

Figure 3.4. 17. Plaque morphology of OROV on ISG-expressing cell-lines.

A plaque assay was carried out on confluent monolayers of ISG-expressing cells, in 6-well plates. 4 day p.i cells were fixed and stained with crystal violet.

3.4.10 Replication of recombinant viruses in mosquito cell-lines

Lastly, growth kinetics of rOROV, delNSmOROV and delNSsOROV viruses in mosquito cell-lines U4.4 (*Aedes albopictus*) and Aag2 (*Aedes aegypti*) were compared. Interestingly, and unlike the situation in mammalian cells, delNSsOROV grows to similar levels as rOROV (Figure. 3.4.18).

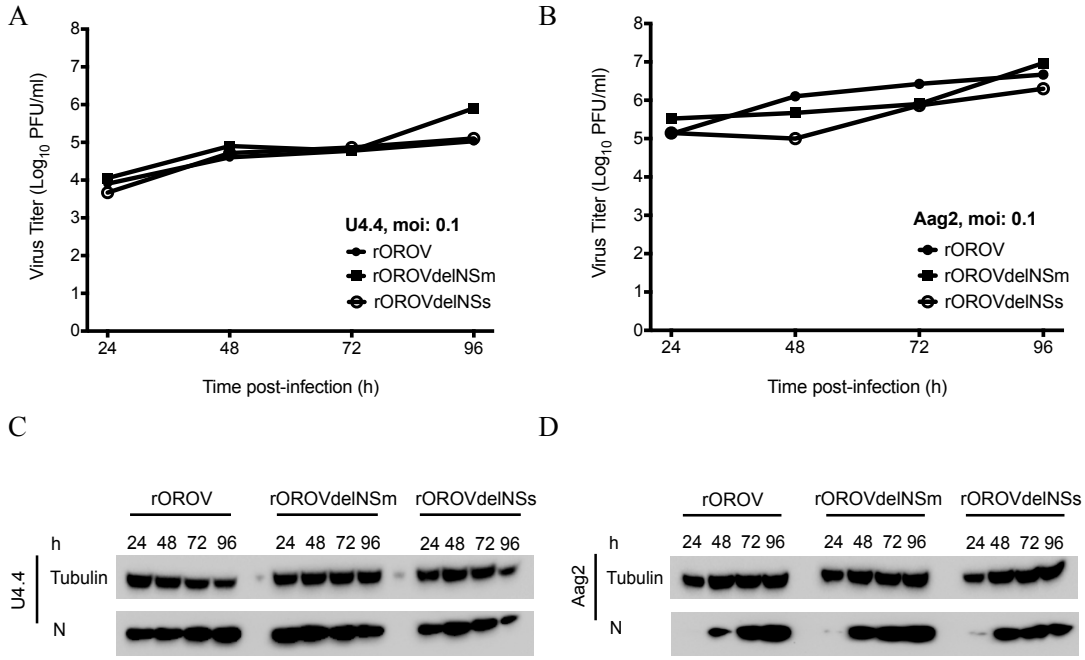

Figure 3.4. 18. Growth kinetics in mosquito cells.

Cells were infected with rOROV, delNSmOROV or delNSsOROV at an MOI of 0.1. At indicated time-points samples were harvested and viral titres determined by plaque assay on BHK-21 cells. Presented graphs are representative experiments. Cell extracts were separated by SDS-PAGE and probed for viral N and Tubulin. (A). Replication in U4.4 cells. (B) Replication in Aag2 cells. (C) N production in U4.4 cells. (D) N production in Aag2 cells.

3.4.11 Discussion

This study describes the successful recovery of OROV in cultured cells entirely from cloned cDNA. The rescued virus (rOROV) replicates similar to the authentic virus (wtOROV) reaching titres of 10^7 PFU/ml (Figure 3.4.2). Using this system, mutant viruses lacking either the NSm or the NSs protein were also generated. Only some bunyaviruses encode these proteins, and until now the exact role played by the NSm protein in orthobunyavirus infections remains unclear. Work on BUNV NSm demonstrated that the protein can localise to the Golgi efficiently on its own (Shi *et al.*, 2006) and may play a role in viral assembly (Shi *et al.*, 2007). In RVFV, the NSm protein is important for infection in mosquitoes by allowing the virus to cross the midgut barrier (Crabtree *et al.*, 2012; Kading *et al.*, 2014). Similarly, in tospoviruses the NSm protein has been shown to be important for virus cell-to-cell spread (Kormelink *et al.*, 1994; Storms *et al.*, 1995; Soellick *et al.*, 2000). Results from this study indicate that for OROV the NSm protein is dispensable for virus replication in cultured cells, as rOROVdelNSm grows and replicates similar to the rOROV virus (Figure 3.4.7.A, C; Figure 3.4.9; Figure 3.4.19). Chapter 3, Section 1, discussed the sequence similarity of the M segment genes between different OROV reassortants, and noted that the NSm region of the M polyprotein of all these viruses is highly conserved when compared to the Gn and Gc glycoproteins, which could indicate that this portion of the polyprotein is less prone to mutation due to a common, yet unknown, selective pressure. Future work could include performing mutations on the NSm coding sequence and monitor for effects on virus replication in more relevant primary cell-lines and *in vivo* models, such as insects. Similarly, the rOROV2080S mutant generated here would also require *in vivo* characterization in order to determine if the S segment difference observed between OROV isolates (Chapter 3, Section 1) offers any advantage over the prototype BeAn19991 S segment, as the current study was not sufficient to determine this.

As with other NSs-encoding bunyaviruses OROV NSs protein is an IFN antagonist and by deleting the NSs ORF, OROV induces high levels of IFN and thus induces STAT1 phosphorylation and MxA expression (Figure 3.4.10, rOROVdelNSs). Interestingly, the C-terminal truncated NSs mutant is also incapable of inhibiting type I IFN production (Figure 3.4.10, rOROV246NSs). Work on BUNV and RVFV has demonstrated that

NSs inhibits IFN-β activation downstream of transcriptional activation through disruption of the DNA-dependent RNA polymerase II (RNAPII) activity (Weber *et al.*, 2002; Kohl *et al.*, 2003b; Billecocq *et al.*, 2004). BUNV NSs interacts with subunit MED8 of the RNAPII regulatory module (Leonard *et al.*, 2006) preventing Ser2 phosphorylation of RNAP II CTD and hence prevents elongation and 3'-end processing of the nascent mRNA transcript (Robinson *et al.*, 2012; Corden, 2013; Eick & Geyer, 2013). This was initially thought to be due to an interaction of BUNV NSs C-terminus (aa 83 – 91) with MED8, however a BUNV NSs mutant lacking an N-terminus of 21 amino acids is also unable to degrade RNAPII, indicating that both the C- and the N-terminus are important for BUNV NSs function (Thomas *et al.*, 2004; Leonard *et al.*, 2006; van Knippenberg *et al.*, 2010). The BUNV MED8 binding domain was mapped to a C-terminal amino acid motif 'LPS', which is conserved in orthobunyavirus NSs proteins (Leonard *et al.*, 2006), and interestingly OROV C-terminal mutant rOROV246NSs also lacks a similar motif 'LPC' (Figure 3.4.19.A). This 'LPC' motif is conserved amongst only the Clade A viruses in the Simbu serogroup (Figure 3.4.19, B). Whether the inability of rOROV246NSs to inhibit IFN production is due to its lack of the MED8 binding domain will need to be investigated in follow-up studies. LACV and SBV NSs function as IFN antagonists by targeting RNAPII for degradation by the proteasome (Blakqori *et al.*, 2007; Verbruggen *et al.*, 2011; Barry *et al.*, 2014). Mutations to the C-terminus of SBV NSs have also been shown to affect the protein's ability to degrade RNAPII (Barry *et al.*, 2014). In the phlebovirus RVFV the NSs protein interacts with subunits of the general transcription factor TFIIH, which also has a role in RNAPI transcription (Assfalg *et al.*, 2012). SFTSV NSs forms viral inclusion bodies in the cytoplasm and uses these to capture kinases TBK1 and IKKε, and proteins STAT1 and STAT2 (Ning *et al.*, 2014; Ning *et al.*, 2015). Recently a study comparing 6-week old C57BL/6 mice knockout mutants demonstrated that MAVS activation independent of MDA5 plays a crucial role in type 1 IFN signalling during OROV infection (Proenca-Modena *et al.*, 2015a), it would be interesting to see how the rOROVdelNSs and rOROV246NSs mutants replicate it such *in vivo* systems.

This study also demonstrates that OROV is sensitive to IFN-α, however to see maximal effects cells have to be treated for 24 h prior to infection (Figure 3.4.12, rOROV).

Addition of 10,000 U/ml of IFN-α 2 h prior to infection decreases OROV titres by 2 logs in comparison to a 4-log decrease at 24 h. This is likely because priming cells 24 h prior to infection allows the cells sufficient time to mount a complete IFN response in comparison to what maybe seen at a 2 h priming period. In addition, results also show that addition of IFN-α to cells once OROV infection is established has no affect on virus yields (Figure 3.4.12, rOROV; +2h, +24h). In contrast to OROV, BUNV appears to be highly sensitive to IFN-α, with a complete inhibition of virus growth at 10,000 U/ml of IFN-α either 24 h or 2 h pre-infection or 2 h post-infection (Figure 3.4.12 and Figure 3.4.15). These findings are consistent with previously published work demonstrating a resistance of OROV to the antiviral effects of IFN-α both *in vivo* and *in vitro* in comparison to other pathogenic orthobunyaviruses (Livonesi *et al.*, 2007b). The reasons for the differences in relative sensitivity of OROV and BUNV to IFN-α will need to be investigated in follow-up studies, but may, for example, be due to the differential effects of certain ISGs on these viruses, or on the ability of OROV to more rapidly switch off host cell gene expression than BUNV. Also, OROV is a virus of primate origin and maybe better adapted to a primate system, and hence the effects seen maybe cell-specific. Whatever the reason, the increased resistance of OROV to IFN-α is not due to expression of the NSs protein (Figure 3.4.14; rOROVdelNSs). The NSs of OROV appears to be inhibitory to the IFN induction (Figure 3.4.10), however whether it also interacts with the signalling pathway is currently unknown. Additional roles for the bunyavirus NSs protein in the virus life-cycle are still being understood, and work in a minigenome system has shown that it may have a regulatory role on the viral polymerase (Weber *et al.*, 2001; Elliott & Schmaljohn, 2013; Brennan *et al.*, 2015). Interestingly both rOROVdelNSs and rOROV246NSs are attenuated in Vero E6 (Figure 2.4.7.A) and in BHK-21 (Figure 2.4.7.C) cells, both of which are IFN deficient. Preliminary work with 246NSs (cloned into expression plasmid pTM1) demonstrates that this protein still retains the ability to decrease minigenome activity, whilst is unable to inhibit *Renilla* activity from a CMV polII-driven plasmid (Appendix; Supplementary Figure).

In an attempt to identify NSs functional domains three additional OROV NSs mutant viruses were generated (Appendix; Supplementary Figure; 48NSs, 90NSs and 159NSs).

These viruses were attenuated in cell culture and were unable to inhibit IFN production, similar to rOROVdelNSs and rOROV246NSs (Figure 4.1.D). However, due to the unavailability of an OROV NSs antibody to confirm the expression of these NSs truncations, the viruses were not studied further. This is worth pursuing in the future.

Work using ISG-expressing cell-lines generated by Mr. Junjie Feng (Figure 3.4.16; Figure 3.4.17) demonstrates that OROV is sensitive to the effects of certain ISGs. In particular human ISG20 decreases OROV titres over 2 logs and results in significant reduction in plaque size. It is interesting that OROV demonstrated an increased sensitivity towards human ISG20 in comparison to the macaque orthologue (Figure 3.4.16; Figure 3.4.17; ISG20 Hs and ISG20 Mm). ISG20 (IFN-stimulated gene 20 KDa protein) which is a 3′ to 5′ exonuclease has previously been shown to possess antiviral properties against a number of RNA viruses (eg. Influenza virus, Vesicular stomatitis virus and EMCV; (Espert *et al.*, 2003)). Human IRF1 was also shown to decrease OROV titres by almost 2 logs, however no reduction in plaque size was observed (Figure 3.4.16 and Figure 3.4.17; IRF1 Hs42). IRF-1 belongs to a family of IFN-regulatory factors and recently published work using mice knockout mutants have demonstrated that IRF-3 and IRF-4 together possess a protective role against OROV infection (Proenca-Modena *et al.*, 2015a), whilst IRF-5 indirectly inhibits OROV neuroinvasion (Proenca-Modena *et al.*, 2015b).

In conclusion, the work presented in this study has shown that we are able to generate infectious OROV entirely from cDNA. The OROV NSs protein similar to other bunyaviruses is an IFN antagonist, whilst the NSm protein appears to be non-essential for virus replication in cultured cells that were tested.

3.4.12 Summary

1. OROV strain BeAn19991 has been successfully rescued entirely from cDNA copies of its genome.
2. OROV mutants lacking either the NSm or the NSs proteins have been generated.
3. OROV NSs protein is an IFN antagonist, and the C-terminal nine residues of the protein are important for functionality.
4. Deletion of OROV NSm protein did not affect viral replication in mammalian or insect cell-lines that were tested.
5. OROV displays a level of tolerance towards the effects of IFN-α in contrast to BUNV.

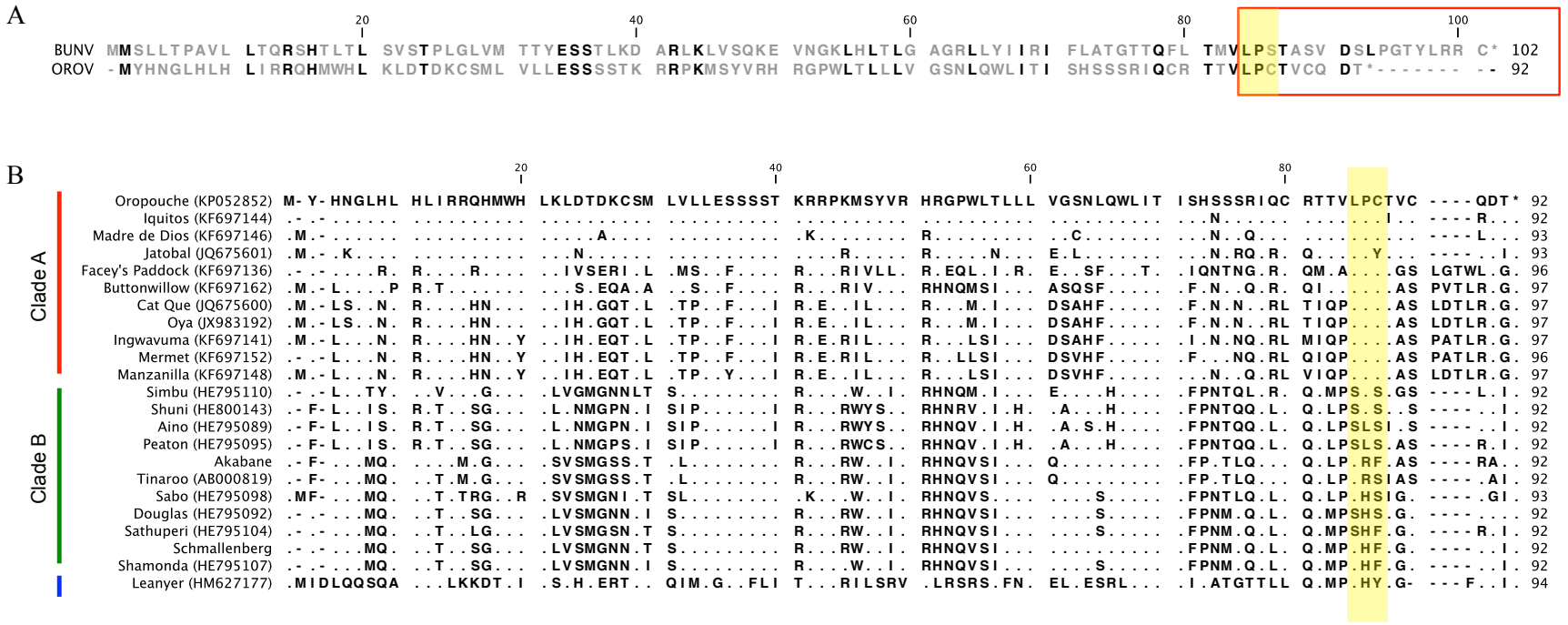

Figure 3.4. 19. NSs protein alignment.

(A). Alignment of BUNV and OROV NSs proteins. The red box highlights the residues deleted in OROV C-terminal NSs mutant (246NSsOROV). The yellow highlight shows the 'LPS' motif that is conserved in orthobunyavirus NSs proteins as described in (Leonard *et al.*, 2006) (B). Alignment of all Simbu serogroup virus NSs proteins. Amino acid residues LPC (highlighted in yellow) are conserved amongst all the Clade A Simbu viruses.

Chapter IV

General Discussion

Chapter IV. General Discussion

4.1. Fulfilment of project aims

The aim of this PhD project was to establish a suite of reverse genetics tools for OROV in order to allow research on this virus at a molecular level. The project successfully fulfilled this aim with the establishment of both a minigenome and VLP assay (Chapter 3, Section 2), which ultimately led to the successful recovery of infectious OROV (Chapter 3, Section 4).

During attempts to establish OROV reverse genetics, the project encountered several hurdles resulting from inconsistencies and inaccuracies within the published genome sequences. Investigating these further revealed that the previously published reference OROV genome sequences in fact contained significant errors. Errors were located in the 3' and 5' UTR regions of all three OROV genome segments, including the absence of a mismatch at nucleotide position 9 of the panhandle sequence in each segment as well as the absence of 204 nucleotides at the 3' end of the S segment (Chapter 3, Section 2). These findings highlighted the importance of establishing protocols for viral genome sequencing that are not reliant on the use of consensus primers. Advances in deep sequencing technology will now allow more accurate determination of viral consensus sequences. However, many orthobunyaviral 3' UTR regions are often poly-A rich and difficult to determine even with modern sequencing methodologies. Therefore, the use of dedicated techniques such as 3' and 5' RACE are generally required in order to confirm these terminal sequences, as evidenced by my work on the OROV S segment. Errors were also found in the published L and M ORFs and this was specific to OROV strain BeAn19991. All discrepancies obtained in this project were confirmed as accurate by functional assays, and hence the re-determined OROV genome sequences were submitted to GenBank (L, KP052850; M, KP052851 and S, KP052852).

Results from this PhD project resulted in the need to re-evaluate OROV phylogeny. Previously published data suggested that OROV could be classified into 4 Genotypes based on full-length N ORF sequences. However, results from Chapter 3, Section 1

revealed a high degree of nucleotide conservation in the N ORF throughout the available OROV sequences, meaning that classification based solely on this region would not accurately reveal the full diversity of circulating OROV strains. My research has reinforced the importance of using full-length genome sequencing to establish accurate and robust viral phylogenies, as well as to investigate the evolutionary trajectory of a virus. The project also identified a novel OROV reassortant, which we named Perdoes virus, after the municipality in Brazil from where it was isolated. Perdoes virus contains L and S segments of OROV, and an M segment of a yet unidentified Simbu virus. Identification of Perdoes virus was important as this suggested that OROV has a broader geographic distribution within Brazil than originally appreciated. Genome sequences for Perdoes virus and OROV clinical isolates that were sequenced during this work have been submitted to GenBank.

The establishment of a successful and reproducible reverse genetic system for OROV during this PhD project has allowed for the generation of OROV mutant viruses lacking either the NSm or the NSs coding regions. Characterisation of the recombinant viruses carried out *in vitro* demonstrated that, as for other NSs-encoding bunyaviruses, the NSs protein of OROV is the main IFN antagonist. Additionally, my research further demonstrated the importance of the nine C-terminal amino acids of OROV NSs in the IFN antagonistic activity. In addition to this I also studied the sensitivity of OROV to IFN-α, in comparison to the family prototype BUNV. Here, I found that OROV was capable of replicating at high doses of IFN-α (10,000 U/ml), whilst BUNV was unable to do so. OROV NSs mutants also displayed the same level of sensitivity as OROV, further indicating that the NSs protein may not be responsible for this characteristic. The project also demonstrated that a mutant OROV lacking a complete NSm protein displayed *in vitro* properties similar to the wild-type virus, suggesting that the NSm protein is dispensible for virus replication in mammalian and mosquito cell-lines that were tested.

4.2. Worth of the project in a wider context and potential for future research

This PhD project has highlighted the importance of obtaining an accurate consensus sequence for a virus population, particularly when that information is required for molecular biological analysis. Reverse genetics systems are powerful tools in virus research, but can be hindered without accurate genetic information. A number of bunyavirus sequences publically available are either incomplete or inaccurate, especially in the UTR sequences. Some viral sequences also contain host-cell sequences attached to the ends, a result of *de novo* assembly of deep sequencing data. One example of this is the published M segment sequence for LENV (GenBank accession no. HM627176). This sequence appears to contain non-viral nucleotides before the start of the actual virus 5' UTR, and was identified during generation of a LENV minigenome in Chapter 3, Section 3. Therefore a careful review of sequences before being deposited into public databases and retracting or correcting sequences with errors would be beneficial to researchers who then use that information in downstream analysis.

Work from this project has resulted in the first complete genome sequences for several OROV field isolate strains, and has highlighted the usefulness of obtaining complete genetic data. Often only partial genetic information is used in phylogenetic analysis, as has been the case with OROV, however as shown in this PhD, this results in loss of valuable information. The OROV field isolates that were obtained in 2009 and 2012 revealed a loss of 11 residues in the S segment 3' UTR when compared to strains BeAn19991 and TRVL-9760, isolated in 1960 and 1955 respectively. This loss of nucleotides is intriguing; unfortunately the significance of this finding could not be determined within the context of this PhD. It is however worth pursuing. Additionally, if isolates from various outbreaks and time-periods were to be re-sequenced completely, this may provide a more accurate description of the molecular epidemiology of OROV.

OROV is a public health threat in Central and South America, where it causes periodic outbreaks of flu-like illness. In Brazil, the virus is the second most frequent cause of

arboviral febrile illness after dengue and given the current rates of urban expansion it is probable that more outbreaks of this emerging viral zoonosis will occur. Hence the information gathered from this study and the tools established will play a crucial role in further understanding the OROV infectious life-cycle. Initial follow-up studies from the work started in this PhD could involve further investigations into the roles played by OROV NSs. For example, due to project time constraints research into the OROV NSs mechanisms of action were not considered. Previous work on BUNV has shown that the NSs C-terminus interacts with MED8 subunit of the RNAPII regulatory module (Leonard *et al.*, 2006) and it would therefore be interesting to determine if the same is true for OROV. Also, recently published work using knock out mouse models have identified different parts of the IFN pathway that are important for OROV disease progression (Proenca-Modena *et al.*, 2015b; Proenca-Modena *et al.*, 2015a). These *in vivo* systems can be used in conjunction with the recombinant delNSsOROV and 246NSsOROV viruses to further study the role NSs plays during infection.

Additional roles for NSs in virus replication could also be investigated. In an attempt to identify NSs functional domains, three OROV NSs mutant viruses were generated in this PhD (Chapter 3, Section 4; Appendix Supplementary Figure; 48NSs, 90NSs and 159NSs). Unfortunately due to the lack of a NSs antibody the expression of these truncated NSs proteins could not be confirmed, and unlike the 246NSsOROV (Chapter 3, Section 4, Figure 3.4.8) visible NSs bands were not observed via metabolic labelling. As an observation, the amount of N production in these three viruses was similar to the 246NSsOROV virus and not the delNSsOROV virus (Chapter 3, Section 4, Figure 3.4.7). It is probable that these viruses express unstable NSs proteins. Obtaining a NSs antibody could allow future characterization of these viruses, and would be beneficial to confirm NSs expression during transient transfection experiments, as well as to monitor cellular localisation of NSs. Attempts to express stable amounts of OROV NSs protein using a bacterial expression system, as well as in insect cells (Dr. Ping Li, MRC-University of Glasgow) for antibody production were unsuccessful during this PhD.

The NSs protein of Simbu viruses are highly conserved (Figure 3.4.19). Future projects investigating OROV NSs may benefit from generating an ambisense S segment similar

to the recently established BUNV system (van Knippenberg & Elliott, 2015), as this would allow point mutations and deletions of the protein to be studied in the context of OROV infection. As described for BUNV (Shi *et al.*, 2010), and in collaboration with Dr. Gustavo Olszanski Acrani (University of Sao Paulo, Brazil) attempts were also made to generate OROV viruses that express fluorescent proteins. Although unsuccessful, the subsequent discovery that NSm protein is dispensable for *in vitro* replication of OROV means that replacing this region with a fluorescent tag should be considered. However, the role the NSm protein plays during *in vivo* infections is completely unknown. Furthermore, the NSm protein is highly conserved in viruses from the Oropouche species, which demonstrates positive selective pressure on this gene. Therefore further investigations into the functions of NSm are therefore likely to reveal important insights into the molecular pathogenesis and host range of OROV.

Members of the species Oropouche virus display a broad phylogenetic diversity predominately due to the M segment. Viruses IQTV and MDDV, isolated in Peru and Venezuela, respectively, cause disease in humans (Aguilar *et al.*, 2011; Ladner *et al.*, 2014), whilst Perdoes virus (Chapter 3, Section 1) and the more divergent JATV (Figueiredo & Da Rosa, 1988) isolated in Brazil, have only been found in non-human primates. The variations observed in the M segments of these viruses could have resulted from either genomic reassortment or extensive adaptation to different hosts and habitats. Using the OROV reverse genetics system established here it would now be possible to study in detail these differences in terms of pathogenesis, virulence outcome and host range of these viruses. This work would contribute to understanding the evolution of Clade A Simbu serogroup viruses within South America. It would also be interesting to compare these viruses in terms of their IFN sensitivity, as work from this PhD has shown that OROV NSs protein may not be solely responsible for host cell protein shut off and the relative resistance of OROV to IFN-α treatment. Additionally, questions regarding host-pathogen interactions and species-specific barriers can now be investigated. OROV is closely related to veterinary pathogen SBV, another Simbu virus, which is also spread by biting midges from the genus *Culicoides*. Using the previously described reverse genetics system for SBV (Elliott *et al.*, 2013; Varela *et al.*,

2013) and the newly established OROV rescue system we can begin to understand the basis for OROV pathogenicity in humans.

In an attempt to shed light on orthobunyavirus reassortment Chapter 3, Section 3 utilised the newly established OROV minigenome system to study protein-protein and protein-RNA interactions between OROV and SBV. Results from that analysis has led to the hypotheses that the M UTR of orthobunyaviruses may be a potential determinant contributing to reassortment. Time constraints prevented further work in this area, however this analysis has established that OROV and SBV possess the ability to reassort. Future work could involve investigating the M UTR of various orthobunyaviruses, and chimeras of various M UTRs should also be generated and tested for functionality with various N and L proteins. Potentially generating L protein chimeras between OROV and SBV may also prove informative. The difference between M UTR nucleotide positions 8 and 9 of the Clade A and Clade B Simbu viruses is intriguing, the availability of complete orthobunyavirus sequences would be beneficial to allow a comprehensive analysis of this region and to determine if there is any relevance towards the virus host species.

Finally, the prevalence of OROV in Central and South America in unknown, and this is mainly due to the lack of a reliable diagnostics and the presence of other endemic viral infections such as dengue, chikungunya and Mayaro fevers that present similar signs and symptoms in patients ((Moreli & da Costa, 2013); personal communication, Professor Pedro Vasconcelos, Evandro Chagas Institute in Belem, Brazil). Developing an OROV VLP-based diagnostic tool similar to that described for CCHFV (Devignot *et al.*, 2015) may be a way to solve this problem. In addition to this, improvements in patient data entry at reference laboratories will also contribute to a better understanding of OROV epidemiology within South America.

4.3. Conclusions

The overall aims of this PhD project were fulfilled and the work presented will now enable us to study OROV in more detail in order to establish the molecular details involved in viral replication and pathogenesis, and potentially generate attenuated vaccine strains. The work presented here is an important move forward towards a better understanding of this important yet neglected human pathogen.

Chapter V

Appendices

Chapter V. Appendices

Supplementary Table

Isolate	Year	Country (State)	Host	Accession Number (L, M, S)		
TRVL9760	1955	Trinidad	Human	N/A	AF312381	AF164531
BeAr19886	1960	Brazil (Para)	*Ochlerotatus serratus*	HQ830408	HQ830373	HM470107
BeAn19991	1960	Brazil (Para)	*Bradypus tridactylus*	KP052850	KP052851	KP052852
BeH29086	1961	Brazil (Para)	Human	HQ830409	HQ830374	HM470108
BeH29090	1961	Brazil (Para)	Human	HQ830410	HQ830375	HM470109
BeAn84785	1965	Brazil	*Bradypus tridactylus*	KF697154	KF697155	KF697156
BeH121923	1967	Brazil (Para)	Human	HQ830411	HQ830376	HM470110
AR136921	1968	Brazil (Para)	*Culex quinquefasciatus*	HQ830412	HQ830377	HQ830443
BeAn206119	1971	Brazil (Para)	*Bradypus tridactylus*	HQ830413	HQ830378	AY993909
BeAn208402	1971	Brazil (Para)	*Bradypus tridactylus*	HQ830414	HQ830379	AY993910
BeAn208819	1971	Brazil (Para)	*Bradypus tridactylus*	HQ830415	HQ830380	AY993911
BeAn208823	1971	Brazil (Para)	*Bradypus tridactylus*	N/A	N/A	AY993912
H244576	1973	N/A	Human	N/A	N/A	HQ830444
AusCh16129	1974	Australia	Mosquito	KF697138	KF697137	AF362400
PanAn48878	1975	Panama	*Bradypus variegatus*	KF697157	KF697159	KF697158
H271078	1975	Brazil (Para)	Human	N/A	N/A	HQ830445
BeAr271708	1975	Brazil	Human	N/A	N/A	HM470113
BeH271815	1975	Brazil (Para)	Human	N/A	N/A	AF164533
BeH355173	1978	Brazil (Para)	Human	HQ830416	HQ830381	HM470114
BeH355186	1978	Brazil	Human	N/A	N/A	HM470115
H356898	1978	Brazil (Para)	Human	N/A	N/A	HQ830447
H366781	1979	N/A	Human	N/A	N/A	HQ830449
AR366927	1979	Brazil (Para)	*Culicoides paraensis*	HQ830417	HQ830382	HQ830448
BeH381114	1980	Brazil (Para)	Human	N/A	N/A	AF164535
H384192	1980	N/A	Human	N/A	N/A	HQ830450
H384193	1980	N/A	Human	N/A	N/A	HQ830451
H385591	1980	N/A	Human	HQ830418	HQ830383	HQ830452
H389865	1980	Brazil (Amazonas)	Human	HQ830419	HQ830384	HQ830453
BeH390233	1980	Brazil (Amazonas)	Human	N/A	N/A	AF164536
H390242	1980	Brazil (Amazonas)	Human	HQ830420	HQ830385	HQ830454
BeAn423380	1984	Brazil	*Nasua*	JQ675603	JQ675602	JQ675601

Isolate	Year	Country (State)	Host	Accession Number (L, M, S)		
			nasua			
BeH472200	1988	Brazil (Maranhao)	Human	N/A	N/A	AF164537
BeH472204	1988	Brazil (Maranhao)	Human	N/A	N/A	AF164538
H472433	1988	Brazil (Maranhao)	Human	HQ830421	HQ830386	HQ830455
H472435	1988	Brazil (Maranhao)	Human	HQ830422	HQ830387	HQ830456
BeAr473358	1988	Brazil (Maranhao)	*Culicoides paraensis*	N/A	N/A	AF164539
BeH475248	1988	Brazil (Para)	Human	N/A	N/A	AF164540
GML444477	1989	Panama (Chame)	Human	N/A	N/A	AF164555
GML444911	1989	Panama (Chame)	Human	N/A	N/A	AF164556
GML445252	1989	Panama (San Miguelito)	Human	N/A	N/A	AF164557
GML450093	1989	Panama (Chilibre)	Human	N/A	N/A	AF164558
H498913	1990	Brazil (Rondonia)	Human	HQ830423	HQ830388	HQ830457
BeH504514	1991	Brazil (Para)	Human	N/A	N/A	AF164541
BeH505442	1991	Brazil (Rondonia)	Human	N/A	N/A	AF164542
BeH505663	1991	Brazil (Rondonia)	Human	N/A	N/A	AF164543
H505764	1991	Brazil (Rondonia)	Human	N/A	N/A	HQ830458
H505768	1991	Brazil (Rondonia)	Human	HQ830424	HQ830389	HQ830459
H505805	1991	Brazil (Rondonia)	Human	N/A	N/A	HQ830460
IQT1690	1992	Peru (Iquitos)	Human	KC759125	KC759126	KC759127
MD023	1993	Peru (Madre de Dios)	Human	N/A	N/A	AF164550
DEI209	1993	Peru (Iquitos)	Human	N/A	N/A	AF164551
BeH521086	1993	Brazil (Maranhao)	Human	HQ830425	HQ830390	AY704559
H532314	1994	Brazil (Para)	Human	HQ830426	HQ830391	HQ830461
H532422	1994	Brazil (Para)	Human	HQ830427	HQ830392	HQ830462
H532490	1994	Brazil (Para)	Human	HQ830428	HQ830393	HQ830463
H532500	1994	Brazil (Para)	Human	HQ830429	HQ830394	HQ830464
BeH541140	1994	Brazil (Para)	Human	HQ830430	HQ830395	HM470126
BeH541863	1996	Brazil (Para)	Human	N/A	N/A	AF164544
BeH543033	1996	Brazil (Para)	Human	N/A	N/A	AF164545
BeH543087	1996	Brazil (Acre)	Human	N/A	N/A	AF164547
H543091	1996	Brazil (Acre)	Human	N/A	N/A	HQ830465
H543100	1996	Brazil (Acre)	Human	HQ830431	HQ830396	HQ830466

Isolate	Year	Country (State)	Host	Accession Number (L, M, S)		
BeH543618	1996	Brazil (Para)	Human	N/A	N/A	AF164548
H543629	1996	Brazil (Para)	Human	HQ830432	HQ830397	HQ830467
BeH543638	1996	Brazil	Human	N/A	N/A	HM470128
BeH543639	1996	Brazil	Human	N/A	N/A	HM470129
BeH543733	1996	Brazil (Para)	Human	N/A	N/A	AY704560
H543760	1996	Brazil (Para)	Human	HQ830433	HQ830398	HQ830470
H543857	1996	Brazil (Para)	Human	HQ830434	HQ830399	HQ830471
BeH543880	1996	Brazil	Human	N/A	N/A	HM470132
BeH544552	1996	Brazil (Para)	Human	N/A	N/A	AF164546
IQT4083	1997	Peru (Iquitos)	Human	N/A	N/A	AF164552
IQT7085	1998	Peru (Iquitos)	Human	N/A	N/A	AF164554
01-812-98	1998	Peru (Iquitos)	Human	N/A	N/A	AF164553
IQT9924	1999	Peru	Human	KF697142	KF697143	KF697144
BeAn622998	2000	Brazil (Minas Gerais)	*Callitrhix penicillata*	HQ830436	HQ830401	AY117135
BeH622544	2002	Brazil (Tocantins)	Human	N/A	N/A	EF467368
PPS522H669314	2003	Brazil (Para)	Human	HQ830435	HQ830400	EF467370
PPS523H669315	2003	Brazil (Para)	Human	HQ830437	HQ830402	EF467369
BR/2004/Acre27	2004	Brazil (Acre)	Human	N/A	N/A	EU561644
PMOH682426	2004	Brazil (Para)	Human	HQ830438	HQ830403	EF467371
PMOH682431	2004	Brazil (Para)	Human	HQ830439	HQ830404	EF467372
AMLq13	2005	Brazil (Mananus)	Human	N/A	N/A	HM107840
AMLq14	2006	Brazil (Manaus)	Human	N/A	N/A	HM107841
BeH706890	2006	Brazil (Para)	Human	N/A	N/A	HM470133
BeH706893	2006	Brazil (Para)	Human	N/A	N/A	HM470134
BeH707157	2006	Brazil (Para)	Human	N/A	N/A	HM470136
BeH707287	2006	Brazil (Para)	Human	HQ830441	HQ830406	HM470137
H708139	2006	Brazil (Para)	Human	HQ830440	HQ830405	HQ830475
H708717	2006	Brazil (Para)	Human	HQ830442	HQ830407	HQ830477
AMLq16	2007	Brazil (Manaus)	Human	N/A	N/A	HM107842
FMD1303	2007	Peru	Human	KF697147	KF697145	KF697146
H75955	2009	Brazil (Amapa)	Human	N/A	N/A	HQ830483
H758669	2009	Brazil (Amapa)	Human	N/A	N/A	HQ830479
H758687	2009	Brazil (Amapa)	Human	N/A	N/A	HQ830478
H759018	2009	Brazil (Amapa)	Human	N/A	N/A	HQ830486
*BeH759021	2009	Brazil	Human			

Isolate	Year	Country (State)	Host	Accession Number (L, M, S)		
		(Amapa)				
*BeH759022	2009	Brazil (Amapa)	Human			
H759023	2009	Brazil (Amapa)	Human	N/A	N/A	HQ830487
*BeH759024	2009	Brazil (Amapa)	Human			
*BeH759025	2009	Brazil (Amapa)	Human			
H759038	2009	Brazil (Amapa)	Human	N/A	N/A	HQ830484
*BeH759040	2009	Brazil (Amapa)	Human			
H759041	2009	Brazil (Amapa)	Human	N/A	N/A	HQ830488
H759042	2009	Brazil (Amapa)	Human	N/A	N/A	HQ830489
H759043	2009	Brazil (Amapa)	Human	N/A	N/A	HQ830490
H759044	2009	Brazil (Amapa)	Human	N/A	N/A	HQ830491
*BeH759146	2009	Brazil (Amapa)	Human			
H759483	2009	Brazil (Amapa)	Human	N/A	N/A	HQ830492
H759525	2009	Brazil (Amapa)	Human	N/A	N/A	HQ830480
*BeH759529	2009	Brazil (Amapa)	Human			
H759531	2009	Brazil (Amapa)	Human	N/A	N/A	HQ830482
H759541	2009	Brazil (Amapa)	Human	N/A	N/A	HQ830481
H759562	2009	Brazil (Amapa)	Human	N/A	N/A	HQ830485
*BeH759620	2009	Brazil (Amapa)	Human			
TVP19255	2010	Venezuela (Anzoategui)	Cebus sp	KJ866391	KJ866390	KJ866389
*BeAN789726	2012	Brazil (Minas Gerais)	*Callitrhix penicillata*			
*BeAN790177	2012	Brazil (Minas Gerais)	*Callitrhix penicillata*			
BeH379693	N/A	N/A	Human	N/A	N/A	AF164534
GML444479	N/A	Panama	Human	N/A	N/A	KC759130
BeH543745	N/A	Brazil (Para)	Human	N/A	N/A	AY704561
BeH543790	N/A	Brazil (Para)	Human	N/A	N/A	AY704567

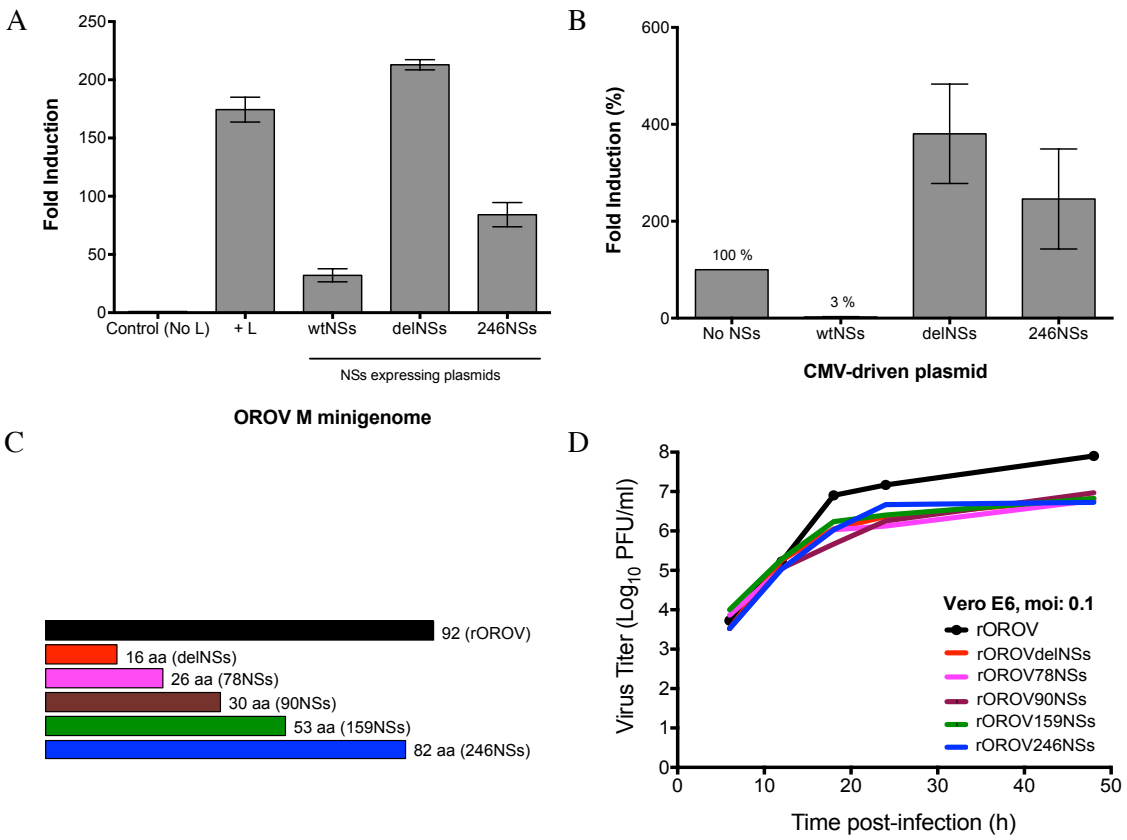

Supplementary Figure. OROV NSs characterisation.

(A) Minigenome assay. BSR-T7/5 cells were co-transfected with pTM1OROV-N (250 ng), pTM1OROV-L (250 ng), pTM1-FF-luc (25 ng) and pTVT7OROVMRen(–) (125 ng), along with indicated NSs-expressing plasmids (125 ng). Luciferase values were measured 24 h p.t using a Dual-luciferase Reporter Assay kit (Promega). Experiment was carried out in triplicate. (B) CMV-driven reporter gene expression. BSR-T7/5 were co-transfected with phRL-CMV (125 ng), pTM1-FF-luc (125 ng) along with indicated NSs-expressing plasmids (125 ng). Luciferase activity measured as in (A). Values are plotted as fold-induction over Control (No NSs), set at 100% activity. Experiment was carried out in triplicates. (C) Schematic of C-terminal NSs truncations that were generated. Black, wild-type. (D) Growth-kinetics of mutant NSs viruses in Vero E6 cells. Cells were infected with indicated viruses at MOI 0.1 PFU/ml, and at indicated time-points harvested and titrated on BHK-21 cells. Graph is a representative experiment.

Chapter VI

References

Chapter VI. References

Acrani, G. O., Gomes, R., Proenca-Modena, J. L., da Silva, A. F., Carminati, P. O., Silva, M. L., Santos, R. I. & Arruda, E. (2010). Apoptosis induced by Oropouche virus infection in HeLa cells is dependent on virus protein expression. *Virus research* **149**, 56-63.

Acrani, G. O., Tilston-Lunel, N. L., Spiegel, M., Weidemann, M., Dilcher, M., da Silva, D. E., Nunes, M. R. & Elliott, R. M. (2014). Establishment of a minigenome system for Oropouche virus reveals the S genome segment to be significantly longer than reported previously. *The Journal of general virology* **95**, 513-523.

Aguilar, P. V., Barrett, A. D., Saeed, M. F., Watts, D. M., Russell, K., Guevara, C., Ampuero, J. S., Suarez, L., Cespedes, M. & other authors (2011). Iquitos Virus: A Novel Reassortant Orthobunyavirus Associated with Human Illness in Peru. *PLoS neglected tropical diseases* **5**, e1315.

Alff, P. J., Gavrilovskaya, I. N., Gorbunova, E., Endriss, K., Chong, Y., Geimonen, E., Sen, N., Reich, N. C. & Mackow, E. R. (2006). The pathogenic NY-1 hantavirus G1 cytoplasmic tail inhibits RIG-I- and TBK-1-directed interferon responses. *Journal of virology* **80**, 9676-9686.

Allen, B. L. & Taatjes, D. J. (2015). The Mediator complex: a central integrator of transcription. *Nature Reviews Molecular Cell Biology* **16**, 155-166.

Anderson, C. R., Spence, L., Downs, W. G. & Aitken, T. H. (1961). Oropouche virus: a new human disease agent from Trinidad, West Indies. *The American journal of tropical medicine and hygiene* **10**, 574-578.

Andersson, I., Bladh, L., Mousavi-Jazi, M., Magnusson, K.-E., Lundkvist, Å., Haller, O. & Mirazimi, A. (2004). Human MxA Protein Inhibits the Replication of Crimean-Congo Hemorrhagic Fever Virus. *Journal of virology* **78**, 4323-4329.

Aquino, V. H. & Figueiredo, L. T. (2004). Linear amplification followed by single primer polymerase chain reaction to amplify unknown DNA fragments: complete nucleotide sequence of Oropouche virus M RNA segment. *Journal of virological methods* **115**, 51-57.

Aquino, V. H., Moreli, M. L. & Moraes Figueiredo, L. T. (2003). Analysis of oropouche virus L protein amino acid sequence showed the presence of an additional conserved region that could harbour an important role for the polymerase activity. *Archives of virology* **148**, 19-28.

Assfalg, R., Lebedev, A., Gonzalez, O. G., Schelling, A., Koch, S. & Iben, S. (2012). TFIIH is an elongation factor of RNA polymerase I. *Nucleic acids research* **40**, 650-659.

Ausubel, F. M. (2005). Are innate immune signaling pathways in plants and animals conserved? *Nature Immunology* **6**, 973-979.

Azevedo, R. S. d. S., Nunes, M. R. T., Chiang, J. O., Bensabath, G., Vasconcelos, H. B., Pinto, A. Y. d. N., Martins, L. C., Monteiro, H. A. d. O., Rodrigues, S. G. & other authors (2007). Reemergence of Oropouche fever, northern Brazil. *Emerging infectious diseases* **13**, 912-915.

Baisley, K. J., Watts, D. M., Munstermann, L. E. & Wilson, M. L. (1998). Epidemiology of endemic Oropouche virus transmission in upper Amazonian Peru. *The American journal of tropical medicine and hygiene* **59**, 710-716.

Baldauf, S. L. (2003). Phylogeny for the faint of heart: a tutorial. *Trends in genetics : TIG* **19**, 345-351.

Bangphoomi, N., Takenaka-Uema, A., Sugi, T., Kato, K., Akashi, H. & Horimoto, T. (2014). Akabane virus utilizes alternative endocytic pathways to entry into mammalian cell lines. *The Journal of veterinary medical science / the Japanese Society of Veterinary Science* **76**, 1471-1478.

Barr, J. N. & Wertz, G. W. (2004). Bunyamwera bunyavirus RNA synthesis requires cooperation of 3'- and 5'-terminal sequences. *Journal of virology* **78**, 1129-1138.

Barr, J. N. & Wertz, G. W. (2005). Role of the Conserved Nucleotide Mismatch within 3′- and 5′-Terminal Regions of Bunyamwera Virus in Signaling Transcription. *Journal of virology* **79**, 3586-3594.

Barr, J. N., Rodgers, J. W. & Wertz, G. W. (2005). The Bunyamwera virus mRNA transcription signal resides within both the 3' and the 5' terminal regions and allows ambisense transcription from a model RNA segment. *Journal of virology* **79**, 12602-12607.

Barr, J. N., Rodgers, J. W. & Wertz, G. W. (2006). Identification of the Bunyamwera bunyavirus transcription termination signal. *The Journal of general virology* **87**, 189-198.

Barr, J. N., Elliott, R. M., Dunn, E. F. & Wertz, G. W. (2003). Segment-specific terminal sequences of Bunyamwera bunyavirus regulate genome replication. *Virology* **311**, 326-338.

Barry, G., Varela, M., Ratinier, M., Blomstrom, A. L., Caporale, M., Seehusen, F., Hahn, K., Schnettler, E., Baumgartner, W. & other authors (2014). NSs protein of Schmallenberg virus counteracts the antiviral response of the cell by inhibiting its transcriptional machinery. *The Journal of general virology* **95**, 1640-1646.

Barzon, L., Lavezzo, E., Militello, V., Toppo, S. & Palù, G. (2011). Applications of Next-Generation Sequencing Technologies to Diagnostic Virology. *International Journal of Molecular Sciences* **12**, 7861.

Bastos Mde, S., Figueiredo, L. T., Naveca, F. G., Monte, R. L., Lessa, N., Pinto de Figueiredo, R. M., Gimaque, J. B., Pivoto Joao, G., Ramasawmy, R. & other authors (2012). Identification of Oropouche Orthobunyavirus in the cerebrospinal fluid of three patients in the Amazonas, Brazil. *The American journal of tropical medicine and hygiene* **86**, 732-735.

Bergeron, E., Albarino, C. G., Khristova, M. L. & Nichol, S. T. (2010). Crimean-Congo hemorrhagic fever virus-encoded ovarian tumor protease activity is dispensable for virus RNA polymerase function. *Journal of virology* **84**, 216-226.

Bergeron, E., Zivcec, M., Chakrabarti, A. K., Nichol, S. T., Albarino, C. G. & Spiropoulou, C. F. (2015). Recovery of Recombinant Crimean Congo Hemorrhagic Fever Virus Reveals a Function for Non-structural Glycoproteins Cleavage by Furin. *PLoS pathogens* **11**, e1004879.

Bernardes-Terzian, A. C., de-Moraes-Bronzoni, R. V., Drumond, B. P., Da Silva-Nunes, M., da-Silva, N. S., Urbano-Ferreira, M., Speranca, M. A. &

Nogueira, M. L. (2009). Sporadic oropouche virus infection, acre, Brazil. *Emerging infectious diseases* **15**, 348-350.

Billecocq, A., Gauliard, N., Le May, N., Elliott, R. M., Flick, R. & Bouloy, M. (2008). RNA polymerase I-mediated expression of viral RNA for the rescue of infectious virulent and avirulent Rift Valley fever viruses. *Virology* **378**, 377-384.

Billecocq, A., Spiegel, M., Vialat, P., Kohl, A., Weber, F., Bouloy, M. & Haller, O. (2004). NSs protein of Rift Valley fever virus blocks interferon production by inhibiting host gene transcription. *Journal of virology* **78**, 9798-9806.

Blakqori, G. & Weber, F. (2005). Efficient cDNA-based rescue of La Crosse bunyaviruses expressing or lacking the nonstructural protein NSs. *Journal of virology* **79**, 10420-10428.

Blakqori, G., Lowen, A. C. & Elliott, R. M. (2012). The small genome segment of Bunyamwera orthobunyavirus harbours a single transcription-termination signal. *The Journal of general virology* **93**, 1449-1455.

Blakqori, G., Kochs, G., Haller, O. & Weber, F. (2003). Functional L polymerase of La Crosse virus allows in vivo reconstitution of recombinant nucleocapsids. *The Journal of general virology* **84**, 1207-1214.

Blakqori, G., Delhaye, S., Habjan, M., Blair, C. D., Sanchez-Vargas, I., Olson, K. E., Attarzadeh-Yazdi, G., Fragkoudis, R., Kohl, A. & other authors (2007). La Crosse bunyavirus nonstructural protein NSs serves to suppress the type I interferon system of mammalian hosts. *Journal of virology* **81**, 4991-4999.

Bouloy, M. & Flick, R. (2009). Reverse genetics technology for Rift Valley fever virus: current and future applications for the development of therapeutics and vaccines. *Antiviral research* **84**, 101-118.

Bouloy, M., Janzen, C., Vialat, P., Khun, H., Pavlovic, J., Huerre, M. & Haller, O. (2001). Genetic evidence for an interferon-antagonistic function of rift valley fever virus nonstructural protein NSs. *Journal of virology* **75**, 1371-1377.

Bowden, T. A., Bitto, D., McLees, A., Yeromonahos, C., Elliott, R. M. & Huiskonen, J. T. (2013). Orthobunyavirus Ultrastructure and the Curious Tripodal Glycoprotein Spike. *PLoS pathogens* **9**, e1003374.

Brennan, B., Li, P. & Elliott, R. M. (2011). Generation and characterization of a recombinant Rift Valley fever virus expressing a V5 epitope-tagged RNA-dependent RNA polymerase. *The Journal of general virology* **92**, 2906-2913.

Brennan, B., Welch, S. R. & Elliott, R. M. (2014). The Consequences of Reconfiguring the Ambisense S Genome Segment of Rift Valley Fever Virus on Viral Replication in Mammalian and Mosquito Cells and for Genome Packaging. *PLoS pathogens* **10**, e1003922.

Brennan, B., Li, P., Zhang, S., Li, A., Liang, M., Li, D. & Elliott, R. M. (2015). Reverse genetics system for severe fever with thrombocytopenia syndrome virus. *Journal of virology* **89**, 3026-3037.

Bridgen, A. & Elliott, R. M. (1996). Rescue of a segmented negative-strand RNA virus entirely from cloned complementary DNAs. *Proceedings of the National Academy of Sciences of the United States of America* **93**, 15400-15404.

Bridgen, A., Weber, F., Fazakerley, J. K. & Elliott, R. M. (2001). Bunyamwera bunyavirus nonstructural protein NSs is a nonessential gene product that contributes to viral pathogenesis. *Proceedings of the National Academy of Sciences of the United States of America* **98**, 664-669.

Briese, T., Calisher, C. H. & Higgs, S. (2013). Viruses of the family Bunyaviridae: are all available isolates reassortants? *Virology* **446**, 207-216.

Buchholz, U. J., Finke, S. & Conzelmann, K. K. (1999). Generation of Bovine Respiratory Syncytial Virus (BRSV) from cDNA: BRSV NS2 Is Not Essential for Virus Replication in Tissue Culture, and the Human RSV Leader Region Acts as a Functional BRSV Genome Promoter. *Journal of virology* **73**, 251-259.

Capodagli, G. C., McKercher, M. A., Baker, E. A., Masters, E. M., Brunzelle, J. S. & Pegan, S. D. (2011). Structural Analysis of a Viral Ovarian Tumor Domain Protease from the Crimean-Congo Hemorrhagic Fever Virus in Complex with Covalently Bonded Ubiquitin. *Journal of virology* **85**, 3621-3630.

Carlton-Smith, C. & Elliott, R. M. (2012). Viperin, MTAP44, and protein kinase R contribute to the interferon-induced inhibition of Bunyamwera Orthobunyavirus replication. *Journal of virology* **86**, 11548-11557.

Carpenter, S., Groschup, M. H., Garros, C., Felippe-Bauer, M. L. & Purse, B. V. (2013). Culicoides biting midges, arboviruses and public health in Europe. *Antiviral research* **100**, 102-113.

Carroll, M. W., Matthews, D. A., Hiscox, J. A., Elmore, M. J., Pollakis, G., Rambaut, A., Hewson, R., Garcia-Dorival, I., Bore, J. A. & other authors (2015). Temporal and spatial analysis of the 2014-2015 Ebola virus outbreak in West Africa. *Nature* **524**, 97-101.

Carter, S. D., Surtees, R., Walter, C. T., Ariza, A., Bergeron, E., Nichol, S. T., Hiscox, J. A., Edwards, T. A. & Barr, J. N. (2012). Structure, function, and evolution of the Crimean-Congo hemorrhagic fever virus nucleocapsid protein. *Journal of virology* **86**, 10914-10923.

Center for Genome Innovation University of Connecticut, Roche/454: GS FLX+, http://cgi.uconn.edu/roche454-gs-flx/.

Chinsangaram, J., Piccone, M. E. & Grubman, M. J. (1999). Ability of foot-and-mouth disease virus to form plaques in cell culture is associated with suppression of alpha/beta interferon. *Journal of virology* **73**, 9891-9898.

Choi, Y., Kwon, Y. C., Kim, S. I., Park, J. M., Lee, K. H. & Ahn, B. Y. (2008). A hantavirus causing hemorrhagic fever with renal syndrome requires gC1qR/p32 for efficient cell binding and infection. *Virology* **381**, 178-183.

Cifuentes-Munoz, N., Salazar-Quiroz, N. & Tischler, N. D. (2014). Hantavirus Gn and Gc envelope glycoproteins: key structural units for virus cell entry and virus assembly. *Viruses* **6**, 1801-1822.

Cifuentes-Munoz, N., Barriga, G. P., Valenzuela, P. D. & Tischler, N. D. (2011). Aromatic and polar residues spanning the candidate fusion peptide of the Andes virus Gc protein are essential for membrane fusion and infection. *The Journal of general virology* **92**, 552-563.

Colon-Ramos, D. A., Irusta, P. M., Gan, E. C., Olson, M. R., Song, J., Morimoto, R. I., Elliott, R. M., Lombard, M., Hollingsworth, R. & other authors (2003). Inhibition of translation and induction of apoptosis by Bunyaviral nonstructural proteins bearing sequence similarity to reaper. *Molecular biology of the cell* **14**, 4162-4172.

Corden, J. L. (2013). RNA Polymerase II C-Terminal Domain: Tethering Transcription to Transcript and Template. *Chemical Reviews* **113**, 8423-8455.

Cosset, F. L. & Lavillette, D. (2011). Cell entry of enveloped viruses. *Advances in genetics* **73**, 121-183.

Crabtree, M. B., Kent Crockett, R. J., Bird, B. H., Nichol, S. T., Erickson, B. R., Biggerstaff, B. J., Horiuchi, K. & Miller, B. R. (2012). Infection and transmission of Rift Valley fever viruses lacking the NSs and/or NSm genes in mosquitoes: potential role for NSm in mosquito infection. *PLoS neglected tropical diseases* **6**, e1639.

Darriba, D., Taboada, G. L., Doallo, R. & Posada, D. (2012). jModelTest 2: more models, new heuristics and parallel computing. *Nature methods* **9**, 772.

Dawood, F. S., Jain, S., Finelli, L., Shaw, M. W., Lindstrom, S., Garten, R. J., Gubareva, L. V., Xu, X., Bridges, C. B. & other authors (2009). Emergence of a novel swine-origin influenza A (H1N1) virus in humans. *The New England journal of medicine* **360**, 2605-2615.

de Boer, S. M., Kortekaas, J., Spel, L., Rottier, P. J., Moormann, R. J. & Bosch, B. J. (2012a). Acid-activated structural reorganization of the Rift Valley fever virus Gc fusion protein. *Journal of virology* **86**, 13642-13652.

de Boer, S. M., Kortekaas, J., de Haan, C. A., Rottier, P. J., Moormann, R. J. & Bosch, B. J. (2012b). Heparan sulfate facilitates Rift Valley fever virus entry into the cell. *Journal of virology* **86**, 13767-13771.

de Brito Magalhaes, C. L., Drumond, B. P., Novaes, R. F., Quinan, B. R., de Magalhaes, J. C., dos Santos, J. R., Pinto Cdo, A., Assis, M. T., Bonjardim, C. A. & other authors (2011). Identification of a phylogenetically distinct orthobunyavirus from group C. *Archives of virology* **156**, 1173-1184.

Desmyter, J., Melnick, J. L. & Rawls, W. E. (1968). Defectiveness of Interferon Production and of Rubella Virus Interference in a Line of African Green Monkey Kidney Cells (Vero). *Journal of virology* **2**, 955-961.

Dessau, M. & Modis, Y. (2013). Crystal structure of glycoprotein C from Rift Valley fever virus. *Proceedings of the National Academy of Sciences of the United States of America* **110**, 1696-1701.

Devignot, S., Bergeron, E., Nichol, S., Mirazimi, A. & Weber, F. (2015). A virus-like particle system identifies the endonuclease domain of Crimean-Congo hemorrhagic fever virus. *Journal of virology* **89**, 5957-5967.

Dilcher, M., Alves, M. J., Finkeisen, D., Hufert, F. & Weidmann, M. (2012). Genetic characterization of Bhanja virus and Palma virus, two tick-borne phleboviruses. *Virus genes* **45**, 311-315.

Dixon, K. E., Travassos da Rosa, A. P., Travassos da Rosa, J. F. & Llewellyn, C. H. (1981). Oropouche virus. II. Epidemiological observations during an epidemic in Santarem, Para, Brazil in 1975. *The American journal of tropical medicine and hygiene* **30**, 161-164.

Dong, H., Li, P., Elliott, R. M. & Dong, C. (2013a). Structure of Schmallenberg orthobunyavirus nucleoprotein suggests a novel mechanism of genome encapsidation. *Journal of virology* **87**, 5593-5601.

Dong, H., Li, P., Bottcher, B., Elliott, R. M. & Dong, C. (2013b). Crystal structure of Schmallenberg orthobunyavirus nucleoprotein-RNA complex reveals a novel RNA sequestration mechanism. *RNA (New York, NY)* **19**, 1129-1136.

Dudas, G. & Obbard, D. J. (2015). Are arthropods at the heart of virus evolution? *eLife* **4**, e06837.

Dunn, E. F., Pritlove, D. C. & Elliott, R. M. (1994). The S RNA genome segments of Batai, Cache Valley, Guaroa, Kairi, Lumbo, Main Drain and Northway

bunyaviruses: sequence determination and analysis. *The Journal of general virology* **75 (Pt 3)**, 597-608.

Dunn, E. F., Pritlove, D. C., Jin, H. & Elliott, R. M. (1995). Transcription of a recombinant bunyavirus RNA template by transiently expressed bunyavirus proteins. *Virology* **211**, 133-143.

Eick, D. & Geyer, M. (2013). The RNA Polymerase II Carboxy-Terminal Domain (CTD) Code. *Chemical Reviews* **113**, 8456-8490.

Eifan, S. A. & Elliott, R. M. (2009). Mutational analysis of the Bunyamwera orthobunyavirus nucleocapsid protein gene. *Journal of virology* **83**, 11307-11317.

Elliott, R. & Weber, F. (2009). Bunyaviruses and the Type I Interferon System. *Viruses* **1**, 1003-1021.

Elliott, R. M. (1989). Nucleotide sequence analysis of the small (S) RNA segment of Bunyamwera virus, the prototype of the family Bunyaviridae. *The Journal of general virology* **70 (Pt 5)**, 1281-1285.

Elliott, R. M. (2014). Orthobunyaviruses: recent genetic and structural insights. *Nature reviews Microbiology* **12**, 673-685.

Elliott, R. M. & McGregor, A. (1989). Nucleotide sequence and expression of the small (S) RNA segment of Maguari bunyavirus. *Virology* **171**, 516-524.

Elliott, R. M. & Blakqori, G. (2011). Molecular Biology of Orthobunyaviruses. In *Bunyaviridae: Molecular and Cellular Biology*. Edited by A. Plyusnin & R. M. Elliott. Norfolk, UK: Caister Academic Press.

Elliott, R. M. & Schmaljohn, C. S. (2013). Chapter 42, Bunyaviridae In *Fields Virology*, 6th edn, vol. 2. Edited by D. M. Knipe & P. Howley.

Elliott, R. M. & Brennan, B. (2014). Emerging phleboviruses. *Current opinion in virology* **5**, 50-57.

Elliott, R. M., Schmaljohn, C. S. & Collett, M. S. (1991). Bunyaviridae Genome Structure and Gene Expression. In *Bunyaviridae* (Current Topics in Microbiology and Immunology), vol. 169, pp. 91-141. Edited by D. Kolakofsky: Springer Berlin Heidelberg.

Elliott, R. M., Blakqori, G., van Knippenberg, I. C., Koudriakova, E., Li, P., McLees, A., Shi, X. & Szemiel, A. M. (2013). Establishment of a reverse genetics system for Schmallenberg virus, a newly emerged orthobunyavirus in Europe. *The Journal of general virology* **94**, 851-859.

Emeny, J. M. & Morgan, M. J. (1979). Regulation of the Interferon System: Evidence that Vero Cells have a Genetic Defect in Interferon Production. *The Journal of general virology* **43**, 247-252.

Enami, M. & Palese, P. (1991). High-efficiency formation of influenza virus transfectants. *Journal of Virology* **65**, 2711-2713.

Epidemiological Alert (2010). Outbreak of Oropouche Fever, Current Situation. Pan American Health Organization.

Epidemiological Bulletin (1982). Oropouche Fever in Brazil. In *Pan American Health Organization*. 3 (5).

Erixon, P., Svennblad, B., Britton, T. & Oxelman, B. (2003). Reliability of Bayesian posterior probabilities and bootstrap frequencies in phylogenetics. *Systematic biology* **52**, 665-673.

Espert, L., Degols, G., Gongora, C., Blondel, D., Williams, B. R., Silverman, R. H. & Mechti, N. (2003). ISG20, a New Interferon-induced RNase Specific for

Single-stranded RNA, Defines an Alternative Antiviral Pathway against RNA Genomic Viruses. *Journal of Biological Chemistry* **278**, 16151-16158.

Fazakerley, J. K., Gonzalez-Scarano, F., Strickler, J., Dietzschold, B., Karush, F. & Nathanson, N. (1988). Organization of the middle RNA segment of snowshoe hare Bunyavirus. *Virology* **167**, 422-432.

Ferron, F., Li, Z., Danek, E. I., Luo, D., Wong, Y., Coutard, B., Lantez, V., Charrel, R., Canard, B. & other authors (2011). The Hexamer Structure of the Rift Valley Fever Virus Nucleoprotein Suggests a Mechanism for its Assembly into Ribonucleoprotein Complexes. *PLoS pathogens* **7**, e1002030.

Figueiredo, L. T. & Da Rosa, A. P. (1988). Jatobal virus antigenic characterization by ELISA and neutralization test using EIA as indicator, on tissue culture. *Memorias do Instituto Oswaldo Cruz* **83**, 161-164.

Fitzgerald, K. A., McWhirter, S. M., Faia, K. L., Rowe, D. C., Latz, E., Golenbock, D. T., Coyle, A. J., Liao, S.-M. & Maniatis, T. (2003). IKK[epsi] and TBK1 are essential components of the IRF3 signaling pathway. *Nature Immunology* **4**, 491-496.

Flick, K., Hooper, J., Schmaljohn, C., Pettersson, R., Feldmann, H. & Flick, R. (2003a). Rescue of Hantaan virus minigenomes. *Virology* **306**, 219-224.

Flick, K., Katz, A., Overby, A., Feldmann, H., Pettersson, R. F. & Flick, R. (2004). Functional analysis of the noncoding regions of the Uukuniemi virus (Bunyaviridae) RNA segments. *Journal of virology* **78**, 11726-11738.

Flick, R. & Pettersson, R. F. (2001). Reverse genetics system for Uukuniemi virus (Bunyaviridae): RNA polymerase I-catalyzed expression of chimeric viral RNAs. *Journal of Virology* **75**, 1643-1655.

Flick, R., Flick, K., Feldmann, H. & Elgh, F. (2003b). Reverse genetics for Crimean-Congo hemorrhagic fever virus. *Journal of Virology* **77**, 5997-6006.

Fontana, J., Lopez-Montero, N., Elliott, R. M., Fernandez, J. J. & Risco, C. (2008). The unique architecture of Bunyamwera virus factories around the Golgi complex. *Cellular microbiology* **10**, 2012-2028.

Forshey, B. M., Guevara, C., Laguna-Torres, V. A., Cespedes, M., Vargas, J., Gianella, A., Vallejo, E., Madrid, C., Aguayo, N. & other authors (2010). Arboviral Etiologies of Acute Febrile Illnesses in Western South America, 2000–2007. *PLoS neglected tropical diseases* **4**, e787.

Fraser, D., Mahler, H. R., Shug, A. L. & Thomas, C. A. (1957). The infection of sub-cellular Escherichia Coli, strain B, with a DNA preparation from T2 bacteriophage. *Proceedings of the National Academy of Sciences of the United States of America* **43**, 939-947.

Freiberg, A. N., Sherman, M. B., Morais, M. C., Holbrook, M. R. & Watowich, S. J. (2008). Three-dimensional organization of Rift Valley fever virus revealed by cryoelectron tomography. *Journal of virology* **82**, 10341-10348.

Frese, M., Kochs, G., Feldmann, H., Hertkorn, C. & Haller, O. (1996). Inhibition of bunyaviruses, phleboviruses, and hantaviruses by human MxA protein. *Journal of virology* **70**, 915-923.

Frias-Staheli, N., Giannakopoulos, N. V., Kikkert, M., Taylor, S. L., Bridgen, A., Paragas, J., Richt, J. A., Rowland, R. R., Schmaljohn, C. S. & other authors (2007). Ovarian Tumor Domain-Containing Viral Proteases Evade Ubiquitin- and ISG15-Dependent Innate Immune Responses. *Cell host & microbe* **2**, 404-416.

Fuller, F. & Bishop, D. H. (1982). Identification of virus-coded nonstructural polypeptides in bunyavirus-infected cells. *Journal of virology* **41**, 643-648.

Fuller, F., Bhown, A. S. & Bishop, D. H. (1983). Bunyavirus nucleoprotein, N, and a non-structural protein, NSS, are coded by overlapping reading frames in the S RNA. *The Journal of general virology* **64 (Pt 8)**, 1705-1714.

García-Sastre, A. & Biron, C. A. (2006). Type 1 Interferons and the Virus-Host Relationship: A Lesson in Détente. *Science (New York, NY)* **312**, 879-882.

Garcin, D., Lezzi, M., Dobbs, M., Elliott, R. M., Schmaljohn, C., Kang, C. Y. & Kolakofsky, D. (1995). The 5' ends of Hantaan virus (Bunyaviridae) RNAs suggest a prime-and-realign mechanism for the initiation of RNA synthesis. *Journal of virology* **69**, 5754-5762.

Garry, C. E. & Garry, R. F. (2004). Proteomics computational analyses suggest that the carboxyl terminal glycoproteins of Bunyaviruses are class II viral fusion protein (beta-penetrenes). *Theoretical biology & medical modelling* **1**, 10.

Gatherer, D. (2014). The 2014 Ebola virus disease outbreak in West Africa. *The Journal of general virology* **95**, 1619-1624.

Gauliard, N., Billecocq, A., Flick, R. & Bouloy, M. (2006). Rift Valley fever virus noncoding regions of L, M and S segments regulate RNA synthesis. *Virology* **351**, 170-179.

Gavrilovskaya, I. N., Brown, E. J., Ginsberg, M. H. & Mackow, E. R. (1999). Cellular Entry of Hantaviruses Which Cause Hemorrhagic Fever with Renal Syndrome Is Mediated by β(3) Integrins. *Journal of virology* **73**, 3951-3959.

Gavrilovskaya, I. N., Shepley, M., Shaw, R., Ginsberg, M. H. & Mackow, E. R. (1998). beta3 Integrins mediate the cellular entry of hantaviruses that cause respiratory failure. *Proceedings of the National Academy of Sciences of the United States of America* **95**, 7074-7079.

Gerlach, P., Malet, H., Cusack, S. & Reguera, J. (2015). Structural Insights into Bunyavirus Replication and Its Regulation by the vRNA Promoter. *Cell* **161**, 1267-1279.

Gerrard, S. R., Li, L., Barrett, A. D. & Nichol, S. T. (2004). Ngari virus is a Bunyamwera virus reassortant that can be associated with large outbreaks of hemorrhagic fever in Africa. *Journal of virology* **78**, 8922-8926.

Ghanem, A., Kern, A. & Conzelmann, K. K. (2012). Significantly improved rescue of rabies virus from cDNA plasmids. *European Journal of Cell Biology* **91**, 10-16.

Goodbourn, S., Didcock, L. & Randall, R. E. (2000). Interferons: cell signalling, immune modulation, antiviral response and virus countermeasures. *The Journal of general virology* **81**, 2341-2364.

Grada, A. & Weinbrecht, K. (2013). Next-Generation Sequencing: Methodology and Application. *Journal of Investigative Dermatology* **133**, e11.

Guindon, S., Dufayard, J. F., Lefort, V., Anisimova, M., Hordijk, W. & Gascuel, O. (2010). New algorithms and methods to estimate maximum-likelihood phylogenies: assessing the performance of PhyML 3.0. *Systematic biology* **59**, 307-321.

Guu, T. Y., Zheng, W. & Tao, Y. (2012). Bunyavirus: Structure and Replication. In *Viral Molecular Machines* (Advances in Experimental Medicine and Biology), vol. 726, pp. 245-266. Edited by M. G. Rossmann & V. B. Rao: Springer US.

Habjan, M., Penski, N., Wagner, V., Spiegel, M., Overby, A. K., Kochs, G., Huiskonen, J. T. & Weber, F. (2009a). Efficient production of Rift Valley

fever virus-like particles: The antiviral protein MxA can inhibit primary transcription of bunyaviruses. *Virology* **385**, 400-408.

Habjan, M., Pichlmair, A., Elliott, R. M., Overby, A. K., Glatter, T., Gstaiger, M., Superti-Furga, G., Unger, H. & Weber, F. (2009b). NSs protein of rift valley fever virus induces the specific degradation of the double-stranded RNA-dependent protein kinase. *Journal of virology* **83**, 4365-4375.

Hacker, J. K. & Hardy, J. L. (1997). Adsorptive endocytosis of California encephalitis virus into mosquito and mammalian cells: a role for G1. *Virology* **235**, 40-47.

Hale, B. G., Knebel, A., Botting, C. H., Galloway, C. S., Precious, B. L., Jackson, D., Elliott, R. M. & Randall, R. E. (2009). CDK/ERK-mediated phosphorylation of the human influenza A virus NS1 protein at threonine-215. *Virology* **383**, 6-11.

Hart, T. J., Kohl, A. & Elliott, R. M. (2009). Role of the NSs protein in the zoonotic capacity of Orthobunyaviruses. *Zoonoses and public health* **56**, 285-296.

Helgason, E., Phung, Q. T. & Dueber, E. C. Recent insights into the complexity of Tank-binding kinase 1 signaling networks: The emerging role of cellular localization in the activation and substrate specificity of TBK1. *FEBS Letters* **587**, 1230-1237.

Hewlett, M. J., Pettersson, R. F. & Baltimore, D. (1977). Circular forms of Uukuniemi virion RNA: an electron microscopic study. *Journal of virology* **21**, 1085-1093.

Hoffmann, B., Scheuch, M., Hoper, D., Jungblut, R., Holsteg, M., Schirrmeier, H., Eschbaumer, M., Goller, K. V., Wernike, K. & other authors (2012). Novel orthobunyavirus in Cattle, Europe, 2011. *Emerging infectious diseases* **18**, 469-472.

Hoffmann, H. H., Schneider, W. M. & Rice, C. M. (2015). Interferons and viruses: an evolutionary arms race of molecular interactions. *Trends in immunology* **36**, 124-138.

Hofmann, H., Li, X., Zhang, X., Liu, W., Kuhl, A., Kaup, F., Soldan, S. S., Gonzalez-Scarano, F., Weber, F. & other authors (2013). Severe fever with thrombocytopenia virus glycoproteins are targeted by neutralizing antibodies and can use DC-SIGN as a receptor for pH-dependent entry into human and animal cell lines. *Journal of virology* **87**, 4384-4394.

Hollidge, B. S., Nedelsky, N. B., Salzano, M. V., Fraser, J. W., Gonzalez-Scarano, F. & Soldan, S. S. (2012). Orthobunyavirus entry into neurons and other mammalian cells occurs via clathrin-mediated endocytosis and requires trafficking into early endosomes. *Journal of virology* **86**, 7988-8001.

Holmes, E. C. & Rambaut, A. (2004). Viral evolution and the emergence of SARS coronavirus. *Philosophical transactions of the Royal Society of London Series B, Biological sciences* **359**, 1059-1065.

Honig, J. E., Osborne, J. C. & Nichol, S. T. (2004). Crimean-Congo hemorrhagic fever virus genome L RNA segment and encoded protein. *Virology* **321**, 29-35.

Huiskonen, J. T., Overby, A. K., Weber, F. & Grunewald, K. (2009). Electron cryo-microscopy and single-particle averaging of Rift Valley fever virus: evidence for GN-GC glycoprotein heterodimers. *Journal of virology* **83**, 3762-3769.

Huiskonen, J. T., Hepojoki, J., Laurinmaki, P., Vaheri, A., Lankinen, H., Butcher, S. J. & Grunewald, K. (2010). Electron cryotomography of Tula hantavirus

suggests a unique assembly paradigm for enveloped viruses. *Journal of virology* **84**, 4889-4897.

Hunt, A. R. & Calisher, C. H. (1979). Relationships of bunyamwera group viruses by neutralization. *The American journal of tropical medicine and hygiene* **28**, 740-749.

Ikegami, T., Peters, C. J. & Makino, S. (2005). Rift valley fever virus nonstructural protein NSs promotes viral RNA replication and transcription in a minigenome system. *Journal of virology* **79**, 5606-5615.

Ikegami, T., Won, S., Peters, C. J. & Makino, S. (2006). Rescue of infectious rift valley fever virus entirely from cDNA, analysis of virus lacking the NSs gene, and expression of a foreign gene. *Journal of virology* **80**, 2933-2940.

Ikegami, T., Won, S., Peters, C. J. & Makino, S. (2007). Characterization of Rift Valley fever virus transcriptional terminations. *Journal of virology* **81**, 8421-8438.

illumina http://www.illumina.com.

IonTorrent (ThermoFisher Scientific). https://ioncommunity.thermofisher.com/welcome.

Iroegbu, C. U. & Pringle, C. R. (1981). Genetic interactions among viruses of the Bunyamwera complex. *Journal of virology* **37**, 383-394.

Iwasaki, A. (2012). A virological view of innate immune recognition. *Annual Review of Microbiology* **66**, 177-196.

Jaaskelainen, K. M., Kaukinen, P., Minskaya, E. S., Plyusnina, A., Vapalahti, O., Elliott, R. M., Weber, F., Vaheri, A. & Plyusnin, A. (2007). Tula and Puumala hantavirus NSs ORFs are functional and the products inhibit activation of the interferon-beta promoter. *Journal of medical virology* **79**, 1527-1536.

Jacoby, D. R., Cooke, C., Prabakaran, I., Boland, J., Nathanson, N. & Gonzalez-Scarano, F. (1993). Expression of the La Crosse M segment proteins in a recombinant vaccinia expression system mediates pH-dependent cellular fusion. *Virology* **193**, 993-996.

Jin, H. & Elliott, R. M. (1991). Expression of functional Bunyamwera virus L protein by recombinant vaccinia viruses. *Journal of virology* **65**, 4182-4189.

Jin, H. & Elliott, R. M. (1992). Mutagenesis of the L protein encoded by Bunyamwera virus and production of monospecific antibodies. *The Journal of general virology* **73 (Pt 9)**, 2235-2244.

Jin, H. & Elliott, R. M. (1993a). Non-viral sequences at the 5' ends of Dugbe nairovirus S mRNAs. *The Journal of general virology* **74 (Pt 10)**, 2293-2297.

Jin, H. & Elliott, R. M. (1993b). Characterization of Bunyamwera virus S RNA that is transcribed and replicated by the L protein expressed from recombinant vaccinia virus. *Journal of virology* **67**, 1396-1404.

Jin, M., Park, J., Lee, S., Park, B., Shin, J., Song, K. J., Ahn, T. I., Hwang, S. Y., Ahn, B. Y. & other authors (2002). Hantaan virus enters cells by clathrin-dependent receptor-mediated endocytosis. *Virology* **294**, 60-69.

Johnson, K. N., Zeddam, J. L. & Ball, L. A. (2000). Characterization and construction of functional cDNA clones of Pariacoto virus, the first Alphanodavirus isolated outside Australasia. *Journal of virology* **74**, 5123-5132.

Kading, R. C., Crabtree, M. B., Bird, B. H., Nichol, S. T., Erickson, B. R., Horiuchi, K., Biggerstaff, B. J. & Miller, B. R. (2014). Deletion of the NSm Virulence Gene of Rift Valley Fever Virus Inhibits Virus Replication in and

Dissemination from the Midgut of *Aedes aegypti* Mosquitoes. *PLoS neglected tropical diseases* **8**, e2670.

Kampmann, T., Mueller, D. S., Mark, A. E., Young, P. R. & Kobe, B. (2006). The Role of Histidine Residues in Low-pH-Mediated Viral Membrane Fusion. *Structure* **14**, 1481-1487.

Kanerva, M., Melen, K., Vaheri, A. & Julkunen, I. (1996). Inhibition of puumala and tula hantaviruses in Vero cells by MxA protein. *Virology* **224**, 55-62.

Kang, J. I., Park, S. H., Lee, P. W. & Ahn, B. Y. (1999). Apoptosis is induced by hantaviruses in cultured cells. *Virology* **264**, 99-105.

Karlberg, H., Tan, Y.-J. & Mirazimi, A. (2011). Induction of Caspase Activation and Cleavage of the Viral Nucleocapsid Protein in Different Cell Types during Crimean-Congo Hemorrhagic Fever Virus Infection. *The Journal of Biological Chemistry* **286**, 3227-3234.

Kaukinen, P., Vaheri, A. & Plyusnin, A. (2003). Mapping of the regions involved in homotypic interactions of Tula hantavirus N protein. *Journal of virology* **77**, 10910-10916.

Kaukinen, P., Koistinen, V., Vapalahti, O., Vaheri, A. & Plyusnin, A. (2001). Interaction between molecules of hantavirus nucleocapsid protein. *The Journal of general virology* **82**, 1845-1853.

Kawaoka, Y. & Neumann, G. (2004). Reverse Genetics Systems for the Generation of Segmented Negative-Sense RNA Viruses Entirely from Cloned cDNA. In *Biology of Negative Strand RNA Viruses: The Power of Reverse Genetics*. Edited by Y. Kawaoka: Springer.

Kielian, M., Chanel-Vos, C. & Liao, M. (2010). Alphavirus Entry and Membrane Fusion. *Viruses* **2**, 796-825.

Killip, M. J., Young, D. F., Gatherer, D., Ross, C. S., Short, J. A., Davison, A. J., Goodbourn, S. & Randall, R. E. (2013). Deep sequencing analysis of defective genomes of parainfluenza virus 5 and their role in interferon induction. *Journal of virology* **87**, 4798-4807.

Kinsella, E., Martin, S. G., Grolla, A., Czub, M., Feldmann, H. & Flick, R. (2004). Sequence determination of the Crimean-Congo hemorrhagic fever virus L segment. *Virology* **321**, 23-28.

Kochs, G., Janzen, C., Hohenberg, H. & Haller, O. (2002). Antivirally active MxA protein sequesters La Crosse virus nucleocapsid protein into perinuclear complexes. *Proceedings of the National Academy of Sciences of the United States of America* **99**, 3153-3158.

Kohl, A., Dunn, E. F., Lowen, A. C. & Elliott, R. M. (2004a). Complementarity, sequence and structural elements within the 3' and 5' non-coding regions of the Bunyamwera orthobunyavirus S segment determine promoter strength. *The Journal of general virology* **85**, 3269-3278.

Kohl, A., Lowen, A. C., Leonard, V. H. & Elliott, R. M. (2006). Genetic elements regulating packaging of the Bunyamwera orthobunyavirus genome. *The Journal of general virology* **87**, 177-187.

Kohl, A., Bridgen, A., Dunn, E., Barr, J. N. & Elliott, R. M. (2003a). Effects of a point mutation in the 3' end of the S genome segment of naturally occurring and engineered Bunyamwera viruses. *The Journal of general virology* **84**, 789-793.

Kohl, A., Clayton, R. F., Weber, F., Bridgen, A., Randall, R. E. & Elliott, R. M. (2003b). Bunyamwera virus nonstructural protein NSs counteracts interferon

regulatory factor 3-mediated induction of early cell death. *Journal of virology* **77**, 7999-8008.

Kohl, A., Hart, T. J., Noonan, C., Royall, E., Roberts, L. O. & Elliott, R. M. (2004b). A bunyamwera virus minireplicon system in mosquito cells. *Journal of virology* **78**, 5679-5685.

Kormelink, R., Storms, M., Van Lent, J., Peters, D. & Goldbach, R. (1994). Expression and subcellular location of the NSM protein of tomato spotted wilt virus (TSWV), a putative viral movement protein. *Virology* **200**, 56-65.

Kotwal, G. J., Hatch, S. & Marshall, W. L. (2012). Viral Infection: An Evolving Insight into the Signal Transduction Pathways Responsible for the Innate Immune Response. *Advances in Virology* **2012**, 11.

Kraatz, F., Wernike, K., Hechinger, S., Konig, P., Granzow, H., Reimann, I. & Beer, M. (2015). Deletion mutants of schmallenberg virus are avirulent and protect from virus challenge. *Journal of virology* **89**, 1825-1837.

Krautkramer, E. & Zeier, M. (2008). Hantavirus causing hemorrhagic fever with renal syndrome enters from the apical surface and requires decay-accelerating factor (DAF/CD55). *Journal of virology* **82**, 4257-4264.

Kreher, F., Tamietti, C., Gommet, C., Guillemot, L., Ermonval, M., Failloux, A. B., Panthier, J. J., Bouloy, M. & Flamand, M. (2014). The Rift Valley fever accessory proteins NSm and P78/NSm-GN are distinct determinants of virus propagation in vertebrate and invertebrate hosts. *Emerging Microbes & Infections* **3**, e71.

Krug, R. M., Broni, B. A. & Bouloy, M. (1979). Are the 5' ends of influenza viral mRNAs synthesized in vivo donated by host mRNAs? *Cell* **18**, 329-334.

Kuismanen, E., Hedman, K., Saraste, J. & Pettersson, R. F. (1982). Uukuniemi virus maturation: accumulation of virus particles and viral antigens in the Golgi complex. *Molecular and cellular biology* **2**, 1444-1458.

Kukkonen, S. K., Vaheri, A. & Plyusnin, A. (2004). Tula hantavirus L protein is a 250 kDa perinuclear membrane-associated protein. *The Journal of general virology* **85**, 1181-1189.

Ladner, J. T., Savji, N., Lofts, L., Travassos da Rosa, A., Wiley, M. R., Gestole, M. C., Rosen, G. E., Guzman, H., Vasconcelos, P. F. & other authors (2014). Genomic and phylogenetic characterization of viruses included in the Manzanilla and Oropouche species complexes of the genus Orthobunyavirus, family Bunyaviridae. *The Journal of general virology* **95**, 1055-1066.

Lambert, A. J. & Lanciotti, R. S. (2008). Molecular characterization of medically important viruses of the genus Orthobunyavirus. *The Journal of general virology* **89**, 2580-2585.

Lanciotti, R. S., Kosoy, O. I., Bosco-Lauth, A. M., Pohl, J., Stuchlik, O., Reed, M. & Lambert, A. J. (2013). Isolation of a novel orthobunyavirus (Brazoran virus) with a 1.7 kb S segment that encodes a unique nucleocapsid protein possessing two putative functional domains. *Virology* **444**, 55-63.

Lappin, D. F., Nakitare, G. W., Palfreyman, J. W. & Elliott, R. M. (1994). Localization of Bunyamwera bunyavirus G1 glycoprotein to the Golgi requires association with G2 but not with NSm. *The Journal of general virology* **75**, 3441-3451.

Le May, N., Dubaele, S., De Santis, L. P., Billecocq, A., Bouloy, M. & Egly, J.-M. (2004). TFIIH Transcription Factor, a Target for the Rift Valley Hemorrhagic Fever Virus. *Cell* **116**, 541-550.

Le May, N., Mansuroglu, Z., Leger, P., Josse, T., Blot, G., Billecocq, A., Flick, R., Jacob, Y., Bonnefoy, E. & other authors (2008). A SAP30 complex inhibits IFN-beta expression in Rift Valley fever virus infected cells. *PLoS pathogens* **4**, e13.

Leonard, V. H., Kohl, A., Hart, T. J. & Elliott, R. M. (2006). Interaction of Bunyamwera Orthobunyavirus NSs protein with mediator protein MED8: a mechanism for inhibiting the interferon response. *Journal of virology* **80**, 9667-9675.

Leonard, V. H., Kohl, A., Osborne, J. C., McLees, A. & Elliott, R. M. (2005). Homotypic interaction of Bunyamwera virus nucleocapsid protein. *Journal of virology* **79**, 13166-13172.

Li, B., Wang, Q., Pan, X., Fernandez de Castro, I., Sun, Y., Guo, Y., Tao, X., Risco, C., Sui, S. F. & other authors (2013). Bunyamwera virus possesses a distinct nucleocapsid protein to facilitate genome encapsidation. *Proceedings of the National Academy of Sciences of the United States of America* **110**, 9048-9053.

Li, C.-X., Shi, M., Tian, J.-H., Lin, X.-D., Kang, Y.-J., Chen, L.-J., Qin, X.-C., Xu, J., Holmes, E. C. & other authors (2015). Unprecedented genomic diversity of RNA viruses in arthropods reveals the ancestry of negative-sense RNA viruses. *eLife* **4**, e05378.

Li, D. (2013). A highly pathogenic new bunyavirus emerged in China. *Emerging Microbes & Infections* **2**, e1.

Li, X. D., Kukkonen, S., Vapalahti, O., Plyusnin, A., Lankinen, H. & Vaheri, A. (2004). Tula hantavirus infection of Vero E6 cells induces apoptosis involving caspase 8 activation. *The Journal of general virology* **85**, 3261-3268.

Li, X. D., Makela, T. P., Guo, D., Soliymani, R., Koistinen, V., Vapalahti, O., Vaheri, A. & Lankinen, H. (2002). Hantavirus nucleocapsid protein interacts with the Fas-mediated apoptosis enhancer Daxx. *The Journal of general virology* **83**, 759-766.

Livonesi, M. C., Moro de Sousa, R. L. & Moraes Figueiredo, L. T. (2007a). In vitro study of antiviral activity of mycophenolic acid on Brazilian orthobunyaviruses. *Intervirology* **50**, 204-208.

Livonesi, M. C., De Sousa, R. L., Badra, S. J. & Figueiredo, L. T. (2006). In vitro and in vivo studies of ribavirin action on Brazilian Orthobunyavirus. *The American journal of tropical medicine and hygiene* **75**, 1011-1016.

Livonesi, M. C., de Sousa, R. L., Badra, S. J. & Figueiredo, L. T. (2007b). In vitro and in vivo studies of the Interferon-alpha action on distinct Orthobunyavirus. *Antiviral research* **75**, 121-128.

Lole, K. S., Bollinger, R. C., Paranjape, R. S., Gadkari, D., Kulkarni, S. S., Novak, N. G., Ingersoll, R., Sheppard, H. W. & Ray, S. C. (1999). Full-length human immunodeficiency virus type 1 genomes from subtype C-infected seroconverters in India, with evidence of intersubtype recombination. *Journal of virology* **73**, 152-160.

Lopez, N., Muller, R., Prehaud, C. & Bouloy, M. (1995). The L protein of Rift Valley fever virus can rescue viral ribonucleoproteins and transcribe synthetic genome-like RNA molecules. *Journal of virology* **69**, 3972-3979.

Lowen, A. C. & Elliott, R. M. (2005). Mutational analyses of the nonconserved sequences in the Bunyamwera Orthobunyavirus S segment untranslated regions. *Journal of virology* **79**, 12861-12870.

Lowen, A. C., Noonan, C., McLees, A. & Elliott, R. M. (2004). Efficient bunyavirus rescue from cloned cDNA. *Virology* **330**, 493-500.

Lowen, A. C., Boyd, A., Fazakerley, J. K. & Elliott, R. M. (2005). Attenuation of bunyavirus replication by rearrangement of viral coding and noncoding sequences. *Journal of virology* **79**, 6940-6946.

Lozach, P. Y., Kuhbacher, A., Meier, R., Mancini, R., Bitto, D., Bouloy, M. & Helenius, A. (2011). DC-SIGN as a receptor for phleboviruses. *Cell host & microbe* **10**, 75-88.

Lozach, P. Y., Mancini, R., Bitto, D., Meier, R., Oestereich, L., Overby, A. K., Pettersson, R. F. & Helenius, A. (2010). Entry of bunyaviruses into mammalian cells. *Cell host & microbe* **7**, 488-499.

Luytjes, W., Krystal, M., Enami, M., Parvin, J. D. & Palese, P. (1989). Amplification, expression, and packaging of foreign gene by influenza virus. *Cell* **59**, 1107-1113.

Margulies, M., Egholm, M., Altman, W. E., Attiya, S., Bader, J. S., Bemben, L. A., Berka, J., Braverman, M. S., Chen, Y.-J. & other authors (2005). Genome sequencing in microfabricated high-density picolitre reactors. *Nature* **437**, 376-380.

Marston, D., McElhinney, L., Ellis, R., Horton, D., Wise, E., Leech, S., David, D., de Lamballerie, X. & Fooks, A. (2013). Next generation sequencing of viral RNA genomes. *BMC Genomics* **14**, 444.

Martin, D. P., Lemey, P., Lott, M., Moulton, V., Posada, D. & Lefeuvre, P. (2010). RDP3: a flexible and fast computer program for analyzing recombination. *Bioinformatics (Oxford, England)* **26**, 2462-2463.

Matsuno, K., Weisend, C., Travassos da Rosa, A. P., Anzick, S. L., Dahlstrom, E., Porcella, S. F., Dorward, D. W., Yu, X. J., Tesh, R. B. & other authors (2013). Characterization of the Bhanja serogroup viruses (Bunyaviridae): a novel species of the genus Phlebovirus and its relationship with other emerging tick-borne phleboviruses. *Journal of virology* **87**, 3719-3728.

Matsuoka, Y., Ihara, T., Bishop, D. H. & Compans, R. W. (1988). Intracellular accumulation of Punta Toro virus glycoproteins expressed from cloned cDNA. *Virology* **167**, 251-260.

Mazel-Sanchez, B. & Elliott, R. M. (2012). Attenuation of bunyamwera orthobunyavirus replication by targeted mutagenesis of genomic untranslated regions and creation of viable viruses with minimal genome segments. *Journal of virology* **86**, 13672-13678.

Mazel-Sanchez, B. & Elliott, R. M. (2015). Evolution of the Bunyamwera virus polymerase to accommodate deletions within genomic untranslated region sequences. *Journal of virology*.

Mercer, D. R. & Castillo-Pizango, M. J. (2005). Changes in relative species compositions of biting midges (Diptera: Ceratopogonidae) and an outbreak of Oropouche virus in Iquitos, Peru. *Journal of medical entomology* **42**, 554-558.

Mercer, J., Schelhaas, M. & Helenius, A. (2010). Virus entry by endocytosis. *Annual review of biochemistry* **79**, 803-833.

Mir, M. A. & Panganiban, A. T. (2004). Trimeric hantavirus nucleocapsid protein binds specifically to the viral RNA panhandle. *Journal of virology* **78**, 8281-8288.

Mir, M. A., Duran, W. A., Hjelle, B. L., Ye, C. & Panganiban, A. T. (2008). Storage of cellular 5′ mRNA caps in P bodies for viral cap-snatching. *Proceedings of the National Academy of Sciences*.

Mohamed, M., McLees, A. & Elliott, R. M. (2009). Viruses in the Anopheles A, Anopheles B, and Tete Serogroups in the Orthobunyavirus Genus (Family Bunyaviridae) Do Not Encode an NSs Protein. *Journal of virology* **83**, 7612-7618.

Moreli, M. L. & da Costa, V. G. (2013). A systematic review of molecular diagnostic methods for the detection of arboviruses in clinical specimens in Brazil and the importance of a differential diagnosis. *Virology Discovery* **1**.

Moss, B., Elroy-Stein, O., Mizukami, T., Alexander, W. A. & Fuerst, T. R. (1990). New mammalian expression vectors. *Nature* **348**, 91-92.

Mourao, M. P., Bastos, M. S., Gimaqu, J. B., Mota, B. R., Souza, G. S., Grimmer, G. H., Galusso, E. S., Arruda, E. & Figueiredo, L. T. (2009). Oropouche fever outbreak, Manaus, Brazil, 2007-2008. *Emerging infectious diseases* **15**, 2063-2064.

Mudhasani, R., Tran, J. P., Retterer, C., Radoshitzky, S. R., Kota, K. P., Altamura, L. A., Smith, J. M., Packard, B. Z., Kuhn, J. H. & other authors (2013). IFITM-2 and IFITM-3 but not IFITM-1 restrict Rift Valley fever virus. *Journal of virology* **87**, 8451-8464.

Mueller, D. S., Kampmann, T., Yennamalli, R., Young, P. R., Kobe, B. & Mark, A. E. (2008). Histidine protonation and the activation of viral fusion proteins. *Biochemical Society transactions* **36**, 43-45.

Muller, R., Poch, O., Delarue, M., Bishop, D. H. & Bouloy, M. (1994). Rift Valley fever virus L segment: correction of the sequence and possible functional role of newly identified regions conserved in RNA-dependent polymerases. *The Journal of general virology* **75 (Pt 6)**, 1345-1352.

Murray, K., Rogers, R., Selvey, L., Selleck, P., Hyatt, A., Gould, A., Gleeson, L., Hooper, P. & Westbury, H. (1995). A novel morbillivirus pneumonia of horses and its transmission to humans. *Emerging infectious diseases* **1**, 31-33.

Nakitare, G. W. & Elliott, R. M. (1993). Expression of the Bunyamwera virus M genome segment and intracellular localization of NSm. *Virology* **195**, 511-520.

Nguyen, M. & Haenni, A. L. (2003). Expression strategies of ambisense viruses. *Virus research* **93**, 141-150.

Ning, Y. J., Feng, K., Min, Y. Q., Cao, W. C., Wang, M., Deng, F., Hu, Z. & Wang, H. (2015). Disruption of Type I Interferon Signaling by NSs Protein of Severe Fever with Thrombocytopenia Syndrome Virus via Hijacking STAT2 and STAT1 into Inclusion Bodies. *Journal of virology*.

Ning, Y. J., Wang, M., Deng, M., Shen, S., Liu, W., Cao, W. C., Deng, F., Wang, Y. Y., Hu, Z. & other authors (2014). Viral suppression of innate immunity via spatial isolation of TBK1/IKKepsilon from mitochondrial antiviral platform. *Journal of molecular cell biology* **6**, 324-337.

Niu, F., Shaw, N., Wang, Y. E., Jiao, L., Ding, W., Li, X., Zhu, P., Upur, H., Ouyang, S. & other authors (2013). Structure of the Leanyer orthobunyavirus nucleoprotein-RNA complex reveals unique architecture for RNA

encapsidation. *Proceedings of the National Academy of Sciences of the United States of America* **110**, 9054-9059.

Nunes, M. R., Martins, L. C., Rodrigues, S. G., Chiang, J. O., Azevedo Rdo, S., da Rosa, A. P. & Vasconcelos, P. F. (2005). Oropouche virus isolation, southeast Brazil. *Emerging infectious diseases* **11**, 1610-1613.

Ogawa, Y., Sugiura, K., Kato, K., Tohya, Y. & Akashi, H. (2007). Rescue of Akabane virus (family Bunyaviridae) entirely from cloned cDNAs by using RNA polymerase I. *The Journal of general virology* **88**, 3385-3390.

Ogino, M., Yoshimatsu, K., Ebihara, H., Araki, K., Lee, B.-H., Okumura, M. & Arikawa, J. (2004). Cell Fusion Activities of Hantaan Virus Envelope Glycoproteins. *Journal of virology* **78**, 10776-10782.

Olal, D., Dick, A., Woods, V. L., Jr., Liu, T., Li, S., Devignot, S., Weber, F., Saphire, E. O. & Daumke, O. (2014). Structural insights into RNA encapsidation and helical assembly of the Toscana virus nucleoprotein. *Nucleic acids research* **42**, 6025-6037.

Osborne, J. C. & Elliott, R. M. (2000). RNA Binding Properties of Bunyamwera Virus Nucleocapsid Protein and Selective Binding to an Element in the 5′ Terminus of the Negative-Sense S Segment. *Journal of virology* **74**, 9946-9952.

Overby, A. K., Pettersson, R. F., Grünewald, K. & Huiskonen, J. T. (2008). Insights into bunyavirus architecture from electron cryotomography of Uukuniemi virus. *Proceedings of the National Academy of Sciences of the United States of America* **105**, 2375-2379.

Överby, A. K., Pettersson, R. F., Grünewald, K. & Huiskonen, J. T. (2008). Insights into bunyavirus architecture from electron cryotomography of Uukuniemi virus. *Proceedings of the National Academy of Sciences of the United States of America* **105**, 2375-2379.

Park, S.-W., Han, M.-G., Park, C., Ju, Y. R., Ahn, B.-Y. & Ryou, J. (2013). Hantaan virus nucleocapsid protein stimulates MDM2-dependent p53 degradation. *The Journal of general virology* **94**, 2424-2428.

Patterson, J. L., Holloway, B. & Kolakofsky, D. (1984). La Crosse virions contain a primer-stimulated RNA polymerase and a methylated cap-dependent endonuclease. *Journal of virology* **52**, 215-222.

Pekosz, A., Phillips, J., Pleasure, D., Merry, D. & Gonzalez-Scarano, F. (1996). Induction of apoptosis by La Crosse virus infection and role of neuronal differentiation and human bcl-2 expression in its prevention. *Journal of virology* **70**, 5329-5335.

Perrotta, A. T. & Been, M. D. (1990). The self-cleaving domain from the genomic RNA of hepatitis delta virus: sequence requirements and the effects of denaturant. *Nucleic Acids Research* **18**, 6821-6827.

Persson, R. & Pettersson, R. F. (1991). Formation and intracellular transport of a heterodimeric viral spike protein complex. *The Journal of cell biology* **112**, 257-266.

Pinheiro F P, T. d. R. A. P. A., Vasconcelos P F C (2004). Bunyaviridae: Other Bunyaviridae - Oropouche Fever In *Text book of Pediatric Infectious Diseases*, Fifth edn, vol. 2, pp. 2418–2423. Edited by R. D. Feigin. Philadelphia: Saunders: Elsevier Health Sciences.

Pinheiro, F. P., Travassos da Rosa, A. P. A. & Vasconcelos, P. F. (1998). An overview of Oropouche fever epidemics in Brazil and neighbouring countries. In

An overview of arbovirology in Brazil and neighbouring countries Belem, Brazil, pp. 186-192. Edited by V. P. F. C. Travassos da Rosa A P A, Travassos da Rosa J F S. The Evandro Chagas Institute.

Pinheiro, F. P., Travassos da Rosa, A. P., Travassos da Rosa, J. F. & Bensabath, G. (1976). An outbreak of Oropouche virus diease in the vicinity of Santarem, Para, Brazil. *Tropenmedizin und Parasitologie* **27**, 213-223.

Pinheiro, F. P., Hoch, A. L., Gomes, M. L. & Roberts, D. R. (1981a). Oropouche virus. IV. Laboratory transmission by *Culicoides paraensis*. *The American journal of tropical medicine and hygiene* **30**, 172-176.

Pinheiro, F. P., Travassos da Rosa, A. P., Gomes, M. L., LeDuc, J. W. & Hoch, A. L. (1982a). Transmission of Oropouche virus from man to hamster by the midge *Culicoides paraensis*. *Science (New York, NY)* **215**, 1251-1253.

Pinheiro, F. P., Rocha, A. G., Freitas, R. B., Ohana, B. A., Travassos da Rosa, A. P., Rogerio, J. S. & Linhares, A. C. (1982b). [Meningitis associated with Oropouche virus infections]. *Revista do Instituto de Medicina Tropical de Sao Paulo* **24**, 246-251.

Pinheiro, F. P., Travassos da Rosa, A. P., Travassos da Rosa, J. F., Ishak, R., Freitas, R. B., Gomes, M. L., LeDuc, J. W. & Oliva, O. F. (1981b). Oropouche virus. I. A review of clinical, epidemiological, and ecological findings. *The American journal of tropical medicine and hygiene* **30**, 149-160.

Pinheiro, F. P., M.; Bensabath, G.; Causey, O. R.; Shope, R E (1962). Epidemia de vírus Oropouche em Belém. *Revista do Serviço Especial de Saúde* **12**, 15 - 23.

Plaschka, C., Lariviere, L., Wenzeck, L., Seizl, M., Hemann, M., Tegunov, D., Petrotchenko, E. V., Borchers, C. H., Baumeister, W. & other authors (2015). Architecture of the RNA polymerase II-Mediator core initiation complex. *Nature* **518**, 376-380.

Plassmeyer, M. L., Soldan, S. S., Stachelek, K. M., Martín-García, J. & González-Scarano, F. (2005). California serogroup Gc (G1) glycoprotein is the principal determinant of pH-dependent cell fusion and entry. *Virology* **338**, 121-132.

Plassmeyer, M. L., Soldan, S. S., Stachelek, K. M., Roth, S. M., Martin-Garcia, J. & Gonzalez-Scarano, F. (2007). Mutagenesis of the La Crosse Virus glycoprotein supports a role for Gc (1066-1087) as the fusion peptide. *Virology* **358**, 273-282.

Plotch, S. J., Bouloy, M. & Krug, R. M. (1979). Transfer of 5′-terminal cap of globin mRNA to influenza viral complementary RNA during transcription in vitro. *Proceedings of the National Academy of Sciences of the United States of America* **76**, 1618-1622.

Poch, O., Sauvaget, I., Delarue, M. & Tordo, N. (1989). Identification of four conserved motifs among the RNA-dependent polymerase encoding elements. *The EMBO journal* **8**, 3867-3874.

Pollitt, E., Zhao, J., Muscat, P. & Elliott, R. M. (2006). Characterization of Maguari orthobunyavirus mutants suggests the nonstructural protein NSm is not essential for growth in tissue culture. *Virology* **348**, 224-232.

Pringle, C. R., Lees, J. F., Clark, W. & Elliott, R. M. (1984). Genome subunit reassortment among Bunyaviruses analysed by dot hybridization using molecularly cloned complementary DNA probes. *Virology* **135**, 244-256.

Proenca-Modena, J. L., Sesti-Costa, R., Pinto, A. K., Richner, J. M., Lazear, H. M., Lucas, T., Hyde, J. L. & Diamond, M. S. (2015a). Oropouche virus infection

and pathogenesis are restricted by MAVS, IRF-3, IRF-7, and type I interferon signaling pathways in nonmyeloid cells. *Journal of virology* **89**, 4720-4737.

Proenca-Modena, J. L., Hyde, J. L., Sesti-Costa, R., Lucas, T., Pinto, A. K., Richner, J. M., Gorman, M. J., Lazear, H. M. & Diamond, M. S. (2015b). IRF-5-dependent signaling restricts Orthobunyavirus dissemination to the central nervous system. *Journal of virology*.

Quinones-Mateu, M. E., Avila, S., Reyes-Teran, G. & Martinez, M. A. (2014). Deep sequencing: becoming a critical tool in clinical virology. *Journal of clinical virology : the official publication of the Pan American Society for Clinical Virology* **61**, 9-19.

Racaniello, V. R. & Baltimore, D. (1981). Cloned poliovirus complementary DNA is infectious in mammalian cells. *Science (New York, NY)* **214**, 916-919.

Raftery, M. J., Lalwani, P., Krautkrmer, E., Peters, T., Scharffetter-Kochanek, K., Kruger, R., Hofmann, J., Seeger, K., Kruger, D. H. & other authors (2014). beta2 integrin mediates hantavirus-induced release of neutrophil extracellular traps. The *Journal of Experimental Medicine* **211**, 1485-1497.

Raj, V. S., Farag, E. A., Reusken, C. B., Lamers, M. M., Pas, S. D., Voermans, J., Smits, S. L., Osterhaus, A. D., Al-Mawlawi, N. & other authors (2014). Isolation of MERS coronavirus from a dromedary camel, Qatar, 2014. *Emerging infectious diseases* **20**, 1339-1342.

Raju, R. & Kolakofsky, D. (1989). The ends of La Crosse virus genome and antigenome RNAs within nucleocapsids are base paired. *Journal of virology* **63**, 122-128.

Randall, R. E. & Goodbourn, S. (2008). Interferons and viruses: an interplay between induction, signalling, antiviral responses and virus countermeasures. *The Journal of general virology* **89**, 1-47.

Raymond, D. D., Piper, M. E., Gerrard, S. R. & Smith, J. L. (2010). Structure of the Rift Valley fever virus nucleocapsid protein reveals another architecture for RNA encapsidation. *Proceedings of the National Academy of Sciences of the United States of America* **107**, 11769-11774.

Reguera, J., Weber, F. & Cusack, S. (2010). Bunyaviridae RNA Polymerases (L-Protein) Have an N-Terminal, Influenza-Like Endonuclease Domain, Essential for Viral Cap-Dependent Transcription. *PLoS pathogens* **6**, e1001101.

Reguera, J., Malet, H., Weber, F. & Cusack, S. (2013). Structural basis for encapsidation of genomic RNA by La Crosse Orthobunyavirus nucleoprotein. *Proceedings of the National Academy of Sciences of the United States of America* **110**, 7246-7251.

Reich, S., Guilligay, D., Pflug, A., Malet, H., Berger, I., Crepin, T., Hart, D., Lunardi, T., Nanao, M. & other authors (2014). Structural insight into cap-snatching and RNA synthesis by influenza polymerase. *Nature* **516**, 361-366.

Reikine, S., Nguyen, J. B. & Modis, Y. (2014). Pattern Recognition and Signaling Mechanisms of RIG-I and MDA5. *Frontiers in Immunology* **5**, 342.

Rezelj, V. V., Overby, A. K. & Elliott, R. M. (2015). Generation of mutant Uukuniemi viruses lacking the nonstructural protein NSs by reverse genetics indicates that NSs is a weak interferon antagonist. *Journal of virology*.

Richmond, K. E., Chenault, K., Sherwood, J. L. & German, T. L. (1998). Characterization of the Nucleic Acid Binding Properties of Tomato Spotted Wilt Virus Nucleocapsid Protein. *Virology* **248**, 6-11.

Roberts, D. R., Hoch, A. L., Dixon, K. E. & Llewellyn, C. H. (1981). Oropouche virus. III. Entomological observations from three epidemics in Para, Brazil, 1975. *The American journal of tropical medicine and hygiene* **30**, 165-171.

Roberts, D. R., Pinheiro, F. d. P., Hoch, A. L., LeDuc, J. W., Peterson, N. E., Santos, M. A. V. & Western, K. A. (1977). Vectors and Natural Reservoirs of Oropouche virus in the Amazon Region: U. S. Army Medical Research and Development Comand Washington , D.C. 20314.

Robinson, P. J. J., Bushnell, D. A., Trnka, M. J., Burlingame, A. L. & Kornberg, R. D. (2012). Structure of the Mediator Head module bound to the carboxy-terminal domain of RNA polymerase II. *Proceedings of the National Academy of Science USA* **109**, 17931-17935.

Roche http://www.454.com.

Rodrigues, A. H., Santos, R. I., Arisi, G. M., Bernardes, E. S., Silva, M. L., Rossi, M. A., Lopes, M. B. & Arruda, E. (2011). Oropouche virus experimental infection in the golden hamster (Mesocrisetus auratus). *Virus research* **155**, 35-41.

Rogers, K. M. & Heise, M. (2009). Modulation of cellular tropism and innate antiviral response by viral glycans. *Journal of innate immunity* **1**, 405-412.

Ronquist, F. & Huelsenbeck, J. P. (2003). MrBayes 3: Bayesian phylogenetic inference under mixed models. *Bioinformatics (Oxford, England)* **19**, 1572-1574.

Rosa, A. P., Rodrigues, S. G., Nunes, M. R., Magalhaes, M. T., Rosa, J. F. & Vasconcelos, P. F. (1996). [Outbreak of oropouche virus fever in Serra Pelada, municipality of Curionopolis, Para, 1994]. *Revista da Sociedade Brasileira de Medicina Tropical* **29**, 537-541.

Rothberg, J. M., Hinz, W., Rearick, T. M., Schultz, J., Mileski, W., Davey, M., Leamon, J. H., Johnson, K., Milgrew, M. J. & other authors (2011). An integrated semiconductor device enabling non-optical genome sequencing. *Nature* **475**, 348-352.

Roulston, A., Marcellus, R. C. & Branton, P. E. (1999). Viruses and apoptosis. *Annual Review of Microbiology* **53**, 577-628.

Saeed, M. F., Wang, H., Nunes, M., Vasconcelos, P. F., Weaver, S. C., Shope, R. E., Watts, D. M., Tesh, R. B. & Barrett, A. D. (2000). Nucleotide sequences and phylogeny of the nucleocapsid gene of Oropouche virus. *The Journal of general virology* **81**, 743-748.

Saeed, M. F., Wang, H., Suderman, M., Beasley, D. W., Travassos da Rosa, A., Li, L., Shope, R. E., Tesh, R. B. & Barrett, A. D. (2001). Jatobal virus is a reassortant containing the small RNA of Oropouche virus. *Virus research* **77**, 25-30.

Salanueva, I. J., Novoa, R. R., Cabezas, P., Lopez-Iglesias, C., Carrascosa, J. L., Elliott, R. M. & Risco, C. (2003). Polymorphism and structural maturation of bunyamwera virus in Golgi and post-Golgi compartments. *Journal of virology* **77**, 1368-1381.

Santos, R. I., Bueno-Junior, L. S., Ruggiero, R. N., Almeida, M. F., Silva, M. L., Paula, F. E., Correa, V. M. & Arruda, E. (2014). Spread of Oropouche virus into the central nervous system in mouse. *Viruses* **6**, 3827-3836.

Santos, R. I., Almeida, M. F., Paula, F. E., Rodrigues, A. H., Saranzo, A. M., Paula, A. E., Silva, M. L., Correa, V. M., Acrani, G. O. & other authors (2012).

Experimental infection of suckling mice by subcutaneous inoculation with Oropouche virus. *Virus research* **170**, 25-33.

Santos, R. I. M., Rodrigues, A. H., Silva, M. L., Mortara, R. A., Rossi, M. A., Jamur, M. C., Oliver, C. & Arruda, E. (2008). Oropouche virus entry into HeLa cells involves clathrin and requires endosomal acidification. *Virus research* **138**, 139-143.

Schaefer, T. M., Desouza, K., Fahey, J. V., Beagley, K. W. & Wira, C. R. (2004). Toll-like receptor (TLR) expression and TLR-mediated cytokine/chemokine production by human uterine epithelial cells. *Immunology* **112**, 428-436.

Schneider, W. M., Chevillotte, M. D. & Rice, C. M. (2014). Interferon-stimulated genes: a complex web of host defenses. *Annual review of immunology* **32**, 513-545.

Schnell, M. J., Mebatsion, T. & Conzelmann, K. K. (1994). Infectious rabies viruses from cloned cDNA. *EMBO J* **13**, 4195-4203.

Severson, W. E., Xu, X. & Jonsson, C. B. (2001). cis-Acting signals in encapsidation of Hantaan virus S-segment viral genomic RNA by its N protein. *Journal of virology* **75**, 2646-2652.

Sherman, M. B., Freiberg, A. N., Holbrook, M. R. & Watowich, S. J. (2009). Single-particle cryo-electron microscopy of Rift Valley fever virus. *Virology* **387**, 11-15.

Shi, X. & Elliott, R. M. (2004). Analysis of N-linked glycosylation of hantaan virus glycoproteins and the role of oligosaccharide side chains in protein folding and intracellular trafficking. *Journal of virology* **78**, 5414-5422.

Shi, X. & Elliott, R. M. (2009). Generation and analysis of recombinant Bunyamwera orthobunyaviruses expressing V5 epitope-tagged L proteins. *The Journal of general virology* **90**, 297-306.

Shi, X., Brauburger, K. & Elliott, R. M. (2005). Role of N-linked glycans on bunyamwera virus glycoproteins in intracellular trafficking, protein folding, and virus infectivity. *Journal of virology* **79**, 13725-13734.

Shi, X., Kohl, A., Li, P. & Elliott, R. M. (2007). Role of the cytoplasmic tail domains of Bunyamwera orthobunyavirus glycoproteins Gn and Gc in virus assembly and morphogenesis. *Journal of virology* **81**, 10151-10160.

Shi, X., van Mierlo, J. T., French, A. & Elliott, R. M. (2010). Visualizing the replication cycle of bunyamwera orthobunyavirus expressing fluorescent protein-tagged Gc glycoprotein. *Journal of virology* **84**, 8460-8469.

Shi, X., Goli, J., Clark, G., Brauburger, K. & Elliott, R. M. (2009). Functional analysis of the Bunyamwera orthobunyavirus Gc glycoprotein. *The Journal of general virology* **90**, 2483-2492.

Shi, X., Kohl, A., Leonard, V. H., Li, P., McLees, A. & Elliott, R. M. (2006). Requirement of the N-terminal region of orthobunyavirus nonstructural protein NSm for virus assembly and morphogenesis. *Journal of virology* **80**, 8089-8099.

Sievers, F., Wilm, A., Dineen, D., Gibson, T. J., Karplus, K., Li, W., Lopez, R., McWilliam, H., Remmert, M. & other authors (2011). Fast, scalable generation of high-quality protein multiple sequence alignments using Clustal Omega. *Molecular systems biology* **7**, 539.

Simon, M., Johansson, C. & Mirazimi, A. (2009). Crimean-Congo hemorrhagic fever virus entry and replication is clathrin-, pH- and cholesterol-dependent. *The Journal of general virology* **90**, 210-215.

Smith, G. C. & Francy, D. B. (1991). Laboratory studies of a Brazilian strain of *Aedes albopictus* as a potential vector of Mayaro and Oropouche viruses. *Journal of the American Mosquito Control Association* **7**, 89-93.

Soellick, T., Uhrig, J. F., Bucher, G. L., Kellmann, J. W. & Schreier, P. H. (2000). The movement protein NSm of tomato spotted wilt tospovirus (TSWV): RNA binding, interaction with the TSWV N protein, and identification of interacting plant proteins. *Proceedings of the National Academy of Sciences of the United States of America* **97**, 2373-2378.

Solid (ThermoFisher Scientific). http://solid.appliedbiosystems.com.

Spann, K. M., Tran, K. C., Chi, B., Rabin, R. L. & Collins, P. L. (2004). Suppression of the induction of alpha, beta, and lambda interferons by the NS1 and NS2 proteins of human respiratory syncytial virus in human epithelial cells and macrophages [corrected]. *Journal of virology* **78**, 4363-4369.

Stobart, C. C. & Moore, M. L. (2014). RNA virus reverse genetics and vaccine design. *Viruses* **6**, 2531-2550.

Storms, M. M., Kormelink, R., Peters, D., Van Lent, J. W. & Goldbach, R. W. (1995). The nonstructural NSm protein of tomato spotted wilt virus induces tubular structures in plant and insect cells. *Virology* **214**, 485-493.

Strandin, T., Hepojoki, J. & Vaheri, A. (2013). Cytoplasmic tails of bunyavirus Gn glycoproteins-Could they act as matrix protein surrogates? *Virology* **437**, 73-80.

Streitenfeld, H., Boyd, A., Fazakerley, J. K., Bridgen, A., Elliott, R. M. & Weber, F. (2003). Activation of PKR by Bunyamwera virus is independent of the viral interferon antagonist NSs. *Journal of virology* **77**, 5507-5511.

Suyama, M., Torrents, D. & Bork, P. (2006). PAL2NAL: robust conversion of protein sequence alignments into the corresponding codon alignments. *Nucleic acids research* **34**, W609-612.

Talmon, Y., Prasad, B. V., Clerx, J. P., Wang, G. J., Chiu, W. & Hewlett, M. J. (1987). Electron microscopy of vitrified-hydrated La Crosse virus. *Journal of virology* **61**, 2319-2321.

Tamura, K., Stecher, G., Peterson, D., Filipski, A. & Kumar, S. (2013). MEGA6: Molecular Evolutionary Genetics Analysis version 6.0. *Molecular biology and evolution* **30**, 2725-2729.

Tan, J. K. & O'Neill, H. C. (2005). Maturation requirements for dendritic cells in T cell stimulation leading to tolerance versus immunity. *Journal of leukocyte biology* **78**, 319-324.

Taniguchi, T., Palmieri, M. & Weissmann, C. (1978). Q[beta] DNA-containing hybrid plasmids giving rise to Q[beta] phage formation in the bacterial host. *Nature* **274**, 223-228.

Taylor, S. L., Krempel, R. L. & Schmaljohn, C. S. (2009). Inhibition of TNF-alpha-induced activation of NF-kappaB by hantavirus nucleocapsid proteins. *Annals of the New York Academy of Sciences* **1171 Suppl 1**, E86-93.

Terasaki, K., Won, S. & Makino, S. (2013). The C-Terminal Region of Rift Valley Fever Virus NSm Protein Targets the Protein to the Mitochondrial Outer Membrane and Exerts Antiapoptotic Function. *Journal of virology* **87**, 676-682.

Terasaki, K., Murakami, S., Lokugamage, K. G. & Makino, S. (2011). Mechanism of tripartite RNA genome packaging in Rift Valley fever virus. *Proceedings of the National Academy of Sciences of the United States of America* **108**, 804-809.

Tesh, R. B. (1994). The emerging epidemiology of Venezuelan hemorrhagic fever and Oropouche fever in tropical South America. *Annals of the New York Academy of Sciences* **740**, 129-137.

Thomas, D., Blakqori, G., Wagner, V., Banholzer, M., Kessler, N., Elliott, R. M., Haller, O. & Weber, F. (2004). Inhibition of RNA Polymerase II Phosphorylation by a Viral Interferon Antagonist. *Journal of Biological Chemistry* **279**, 31471-31477.

Tischler, N. D., Gonzalez, A., Perez-Acle, T., Rosemblatt, M. & Valenzuela, P. D. (2005). Hantavirus Gc glycoprotein: evidence for a class II fusion protein. *The Journal of general virology* **86**, 2937-2947.

Uhrig, J. F., Soellick, T. R., Minke, C. J., Philipp, C., Kellmann, J. W. & Schreier, P. H. (1999). Homotypic interaction and multimerization of nucleocapsid protein of tomato spotted wilt tospovirus: Identification and characterization of two interacting domains. *Proceedings of the National Academy of Science USA* **96**, 55-60.

Uppal, P. K. (2000). Emergence of Nipah virus in Malaysia. *Annals of the New York Academy of Sciences* **916**, 354-357.

van Knippenberg, I. & Elliott, R. M. (2015). Flexibility of bunyavirus genomes: creation of an orthobunyavirus with an ambisense s segment. *Journal of virology* **89**, 5525-5535.

van Knippenberg, I., Carlton-Smith, C. & Elliott, R. M. (2010). The N-terminus of Bunyamwera orthobunyavirus NSs protein is essential for interferon antagonism. *The Journal of general virology* **91**, 2002-2006.

Varela, M., Schnettler, E., Caporale, M., Murgia, C., Barry, G., McFarlane, M., McGregor, E., Piras, I. M., Shaw, A. & other authors (2013). Schmallenberg virus pathogenesis, tropism and interaction with the innate immune system of the host. *PLoS pathogens* **9**, e1003133.

Vasconcelos, H. B., Nunes, M. R., Casseb, L. M., Carvalho, V. L., Pinto da Silva, E. V., Silva, M., Casseb, S. M. & Vasconcelos, P. F. (2011). Molecular epidemiology of Oropouche virus, Brazil. *Emerging infectious diseases* **17**, 800-806.

Vasconcelos, H. B., Azevedo, R. S. S., Casseb, S. M., Nunes-Neto, J. P., Chiang, J. O., Cantuária, P. C., Segura, M. N. O., Martins, L. C., Monteiro, H. A. O. & other authors (2009). Oropouche fever epidemic in Northern Brazil: epidemiology and molecular characterization of isolates. *Journal of clinical virology* **44**, 129-133.

Vasconcelos, P. F., Travassos Da Rosa, J. F., Guerreiro, S. C., Degallier, N., Travassos Da Rosa, E. S. & Travassos Da Rosa, A. P. (1989). [1st register of an epidemic caused by Oropouche virus in the states of Maranhao and Goias, Brazil]. *Revista do Instituto de Medicina Tropical de Sao Paulo* **31**, 271-278.

Vasconcelos, P. F., Travassos da Rosa, A. P., Rodrigues, S. G., Travassos da Rosa, E. S., Degallier, N. & Travassos da Rosa, J. F. (2001). Inadequate management of natural ecosystem in the Brazilian Amazon region results in the emergence and reemergence of arboviruses. *Cadernos de saude publica* **17 Suppl**, 155-164.

Vera-Otarola, J., Solis, L., Soto-Rifo, R., Ricci, E. P., Pino, K., Tischler, N. D., Ohlmann, T., Darlix, J.-L. & López-Lastra, M. (2012). The Andes Hantavirus

NSs Protein Is Expressed from the Viral Small mRNA by a Leaky Scanning Mechanism. *Journal of virology* **86**, 2176-2187.

Verbruggen, P., Ruf, M., Blakqori, G., Overby, A. K., Heidemann, M., Eick, D. & Weber, F. (2011). Interferon antagonist NSs of La Crosse virus triggers a DNA damage response-like degradation of transcribing RNA polymerase II. *Journal of Biological Chemistry* **286**, 3681-3692.

von Bonsdorff, C. H. & Pettersson, R. (1975). Surface structure of Uukuniemi virus. *Journal of virology* **16**, 1296-1307.

Walpita, P. & Flick, R. (2005). Reverse genetics of negative-stranded RNA viruses: a global perspective. *FEMS microbiology letters* **244**, 9-18.

Walter, C. T., Costa Bento, D. F., Guerrero Alonso, A. & Barr, J. N. (2011). Amino acid changes within the Bunyamwera virus nucleocapsid protein differentially affect the mRNA transcription and RNA replication activities of assembled ribonucleoprotein templates. *Journal of General Virology* **92**, 80-84.

Wang, H., Beasley, D. W., Li, L., Holbrook, M. R. & Barrett, A. D. (2001). Nucleotide sequence and deduced amino acid sequence of the medium RNA segment of Oropouche, a Simbu serogroup virus: comparison with the middle RNA of Bunyamwera and California serogroup viruses. *Virus research* **73**, 153-162.

Watts, D. M., Phillips, I., Callahan, J. D., Griebenow, W., Hyams, K. C. & Hayes, C. G. (1997). Oropouche virus transmission in the Amazon River basin of Peru. *The American journal of tropical medicine and hygiene* **56**, 148-152.

Weber, F. (2015). The catcher in the RIG-I. *Cytokine* **76**, 38-41.

Weber, F., Dunn, E. F., Bridgen, A. & Elliott, R. M. (2001). The Bunyamwera virus nonstructural protein NSs inhibits viral RNA synthesis in a minireplicon system. *Virology* **281**, 67-74.

Weber, F., Bridgen, A., Fazakerley, J. K., Streitenfeld, H., Kessler, N., Randall, R. E. & Elliott, R. M. (2002). Bunyamwera bunyavirus nonstructural protein NSs counteracts the induction of alpha/beta interferon. *Journal of virology* **76**, 7949-7955.

White, J., Matlin, K. & Helenius, A. (1981). Cell fusion by Semliki Forest, influenza, and vesicular stomatitis viruses. *The Journal of cell biology* **89**, 674-679.

Yanase, T., Aizawa, M., Kato, T., Yamakawa, M., Shirafuji, H. & Tsuda, T. (2010). Genetic characterization of Aino and Peaton virus field isolates reveals a genetic reassortment between these viruses in nature. *Virus research* **153**, 1-7.

Zhang, X., Liu, Y., Zhao, L., Li, B., Yu, H., Wen, H. & Yu, X. J. (2013). An emerging hemorrhagic fever in China caused by a novel bunyavirus SFTSV. *Science China Life sciences* **56**, 697-700.

Chapter VII

Publications

Journal of General Virology (2015), **96**, 513–523 **DOI** 10.1099/jgv.0.000005

Establishment of a minigenome system for Oropouche virus reveals the S genome segment to be significantly longer than reported previously

Gustavo Olszanski Acrani,[1,2]† Natasha L. Tilston-Lunel,[1,3]† Martin Spiegel,[4] Manfred Weidmann,[4]‡ Meik Dilcher,[4] Daisy Elaine Andrade da Silva,[5] Marcio R. T. Nunes[5] and Richard M. Elliott[1]

Correspondence
Richard M. Elliott
richard.elliott@glasgow.ac.uk

[1]MRC-University of Glasgow Centre for Virus Research, 464 Bearsden Road, Glasgow G61 1QH, Scotland, UK

[2]Department of Cell and Molecular Biology, University of Sao Paulo School of Medicine, 3900, Av. Bandeirantes, Ribeirão Preto, SP 14049-900, Brazil

[3]Biomedical Sciences Research Complex, School of Biology, University of St Andrews, St Andrews KY16 9ST, Scotland, UK

[4]Department of Virology, University Medical Center Göttingen, Kreuzbergring 57, 37075 Göttingen, Germany

[5]Center for Technological Innovation, Instituto Evandro Chagas, Ananindeua, Brazil

Oropouche virus (OROV) is a medically important orthobunyavirus, which causes frequent outbreaks of a febrile illness in the northern parts of Brazil. However, despite being the cause of an estimated half a million human infections since its first isolation in Trinidad in 1955, details of the molecular biology of this tripartite, negative-sense RNA virus remain limited. We have determined the complete nucleotide sequence of the Brazilian prototype strain of OROV, BeAn 19991, and found a number of differences compared with sequences in the database. Most notable were that the S segment contained an additional 204 nt at the 3′ end and that there was a critical nucleotide mismatch at position 9 within the base-paired terminal panhandle structure of each genome segment. In addition, we obtained the complete sequence of the Trinidadian prototype strain TRVL-9760 that showed similar characteristics to the BeAn 19991 strain. By using a T7 RNA polymerase-driven minigenome system, we demonstrated that cDNA clones of the BeAn 19991 L and S segments expressed functional proteins, and also that the newly determined terminal untranslated sequences acted as functional promoters in the minigenome assay. By co-transfecting a cDNA to the viral glycoproteins, virus-like particles were generated that packaged a minigenome and were capable of infecting naive cells.

Received 16 September 2014
Accepted 3 November 2014

INTRODUCTION

Oropouche virus (OROV) is one of the most important arboviruses in Brazil, after dengue virus and yellow fever virus, and was first isolated in 1955 from a febrile patient in Trinidad (Anderson *et al.*, 1961). Subsequently, the virus was isolated in Brazil in 1960 from the blood of a pale-throated three-toed sloth, *Bradypus tridactylus*, at a forest camp-site during construction of the Belém–Brasilia highway, just before the first documented epidemic in Brazil in 1961 (Pinheiro *et al.*, 1962). It is estimated that half a million OROV infections have occurred in >30 outbreaks since the virus became recognized, but it is probable that the actual numbers are much higher as cases may be masked by other febrile illnesses, such as dengue or Mayaro fever, and diseases caused by other orthobunyaviruses, such as Guama virus, that are prevalent in the region (reviewed by Vasconcelos *et al.*, 2011). OROV has also been isolated from various mosquito species (e.g. *Coquillettidia venezuelensis* and *Ochlerotatus serratus*), but during epidemics OROV is transmitted to humans by the biting midge *Culicoides paraensis* (Pinheiro *et al.*, 1981a, b, 1982).

†These authors contributed equally to this work.

‡Present address: Institute of Aquaculture, Pathfoot Building, University of Stirling, Stirling FK9 4LA, Scotland, UK.

The GenBank/EMBL/DDBJ accession numbers for the sequences of the segments of OROV strains BeAn 19991 and TRVL-9760 are KP052850–KP052852 and KP026179–KP026181, respectively.

OROV belongs to the Simbu serogroup of the genus *Orthobunyavirus*. The serogroup also includes a number of veterinary pathogens such as Akabane, Aino, Shuni, Sabo and Douglas viruses, as well the newly emerged Schmallenberg virus (Afonso *et al.*, 2014). OROV is currently the only known human pathogen in the serogroup and recent phylogenetic analysis (Ladner *et al.*, 2014b) places it in a clade separate from the other members. Like all bunyaviruses, the OROV genome consists of three segments of negative-sense ssRNA designated large (L), medium (M) and small (S). The L segment encodes the viral polymerase (L protein), and the M segment encodes the glycoproteins Gn and Gc, along with a non-structural protein called NSm. The S segment encodes the viral nucleocapsid protein (N) and a second non-structural protein (NSs) in overlapping reading frames, although both proteins are translated from the same mRNA (Elliott, 2014; Plyusnin & Elliott, 2011). The terminal sequences at the 3′ and 5′ ends of each segment are complementary, allowing the formation of a panhandle structure that is crucial for genome replication and transcription (Barr *et al.*, 2003; Barr & Wertz, 2004; Kohl *et al.*, 2004).

The epidemiology and genetic variation of OROV has been widely studied, and phylogenetic analysis of numerous partial S segment sequences (mainly N ORF sequences), together with more limited partial sequence data on the M and L segments, suggested the existence of four genotypes (reviewed by Vasconcelos *et al.*, 2011). However, much less is known about the general molecular biology of OROV or virus–host interactions. To facilitate such investigations we intended to develop a reverse genetics system for OROV, as has been reported for other orthobunyaviruses (Elliott, 2012), including two Simbu group viruses: Akabane virus (Ogawa *et al.*, 2007) and Schmallenberg virus (Elliott *et al.*, 2013; Varela *et al.*, 2013). When we produced cDNA clones of the OROV genome segments, we noticed several discrepancies between the viral sequences we obtained and the sequences in the database, notably that the S segment contained an additional 204 nt. The functionality of our cDNA clones was confirmed by establishing minigenome (Blakqori *et al.*, 2003; Weber *et al.*, 2002) and virus-like particle (VLP) (Shi *et al.*, 2007) systems. Our results highlighted the importance of obtaining complete and correct viral sequences, including direct confirmation of the genome termini, in order to establish reverse genetic systems.

RESULTS

Cloning and sequence determination of the genome of OROV strain BeAn 19991

Total RNA was extracted from BHK-21 cells infected with OROV strain BeAn 19991 (prototype Brazilian strain isolated from *B. tridactylus*) and reverse transcribed using random primers. Segment-specific oligonucleotides, based on available complete sequences in GenBank [L, accession number NC_005776.1 (Aquino *et al.*, 2003); M, NC_005775.1 (Wang *et al.*, 2001); and S, NC_005777.1; V. H. Aquino and others, unpublished], were used in PCR (Table 1). Full-length cDNAs were cloned into the T7 RNA polymerase transcription plasmid TVT7R(0,0) (Johnson *et al.*, 2000); the inserts included an extra G residue at their 5′ ends for efficient T7 transcription and the cDNAs were cloned such that T7 polymerase would transcribe anti-genome-sense RNAs, as described previously (Elliott *et al.*, 2013). Descriptions of the sequences in this paper are presented for the antigenome-sense RNA, in the conventional 5′→3′ orientation.

The full-length L segment sequence that we obtained was 6852 nt in length, 6 nt longer than GenBank accession number NC_005776.1. Alignment of our sequence with that of GenBank accession number NC_005776.1 revealed a number of differences in the regions from nt 2405 to 2450 and from nt 2592 to 2617, resulting in amino acid changes in the region from aa 798 to 812 and from aa 860 to 867 (Fig. 1). We verified the sequence of this region by reverse transcription (RT)-PCR amplification of a fragment from nt 2130 to 2980 using specific primers and viral RNA as template. Furthermore, alignment of our sequence with partial sequences of the L segments of OROV strains TRVL-9760, GML-444479 and IQT-1690 (GenBank accession numbers KC759122.1, KC759128.1 and KC759125.1, respectively) revealed that, apart from a few variations at the nucleotide level, the translated amino acid sequence for this region was conserved (Fig. 1). Therefore, we consider the published sequence for the BeAn 19991 L segment contains some errors in this region. In addition, we noted two other amino acid differences: L to F at position 415 and N to D at position 1021. Both of these have been confirmed by independent sequence analysis of our stock of virus, and the F residue at position 415 is also found in the L protein of other strains of OROV (TRVL-9760, GML-444479 and IQT-1690).

The terminal sequences of the L segment UTRs were determined by a 3′ RACE procedure on total infected cell RNA, using oligonucleotides designed to anneal to either the genomic or antigenomic strands. Position 9 of the 5′ UTR was determined as a C residue and the corresponding −9 position in the 3′ UTR was determined as an A residue, resulting in the characteristic mismatch that has been observed in the predicted panhandle structure of other orthobunyavirus genome segments (Kohl *et al.*, 2004). This mismatch is not recorded in the published sequence. Additionally, position 18 at the 5′ end was determined to be a U rather than a C residue, as in the published sequence (Fig. 2).

The full-length M segment was determined to be 4385 nt in length, in agreement with the published sequence. There were a small number of nucleotide variations compared with GenBank accession number NC_005775.1, six of which resulted in amino acid differences: I274F, F587L, K614N, D750G, K981Q and G982S. The sequences encoding these residues were confirmed in independent cDNA clones of the M segment cDNA and also by specific RT-PCR amplification of appropriate regions of the viral RNA. Results from RACE analysis revealed two single nucleotide differences in

Table 1. Oligonucleotides used in this study

Oligonucleotide	Sequence (5′→3′)	Segment/gene	Position
OROLFg	GGGGTACCCGTCTCATATAG**AGTAGTGTGCTCCTATTCCG**	L	1–19
OROL1	GAAGTTAGTTAGATATGTCT	L	3706–3687
OROLRg	GCTCTAGACGTCTCTACCC**AGTAGTGTGCTCCTATTTAG**	L	6833–6852
OROL2	CCCTTGTGAACTCAATGGTA	L	3537–3556
OROMFg	GGGGTACCCGTCTCATATAG**AGTAGTGTGCTACCGGCAACAAACA**	M	1–25
OROMRg	GCTCTAGACGTCTCTACCC**AGTAGTGTGCTACCGACAACAATTT**	M	4508–4484
OROSFg	GGGGTACCCGTCTCATATAG**AGTAGTGTGCTCCACAATTC**	S	1–20
OROSRg	GCTCTAGACGTCTCTACCC**AGTAGTGTGCTCCACTATAT**	S	754–735†
ORODelNSsF	GAGTTCATTTTCAACGA**C**GTACCACAACGGACTACATCTACATTTGATCCGGAGGCAGCATA**C**GT**A**GCATTTGAAGC	delNSs	51–127
ORODelNSsR	GCTTCAAATGC**T**AC**G**TATGCTGCCTCCGGATCAAATGTAGATGTAGTCCGTTGTGGTAC**G**TCGTTGAAAATGAACTC	delNSs	127–51
pTM1-OROVL-F	AAAACACGATAATACC**ATGTCACAACTGTTGCTCAACCAATATCG**	L	44–72
pTM1-OROVL-R	TTAATTAGGCCTCTC**TTAGAAGTCAAATTTGGATTTGCCAGT**	L	6802–6776
pTM1-OROVM-F	AACACGATAATACC**ATGGCGAATTTAATAATTATTTCAATGGTTC**	Glycoprotein	32–62
pTM1-OROVM-R	TTAATTAGGCCTCTC**CTACTTGATTTTCTGCTCCATGGCATATTCTATTTCATGTCTGATT**	Glycoprotein	4294–4249
pTM1-OROVS-F	AAACACGATAATACC**ATGTCAGAGTTCATTTTCAACGATGTACCAC**	N	45–75
pTM1-OROVS-R	TTAATTAGGCCTCTC**CTATATGTCAATTCCGAATTGGCGCAAGAAGTCTCTTGCTGC**	N	740–699
OROVL_anti	ACCTCTCCAAAAATCTCATT	L 5′ UTR	384–365
OROVL_gen	GAACTAGACAATTGTATTCA	L 3′ UTR	6494–6513
OROVM_anti	CTAATATCACATGCTGCTCTACATG	M 5′ UTR	396–372
OROVM_gen	GCACATATCTGTGGGAGAGACAT	M 3′ UTR	3959–3981
OROSlig1	CTTGCGCCAATTCGGAATTGAC	S UTR	713–734
OROSlig2	GGTACATCGTTGAAAATGAAC	S UTR	73–53

*Viral sequences are shown in bold.

†Based on GenBank accession number NC_005777.1.

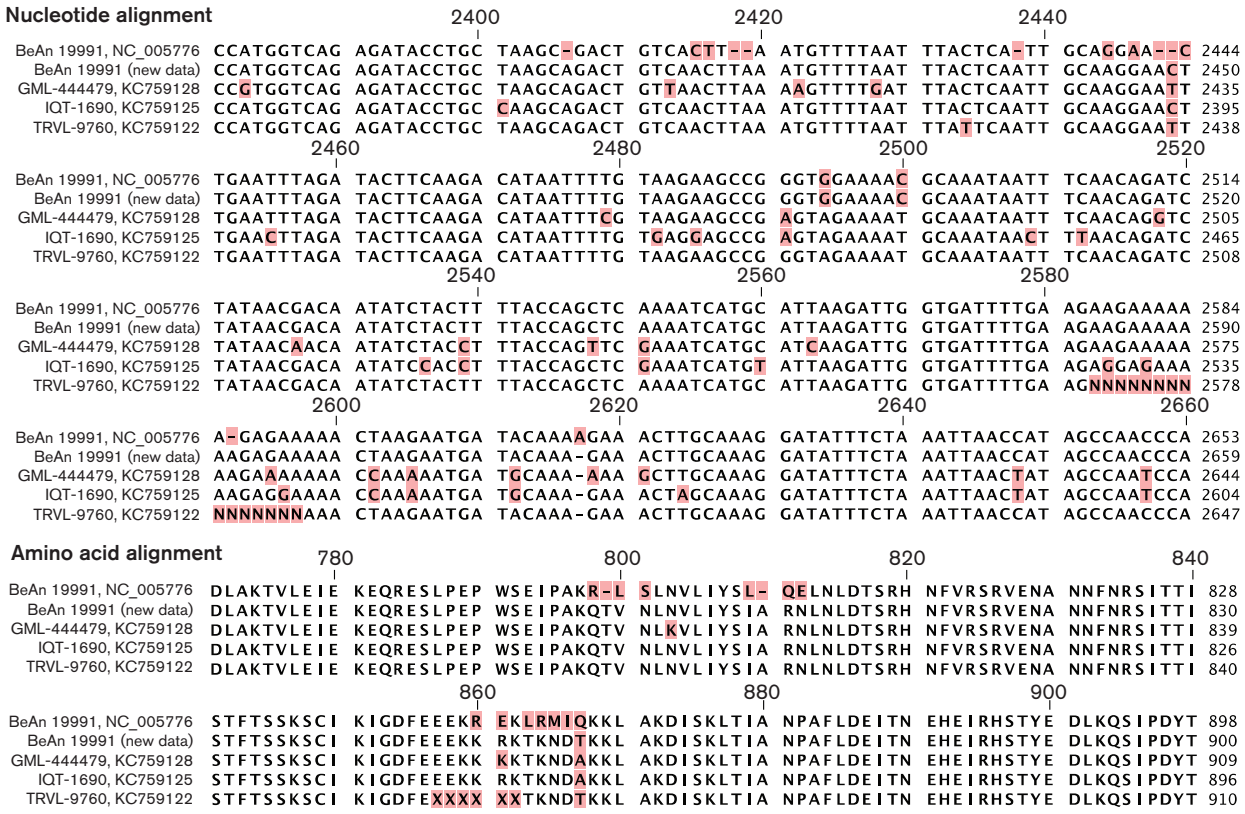

Fig. 1. Alignment of part of the OROV L segment highlighting the differences between the published sequence for the BeAn 19991 strain (GenBank accession number NC_005776) and the sequence obtained in this study (new data), along with three published OROV sequences from different genotypes GML-444479, IQT-1690 and TRVL-9760 (GenBank accession numbers KC759128.1, KC759125.1 and KC759122.1, respectively). The nucleotide alignment is shown in the top panel and the amino acid alignment is shown in the bottom panel. Alignments were performed using CLC Genomics Workbench 6.5.

the 5′ UTR (C at position 9 and A at position 15) and one difference at the 3′ end (U at position 15) compared with the database sequence. Thus, the predicted panhandle has a C/A mismatch at position 9/–9 and a U/A pairing at position 15/–15 (Fig. 2).

The PCR to amplify the S segment surprisingly generated two products of ~750 and 1000 bp (Fig. 3a). After cloning, the sequences of both products were determined. The nucleotide sequence of the smaller fragment was identical to GenBank accession number NC_005777 (V. H. Aquino and others, unpublished) that is described as 'Oropouche virus segment S, complete genome', but no strain designation is given. Saeed *et al.* (2000) reported the complete sequence of the TRVL-9760 strain of OROV also to be 754 nt, although GenBank accession number AF164531 only gives the coding sequence for this strain. In addition, the sequence of the N ORF of the BeAn 19991 was also reported by Saeed *et al.* (2000) (GenBank accession number AF164532) and the amino acid sequence was identical to that that we obtained.

The larger fragment contained an additional 204 nt after the apparent consensus 3′ terminal sequence in the GenBank entry (Fig. 3b).

The DNA products were extracted from the gel and used as templates in further PCR. The shorter template gave rise to a single, similarly sized amplicon, whereas the longer template again generated products ~750 and 1000 bp in length (Fig. 3c). To investigate this observation further, we amplified the S segment of a clinical isolate of OROV (H759025 AMA2080; N. L. Tilston-Lunel, M. R. T. Nunes & R. M. Elliott, unpublished) using the same primers and PCR conditions that were used for BeAn 19991, and again observed two amplified DNA fragments (data not shown). The sequences of both of these amplicons largely matched that of the BeAn 19991 products (data not shown).

Inspection of the 'long' sequence showed that nt 735–752 could allow annealing of the primer used in PCR (Fig. 3d). Thus, binding of the primer to this internal sequence in the S segment would result in a cDNA product with a terminus matching that of the orthobunyavirus consensus sequence, making it appear complete. Using 3′ RACE and RNA ligation methods, we confirmed that the OROV S segment did indeed contain the additional 204 nt at the 3′ end (data not shown). Therefore, the full-length OROV S segment is 958 nt in length.

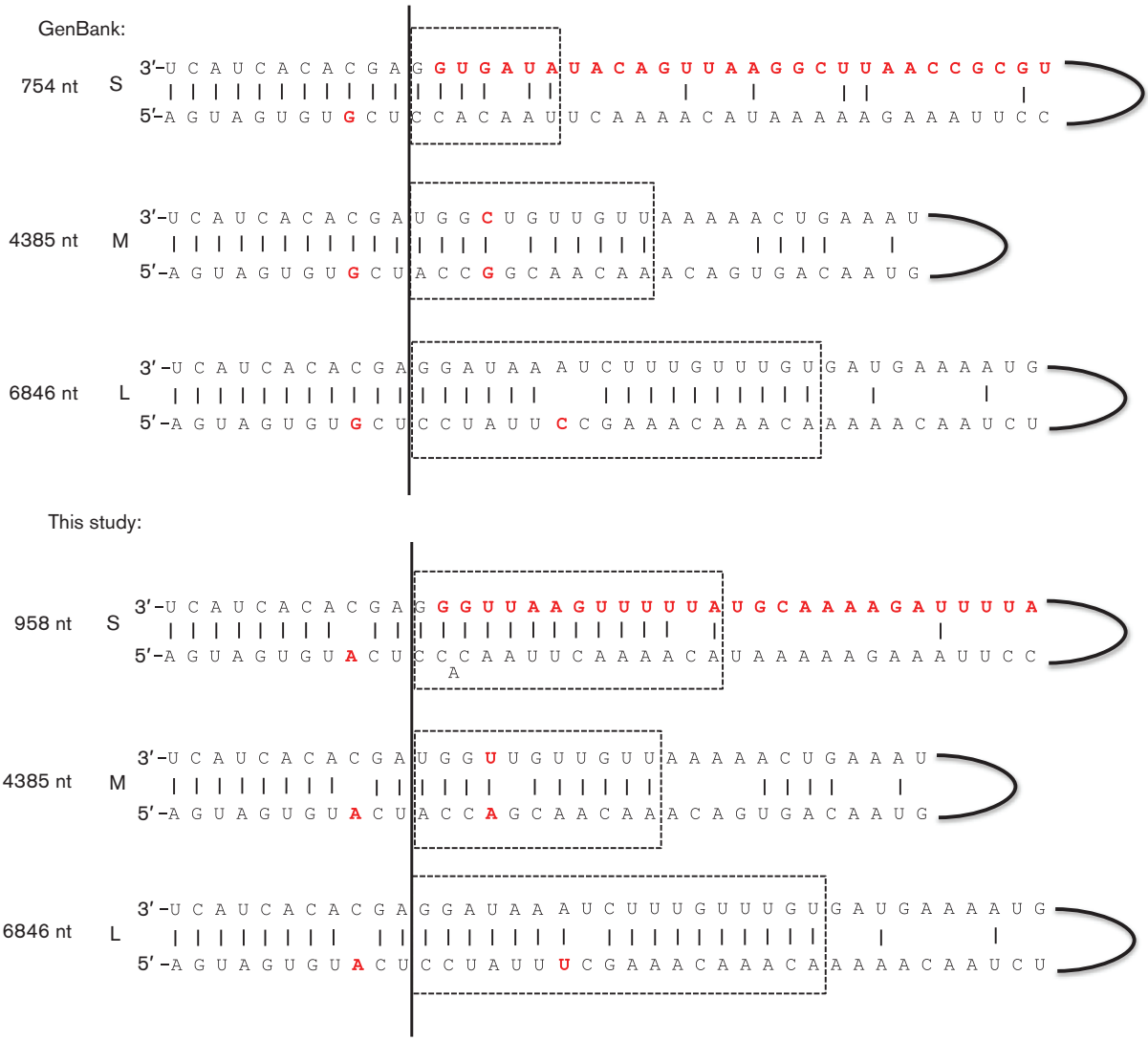

Fig. 2. Comparison of the published and the revised OROV BeAn 19991 UTR sequences shown as a panhandle structure (antigenomic sense). The terminal 11 conserved residues are separated by a vertical line. Differences are highlighted in red.

The corrected sequences of the OROV strain BeAn 19991 genome have been deposited in GenBank with accession numbers KP052850 (L), KP052851 (M) and KP052852 (S).

Sequence determination of the OROV TRVL-9760 strain

Determination of the complete sequence of another strain of OROV, the Trinidadian prototype TRVL-9760, was carried out independently from that of the BeAn 19991 strain. Total RNA was extracted from infected murine type I IFN receptor-deficient (IFNAR$^{-/-}$) cells and reverse transcribed using random hexamer primers. Sequences comprising the L, M and S segment ORFs were amplified by RT-PCR using specific oligonucleotides based on the available sequences (GenBank accession numbers NC_005776.1, NC_005775.1 and NC_005777.1, as described above). Whilst the N ORF sequence was completely amplified in one step, the L and the M segment ORF sequences were amplified as six (L) or three (M) overlapping fragments. The resulting cDNAs were inserted into the TA-vector pCRII and their sequences were determined by Sanger sequencing. In comparison with the BeAn 19991 L ORF sequence (GenBank accession number NC_005776.1), the TRVL-9760 L ORF contained 151 nt exchanges, seven single nucleotide insertions and one single nucleotide deletion. Whilst 134 of the 151 nt exchanges were silent, the nucleotide insertions and deletions which were found from nt 2405 to 2446 and from nt 2592 to 2617 led to several amino acid exchanges and the insertion of two additional amino acids at aa 799 and 810 (Fig. 1). The majority of the amino acid substitutions caused by single nucleotide exchanges were found in the N-terminal half of the L ORF (A136T, M145V, N210S, N273D, Q308K, S313N, I355V, F415L, D442N, T479A, I558M, T640A,

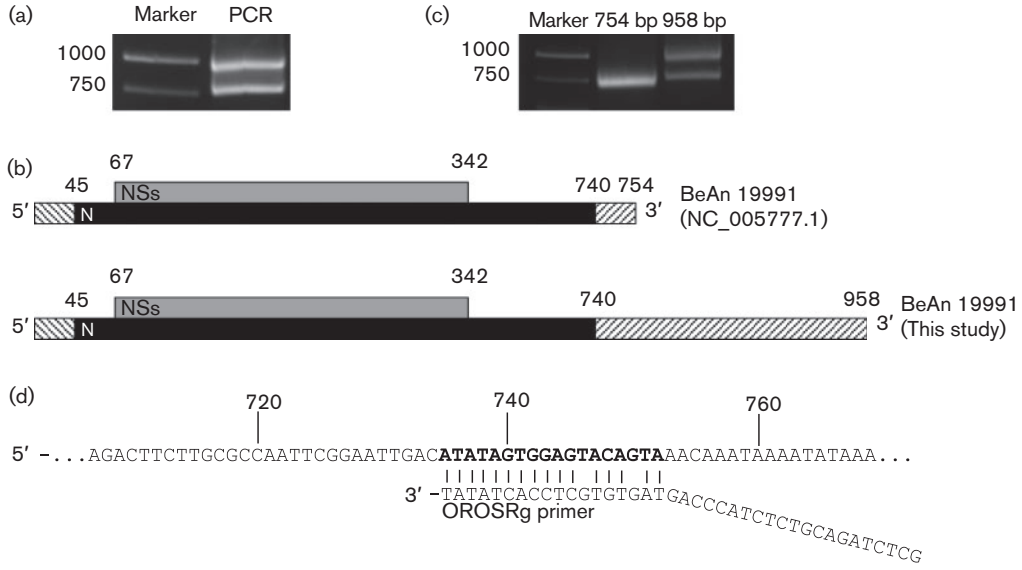

Fig. 3. Analysis of the OROV S segment. (a) Agarose gel electrophoresis of the S segment RT-PCR product. (b) Schematic drawing of the OROV S segment, comparing the published sequence of 754 bp (upper drawing) with the newly determined 958 bp sequence (lower drawing). Black boxes, N ORF; grey boxes, NSs ORF; hatched boxes, UTRs. The sequence is presented in the antigenomic 5′→3′ sense. Numbers indicate nucleotide positions in the sequence. (c) Agarose gel electrophoresis of reamplified DNA products using the 754 and 958 bp PCR products as template. (d) Diagram showing the potential internal binding site (bold) in the OROV S segment. Numbers represent nucleotide positions. OROSRg primer represents the primer sequence that was used in this paper to amplify the S segment.

S921N, L974I and S1021N), whilst only three exchanges were found in the C-terminal half (T1159I, E2056G and R2241K). When compared with the BeAn 19991 M ORF sequence (GenBank accession number NC_005775.1), the TRVL-9760 M ORF showed 100 nt exchanges, with 15 of them leading to amino acid substitutions (S12G, I13V, L67P, A244V, I274F, T463I, A609T, K615N, V732L, D750G, R801K, V846I, S849G, V1241I and M1363I). For the TRVL-9760 N ORF, we detected 13 nt exchanges in comparison to the BeAn 19991 N ORF sequence (GenBank accession number NC_005777.1), but none of these exchanges led to an amino acid substitution. Three of these nucleotide exchanges also affected the overlapping NSs ORF and two of them led to amino acid exchanges (K13R and N74S).

To determine the sequence of the complete L, M and S segments, pyrosequencing was performed. OROV genomic RNA isolated from supernatants of infected murine IFNAR$^{-/-}$ cells was converted to dsDNA by whole-transcriptome amplification, which served as starting material for a shotgun library preparation. After pyrosequencing of the shotgun library, *de novo* assembly with the obtained sequence reads was performed which resulted in sequences for the OROV L, M and S ORFs identical to those obtained by Sanger sequencing. It was not, however, possible to determine the sequences of the non-coding regions by *de novo* assembly. Therefore, an additional reference mapping was performed using the OROV genomic segment sequences from GenBank as reference. With this approach we were able to map the obtained sequence reads to the complete L and the M segment sequences (GenBank accession numbers NC_005776.1 and NC_005775.1). In the case of the S segment, however, it was not possible to map the sequence reads to the 3′ end of the S segment sequence (GenBank accession number NC_005777.1), but mapping was possible for the 5′ non-coding end and the N ORF. We therefore performed another round of reference mapping using an S segment fragment comprising the 5′ end and the N ORF of GenBank accession number NC_005777.1 as reference sequence. Using this approach, the reference mapping resulted in an S segment sequence with an additional 204 nt at the 3′ end.

The complete sequences of the OROV strain TRVL-9760 genome segments have been deposited in GenBank with accession numbers KP026179 (L), KP026180 (M) and KP026181 (S).

Establishment of an OROV minigenome system

Minigenome systems have been described for a number of orthobunyaviruses, and comprise a negative-sense genome analogue encoding a reporter gene that is packaged into ribonucleoprotein complex, transcribed and replicated by co-expressed viral N and L proteins, leading to measurable reporter activity (Elliott, 2012). After confirmation of the nucleotide sequences, the ORFs in each segment are amplified by PCR and subcloned into the pTM1 expression vector (Moss *et al.*, 1990). Minigenome constructs are created by replacing the viral ORF in each segment with the sequence for *Renilla* luciferase and then inverting the insert

in plasmid TVT7R(0,0) (Johnson *et al.*, 2000) so that T7 transcripts would be in the genomic sense (Weber *et al.*, 2001). We first used a minigenome based on the OROV M segment, as studies with Bunyamwera virus (BUNV) showed the M segment minigenome to be the most active (Barr *et al.*, 2003). However, initial attempts using the M segment UTR sequences as reported in GenBank gave low activity over background. When we subsequently obtained the M segment terminal sequences by 3′ RACE analysis and redesigned the minigenome accordingly, with the C/A mismatch at position 9/–9, high levels of luciferase activity were observed, indicating that (i) both N- and L-expressing constructs were functional and (ii) that the M segment UTR sequences determined herein were active promoters. The amounts of transfected N- and L-expressing plasmids were titrated to determine the optimal amounts that gave maximum luciferase activity (data not shown), and the optimized amounts used in all further experiments.

The effects of nucleotide differences in the M segment UTR on minigenome activity are compared in Fig. 4(a). The minigenome with UTR sequences as previously published (9C/G, 15C/G) showed low activity, whereas the minigenome with UTR sequences as determined in our work (9C/A, 15U/A) showed >2000-fold increased activity over background (cells where no L-expressing plasmid was transfected). However, it was not just the mismatch at position 9/–9 that was critical for maximal activity, but also the base-pairing at position 15/–15, as the minigenome with the position 9 C/A mismatch but C/G at position 15/–15 showed only 500-fold increase in activity. Introduction of the U/A pairing was not able to rescue activity when position 9/–9 was C/G and other nucleotide combinations at position 15 were less active than U/A. Taken together, these results highlight the importance of certain residues within the M segment promoter.

The minigenome assay was also used to compare the short and long S segment UTR sequences (Fig. 4b). Minigenome constructs contained the same 5′ UTR and either the 14 nt (as previously published) or 218 nt (as determined herein) long 3′ UTR. The minigenome with the short UTR was inactive, whereas the minigenome with the 218 nt 3′ UTR showed robust luciferase activity. Lastly, we compared L segment-derived minigenomes with either a C or U residue at position 18 in the 5′ UTR. Both minigenomes gave similar high luciferase activity (Fig. 4c).

Together, these results confirmed that the N and L proteins were functional in a minigenome assay, and also that the UTR sequences as determined for the S, M and L segments were functional promoters, and that a base mismatch at position 9/–9 was critical for promoter activity.

VLP production assay

To investigate whether the glycoprotein gene was also functional, a VLP assay was developed. In addition to the M segment minigenome, N- and L-expressing plasmids, cells were also transfected with a plasmid expressing the glycoprotein precursor. Luciferase activity was measured in these donor cells at 24 and 48 h post-transfection (Fig. 5a), and it was noted that there was a significant increase in luciferase activity in cells additionally transfected with the glycoprotein cDNA at 48 h, suggesting spread of VLPs within the culture. The supernatants from transfected cells were harvested at 48 h post-transfection and transferred onto naive BHK-21 cells; luciferase activity in these cells was measured 24 h later. High levels of luciferase activity were recorded in cells exposed to supernatants expressing the glycoproteins (Fig. 5b, L+M) compared with those exposed to supernatants from cells not transfected with the glycoprotein cDNA (Fig. 5b, +L). This is a stringent assay relying only on transcription of the packaged minigenome in the VLP without the need for exogenously supplied viral N and L proteins. Incubation of the supernatant with antibodies to OROV before infection markedly reduced luciferase expression, whereas incubation with an irrelevant antiserum (anti-BUNV serum) had no effect (Fig. 5b). Taken together, these results indicated that the OROV glycoprotein gene cDNA was functional in this VLP assay.

DISCUSSION

A crucial step in developing reverse genetic systems for RNA viruses is obtaining cDNA clones that are representative of the authentic viral genome sequence. As described above, we found a number of sequence differences in our clones derived from the BeAn 19991 strain compared with sequences in the database, including an additional ~200 nt at the 3′ end of the S genome segment, an apparent frame shift in the L segment coding sequence and a critical mismatched nucleotide pair in the terminal panhandle sequence on each segment. These significant differences were confirmed when the complete sequence of the Trinidadian prototype strain TRVL-9760 was also determined.

Early studies comparing orthobunyavirus genome sequences indicated that the terminal 11 nt of each segment exhibited a high degree of conservation, and hence consensus primers based on sequences of Bunyamwera and California serogroup viruses (Dunn *et al.*, 1994; Elliott, 1989a, b; Elliott *et al.*, 1991) have traditionally been used to amplify unknown bunyavirus genomes. However, the actual terminal sequences for the majority of sequences currently available in GenBank have not been verified directly, e.g. by RACE techniques. With regard to the orthobunyavirus 'consensus sequence', there is a single nucleotide difference between the 3′ and 5′ complementary ends such that, using total infected cell RNA as template, mispriming by either primer could occur or a single primer could bind to both genomic and antigenomic RNAs. Indeed, a single primer was used to amplify the OROV M segment (Aquino & Figueiredo, 2004) or the S segments of a range of orthobunyaviruses (Lambert & Lanciotti, 2008). The importance of the terminal sequence has been investigated by minigenome assays for BUNV (Barr & Wertz, 2004; Barr *et al.*, 2003; Dunn *et al.*, 1995; Kohl *et al.*, 2003, 2004) and the

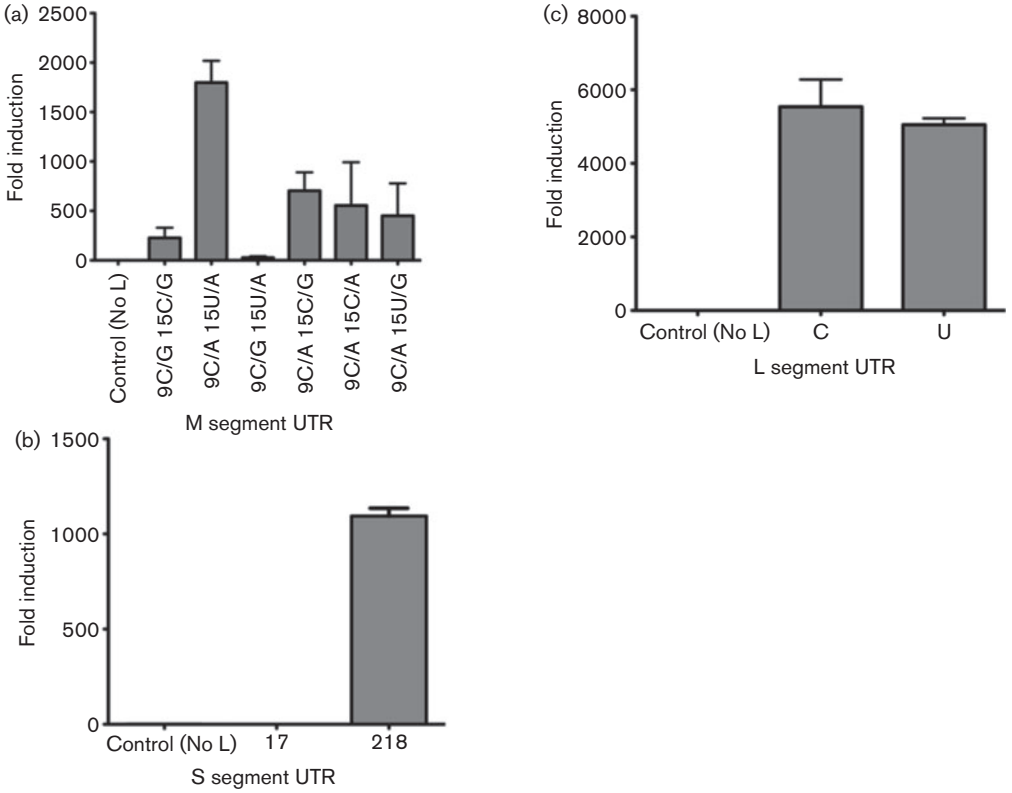

Fig. 4. Minigenome assay. (a) Comparison of M segment-based minigenomes. BSR-T7/5 cells were transfected with 1 μg each pTM1OROV-L and pTM1OROV-N, 0.5 μg M segment minigenome-expressing plasmid, and 100 ng pTM1-FF-Luc; the background control lacked pTM1OROV-L. M segment minigenomes contained different nucleotides at position 9/−9 as indicated. Minigenome activity is expressed as fold induction over the background control. (b) Comparison of S segment minigenomes containing the published (14 nt) or newly defined long (218 nt) 5′ UTR. (c) Comparison of L segment minigenomes containing a C or U at position 18 in the 3′ UTR. Error bars indicate SD.

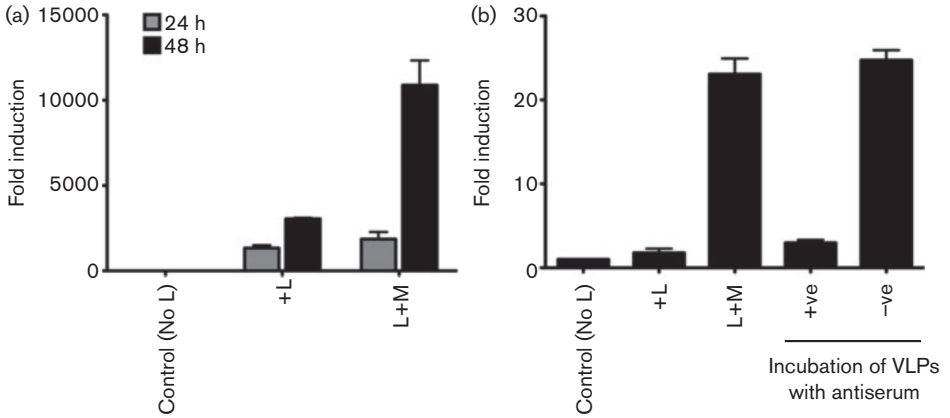

Fig. 5. VLP production assay. BSR-T7/5 cells were transfected with 1 μg each pTM1OROV-L and pTM1OROV-N, 0.5 μg pTM1OROV-M, 0.5 μg M segment minigenome-expressing plasmid, and 100 ng pTM1-FF-Luc; control transfection mixes lacked pTM1OROV-L (No L) or pTM1OROV-M (+L). At 24 or 48 h post-transfection, clarified supernatants were used to infect naive BHK-21 cells, and luciferase activity measured 24 h later. (a) Minigenome activity in transfected BSR-T7/5 cells at 24 or 48 h post-transfection. (b) Minigenome activity in BHK-21 cells infected with supernatants from cells in (a). VLPs were also incubated with anti-OROV antibodies (+ve) or irrelevant antibodies (−ve) before infection of cells as indicated. Error bars indicate SD.

mismatch at position 9/–9 was shown to be crucial for promoter activity (Barr & Wertz, 2005). As more diverse orthobunyavirus genomes have been sequenced, particularly using next-generation sequencing methods (deep sequencing) that are not reliant on specific primers to amplify cDNA, it has become clear that there is more variation in the 'bunyavirus consensus' than observed between Bunyamwera and California serogroup viruses (e.g. Ladner *et al.*, 2014b), highlighting the requirement for direct determination of the terminal sequences. In a similar vein, as the genomes of more members of the genus *Phlebovirus* (another genus in the family *Bunyaviridae*) have been sequenced, it is apparent that the termini also diverge from the 'phlebovirus consensus' (Dilcher *et al.*, 2012a; Elliott & Brennan, 2014; Matsuno *et al.*, 2013).

A recent paper (Ladner *et al.*, 2014a) suggested the standards that should be applied to viral genome sequence determination and we strongly support the recommendations proposed therein.

Saeed *et al.* (2000) reported the first nucleocapsid gene sequences of 28 strains of OROV, including the prototypic Trinidadian OROV isolate TRVL-9760 and the Brazilian isolate BeAn 19991. They determined the complete S segment to be 754 bases and noted the unusually short length of the 3′ UTR, just 14 bases after the translational stop codon, compared with other orthobunyavirus S segments. They employed various experimental procedures to verify the 3′ UTR, including chemical denaturation of the purified viral RNA with methylmercury hydroxide before RT-PCR (in case there was a secondary structure that impeded reverse transcription), and a 5′ RACE procedure using both purified viral RNA and total cellular RNA as starting material (Saeed *et al.*, 2000). All approaches yielded that same short 3′ UTR. Our results indicate that the true length of the S segment is actually 958 nt, which was verified by independent experimental analyses, including deep sequencing of the TRVL-9760 strain. Examination of the correct sequence reveals an internal region highly similar to the terminal sequence that could hybridize with the primer and in our studies resulted in two PCR products. The functionality of the longer 3′ UTR determined in this study was demonstrated in the minigenome assay.

We further confirmed that the sequences of the BeAn 19991 N and L proteins were functional in driving reporter gene expression from minigenomes, and similarly that the determined UTR sequence for all three segments could be used to construct functional minigenomes. Lastly, by co-transfecting a cDNA that expressed the glycoprotein gene, we produced VLPs that were capable of packaging a minigenome and infecting naive cells. Taken together, these data provide strong evidence that the cDNA clones reported in this paper are fully functional and pave the way to establishing a virus rescue system. The availability of such a system will play a crucial role in understanding the molecular biology of this important yet poorly characterized emerging viral zoonosis.

METHODS

Cells and virus. Vero-E6 and murine IFNAR$^{-/-}$ cells were grown in Dulbecco's modified Eagle's medium (Invitrogen) supplemented with 10 % FCS. BHK-21 cells were grown in Glasgow minimal essential medium (GMEM; Invitrogen) supplemented with 10 % newborn calf serum and 10 % tryptose phosphate broth (TPB; Invitrogen). BSR-T7/5 cells, which stably express T7 RNA polymerase (Buchholz *et al.*, 1999), were grown in GMEM supplemented with 10 % FCS, 10 % TPB and 1 mg G418 ml^{-1} (Geneticin; Invitrogen).

OROV strain BeAn 19991 was kindly donated by Professor Luiz Tadeu Moraes Figueiredo (University of Sao Paulo School of Medicine, Ribeirão Preto, Brazil) and strain TRVL-9760 was kindly provided by Dr Robert Shope (University of Texas Medical Branch, Galveston, TX, USA). A sample of total infected cell RNA obtained from strain H759025 AMA2080 was provided by Dr Pedro Vasconcelos (Department of Arboviruses and Hemorrhagic Fevers, Evandro Chagas Institute, Ministry of Health, Ananindeua, Brazil).

All experiments with infectious viruses were conducted under Containment Level 3 laboratory conditions.

Cloning of OROV cDNA. OROV was grown in BHK-21 cells at 37 °C, and after 30 h both cells and supernatant were harvested, and RNA extracted using TRIzol reagent (Invitrogen). cDNAs to each segment were synthesized separately, using segment-specific primers for the L and M segments (OROLFg and OROMFg, Table 1), and random primers (Promega) for the S segment, together with Moloney murine leukemia virus (MMLV) reverse transcriptase (Promega). Each cDNA preparation was used in a segment-specific PCR using the appropriate primer pairs (OROMFg/OROMRg for the M segment and OROSFg/OROSRg for the S segment; Table 1) and KOD Hot Start DNA polymerase (Merck), according to the manufacturer's protocol. The full-length PCR products were cloned into pGEM-T Easy (Promega). After selection of positive clones, the inserts were excised by digestion with *Bsm*BI and ligated into *Bbs*I-linearized plasmid TVT7R(0,0) (Johnson *et al.*, 2000). The L segment cDNA was amplified in two fragments using primer pairs (OROFLg/OROL1 and OROL2/OROLRg; Table 1). The first primer pair amplified nt 1–3706 and the second pair amplified nt 3537–6852, resulting in two PCR products with a 170 bp overlapping region containing a unique *Bsg*I restriction site (nt 3590 in the full-length segment). PCR products were purified from an agarose gel and then cloned into pGEM-T Easy. The inserts were excised by digestion with restriction enzymes *Bsg*I and *Bsm*BI, and the full-length L segment was assembled by ligating both fragments with *Bbs*I-linearized TVT7R(0,0). The cDNA inserts included an extra G residue at their 5′ ends for efficient T7 transcription and the inserts were cloned such that T7 polymerase would transcribe antigenome-sense RNAs. The plasmids were designated pTVTOROVL, pTVTOROVM and pTVTOROVS.

Construction of protein-expressing and minigenome-expressing plasmids. The complete ORFs in the L and M segments were amplified by PCR using specific primers (pTM1 series in Table 1) and the pTVT7 transcription plasmids as templates, and subcloned into expression vector pTM1 (Moss *et al.*, 1990), under the control of the T7 promoter and encephalomyocarditis virus internal ribosome entry site sequence. The constructs were designated pTM1OROV-L and pTM1OROV-M. To generate a plasmid expressing only the N protein, we introduced three point mutations (T68C, T113C and G116A) into pTVTOROVS using primers ORODelNSsF and ORODelNSsR (Table 1), by QuikChange site-directed mutagenesis (Stratagene), prior to PCR amplification of the N ORF. These mutations changed the first and second methionine codons in the NSs ORF into threonine codons, and introduced an in-frame translation stop codon at codon 17; the coding sequence of the overlapping N ORF was unaffected. This plasmid was designated pTM1OROV-N.

The minigenome plasmids were created in three steps. First, the sequence encoding the coding sequence in each pTVT7 clone was deleted by excision PCR, leaving the UTRs intact. These linearized DNAs were then used in an In-Fusion reaction (In-Fusion HD Cloning; Clontech) with PCR-amplified DNA of the *Renilla* luciferase gene. The amplified luciferase gene contained 15 nt extensions homologous to the OROV L, M or S segment UTR sequences in the linearized pTVT7 construct. The UTR–luciferase–UTR sequence was then amplified by PCR using primers containing 15 nt extensions homologous to the T7 terminator (5′ end) and T7 promoter (3′ end). This amplified products were combined with TVT7R(0,0) DNA in an In-Fusion reaction to generate minigenome-expressing plasmids such that in T7 transcripts the *Renilla* luciferase was in the negative sense. These constructs were designated pTVT7OROVSRen(–), pTVT7OROVMRen(–) and pTVT7OROVLRen(–).

Sequencing OROV BeAn 19991 5′ and 3′ termini. As total infected cell RNA contains both genomic and antigenomic segments, 3′ RACE analysis was capable of generating both the 5′ and 3′ terminal sequences using strand-specific primers. Briefly, RNA was polyadenylated (Ambion) for 1 h at 37 °C and then purified using an RNeasy Mini kit (Qiagen). The polyadenylated RNA was then used in a reverse transcription reaction with MMLV reverse transcriptase (Promega) and oligo-d(T) primer, followed by PCR using 3′ PCR anchor primer (Roche) and the appropriate segment specific primer (OROVL_anti/OROVL_gen for the L segment and OROVM_anti/OROVM_gen for the M segment; Table 1) with KOD Hot Start DNA polymerase (Merck). Amplified products were purified on an agarose gel and their nucleotide sequence determined.

To confirm the S segment terminal sequences, total infected cell RNA was first denatured at 90 °C for 3 min and then ligated using T4 RNA ligase (New England Biolabs) for 2 h at 37 °C. The reaction was heat inactivated at 65 °C and purified using an RNeasy Mini kit (Qiagen). cDNA was synthesized using MMLV reverse transcriptase (Promega) and oligonucleotide OROSlig1 (Table 1). PCR was then performed with KOD Hot Start DNA polymerase (Merck) and primers OROSlig1 and OROSlig2 (Table 1). The PCR product was purified on an agarose gel and its nucleotide sequence determined.

Pyrosequencing of the OROV TRVL-9760 strain. OROV TRVL-9760 was grown in IFNAR$^{-/-}$ cells at 37 °C and supernatant was harvested after 48 h. (Preliminary results showed that IFNAR$^{-/-}$ cells gave the highest amounts of genomic RNA in the extracted supernatant compared with Vero-E6 or BHK-21 cells; unpublished observations.) For removal of cell debris, the supernatant was centrifuged at 700 ***g*** for 10 min and at 2800 ***g*** for 5 min, followed by filtration through a 0.2 μm sterile filter. To enrich viral particles, 20 ml cleared supernatant was mixed with 1.48 ml 5 M NaCl and 10.8 ml 30 % PEG8000 in NTE (100 mM NaCl; 10 mM Tris, pH 6.5; 1 mM EDTA), incubated on a shaker for 30 min at 4 °C, and subsequently centrifuged at 6000 ***g*** for 60 min at 4 °C. The virus pellet was resuspended in 500 μl PBS. RNA extraction was performed using PeqGold Trifast (Peqlab). To be able to cover the 3′ terminal parts of the OROV genome segments, 500 ng self-complementary FLAC (full-length amplification of cDNAs) adapters were ligated to 500 ng purified viral RNA as described previously (Dilcher *et al.*, 2012b). To achieve coverage of the 5′ terminal parts, a 5′ RACE RNA adaptor (Ambion) was ligated to the viral RNA after the removal of two phosphate groups via RNA 5′-polyphosphatase. To remove unligated adapters, a subsequent purification step was performed using a CleanAll DNA/RNA Clean-Up and Concentration kit (Norgen Biotek). The concentration of the adaptor-ligated and purified ssRNA was determined by Qant-iT RiboGreen assay (Invitrogen). Then, 60 ng adaptor-ligated viral RNA was amplified and converted to dsDNA using a TransPlex Whole Transciptome Amplification kit (WTA2; Sigma-Aldrich). The newly synthesized dsDNA was purified using a QIAquick PCR Purification kit (Qiagen), and DNA fragments <350 bp were removed using Ampure-XP beads (Agencourt). A sample of 300 ng whole-genome amplified dsDNA was used for Titanium Shotgun Rapid Library Preparation and pyrosequencing on a Genome Sequencer FLX (Roche) as described in the FLX Titanium Protocol (Roche), but omitting the 'DNA fragmentation by nebulization' step. Assembly of the sequenced OROV genome segments was done by means of the Genome Sequencer FLX System software package version 2.3 (GS *De novo* Assembler, GS Reference Mapper) in combination with the commercially available SeqMan Pro version 10.1.1 (DNASTAR, Lasergene).

Minigenome and VLP assays. Subconfluent monolayers of BSR-T7/5 cells were transfected with 1 μg each pTM1OROV-L and pTM1OROV-N, 0.5 μg minigenome-expressing plasmid, and 100 ng pTM1-FF-Luc (Weber *et al.*, 2001). At 24 h post-transfection, *Renilla* and firefly luciferase activities were measured using a Dual-Luciferase Reporter Assay kit (Promega).

To generate VLPs, the M segment minigenome transfection mix was supplemented with 0.5 μg pTM1OROV-M. At 24 and 48 h post-transfection, supernatants were harvested, clarified by centrifugation (4000 r.p.m. for 5 min at 4 °C), digested with benzonase and used to infect BHK-21 cells. *Renilla* activity was measured after 24 h using a Renilla Reporter Assay kit (Promega). To neutralize the VLPs, samples were incubated with hyperimmune mouse ascetic fluid to OROV or with anti-BUNV rabbit antiserum for 1 h at room temperature before infecting BHK-21 cells.

ACKNOWLEDGEMENTS

This work was supported by a Wellcome Trust Senior Investigator Award to R. M. E. (099220), a Medical Research Council postgraduate studentship to N. L. T.-L., a FAPESP-Sao Paulo Research Foundation fellowship to G. O. A. (2013/02798-0, CNPQ) and a CAPES-National Council for the Improvement of Higher Education (Brazil) scholarship to D. E. A. S. (3851/10-9).

REFERENCES

Afonso, A., Abrahantes, J. C., Conraths, F., Veldhuis, A., Elbers, A., Roberts, H., Van der Stede, Y., Méroc, E., Gache, K. & Richardson, J. (2014). The Schmallenberg virus epidemic in Europe – 2011–2013. *Prev Vet Med* **116**, 391–403.

Anderson, C. R., Spence, L., Downs, W. G. & Aitken, T. H. (1961). Oropouche virus: a new human disease agent from Trinidad, West Indies. *Am J Trop Med Hyg* **10**, 574–578.

Aquino, V. H. & Figueiredo, L. T. (2004). Linear amplification followed by single primer polymerase chain reaction to amplify unknown DNA fragments: complete nucleotide sequence of Oropouche virus M RNA segment. *J Virol Methods* **115**, 51–57.

Aquino, V. H., Moreli, M. L. & Moraes Figueiredo, L. T. (2003). Analysis of oropouche virus L protein amino acid sequence showed the presence of an additional conserved region that could harbour an important role for the polymerase activity. *Arch Virol* **148**, 19–28.

Barr, J. N. & Wertz, G. W. (2004). Bunyamwera bunyavirus RNA synthesis requires cooperation of 3′- and 5′-terminal sequences. *J Virol* **78**, 1129–1138.

Barr, J. N. & Wertz, G. W. (2005). Role of the conserved nucleotide mismatch within 3′- and 5′-terminal regions of Bunyamwera virus in signaling transcription. *J Virol* **79**, 3586–3594.

Barr, J. N., Elliott, R. M., Dunn, E. F. & Wertz, G. W. (2003). Segment-specific terminal sequences of Bunyamwera bunyavirus regulate genome replication. *Virology* **311**, 326–338.

Blakqori, G., Kochs, G., Haller, O. & Weber, F. (2003). Functional L polymerase of La Crosse virus allows *in vivo* reconstitution of recombinant nucleocapsids. *J Gen Virol* **84**, 1207–1214.

Buchholz, U. J., Finke, S. & Conzelmann, K. K. (1999). Generation of bovine respiratory syncytial virus (BRSV) from cDNA: BRSV NS2 is not essential for virus replication in tissue culture, and the human RSV leader region acts as a functional BRSV genome promoter. *J Virol* **73**, 251–259.

Dilcher, M., Alves, M. J., Finkeisen, D., Hufert, F. & Weidmann, M. (2012a). Genetic characterization of Bhanja virus and Palma virus, two tick-borne phleboviruses. *Virus Genes* **45**, 311–315.

Dilcher, M., Hasib, L., Lechner, M., Wieseke, N., Middendorf, M., Marz, M., Koch, A., Spiegel, M., Dobler, G. & other authors (2012b). Genetic characterization of Tribeč virus and Kemerovo virus, two tick-transmitted human-pathogenic Orbiviruses. *Virology* **423**, 68–76.

Dunn, E. F., Pritlove, D. C. & Elliott, R. M. (1994). The S RNA genome segments of Batai, Cache Valley, Guaroa, Kairi, Lumbo, Main Drain and Northway bunyaviruses: sequence determination and analysis. *J Gen Virol* **75**, 597–608.

Dunn, E. F., Pritlove, D. C., Jin, H. & Elliott, R. M. (1995). Transcription of a recombinant bunyavirus RNA template by transiently expressed bunyavirus proteins. *Virology* **211**, 133–143.

Elliott, R. M. (1989a). Nucleotide sequence analysis of the large (L) genomic RNA segment of Bunyamwera virus, the prototype of the family *Bunyaviridae*. *Virology* **173**, 426–436.

Elliott, R. M. (1989b). Nucleotide sequence analysis of the small (S) RNA segment of Bunyamwera virus, the prototype of the family *Bunyaviridae*. *J Gen Virol* **70**, 1281–1285.

Elliott, R. M. (2012). Bunyavirus reverse genetics and applications to studying interactions with host cells. In *Reverse Genetics of RNA Viruses: Applications and Perspectives*, pp. 200–223. Edited by A. Bridgen. Chichester: Wiley.

Elliott, R. M. (2014). Orthobunyaviruses: recent genetic and structural insights. *Nat Rev Microbiol* **12**, 673–685.

Elliott, R. M. & Brennan, B. (2014). Emerging phleboviruses. *Curr Opin Virol* **5**, 50–57.

Elliott, R. M., Schmaljohn, C. S. & Collett, M. S. (1991). *Bunyaviridae* genome structure and gene expression. *Curr Top Microbiol Immunol* **169**, 91–141.

Elliott, R. M., Blakqori, G., van Knippenberg, I. C., Koudriakova, E., Li, P., McLees, A., Shi, X. & Szemiel, A. M. (2013). Establishment of a reverse genetics system for Schmallenberg virus, a newly emerged orthobunyavirus in Europe. *J Gen Virol* **94**, 851–859.

Johnson, K. N., Zeddam, J. L. & Ball, L. A. (2000). Characterization and construction of functional cDNA clones of Pariacoto virus, the first Alphanodavirus isolated outside Australasia. *J Virol* **74**, 5123–5132.

Kohl, A., Bridgen, A., Dunn, E., Barr, J. N. & Elliott, R. M. (2003). Effects of a point mutation in the 3′ end of the S genome segment of naturally occurring and engineered Bunyamwera viruses. *J Gen Virol* **84**, 789–793.

Kohl, A., Dunn, E. F., Lowen, A. C. & Elliott, R. M. (2004). Complementarity, sequence and structural elements within the 3′ and 5′ non-coding regions of the Bunyamwera orthobunyavirus S segment determine promoter strength. *J Gen Virol* **85**, 3269–3278.

Ladner, J. T., Beitzel, B., Chain, P. S., Davenport, M. G., Donaldson, E. F., Frieman, M., Kugelman, J. R., Kuhn, J. H., O'Rear, J. & other authors (2014a). Standards for sequencing viral genomes in the era of high-throughput sequencing. *MBio* **5**, e01360–e14.

Ladner, J. T., Savji, N., Lofts, L., Travassos da Rosa, A., Wiley, M. R., Gestole, M. C., Rosen, G. E., Guzman, H., Vasconcelos, P. F. & other authors (2014b). Genomic and phylogenetic characterization of viruses included in the Manzanilla and Oropouche species complexes of the genus *Orthobunyavirus*, family *Bunyaviridae*. *J Gen Virol* **95**, 1055–1066.

Lambert, A. J. & Lanciotti, R. S. (2008). Molecular characterization of medically important viruses of the genus *Orthobunyavirus*. *J Gen Virol* **89**, 2580–2585.

Matsuno, K., Weisend, C., Travassos da Rosa, A. P., Anzick, S. L., Dahlstrom, E., Porcella, S. F., Dorward, D. W., Yu, X. J., Tesh, R. B. & Ebihara, H. (2013). Characterization of the Bhanja serogroup viruses (*Bunyaviridae*): a novel species of the genus *Phlebovirus* and its relationship with other emerging tick-borne phleboviruses. *J Virol* **87**, 3719–3728.

Moss, B., Elroy-Stein, O., Mizukami, T., Alexander, W. A. & Fuerst, T. R. (1990). New mammalian expression vectors. *Nature* **348**, 91–92.

Ogawa, Y., Sugiura, K., Kato, K., Tohya, Y. & Akashi, H. (2007). Rescue of Akabane virus (family *Bunyaviridae*) entirely from cloned cDNAs by using RNA polymerase I. *J Gen Virol* **88**, 3385–3390.

Pinheiro, F. P., Pinheiro, M., Bensabath, G., Causey, O. R. & Shope, R. E. (1962). [Oropouche virus epidemic in Bélem]. *Rev Serv Esp Saude Pub* **12**, 15–23 (in Portugese).

Pinheiro, F. P., Hoch, A. L., Gomes, M. L. & Roberts, D. R. (1981a). Oropouche virus. IV. Laboratory transmission by *Culicoides paraensis*. *Am J Trop Med Hyg* **30**, 172–176.

Pinheiro, F. P., Travassos da Rosa, A. P., Travassos da Rosa, J. F., Ishak, R., Freitas, R. B., Gomes, M. L., LeDuc, J. W. & Oliva, O. F. (1981b). Oropouche virus. I. A review of clinical, epidemiological, and ecological findings. *Am J Trop Med Hyg* **30**, 149–160.

Pinheiro, F. P., Travassos da Rosa, A. P., Gomes, M. L., LeDuc, J. W. & Hoch, A. L. (1982). Transmission of Oropouche virus from man to hamster by the midge *Culicoides paraensis*. *Science* **215**, 1251–1253.

Plyusnin, A. & Elliott, R. M. (editors) (2011). *Bunyaviridae. Molecular and Cellular Biology*. Norfolk: Caister Academic Press.

Saeed, M. F., Wang, H., Nunes, M., Vasconcelos, P. F., Weaver, S. C., Shope, R. E., Watts, D. M., Tesh, R. B. & Barrett, A. D. (2000). Nucleotide sequences and phylogeny of the nucleocapsid gene of Oropouche virus. *J Gen Virol* **81**, 743–748.

Shi, X., Kohl, A., Li, P. & Elliott, R. M. (2007). Role of the cytoplasmic tail domains of Bunyamwera orthobunyavirus glycoproteins Gn and Gc in virus assembly and morphogenesis. *J Virol* **81**, 10151–10160.

Varela, M., Schnettler, E., Caporale, M., Murgia, C., Barry, G., McFarlane, M., McGregor, E., Piras, I. M., Shaw, A. & other authors (2013). Schmallenberg virus pathogenesis, tropism and interaction with the innate immune system of the host. *PLoS Pathog* **9**, e1003133.

Vasconcelos, H. B., Nunes, M. R., Casseb, L. M., Carvalho, V. L., Pinto da Silva, E. V., Silva, M., Casseb, S. M. & Vasconcelos, P. F. (2011). Molecular epidemiology of Oropouche virus, Brazil. *Emerg Infect Dis* **17**, 800–806.

Wang, H., Beasley, D. W., Li, L., Holbrook, M. R. & Barrett, A. D. (2001). Nucleotide sequence and deduced amino acid sequence of the medium RNA segment of Oropouche, a Simbu serogroup virus: comparison with the middle RNA of Bunyamwera and California serogroup viruses. *Virus Res* **73**, 153–162.

Weber, F., Dunn, E. F., Bridgen, A. & Elliott, R. M. (2001). The Bunyamwera virus nonstructural protein NSs inhibits viral RNA synthesis in a minireplicon system. *Virology* **281**, 67–74.

Weber, F., Bridgen, A., Fazakerley, J. K., Streitenfeld, H., Kessler, N., Randall, R. E. & Elliott, R. M. (2002). Bunyamwera bunyavirus nonstructural protein NSs counteracts the induction of alpha/beta interferon. *J Virol* **76**, 7949–7955.

Journal of General Virology (2015), **96**, 1636–1650 **DOI** 10.1099/vir.0.000108

Genetic analysis of members of the species *Oropouche virus* and identification of a novel M segment sequence

Natasha L. Tilston-Lunel,[1,2] Joseph Hughes,[1] Gustavo Olszanski Acrani,[1,3] Daisy E. A. da Silva,[4] Raimunda S. S. Azevedo,[5] Sueli G. Rodrigues,[5] Pedro F. C. Vasconcelos,[5] Marcio R. T. Nunes[4] and Richard M. Elliott[1]

Correspondence
Richard M. Elliott
richard.elliott@glasgow.ac.uk

[1]MRC-University of Glasgow Centre for Virus Research, 464 Bearsden Road, Glasgow G61 1QH, Scotland, UK

[2]Biomedical Sciences Research Complex, School of Biology, University of St Andrews, St Andrews KY16 9ST, Scotland, UK

[3]Department of Cell and Molecular Biology, University of Sao Paulo School of Medicine, 3900, Av Bandeirantes, Ribeirão Preto, SP 14049-900, Brazil

[4]Center for Technological Innovation, Instituto Evandro Chagas, Ananindeua, Brazil

[5]Department of Arbovirology and Hemorrhagic Fevers, Instituto Evandro Chagas, Ananindeua, Brazil

Oropouche virus (OROV) is a public health threat in South America, and in particular in northern Brazil, causing frequent outbreaks of febrile illness. Using a combination of deep sequencing and Sanger sequencing approaches, we determined the complete genome sequences of eight clinical isolates that were obtained from patient sera during an Oropouche fever outbreak in Amapa state, northern Brazil, in 2009. We also report the complete genome sequences of two OROV reassortants isolatd from two marmosets in Minas Gerais state, south-east Brazil, in 2012 that contained a novel M genome segment. Interestingly, all 10 isolates possessed a 947 nt S segment that lacked 11 residues in the S-segment 3′ UTR compared with the recently redetermined Brazilian prototype OROV strain BeAn19991. OROV maybe circulating more widely in Brazil and in the non-human primate population than previously appreciated, and the identification of yet another reassortant highlights the importance of bunyavirus surveillance in South America.

Received 22 January 2015
Accepted 25 February 2015

INTRODUCTION

Oropouche virus (OROV) is a midge-borne orthobunyavirus that causes a febrile illness in humans throughout northern South America. The virus is endemic to Brazil and to date all major outbreaks have been limited to the northern region of the country. The largest known OROV outbreak was recorded in 1980 in the state of Para with an estimated 100 000 cases (Anderson *et al.*, 1961; Borborema *et al.*, 1982; Dixon *et al.*, 1981; LeDuc *et al.*, 1981; Pinheiro *et al.*, 1976; Pinheiro, 1962; Vasconcelos *et al.*, 1989). Due to the similarity of signs and symptoms to other endemic viral diseases such as dengue, chikungunya and Mayaro fevers and the lack of a differential surveillance system, the burden of OROV on the Brazilian public health system and economy remains unclear. In an urban environment, the midge *Culicoides paraensis* transmits OROV among humans (Pinheiro *et al.*, 1981, 1982; Roberts *et al.*, 1977), whilst in the tropical forest the virus has been isolated from the pale-throated three-toed sloth (*Bradypus tridactylus*) and the black-tufted marmoset (*Callithrix penicillata*), although the vectors are largely unknown (Nunes *et al.*, 2005a; Pinheiro *et al.*, 1976).

OROV belongs to the genus *Orthobunyavirus*, the largest of the five genera in the family *Bunyaviridae*, which contains several other important human and veterinary pathogens such as La Crosse, Akabane, Cache Valley and Schmallenberg viruses (Elliott, 2014). OROV is classified in the Simbu serogroup and, like all bunyaviruses, contains a tripartite negative-sense RNA genome. The large (L) segment encodes the viral polymerase, the medium (M)

The GenBank/EMBL/DDBJ accession numbers for the sequences reported in this paper are KP691603–KP691632.

Four supplementary tables are available with the online Supplementary Material.

segment encodes the viral glycoproteins Gn and Gc, and a nonstructural protein, NSm, and the small (S) segment codes for the viral nucleocapsid protein (N) and a second non-structural protein (NSs) from overlapping ORFs (Elliott, 2014; Elliott & Blakqori, 2011). Recently, we reported the complete genome sequence for the prototype Brazilian OROV strain BeAn19991 (GenBank accession numbers KP052850–KP052852). Our analysis corrected several errors in the previously published OROV genome sequences, most notably that the S segment was 958 nt and not the originally published 754 nt (Acrani *et al.*, 2014).

Here, we report the complete genome sequences of eight clinical isolates of OROV and two primate-derived OROV reassortants. The M segment of the reassortant virus was a unique Simbu sequence that fell in the same clade as the Jatobal virus (JATV) M segment. All 10 isolates contained S segments that were 11 nt shorter than the BeAn19991 strain. To our knowledge, this is the first report of complete genome sequences for OROV field isolates, and we discuss the importance of this in terms of understanding the evolutionary history of the virus.

RESULTS

Complete genome sequence of OROV clinical isolates

OROV isolates BeH759021, BeH759022, BeH759024, BeH759025, BeH759040, BeH759146, BeH759529 and BeH759620 represent a small portion of OROV samples that were obtained from febrile humans between June and August 2009 in the town of Mazagão, Amapa state, Brazil (Table 1, Fig. 1). The mean age of the patients was 26.5 years and all had presented a similar clinical picture characterized by fever, headache, arthralgia, myalgia and ocular pain. Genome sequences for these isolates were generated by *de novo* assembly of 1 058 075 trimmed and filtered sequence reads obtained using a Roche 454 sequencer.

The mean S-segment contig length was 867 bases, and by mapping the sequence reads to reference strain BeAn19991 S segment (GenBank accession no. KP052852), we obtained complete S-segment sequences of 947 bases. All S segments were therefore 11 nt shorter than that of the redetermined BeAn19991 strain (Acrani *et al.*, 2014). Ligation of extracted RNA (see Methods) followed by Sanger sequencing was used to confirm the UTR sequences. This revealed that all these isolates lacked nt 781–791 in the S segment of BeAn19991. Additional differences were observed at positions G750A, A754G, C771T, T820C and T888C, resulting in 92.6 % 3′ UTR similarity with BeAn19991 (Fig. 2a). However, despite these differences, promoter activity was similar to that of BeAn19991 (Fig. 2b) when tested in a minigenome assay (Acrani *et al.*, 2014). At the nucleotide level, the N-coding region of these isolates was 95 % similar to that of BeAn19991, but there was 100 % conservation of the translated protein sequence. Unlike in BeAn19991, the NSs-coding region contains tandem AUG translational start codons (a feature

Table 1. Information about samples sequenced in this study

Sample	ID	Isolation date	Host	Country	State	Town	Age (years)	Gender	Source	GenBank accession nos
BeH759021	AMA 2076	23/07/2009	Human	Brazil	Amapa	Mazagao	18	M	Serum	KP691606–KP691608
BeH759022	AMA 2077	24/07/2009	Human	Brazil	Amapa	Mazagao	39	M	Serum	KP691609–KP691611
BeH759024	AMA 2079	24/07/2009	Human	Brazil	Amapa	Mazagao	24	M	Serum	KP691603–KP691605
BeH759025	AMA 2080	24/07/2009	Human	Brazil	Amapa	Mazagao	23	F	Serum	KP691612–KP691614
BeH759040	AMA 2095	23/07/2009	Human	Brazil	Amapa	Mazagao	48	M	Serum	KP691615–KP691617
BeH759146	AMA 2337	20/08/2009	Human	Brazil	Amapa	Mazagao	31	M	Serum	KP691630–KP691632
BeH759529	AMA 2238	17/06/2009	Human	Brazil	Amapa	Mazagao	13	F	Serum	KP691618–KP691620
BeH759620	AMA 2329	23/06/2009	Human	Brazil	Amapa	Mazagao	16	M	Serum	KP691621–KP691623
BeAn789726	PR 4837	2012	*Callithrix penicillata*	Brazil	Minas Gerais	Perdoes	NA	NA	Viscera	KP691624–KP691626
BeAn790177	PR 4843	2012	*Callithrix penicillata*	Brazil	Minas Gerais	Perdoes	NA	NA	Viscera	KP691627–KP691629

M, male; F, female; NA, not applicable.

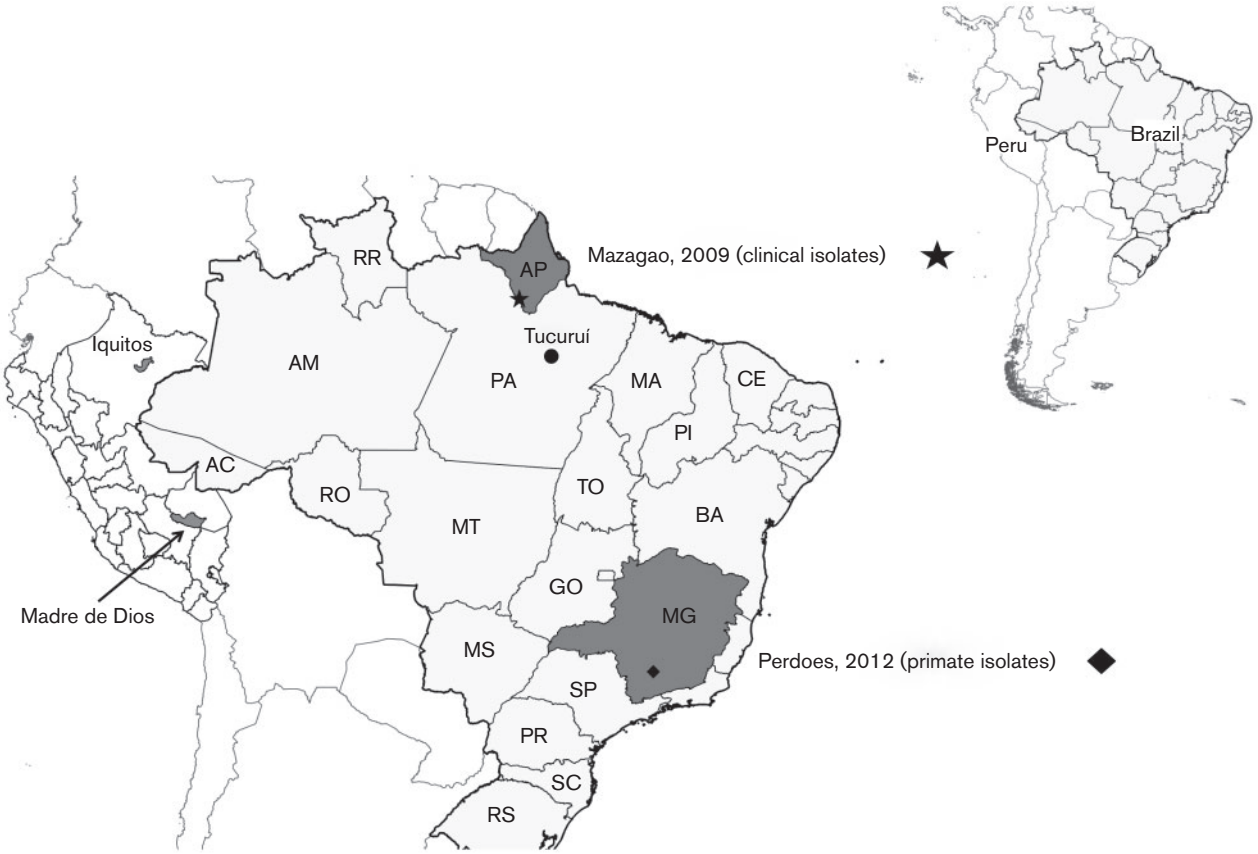

Fig. 1. Location of samples sequenced in this study. The map also shows Iquitos and Madre de Dios in Peru where OROV M segment reassortants were isolated, and Tucuruí, a municipality in Para, Brazil, where JATV was isolated. AC, Acre; AM, Amazonas; AP, Amapa; BA, Bahia; CE, Ceara; GO, Goias; MA, Maranhao; MG, Minas Gerais; MS, Mato Grosso do Sul; MT, Mato Grosso; PA, Para; PI, Piaui; PR, Parana; RO, Rondonia; RR, Roraima; SC, Santa Catarina; SP, Sao Paulo; RS, Rio Grande do Sul; TO, Tocantins.

of many other orthobunyaviruses; Dunn *et al.*, 1994), caused by C/U variation at nt 56. The NSs ORFs of the human isolates also had a difference at position 332 (A→G), resulting in a Gln→Arg change in the NSs protein at position 89.

The amino acid sequences of the M- and L-segment-encoded proteins of the human isolates were 98.5 and 98.0 % similar to the M- and L-segment proteins of BeAn19991, respectively. We were unable to obtain the terminal sequences of the M and L segments from the deep sequencing data, and therefore 3′ rapid amplification of cDNA ends (RACE) analysis was used. The clinical isolates displayed 99 % similarity among each other across the complete L and M segments, but all had identical UTR sequences that showed 90 and 96 % similarity to the L- and M-segment UTRs, respectively, of BeAn19991 (Fig. 2c).

Complete sequence of a novel Simbu virus M segment

The sequences of BeAn789726 and BeAn790177, isolates from two black-tufted marmosets (*Callithrix penicillata*), were obtained using deep sequencing and 3′ RACE analysis. The L and S segments showed 99 and 100 % similarity, respectively, to those of the eight clinical isolates. Unexpectedly, the M segment showed only about 56 % similarity at the nucleotide level to other OROV M-segment sequences (about 48 % at the amino acid level). There was, however, a higher similarity with JATV M segment, strain BeAn423380 (GenBank accession no. AFI24667; 71.6 % at the nucleotide level and 76.5 % at the amino acid level). Alignment of the UTR sequences in Fig. 2(c) shows the 11 nt terminal consensus sequence with the conserved C/A mismatch at position 9/−9. This novel M segment was 4418 nt and encoded a 1417 aa polyprotein. Between BeAn790177 and BeAn789726, we observed two nucleotide differences, a silent mutation at position 1676 (U in An790177, C in An789726), and a second at position 1856 (G in An790177, U in An789726) that caused an amino acid change in the translated protein sequence of K or N at position 611 in the polyprotein.

Phylogenetic analysis

To determine the phylogenetic relationship of the newly sequenced isolates within the Simbu serogroup, we compared

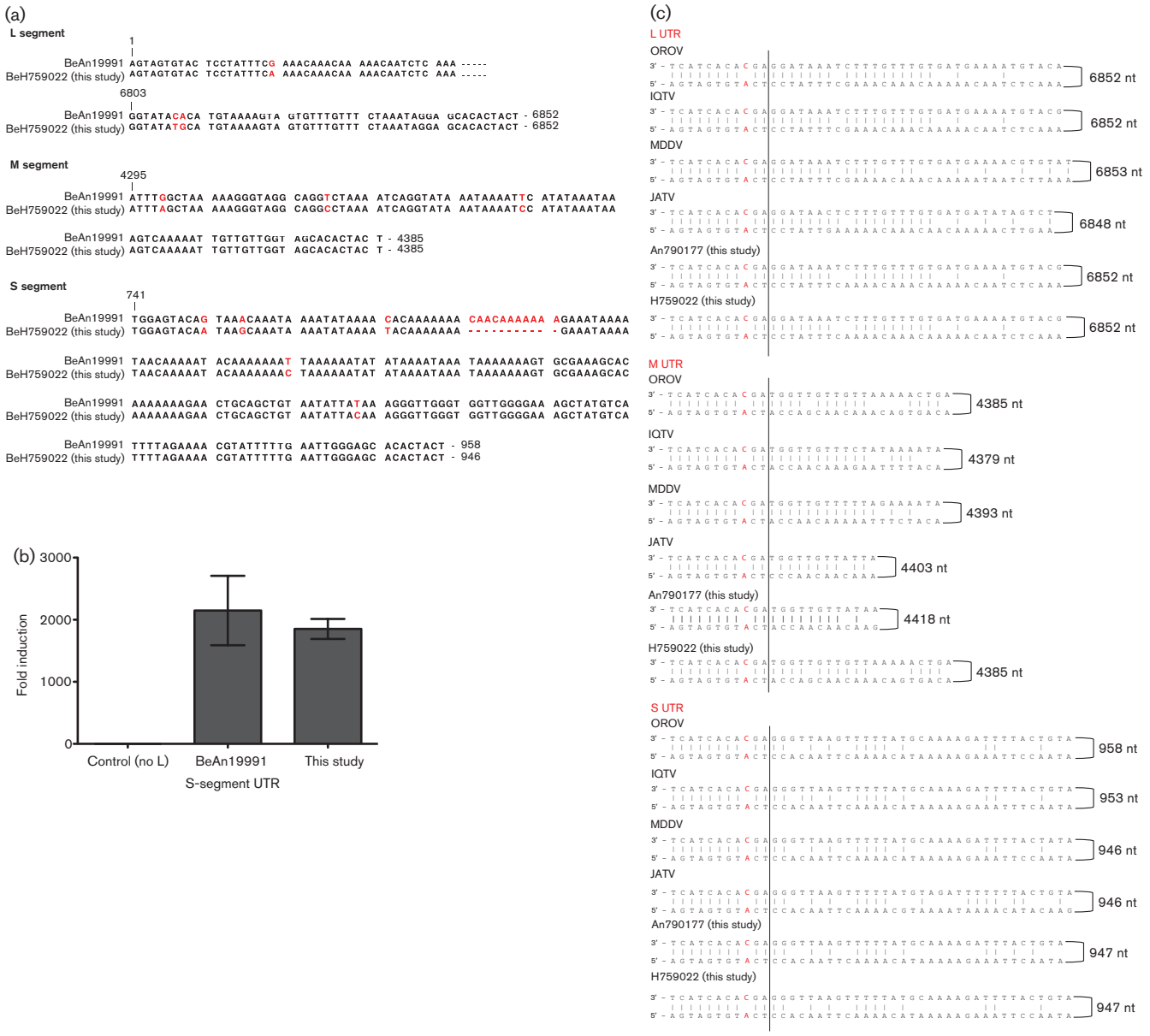

Fig. 2. Comparison of UTR sequences. (a) Comparison of the UTRs of BeH759022 isolate (chosen as a representative of the clinical isolates) with OROV strain BeAn19991. The bases in red highlight differences between BeAn19991 and BeH759022. (b) Minigenome assay. Comparison of S-segment-based minigenomes containing the S UTR of OROV BeAn19991 or the S UTR of the newly sequenced isolates. BSR-T7/5 cells were transfected with pTM1OROV-L and pTM1OROV-N plasmids expressing the L and N proteins, respectively, in addition to an S-segment-minigenome-expressing plasmid and pTM1-FF-Luc expressing firefly luciferase as an internal control. The control cells lacked pTM1OROV-L. Minigenome activity was expressed as fold induction over the background control. (c) Comparison of the M-segment UTRs of the novel M segment (BeAn790177) with those of OROV, Iquitos virus (IQTV), Madre de Dios virus (MDDV) and JATV. The C/A mismatch is highlighted in red. The dotted line indicates the extent of the conserved terminal sequence.

all available Simbu serogroup virus sequences of the three structural genes, L, M polyprotein and N (Table S1, available in the online Supplementary Material). The eight Amapa state clinical isolates cluster as OROV strains for all L, M polyprotein and N genes (Fig. 3). Pairwise comparisons of the polymerase amino acid sequence for all 10 isolates revealed a pairwise *p*-distance of 2 % towards BeAn19991, but the closest relationship was with Iquitos virus (IQTV) L protein (Fig. 4a). The glycoprotein precursor of the eight clinical isolates had a pairwise *p*-distance value of 1 % towards BeAn19991 (Fig. 4a); however, with samples BeAn790177 and BeAn789726, the glycoprotein gene

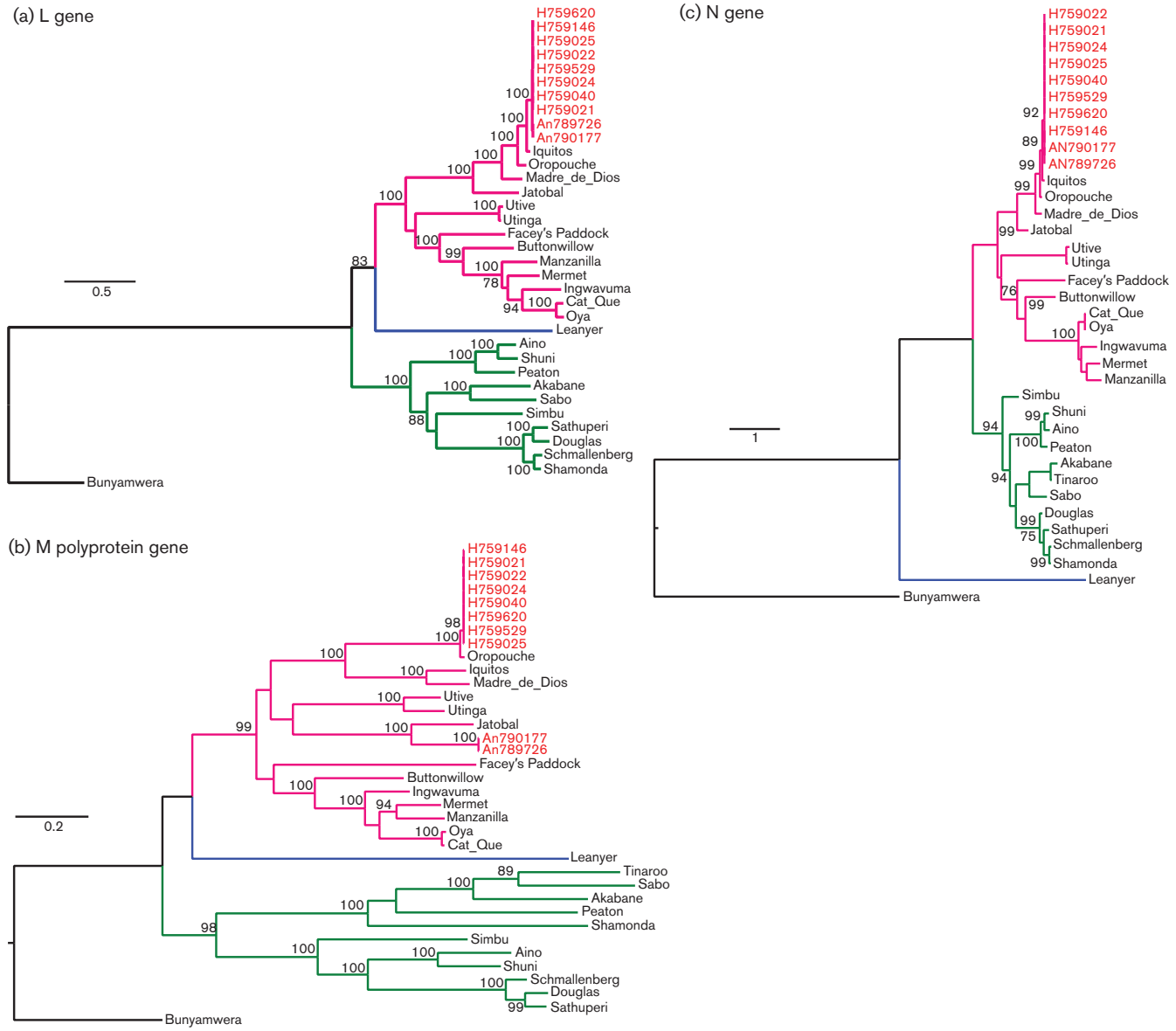

Fig. 3. Phylogenetic trees of the Simbu serogroup viruses. The trees were recreated using a maximum-likelihood method based on the general time reversible model (GTR) with five rate categories and assuming sites are evolutionary invariable, for the L gene (a), the GTR model with discrete gamma distribution for the M polyprotein gene (b) and the Tamura three-parameter model with discrete gamma distribution for the N gene (c). Bars, number of nucleotide substitutions per site. Positions with lower than 95 % site coverage were eliminated. Alignment and analysis were conducted in MEGA6 (Tamura *et al.*, 2013) and final trees were created using FigTree v.1.4.2.

clustered in a clade close to JATV (Fig. 3b) with an amino acid pairwise *p*-distance value of 21 % compared with 48–49 % with IQTV, OROV and Madre de Dios virus (MDDV) (Fig. 4a). A pairwise sliding-window analysis (Fig. 4b) of BeAn790177, IQTV (strain IQT9924), MDDV (strain FMD1303) and JATV (strain BeAn423380) was performed to analyse the level of similarity in the M polyprotein in comparison with OROV (strain BeAn19991). The highest level of similarity between OROV and BeAn790177 occurred between amino acid positions 1141 and 1341.

Genetic relationships among members of the species *Oropouche virus*

OROV showed two clearly identifiable clades for the L and M genes supported by high bootstrap and posterior probabilities (Fig. 5a, b). The trees were topologically different, especially with respect to the M gene of isolates BeAn790177 and BeAn789726, which clustered with high support with JATV (BeAn423380) (Fig. 5b). Interestingly, the Amapa clinical isolates in the L-gene tree clustered with IQTV (IQT9924)

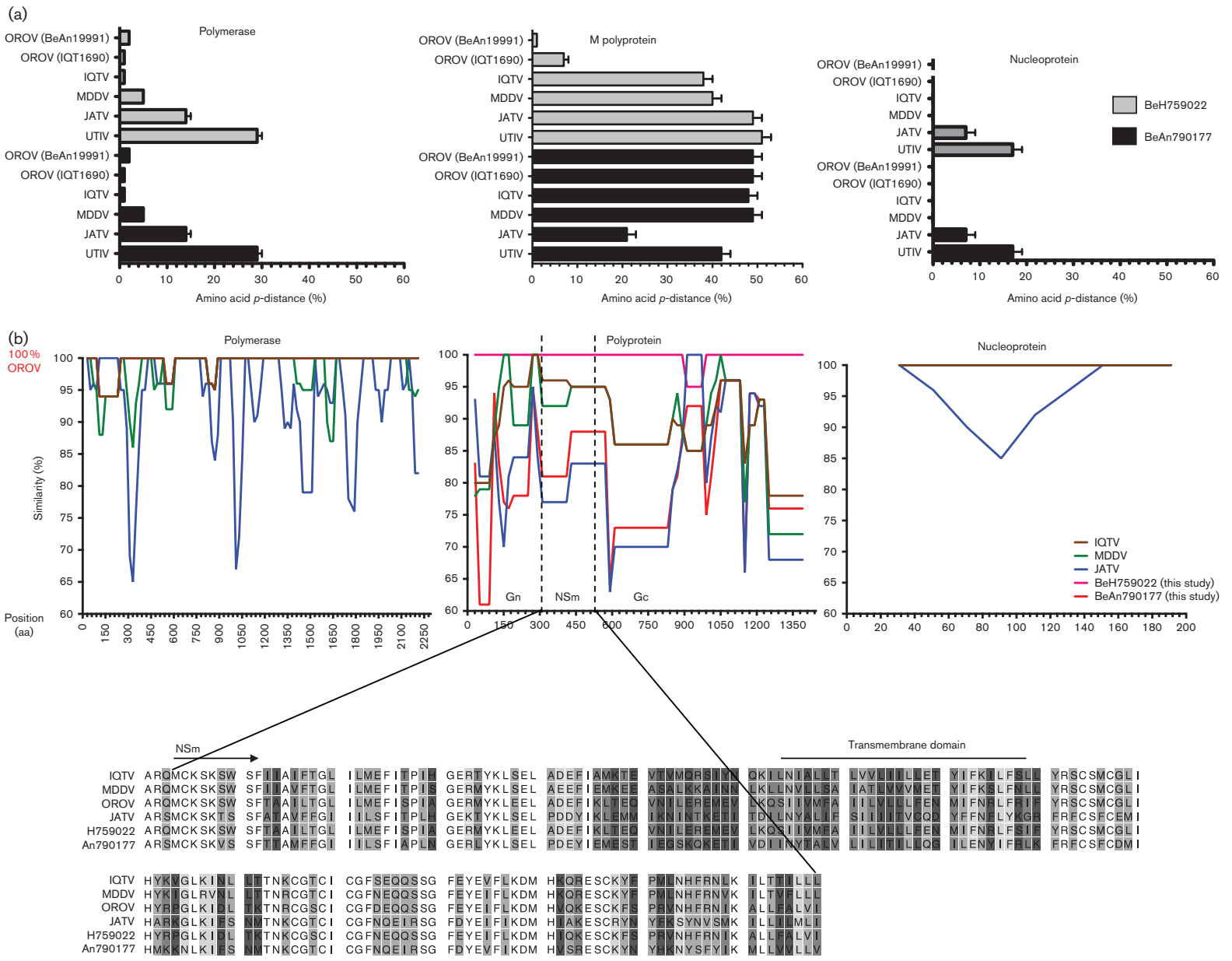

Fig. 4. Amino acid comparisons among viruses comprising the species *Oropouche virus*. (a) Pairwise amino acid *p*-distance scores of BeH759022 and BeAn790177 with *Oropouche virus* species and Utinga virus (UTIV). (b) M-segment deduced amino acid similarity plot using OROV as a query sequence and IQTV, MDDV, JATV and BeAn790177 as reference sequences.

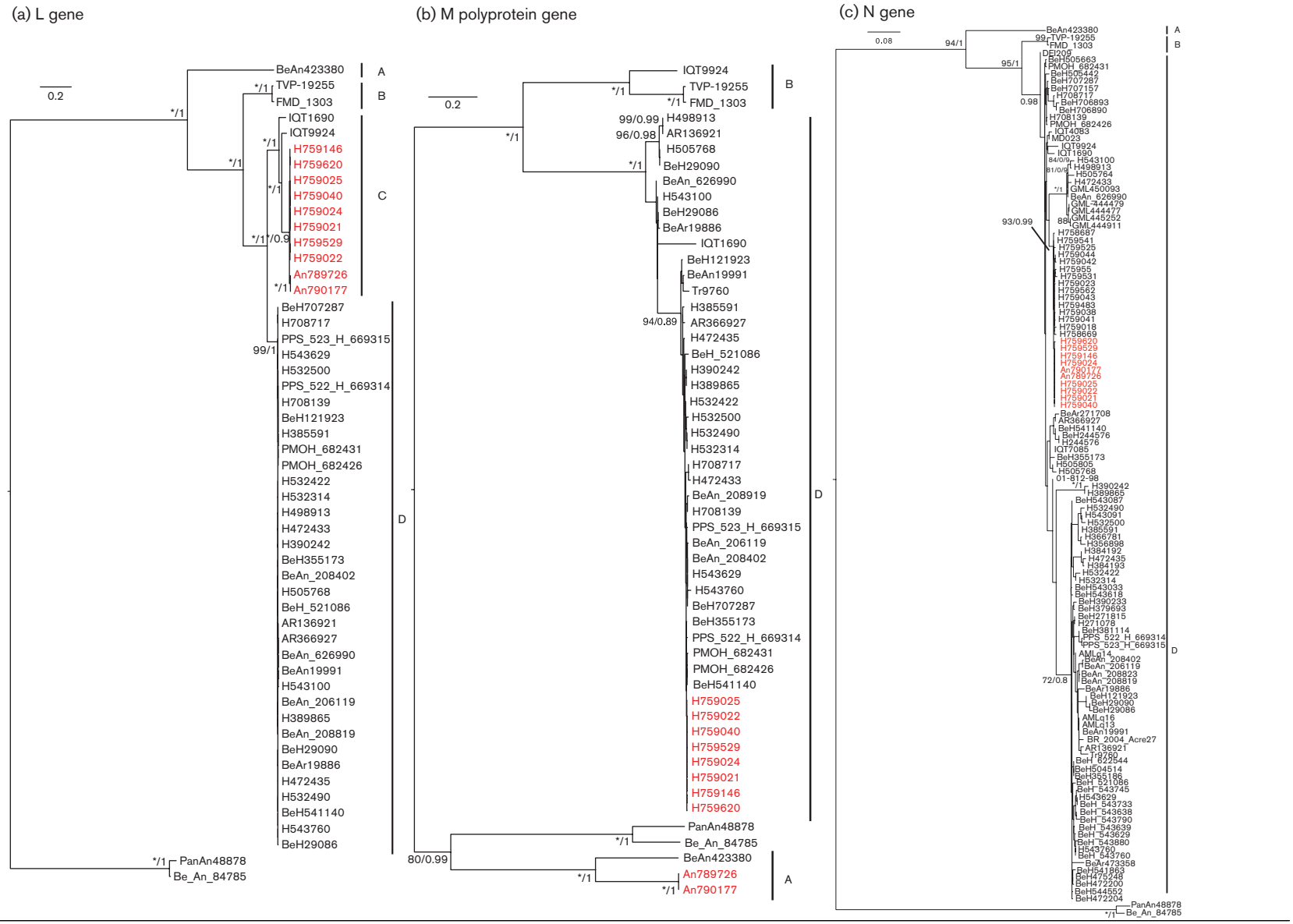

Fig. 5. Phylogenetic trees of viruses comprising members of the species *Oropouche virus*. (a) Maximum-likelihood phylogeny of the L gene with bootstrap support/Bayesian posterior probability shown on the branch. (b) Maximum-likelihood phylogeny of the M polyprotein gene with bootstrap support/Bayesian posterior probability shown on the branch. (c) Maximum-likelihood phylogeny of the N gene with bootstrap supports/Bayesian posterior probability shown on the branch. In (a)–(c), * represents 100 % bootstrap support. Isolates sequenced in this paper are highlighted in red. Full details of the strains used in this analysis are presented in Table S2. Bars, number of nucleotide substitutions per site. Clades A–D are indicated.

Table 2. Summary of RDP analysis to determine potential reassortant isolates

Reassortment event number	Breakpoint positions				Reassortment sequence(s)	Minor parental sequence(s)	Major parental sequence(s)	Detection method						
	In alignment		In reassortment sequence											
	Begin	End	Begin	End				RDP	GENECONV	Bootscan	Maxchi	Chimaera	SiSscan	3Seq
1	1	7481	1	7452	BeAn790177, BeAn789726	H759620, TVP-19255, H759040 FMD_1303, BeH759024, BeAn19991, BeH759146, BeH759021, BeH759025, BeH759529, BeH759022	BeAn423380	NS	5.47E−30	NS	9.21E−91	7.86E−67	3.35E−13	5.74E−27
2	7443	1	7416	1	IQT9924	Unknown (BeAn19991)	BeH759022, BeH759040, BeH759024, BeH759146, BeH759021, BeH759025, BeH759529, BeH759620	4.84E−13	2.40E−13	4.13E−12	2.43E−54	1.09E−44	2.51E−10	8.81E−20
3	7368	52	7341	52	BeH759024, BeH759040, BeH759146, BeH759021, BeH759025, BeH759529, BeH759022, BeH759620	BeAn19991	IQT1690	2.31E−57	1.15E−54	2.79E−58	6.96E−26	7.96E−25	5.79E−43	4.92E−48

Table 2. cont.

Reassortment event number	Breakpoint positions				Reassortment sequence(s)	Minor parental sequence(s)	Major parental sequence(s)	Detection method						
	In alignment		In reassortment sequence											
	Begin	End	Begin	End				RDP	GENECONV	Bootscan	Maxchi	Chimaera	SiSscan	3Seq
4	7469	6833	1361	728	BeH472433, BeH355173, BeAn_208402, PPS_522_H_669314, BeH543760, BeAn19991, BeH498913, BeAR366927, PPS_523_Be H_669315, BeH708139, BeH_521086, BeH543100, BeH472435, BeH543629, BeAn_208819, BeH707287, BeH708717, BeAr19886, BeAn626990, PMO Be H682426, BeAR136921, PMO BeH682431	BeH390242, BeH389865	IQT1690, BeAn789726, IQT9924, BeAn790177	2.18E−08	3.79E−08	9.52E−12	1.98E−12	1.33E−07	3.99E−16	1.56E−11

NS, Not significant.

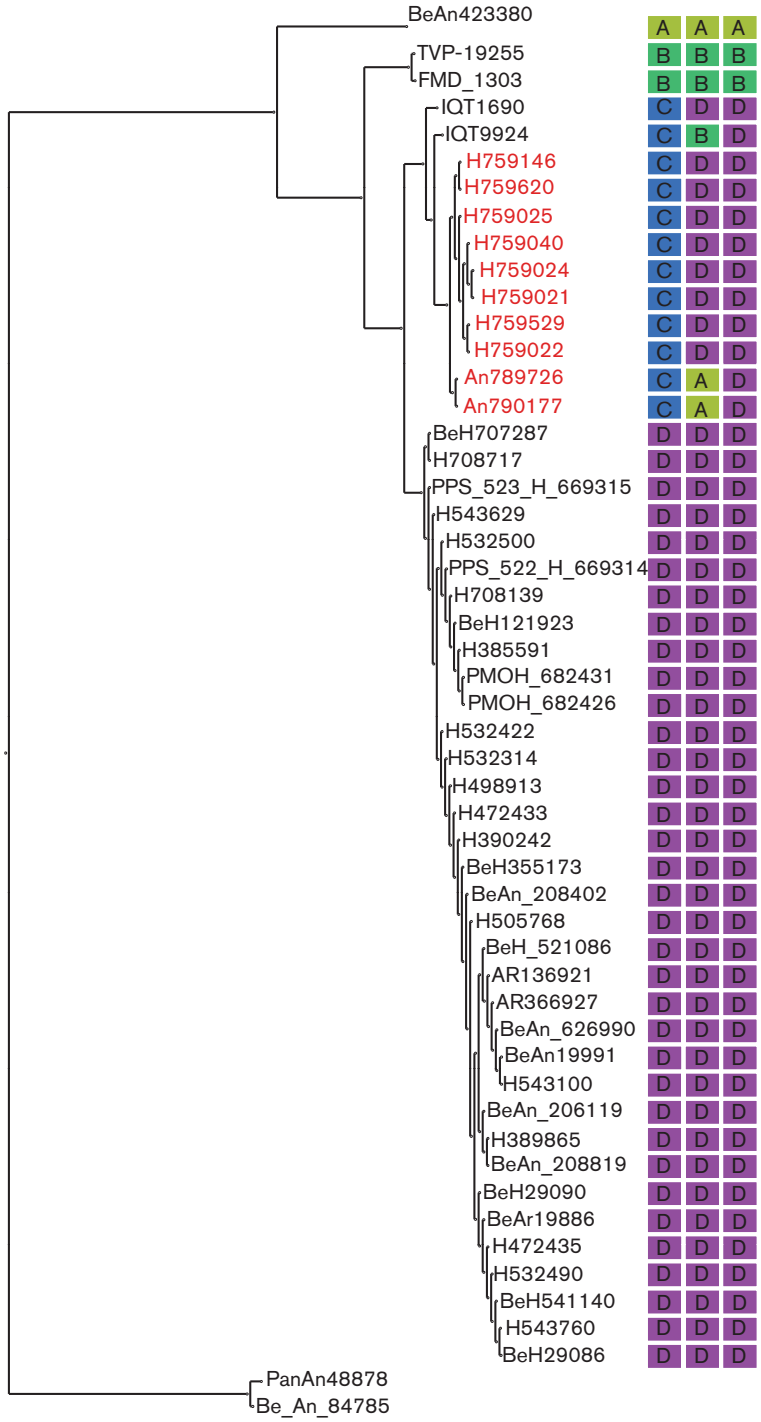

Fig. 6. Reassortment among viruses comprising the species *Oropouche virus*. Maximum-likelihood phylogeny of the L segment with each isolate annotated with their clade assignment (A–D) according to the L-, M- and S-segment phylogenies. The different patterns represent the different interclade reassortments: pattern 1, C-D-D; pattern 2, C-B-D; pattern 3, C-A-D; pattern 4, D. Isolates sequenced in this paper are highlighted in red.

and the Peruvian OROV isolate (IQT1690) with high bootstrap support and posterior probability (100 and 1, respectively) (Fig. 5a). The N-gene phylogeny on the other hand was less resolved, with most isolates belonging to a single clade and all being closely related (Fig. 5c). Using a dataset of concatenated genes for each isolate, analysis with the Recombination Detection Program (RDP) recognized four reassortment events with breakpoints close to the gene boundaries, with 33 isolates identified as reassortants (Table 2). Three of these reassortment events were well supported by the gene phylogenies and formed three different mosaic patterns: (i) IQT1690, BeH759021, BeH759022, BeH759024, BeH759025, BeH759040, BeH759146, BeH759529 and BeH759620; (ii) IQT9924; and (iii) BeAn790177 and BeAn789726. These isolates represented inter-clade reassortants (Fig. 6). The fourth reassortment event (Table 2)

suggested an intra-clade (D) reassortment, for which there was less phylogenetic support.

DISCUSSION

OROV causes a febrile illness in the South American human population, with more than half a million cases reported in Brazil in the last 59 years, and although the annual OROV incidence in the country is unknown, sporadic cases are constantly being picked up, making it a major public health problem. Recently, we corrected the complete genome of the Brazilian prototypic OROV reference strain BeAn19991 (Acrani *et al.*, 2014), a strain that was isolated originally from a pale-throated three-toed sloth (*Bradypus tridactylus*) in 1960 (Pinheiro *et al.*, 1981). In this study, we have described the complete genomic sequences for 10 field samples isolated more recently in Brazil (eight from humans and two from non-human primates), revealing new phylogenetic information on OROV. Phylogenetic analysis of the N gene of several OROV isolates carried out by Saeed *et al.* (2000), and subsequently by several other groups, classified OROV into four genotypes (Aguilar *et al.*, 2011; Azevedo *et al.*, 2007; Nunes *et al.*, 2005a, b; Vasconcelos *et al.*, 2009, 2011). However, the bootstrap values for this classification into four distinct genotypes did not give strong support, prompting us to reanalyse all available OROV sequences in GenBank, along with our newly sequenced field isolates. Our analysis revealed that the N-gene tree lacks structure and that the previously classified genotypes are not clearly distinguishable. The N gene is more conserved compared with the L and M genes where it is possible to distinguish two clades.

Vasconcelos *et al.* (2011) analysed the genetic evolution and dispersal of OROV in South America using samples from 1961 to 2009, the first study aimed at understanding the molecular epidemiology of this human pathogen. However, the results have to be treated with caution as the authors utilized only partial genetic information from each gene and not complete sequences. In the current analyses, complete sequences were analysed. We observed that the S segment 3′ UTR of the field isolates differed from that of BeAn19991 quite significantly (Fig. 2a; residues 781–791 were missing) in both the human and primate virus samples, which were isolated in different geographical regions and at different times (Table 1). For the M-segment UTRs, we noted that the field isolates differed from BeAn19991 at positions G4299A, T4319C and T4343C, whilst for the L segment the differences were observed at G20A, C6809T and A6810G. These findings highlight the need to consider UTR sequences, in addition to coding sequences, when trying to understand the evolutionary history of a virus. Advances in nucleotide sequencing technology mean that full-genome determination is now feasible on a routine basis. The loss of 11 residues in the S segment is intriguing, although it appeared to have no effect on the UTR function when analysed using our minigenome system (Acrani *et al.*, 2014) (Fig. 2b). Previous work, however, has demonstrated that internal deletions in the S-segment UTRs of Bunyamwera virus (BUNV) do not affect virus viability but do interfere with replication causing growth attenuation in cell culture (Lowen & Elliott, 2005). Similar results have also been shown for the BUNV M- and L-segment UTRs (Mazel-Sanchez & Elliott, 2012). The apparent natural deletion of these 11 residues could be important for virus replication efficiency and virus fitness, both *in vitro* and *in vivo*, and are worth pursuing further.

Another interesting finding was the identification of a novel Simbu serogroup virus M segment, in samples BeAn790177 and BeAn789726, obtained from the primate *Callithrix penicillata*. These viruses were isolated in Minas Gerais state, south-east Brazil, 7 years after OROV was first described in this area (Nunes *et al.*, 2005a). Interestingly, the OROV isolate (BeAn626990, GenBank accession no. AY117135) described by Nunes *et al.* (2005a) was also isolated from *Callithrix penicillata*. The S segment of BeAn626990 had a 92 % pairwise sequence identity to the S segments of BeAn790177 and BeAn789726, and clustered separately in the phylogenetic tree (Fig. 5c). L and M sequence information for sample BeAn626990 is currently unavailable, but this virus was identified as OROV based on complement fixation tests that measure antibody responses against the N protein, similar to the way in which the viruses in this study were initially identified as OROV isolates. The fact that OROV has been detected in the area twice is of concern, as it would suggest that the virus is stably circulating in the marmoset population in a region where currently OROV or other Simbu virus outbreaks have not been reported. For epidemiological and phylogenetic research purposes, sequencing of all three segments is crucial so that reassortants such as this are detected. Genetic reassortment is common among segmented viruses such as bunyaviruses (Briese *et al.*, 2013). IQTV and MDDV, both isolated from febrile patients in Peru in 1999 and 2007, respectively, contain L and S segments highly similar to those of OROV, but with M segments that cluster further away from OROV in a sister clade (Aguilar *et al.*, 2011; Briese *et al.*, 2013; Ladner *et al.*, 2014). The L and S segments of the primate-derived virus in this report revealed a similar level of nucleotide identity to that of OROV and IQTV, whilst the M segment was unique and clustered close to JATV. JATV was originally isolated in 1985 from a ring-tailed coati (*Nasua nasua*) in Para, Brazil (Figueiredo & Da Rosa, 1988). In 2001, the S and M segments of JATV were sequenced, classifying this virus as a potential OROV reassortant based on the fact that its N and NSs proteins encoded by the S segment were highly similar to OROV isolates from Peru and that its M segment was unique (Saeed *et al.*, 2001). Recent deep sequencing on the same JATV virus stock now suggests that the S, M and L segments of JATV are more divergent from OROV than initially thought (Ladner *et al.*, 2014). Based on our genetic analysis of the BeAn790177 and BeAn789726 M segments and the significant distance to OROV, IQTV, MDDV and JATV, we propose naming this isolate Perdões virus, after the municipality in which it was isolated.

In this study, we classified the viruses currently comprising the species *Oropouche virus* into clades A, B and D. IQTV fell into its own clade C for the L gene; however, it clustered in clades B and D for the M and N genes, respectively (Fig. 6). In a recent analysis of the species *Manzanilla* and *Oropouche virus*, Ladner *et al.* (2014) suggested that Manzanilla and Utinga viruses could be thought of as distinct strains of a single virus owing to the level of genetic similarity among current members. The authors suggest that this may not be applicable to the species *Oropouche virus* due to the level of M segment differences (Table S3). However, it is possible that these viruses also represent different strains of the same virus but with a higher degree of M-segment divergence. Unlike the L- and S-segment-encoded proteins that function together in RNA synthesis and hence potentially co-evolve together, the M segment codes for the Gc and Gn envelope glycoproteins that are entry binding proteins as well as being major antigenic targets. Selective pressure to produce viable virus in different host species and in different geographical settings could potentially result in higher levels of variation in the M segment. If this were true, we would assume that the non-structural NSm ORF would remain more conserved, and would expect a higher level of variation in the Gn and Gc proteins. It is also interesting to note that most bunyavirus reassortants tend to contain M segments from as-yet-unknown donors (Briese *et al.*, 2013). Pairwise, sliding-window distance analysis of OROV (BeAn19991) and the possible reassortants IQTV, MDDV, JATV and Perdões virus (BeAn790177) indicated an almost equidistant position between IQTV and MDDV, and between the more distant JATV and BeAn790177, with the lowest similarity scores in the N terminus of Gn protein (positions 1–200, Fig. 4b). The similarity pattern for the NSm and Gc ORFs was constant, maintaining the distance between IQTV/MDDV and JATV/An790177 almost unchanged until residue 950, where a sudden variation of sequence divergence could suggest possible recombination. From residues 950 to 1200, we observed a higher degree of variation within a single viral genome for each virus, with a higher percentage of divergence when compared with the rest of the protein. However, this was the region with the highest degree of similarity among all four viral sequences (except OROV), in contrast to what is observed in the rest of the protein, which could suggest that this particular region is subjected to more selective pressure and prone to a higher degree of conservation. It could also suggest that at some point during evolution they all shared the same sequence with a common ancestor, and the distribution to different geographical regions, such as Brazil (Pará, Amazonas, Acre, Rondônia, Amapá Maranhão, Tocantins, Minas Gerais), Peru and Venezuela, to different hosts (humans, *Bradypus trydactulus*, *Callithrix* sp. and wild birds) and to different invertebrate vectors (*Culicoides paraensis*, *Culex quinquefasciatus*, *Coquillettidia venezuelensis* and *Ochlerotatus serratus*) allowed a higher degree of variation through natural selection in the whole M segment, but not in this region, nor in the S and L segments (Baisley *et al.*, 1998; Nunes *et al.*, 2005a; Pinheiro *et al.*, 1982; Vasconcelos *et al.*, 2009). This analysis of the amino acid sequences could suggest that these five viruses are all variants of a single species, contrary to the proposal of Ladner *et al.* (2014) based on the nucleotide sequence. It is interesting that the two viruses closer to OROV (IQTV and MDDV) are human isolates, whilst the ones more distant in this analysis were isolated from animals (JATV and An790177), potentially explaining the different selective pressure and the degree of similarity among these viruses. Whatever the case, OROV, at least for now, is more successful as a human pathogen, and further surveillance of orthobunyaviruses in South America could potentially shed more light on the evolution of the species *Oropouche virus*.

METHODS

Cells and virus. Vero-E6 cells were grown in Dulbecco's modified Eagle's medium supplemented with 10 % FCS. BSR-T7/5 cells that stably express bacteriophage T7 RNA polymerase (Buchholz *et al.*, 1999) were supplied by K. K. Conzelmann (Max von Pettenkofer-Institute, Munich, Germany) and were grown in Glasgow minimal essential medium supplemented with 10 % tryptose phosphate broth, 10 % FCS and 1 mg G418 ml^{-1}. Samples used in this study were obtained from the World Health Organization Reference Centre for Arboviruses at the Department of Arbovirology and Hemorrhagic Fevers, Instituto Evandro Chagas (Ananindeua, Brazil). The eight clinical strains of OROV were obtained originally from human patients in 2009 in the municipality of Mazagao, Amapa state, northern Brazil, and had previously been passaged three times in Vero-E6 cells. Viral isolates PR4843 BeAN790177 and PR4837 BeAN789726 were isolated from liver samples collected from two separate *Callithrix penicillata* found dead in the municipality of Perdões, Minas Gerais state, in 2012. A suspension of monkey viscera prepared with PBS (pH 7.4) and antibiotics (penicillin and streptomycin) was used to inject suckling mice (*Mus musculus*) via the intracranial route. Animals were observed daily and collected immediately when disease was evident. A suspension of mouse brain in PBS was then used to infect Vero-E6 cells and virus was harvested 72 h post-infection. Table 1 and Fig. 1 describe the viral isolates used in the study and the geographical locations.

All experiments with infectious viruses were conducted under Biosafety Level 3 conditions.

RNA extraction, and genome sequencing and assembling. Virus was harvested and filtered through a 0.2 μm sterile filter and concentrated using polyethylene glycol 8000. The virus aggregate was resuspended in 500 μl PBS and treated with 25 U μl^{-1} Benzonase (Novagen) for 30 min at 37 °C. RNA was extracted using TRIzol reagent (Invitrogen) according to the manufacturer's protocol and quantified on a Qubit 2.0 Fluorometer (Invitrogen). The genomes were obtained using the following basic steps: (i) cDNA synthesis using random primers (cDNA Synthesis kit; Roche Life Science); (ii) library preparation (second-strand cDNA synthesis and emulsion PCR); and (iii) nucleotide sequencing using both GS FLX 454 (Roche Life Science) and Ion Torrent (Life Technologies) as described previously (Margulies *et al.*, 2005; Rothberg *et al.*, 2011). The SSF (Standard Flowgram Format) files generated by the GS FLX 454 and Ion Torrent machines containing the sequencing trace data were transferred onto a Linux-based computer for analysis. *De novo* DNA sequence assemblers Newbler v.2.6 (GS Assembler, 454 sequencing, Roche) and Celera were used to assemble reads. Adaptors were first trimmed from generated reads and then assembled to generate contigs. These contigs were then compared against sequences in

GenBank by performing a BLASTX search. Using the top hit generated by BLASTX as a reference sequence, reads were assembled against this to generate more contigs using GS Reference Mapper Software (Roche). Parameters were left at default. Sequences were evaluated for homopolymers before attempting to fill gaps in the genome by the mapping reference method in CLC Genomics Workbench 6 (CLC bio). Scaffold sequences from a consensus of reads and contigs were generated and evaluated before generating the final genome sequence.

Sanger sequencing. Sufficient reads could not be generated to complete the L and M segments of samples BeH759024, BeH759529, BeH759620 and BeH759146, and so the incomplete regions were sequenced via Sanger sequencing. Briefly, reverse transcription-PCR was performed using 10 µl TRIzol-extracted RNA and segment-specific forward or reverse primers, with Moloney murine leukemia virus (M-MLV) reverse transcriptase (Promega). PCR was carried out using KOD Hot Start DNA polymerase (Merck) and the amplified products were purified from agarose gel using a gel extraction kit (Wizard kit; Promega), following the manufacturer's protocol. Entire M segments were amplified using previously described primers OROVMFg and OROVMRg (Acrani *et al.*, 2014) and products were directly sequenced (Table S4). The L segments were amplified as two separate fragments as described previously for BeAN19991 (Acrani *et al.*, 2014) [primers OROVLFg and Ama3082LR (this study), Ama2930LF (this study) and OROVLRg]. Products were cloned separately into the pGEM-T Easy cloning vector and nucleotide sequences were determined using the T7 F and SP6 primers in the first genome walking reaction (Table S4).

Sequencing the viral 5′ and 3′ termini. As described previously (Acrani *et al.*, 2014), total cellular RNA from cells infected with the virus was extracted using TRIzol reagent (Invitrogen) at 48 h post-infection. Both the genomic and anti-genomic 3′ ends were obtained by RACE analysis. RNA was polyadenylated (Ambion) for 1 h at 37 °C and then purified using an RNeasy mini kit (Qiagen). Twelve microlitres of this polyadenylated RNA was then used in a reverse transcription reaction with M-MLV reverse transcriptase (Promega) and Oligo d(T)-Anchor primer (Table S4), followed by a PCR using a PCR Anchor primer and a segment-specific primer (Table S4) with KOD Hot Start DNA polymerase (Merck). Amplified products were gel extracted and purified using a gel extraction kit (Promega Wizard kit), followed by Sanger sequencing.

RNA ligation was carried out by denaturing the RNA at 90 °C for 3 min, and the 3′ and 5′ ends were then ligated using T4 RNA ligase (New England Biolabs) for 2 h at 37 °C. The reaction was heat inactivated at 65 °C and purified using an RNeasy Mini kit (Qiagen). cDNA was synthesized using M-MVL reverse transcriptase (Promega) and primer OROSlig1 (Table S4). PCR was performed using KOD Hot Start DNA polymerase (Merck) and primers OROSlig1 and OROSlig2 (Table S4). The PCR products were gel purified and their nucleotide sequences determined.

Minigenome assay. The OROV minigenome assay was performed as described previously (Acrani *et al.*, 2014). In brief, subconfluent monolayers of BSR-T7/5 cells in 24-well plates were transfected with 250 ng expression plasmids pTM1OROV-L and pTM1OROV-N, 125 ng S-segment-based minigenome plasmid and 25 ng pTM1-FF-Luc (Weber *et al.*, 2001). At 24 h post-transfection, *Renilla* and firefly luciferase activities were measured using a Dual-Luciferase Reporter Assay kit (Promega).

Phylogenetic analysis. Phylogenetic analysis of the 10 isolate sequences was first conducted with available Simbu serogroup viruses (Table S1). The L-, M- and S-segment coding regions were aligned using the MUSCLE algorithm in MEGA6.06 (Tamura *et al.*, 2013). A model test was then performed on this alignment, and the best DNA substitution model was used to generate the phylogenetic trees for the L, glycoprotein and N ORFs using a maximum-likelihood method in MEGA6.06 (Tamura *et al.*, 2013), with 1000 bootstrap replicates. Final trees were recreated using FigTree v.1.4.2. Furthermore, a separate analysis of all 10 isolates along with all OROV isolates was conducted. For this, all OROV sequences were downloaded from GenBank and compiled to include a single sequence for each isolate. Each gene segment was aligned according to the protein alignment using CLUSTAL Omega (Sievers *et al.*, 2011) and PAL2NAL (Suyama *et al.*, 2006). Phylogenetic analyses were reconstructed using the general time reversible (GTR) + GAMMA + I substitution model as selected by the Bayesian Information Criterion (BIC) in jModeltest (Darriba *et al.*, 2012). Maximum-likelihood phylogenies were generated in Phyml (Guindon *et al.*, 2010) using 1000 bootstrap replicates and Bayesian tree reconstruction was carried out using MrBayes (Ronquist & Huelsenbeck, 2003) across four chains for 2 million generations sampling every 100 generations, and stationarity was determined from examination of the log likelihoods and the convergence diagnostics. Trees recovered prior to stationarity being reached were discarded, and Bayesian posterior probabilities of each bipartition, representing the percentage of times each node was recovered, were calculated from a 50 % majority rule consensus of the remaining trees.

Reassortant and genetic divergence analysis. To examine reassortment, all genes were concatenated for isolates that had complete genomes and the concatenated alignment was analysed in RDP3 (Martin *et al.*, 2010) using the various built-in recombination analysis methods. Genetic distances were calculated at the amino acid level using a pairwise *p*-distance method with complete deletion in MEGA6.06 (Tamura *et al.*, 2013). A pairwise sliding-window analysis for the M segment at the amino acid level was performed using SimPlot v.3.5.1 (Lole *et al.*, 1999). Using a 200 bp window, 20 bp step, Kimura (two-parameter) and 1000 bootstrap replications, results were plotted in Prism 6.2.

ACKNOWLEDGEMENTS

We thank João Vianez and Jedson Cardoso for their assistance in *de novo* genome assembly. We thank Clayton Lima, Janaina M. Vasconcelos and Layanna Oliveira for their assistance with the Ion torrent. This work was supported by a Wellcome Trust Senior Investigator Award to R. M. E (99220), and a Medical Research Council postgraduate studentship (1101085) and a Medical Research Council Centenary Award for Early Career Researchers to N. L. T.-L. M. R. T. N was supported by CNPq grant no. 302032/2011-8.

REFERENCES

Acrani, G. O., Tilston-Lunel, N. L., Spiegel, M., Weidemann, M., Dilcher, M., Andrade da Silva, D. E., Nunes, M. R. T. & Elliott, R. M. (2014). Establishment of a minigenome system for Oropouche virus reveals the S genome segment to be significantly longer than reported previously. *J Gen Virol* **96**, 513–523.

Aguilar, P. V., Barrett, A. D., Saeed, M. F., Watts, D. M., Russell, K., Guevara, C., Ampuero, J. S., Suarez, L., Cespedes, M. & other authors (2011). Iquitos virus: a novel reassortant *Orthobunyavirus* associated with human illness in Peru. *PLoS Negl Trop Dis* **5**, e1315.

Anderson, C. R., Spence, L., Downs, W. G. & Aitken, T. H. (1961). Oropouche virus: a new human disease agent from Trinidad, West Indies. *Am J Trop Med Hyg* **10**, 574–578.

Azevedo, R. S. S., Nunes, M. R. T., Chiang, J. O., Bensabath, G., Vasconcelos, H. B., Pinto, A. Y. N., Martins, L. C., Monteiro, H. A. O.,

Rodrigues, S. G. & Vasconcelos, P. F. (2007). Reemergence of Oropouche fever, northern Brazil. *Emerg Infect Dis* **13**, 912–915.

Baisley, K. J., Watts, D. M., Munstermann, L. E. & Wilson, M. L. (1998). Epidemiology of endemic Oropouche virus transmission in upper Amazonian Peru. *Am J Trop Med Hyg* **59**, 710–716.

Borborema, C. A., Pinheiro, F. P., Albuquerque, B. C., da Rosa, A. P., da Rosa, J. F. & Dourado, H. V. (1982). [1st occurrence of outbreaks caused by Oropouche virus in the State of Amazonas]. *Rev Inst Med Trop Sao Paulo* **24**, 132–139 (in Portuguese).

Briese, T., Calisher, C. H. & Higgs, S. (2013). Viruses of the family *Bunyaviridae*: are all available isolates reassortants? *Virology* **446**, 207–216.

Buchholz, U. J., Finke, S. & Conzelmann, K. K. (1999). Generation of bovine respiratory syncytial virus (BRSV) from cDNA: BRSV NS2 is not essential for virus replication in tissue culture, and the human RSV leader region acts as a functional BRSV genome promoter. *J Virol* **73**, 251–259.

Darriba, D., Taboada, G. L., Doallo, R. & Posada, D. (2012). jModelTest 2: more models, new heuristics and parallel computing. *Nat Methods* **9**, 772.

Dixon, K. E., Travassos da Rosa, A. P., Travassos da Rosa, J. F. & Llewellyn, C. H. (1981). Oropouche virus. II. Epidemiological observations during an epidemic in Santarém, Pará, Brazil in 1975. *Am J Trop Med Hyg* **30**, 161–164.

Dunn, E. F., Pritlove, D. C. & Elliott, R. M. (1994). The S RNA genome segments of Batai, Cache Valley, Guaroa, Kairi, Lumbo, Main Drain and Northway bunyaviruses: sequence determination and analysis. *J Gen Virol* **75**, 597–608.

Elliott, R. M. (2014). Orthobunyaviruses: recent genetic and structural insights. *Nat Rev Microbiol* **12**, 673–685.

Elliott, R. M. & Blakqori, G. (2011). Molecular biology of orthobunyaviruses. In *Bunyaviridae: Molecular and Cellular Biology*, pp. 1–39. Edited by A. Plyusnin & R. M. Elliott. Norfork, UK: Caister Academic Press.

Figueiredo, L. T. M. & Da Rosa, A. P. A. T. (1988). Jatobal virus antigenic characterization by ELISA and neutralization test using EIA as indicator, on tissue culture. *Mem Inst Oswaldo Cruz* **83**, 161–164.

Guindon, S., Dufayard, J. F., Lefort, V., Anisimova, M., Hordijk, W. & Gascuel, O. (2010). New algorithms and methods to estimate maximum-likelihood phylogenies: assessing the performance of PhyML 3.0. *Syst Biol* **59**, 307–321.

Ladner, J. T., Savji, N., Lofts, L., Travassos da Rosa, A., Wiley, M. R., Gestole, M. C., Rosen, G. E., Guzman, H., Vasconcelos, P. F. & other authors (2014). Genomic and phylogenetic characterization of viruses included in the Manzanilla and Oropouche species complexes of the genus *Orthobunyavirus*, family *Bunyaviridae*. *J Gen Virol* **95**, 1055–1066.

LeDuc, J. W., Hoch, A. L., Pinheiro, F. P. & da Rosa, A. P. (1981). Epidemic Oropouche virus disease in northern Brazil. *Bull Pan Am Health Organ* **15**, 97–103.

Lole, K. S., Bollinger, R. C., Paranjape, R. S., Gadkari, D., Kulkarni, S. S., Novak, N. G., Ingersoll, R., Sheppard, H. W. & Ray, S. C. (1999). Full-length human immunodeficiency virus type 1 genomes from subtype C-infected seroconverters in India, with evidence of intersubtype recombination. *J Virol* **73**, 152–160.

Lowen, A. C. & Elliott, R. M. (2005). Mutational analyses of the nonconserved sequences in the Bunyamwera Orthobunyavirus S segment untranslated regions. *J Virol* **79**, 12861–12870.

Margulies, M., Egholm, M., Altman, W. E., Attiya, S., Bader, J. S., Bemben, L. A., Berka, J., Braverman, M. S., Chen, Y.-J. & other authors (2005). Genome sequencing in microfabricated high-density picolitre reactors. *Nature* **437**, 376–380.

Martin, D. P., Lemey, P., Lott, M., Moulton, V., Posada, D. & Lefeuvre, P. (2010). RDP3: a flexible and fast computer program for analyzing recombination. *Bioinformatics* **26**, 2462–2463.

Mazel-Sanchez, B. & Elliott, R. M. (2012). Attenuation of bunyamwera orthobunyavirus replication by targeted mutagenesis of genomic untranslated regions and creation of viable viruses with minimal genome segments. *J Virol* **86**, 13672–13678.

Nunes, M. R. T., Martins, L. C., Rodrigues, S. G., Chiang, J. O., Azevedo, R. S. S., Travassos da Rosa, A. P. A. & Vasconcelos, P. F. C. (2005a). Oropouche virus isolation, southeast Brazil. *Emerg Infect Dis* **11**, 1610–1613.

Nunes, M. R. T., Travassos da Rosa, A. P. A., Weaver, S. C., Tesh, R. B. & Vasconcelos, P. F. C. (2005b). Molecular epidemiology of group C viruses (*Bunyaviridae*, *Orthobunyavirus*) isolated in the Americas. *J Virol* **79**, 10561–10570.

Pinheiro, F. P., Pinheiro, M., Bensabath, G., Causey, O. R. & Shope, R. E. (1962). Epidemia de *vírus Oropouche* em Belém. *Rev Serv Especial Saude* **12**, 15–23.

Pinheiro, F. P., Travassos da Rosa, A. P., Travassos da Rosa, J. F. & Bensabath, G. (1976). An outbreak of Oropouche virus diease in the vicinity of Santarem, Para, Brazil. *Tropenmed Parasitol* **27**, 213–223.

Pinheiro, F. P., Hoch, A. L., Gomes, M. L. & Roberts, D. R. (1981). Oropouche virus. IV. Laboratory transmission by *Culicoides paraensis*. *Am J Trop Med Hyg* **30**, 172–176.

Pinheiro, F. P., Travassos da Rosa, A. P., Gomes, M. L., LeDuc, J. W. & Hoch, A. L. (1982). Transmission of Oropouche virus from man to hamster by the midge *Culicoides paraensis*. *Science* **215**, 1251–1253.

Roberts, D. R., Pinheiro, F. P., Hoch, A. L., LeDuc, J. W., Peterson, N. E., Santos, M. A. V., Western, K. A. & Pan American Health Organization Washington DC. (1977). *Vectors and natural reservoirs of Oropouche virus in the Amazon region.* Tech. Rep. NTIS 7815, US Dep. Commer Washington, DC: access. no. AD-A053.

Ronquist, F. & Huelsenbeck, J. P. (2003). MrBayes 3: Bayesian phylogenetic inference under mixed models. *Bioinformatics* **19**, 1572–1574.

Rothberg, J. M., Hinz, W., Rearick, T. M., Schultz, J., Mileski, W., Davey, M., Leamon, J. H., Johnson, K., Milgrew, M. J. & other authors (2011). An integrated semiconductor device enabling non-optical genome sequencing. *Nature* **475**, 348–352.

Saeed, M. F., Wang, H., Nunes, M., Vasconcelos, P. F., Weaver, S. C., Shope, R. E., Watts, D. M., Tesh, R. B. & Barrett, A. D. (2000). Nucleotide sequences and phylogeny of the nucleocapsid gene of Oropouche virus. *J Gen Virol* **81**, 743–748.

Saeed, M. F., Wang, H., Suderman, M., Beasley, D. W., Travassos da Rosa, A., Li, L., Shope, R. E., Tesh, R. B. & Barrett, A. D. (2001). Jatobal virus is a reassortant containing the small RNA of Oropouche virus. *Virus Res* **77**, 25–30.

Sievers, F., Wilm, A., Dineen, D., Gibson, T. J., Karplus, K., Li, W., Lopez, R., McWilliam, H., Remmert, M. & other authors (2011). Fast, scalable generation of high-quality protein multiple sequence alignments using Clustal Omega. *Mol Syst Biol* **7**, 539.

Suyama, M., Torrents, D. & Bork, P. (2006). PAL2NAL: robust conversion of protein sequence alignments into the corresponding codon alignments. *Nucleic Acids Res* **34** (Web Server issue), W609–W612.

Tamura, K., Stecher, G., Peterson, D., Filipski, A. & Kumar, S. (2013). MEGA6: Molecular Evolutionary Genetics Analysis version 6.0. *Mol Biol Evol* **30**, 2725–2729.

Vasconcelos, P. F. C., Travassos Da Rosa, J. F. S., Guerreiro, S. C., Dégallier, N., Travassos Da Rosa, E. S. & Travassos Da Rosa, A. P. A. (1989). [1st register of an epidemic caused by Oropouche

virus in the states of Maranhão and Goiás, Brazil]. *Rev Inst Med Trop Sao Paulo* **31**, 271–278 (in Portuguese).

Vasconcelos, H. B., Azevedo, R. S. S., Casseb, S. M., Nunes-Neto, J. P., Chiang, J. O., Cantuária, P. C., Segura, M. N. O., Martins, L. C., Monteiro, H. A. O. & other authors (2009). Oropouche fever epidemic in Northern Brazil: epidemiology and molecular characterization of isolates. *J Clin Virol* **44**, 129–133.

Vasconcelos, H. B., Nunes, M. R., Casseb, L. M., Carvalho, V. L., Pinto da Silva, E. V., Silva, M., Casseb, S. M. & Vasconcelos, P. F. (2011). Molecular epidemiology of Oropouche virus, Brazil. *Emerg Infect Dis* **17**, 800–806.

Weber, F., Dunn, E. F., Bridgen, A. & Elliott, R. M. (2001). The Bunyamwera virus nonstructural protein NSs inhibits viral RNA synthesis in a minireplicon system. *Virology* **281**, 67–74.

AMERICAN SOCIETY FOR MICROBIOLOGY | Journal of Virology

Generation of Recombinant Oropouche Viruses Lacking the Nonstructural Protein NSm or NSs

Natasha L. Tilston-Lunel,[a,b] Gustavo Olszanski Acrani,[a,c] Richard E. Randall,[b] Richard M. Elliott[a]†

MRC-University of Glasgow Centre for Virus Research, Glasgow, Scotland[a]; Biomedical Sciences Research Complex, University of St. Andrews, St. Andrews, Scotland[b]; Department of Cell and Molecular Biology, University of São Paulo School of Medicine, São Paulo, Brazil[c]

ABSTRACT

Oropouche virus (OROV) is a midge-borne human pathogen with a geographic distribution in South America. OROV was first isolated in 1955, and since then, it has been known to cause recurring outbreaks of a dengue-like illness in the Amazonian regions of Brazil. OROV, however, remains one of the most poorly understood emerging viral zoonoses. Here we describe the successful recovery of infectious OROV entirely from cDNA copies of its genome and generation of OROV mutant viruses lacking either the NSm or the NSs coding region. Characterization of the recombinant viruses carried out *in vitro* demonstrated that the NSs protein of OROV is an interferon (IFN) antagonist as in other NSs-encoding bunyaviruses. Additionally, we demonstrate the importance of the nine C-terminal amino acids of OROV NSs in IFN antagonistic activity. OROV was also found to be sensitive to IFN-α when cells were pretreated; however, the virus was still capable of replicating at doses as high as 10,000 U/ml of IFN-α, in contrast to the family prototype BUNV. We found that OROV lacking the NSm protein displayed characteristics similar to those of the wild-type virus, suggesting that the NSm protein is dispensable for virus replication in the mammalian and mosquito cell lines that were tested.

IMPORTANCE

Oropouche virus (OROV) is a public health threat in Central and South America, where it causes periodic outbreaks of dengue-like illness. In Brazil, OROV is the second most frequent cause of arboviral febrile illness after dengue virus, and with the current rates of urban expansion, more cases of this emerging viral zoonosis could occur. To better understand the molecular biology of OROV, we have successfully rescued the virus along with mutants. We have established that the C terminus of the NSs protein is important in interferon antagonism and that the NSm protein is dispensable for virus replication in cell culture. The tools described in this paper are important in terms of understanding this important yet neglected human pathogen.

Bunyaviruses form a large group of single-stranded negative-sense RNA viruses consisting of important human and veterinary pathogens, such as the recently emerged severe fever with thrombocytopenia syndrome virus (SFTSV) and Schmallenberg virus (SBV). The family is divided into genera *Hantavirus*, *Nairovirus*, *Phlebovirus*, *Tospovirus*, and the largest genus *Orthobunyavirus*, to which Oropouche virus (OROV) belongs (1, 2). OROV causes an acute febrile illness in humans, with signs and symptoms of fever, headache, malaise, myalgia, arthralgia, photophobia, nausea, vomiting, dizziness, and in some cases encephalitis and meningitis. Symptoms last between 2 and 7 days, with some patients reporting a recurrence of these symptoms (3–10). OROV is transmitted among humans via the biting midge *Culicoides paraensis* and is maintained in the wild by circulating in nonhuman primates, such as the pale-throated three-toed sloth (*Bradypus tridactylus*) and the black-tufted marmoset (*Callithrix penicillata*), though the vectors remain largely unknown (3–5, 10–12). Laboratory experiments and epidemiological surveys have reported that mosquitoes *Aedes serratus*, *Aedes scapularis*, *Aedes albopictus*, *Culex fatigans*, *Culex quiquefaciatus*, *Coquilettidia venezuelensis*, and *Psorophora ferox* are susceptible to OROV infection (13–16). Neutralizing antibodies against OROV have also been detected in both wild and domestic birds (10, 14, 15), leading to speculation that birds could be carriers of the virus (A. Barrett, University of Texas Medical Branch, personal communication).

Oropouche fever (OROF) outbreaks have mainly been reported in Brazil's Amazonian cities. OROV, however, was first recorded in Trinidad in 1955 (13). In Brazil, the virus was isolated in 1960 from a dead sloth found near one of the Belem-Brasilia highway construction sites. The following year (1961), in Belem, 11,000 people were reported ill in what became the first OROF outbreak (17). Between 1961 and 2009, over 30 OROF outbreaks were recorded, with an estimated 500,000 cases (13, 17, 18). Outside of Brazil, OROF was reported for the first time in Panama in 1989 and Peru in 1992. The geographic distribution of OROV today includes Brazil, Panama, Peru, and Argentina. Serological evidence suggests that the virus may also be circulating in Ecuador and Bolivia and in nonhuman primates in Colombia (7, 18–23). However, without a differential surveillance system to distinguish infections with similar clinical symptoms, such as OROV and den-

Received 9 November 2015 **Accepted** 15 December 2015

Accepted manuscript posted online 23 December 2015

Citation Tilston-Lunel NL, Acrani GO, Randall RE, Elliott RM. 2016. Generation of recombinant Oropouche viruses lacking the nonstructural protein NSm or NSs. J Virol 90:2616–2627. doi:10.1128/JVI.02849-15.

Editor: B. Williams

Address correspondence to Natasha L. Tilston-Lunel, natasha.tilston@gmail.com.

† Deceased.

N.L.T.-L. and G.O.A. contributed equally to this article.

Supplemental material for this article may be found at http://dx.doi.org/10.1128/JVI.02849-15.

TABLE 1 Oligonucleotides used in this study

Primer	Sequence (5′→3′)	Plasmid
delNSmOROVR	TCCTGCAATTGGTGAGATGAATTC	pTVTOROVdelNSm
delNSmOROVF	GATGAAGATTGCTTATCTAAAGAT	pTVTOROVdelNSm
OROV48NSsF	CAGCATATGTAGCATTTGAAGCTAGATACG	pTVTOROV48delNSs
OROV48NSsR	CGTATCTAGCTTCAAATGCTACATATGCTG	pTVTOROV48delNSs
OROV246NSsF	CGGACAACGGTCTAACCCTGCACCGTCTGT	pTVTOROV246NSs
OROV246NSsR	ACAGACGGTGCAGGGTTAGACCGTTGTCCG	pTVTOROV246NSs
OROVdelNSs2F	GAGTTCATTTTCAACGACGTACCACAACGGACTACATCTACATTTGATCCGGAGGCAG CATACGTAGCATTTGAAGC	pTVTOROVdelNSs2
OROVdelNSs2R	GCTTCAAATGCTACGTATGCTGCCTCCGGATCAAATGTAGATGTAGTCCGTTGTGGTA CGTCGTTGAAAATGAACTC	pTVTOROVdelNSs2

gue, chikungunya, and Mayaro fevers, the exact epidemiology of OROV in Central and South America remains unclear. OROV reassortant viruses have also been isolated in Peru and Venezuela and outside the epidemic zone within Brazil (24–26).

The lack of a reverse genetics system has, until now, limited research on OROV at a molecular level. In order to address this issue, we previously reported the establishment of a minigenome and virus-like particle production assay for OROV (27). In the present paper, we report the recovery of infectious OROV entirely from cDNA plasmids. Like all bunyaviruses, OROV contains a tripartite RNA genome with a large (L) segment that encodes the viral RNA-dependent RNA polymerase, a medium (M) segment that encodes the viral glycoproteins Gn and Gc, and a small (S) segment that encodes the nucleocapsid (N) protein. OROV also encodes two nonstructural proteins, NSm, which is a cotranslationally cleaved product formed along with Gn and Gc from the M segment, and NSs, which is encoded from a downstream AUG site on the same mRNA transcript as the N protein. The rescue system described in this paper is based on a T7 RNA polymerase-driven plasmid system (28). Using this, we have successfully recovered wild-type OROV, along with mutant viruses lacking the NSm or NSs protein. We report here the characterization of these recombinant viruses in cultured cells, as a way to contribute to the understanding of this important yet poorly understood emerging viral zoonosis.

MATERIALS AND METHODS

Cells and viruses. A549 (human alveolar adenocarcinoma epithelial cells), A549/BVDV-NPro (A549 cells that express bovine viral diarrhea virus NPro protein), A549/V (derived from A549 and expressing simian virus 5 V protein), CPT-Tert (sheep choroid plexus cells), DF-1 (chicken embryo fibroblasts), HeLa (human cervical adenocarcinoma epithelial cells), LLC-MK2 (*Macaca mulatta* kidney epithelial cells), MDCK (canine kidney epithelial cells), MRK101 (gray red-backed vole kidney cells), QT-35 (Japanese quail fibrosarcoma cells), Vero-E6 (African green monkey kidney cells), and 2fTGH (human epithelial fibrosarcoma cells) cells were grown in Dulbecco's modified Eagle's medium (DMEM; Invitrogen) supplemented with 10% fetal bovine serum (FBS). BHK-21 (baby hamster kidney fibroblasts) cells were grown in Glasgow minimal essential medium (GMEM; Invitrogen) supplemented with 10% newborn calf serum (NCS) and 10% tryptose phosphate broth (TPB; Invitrogen). BSR-T7/5 cells, which stably express T7 RNA polymerase (29), were grown in GMEM supplemented with 10% FBS, 10% TPB, and 1 mg/ml of G418 (Geneticin; Invitrogen). All mammalian cell lines were grown at 37°C with 5% CO_2.

Mosquito U4.4 cells (*Aedes albopictus* neonatal larvae cells) were grown in Leibovitz 15 medium (Gibco) supplemented with 10% FBS and 10% TPB, while Aag-2 cells (derived from *Aedes aegypti* neonatal larvae) were grown in Schneider's *Drosophila* medium with L-glutamine (Gibco) supplemented with 10% FBS. Both cell lines were maintained at 28°C.

OROV strain BeAn19991 was kindly donated by Luiz Tadeu Moraes Figueiredo (University of São Paulo School of Medicine, Ribeirao Preto, Brazil). OROV isolate BeH759025 was kindly provided by Pedro Vasconcelos (Department of Arboviruses and Hemorrhagic Fevers, Evandro Chagas Institute, Ministry of Health, Ananindeua, Brazil).

All experiments with infectious viruses were conducted under biosafety level 3 (BSL3) conditions.

Plasmids. Plasmids pTVTOROVL, pTVTOROVM, and pTVTOROVS used for OROV rescue have previously been described (27). pTVTOROVdelNSm was created from pTVTOROVM by excision PCR using 5′-phosphorylated primers to delete nucleotides (nt) 1039 to 1476 of the M segment, hence removing the entire NSm open reading frame (ORF) after the first transmembrane domain up to the third transmembrane domain while maintaining the predicted cleavage site that resides between NSm and Gc. pTVTOROVdelNSs and pTVTOROV246NSs were generated by QuikChange site-directed mutagenesis on pTVTOROVS to insert stop codons at specific regions in order to generate viruses with truncated NSs proteins. These plasmids contain mutations at cDNA nt position 116 for pTVTOROVdelNSs and 313 for pTVTOROV246NSs. The N ORF remains unchanged. pTVTOROV2080S was generated by amplifying the full-length S segment of clinical isolate BeH759025 (24). Primers and cloning strategy were the same as for pTVTOROVS (27). All PCRs were carried out using KOD Hot Start DNA polymerase (Merck). Products were gel purified (Promega) and, where needed, ligated using T4 DNA ligase (Promega), as per the manufacturer's protocol. Plasmids were confirmed by nucleotide sequencing (Source Bioscience). Primers used are listed in Table 1.

Generation of recombinant OROV from cDNA. Recombinant OROVs were generated by transfecting BSR-T7/5 cells (1.5×10^5 cells/ml) with 1 μg of pTVTOROVL, pTVTOROVM (or pTVTOROVdelNSm), and pTVTOROVS (or pTVTOROV2080S) using 3 μl of transfection reagent TransIT-LT1 (Mirus Bio LLC) per μg of DNA. By replacing the wild-type (wt) S segment (pTVTOROVS) with 1.5 μg of pTVTOROVdelNSs or pTVTORO246NSs, mutant NSs viruses were generated. Supernatants were harvested 7 days posttransfection (p.t.). Rescue outcome was assessed by plaque assay on BHK-21 cells. All recovered viruses were grown in Vero E6 cells, and genome segments were amplified by reverse transcription-PCR (RT-PCR) for sequence determination (Sanger sequencing).

Plaque assay. Viruses were titrated on BHK-21 cells seeded at a density of 3×10^5 per ml in a 12-well plate, while virus phenotype assays (with various cells) were carried out in 6-well plates. Cell monolayers were infected with either 150 μl (12-well plate) or 200 μl (6-well plate) of virus diluted in phosphate-buffered saline (PBS)–2% NCS. Cells were then overlaid using 0.6% Avicell (FMC) in 2× minimum essential medium (MEM)–2% NCS. Three days postinfection (p.i.), cells were fixed with 4% formaldehyde and stained using crystal violet to visualize plaques.

Virus propagation. Working stocks of recombinant and wt viruses were grown in Vero E6 cells at a multiplicity of infection (MOI) of 0.001. Cells were maintained at 37°C and 5% CO_2 until visible cytopathic effect (CPE) was observed. Virus-containing supernatant was clarified by low-speed centrifugation, and aliquots were stored at −80°C. Recombinant viruses used were at passage 2. All the introduced mutations were confirmed by amplifying the segment in question by RT-PCR, followed by Sanger sequencing with primers covering the region of interest.

RT-PCR. Virion RNA of each passaged virus was extracted using the RNeasy minikit (Qiagen) as per the manufacturer's protocol. RT-PCR was then carried out using segment-specific forward or reverse primers (27), with Moloney murine leukemia virus (MMLV) reverse transcriptase (Promega). PCR was carried out using KOD Hot Start DNA polymerase (Merck), and the amplified products were agarose gel purified (Promega), as per the manufacturer's protocol. Specific regions of each segment were then sequenced via Sanger sequencing (Source Bioscience).

Viral infection. Cells were infected with viruses at the desired MOI for 1 h at 37°C. The cell monolayer was washed three times using PBS, and then complete growth medium was added. At desired time points, virus was harvested or cell lysates were collected. Viral titers were determined by plaque assay on BHK-21 cells for 3 days.

Western blotting. Cell lysates were prepared in lysis buffer (100 mM Tris-HCl [pH 6.8], 4% SDS, 20% glycerol, 200 mM dithiothreitol [DTT], 0.2% bromophenol blue, and 25 U/ml of Benzonase; Novagen), and proteins were then separated on a 4 to 12% gradient NuPAGE bis-Tris gel (Invitrogen) at 180 V for 50 min. Proteins were transferred to a nitrocellulose membrane (Amersham), and a semidry transfer was performed using the Trans-Blot Turbo transfer system (Bio-Rad) at 10 V for 50 min. Membranes were then blocked for 1 h in 5% milk–PBS 0.1% (vol/vol) Tween 20 and incubated in primary antibody overnight at 4°C. Secondary antibody was added for 1 h at 37°C. Proteins were then visualized using SuperSignal WestPico chemiluminescent substrate (Pierce), followed by exposure on a Bio-Rad ChemiDoc imager. Primary antibodies included BUNV anti-N-Rb (1:5,000) (30), anti-MxA (1:500, catalogue no. sc-50509; Santa Cruz Biotech), anti-pSTAT1 (1:750, catalogue no. 9167S; Cell Signaling), anti-STAT1 (1:750, catalogue no. 9172; Cell Signaling), and antitubulin monoclonal antibody (1:5,000, catalogue no. T5168, Sigma). OROV anti-N polyclonal rabbit antibody (1:1,000; GenScript) was a kind gift from Massimo Palmarini (MRC-University of Glasgow Centre for Virus Research). Horseradish peroxidase (HRP)-coupled secondary anti-rabbit (catalogue no. A0545; Sigma) and anti-mouse (catalogue no. A4416; Sigma) antibodies were used at 1:5,000.

Metabolic radiolabeling. Vero E6 cells were grown in 12-well plates and infected at an MOI for 3 of each virus, and at the desired time points, supernatant was removed and cells were starved in methionine- and cysteine-free DMEM at 37°C for 30 min. Cells were then washed and labeled with 10 μCi per well of EasyTag EXPRESS^{35}S mixed in methionine- and cysteine-free DMEM for 2 h at 37°C. Cell were then lysed in 150 μl of lysis buffer (100 mM Tris-HCl [pH 6.8], 4% SDS, 20% glycerol, 200 mM DTT, 0.2% bromophenol blue, and 25 U/ml of Benzonase; Novagen), and proteins were separated by SDS-PAGE. Gels were fixed and dried, and then labeled proteins were visualized by phosphorimaging (Storm840 phosphorimager; Molecular Dynamics).

Biological IFN production assay. A549 cells were grown in 12-well plates and infected at an MOI of 1 for each virus. Twenty-four hours postinfection, supernatant was harvested and treated with UV light (8 W, 254 nm, and 2-cm distance) for 4 min with shaking after 2 min to inactivate any virus. Cells were lysed in 150 μl of lysis buffer (100 mM Tris-HCl [pH 6.8], 4% SDS, 20% glycerol, 200 mM DTT, 0.2% bromophenol blue, and 25 U/ml of Benzonase; Novagen) to check viral N and STAT1 protein levels. Phosphorylated STAT1 and MxA production in each sample was also probed. A549/BVDV-NPro cells grown in a 96-well plate were then treated with the UV-inactivated supernatant for 24 h. These cells were then infected with interferon (IFN)-sensitive encephalomyocarditis virus (EMCV; 0.05 PFU/cell) and incubated for 3 days at 37°C. Cells were fixed in 4% formaldehyde and stained with crystal violet to visualize CPE.

IFN-α sensitivity assay. Vero E6 cells at 1.5×10^5/ml were treated either pre- or post-viral infection with various concentrations of universal type 1 IFN-α (catalogue no. 11200, lot no. 5283; Stratech Scientific). Cells were infected with virus at the desired MOI in PBS–2% FBS for 1 h at 37°C. Cells were washed three times in PBS before medium was replaced with medium with or without IFN-α. Cells were incubated at 37°C for 48 h before harvesting and determination of virus yield by plaque assay on BHK-21 cells. For plaque assays, confluent Vero E6 cells were pretreated with IFN-α for 24 h before the virus was titrated. At 4 days p.i., cells were fixed in 4% formaldehyde and stained with crystal violet. IFN-α was maintained in the medium and Avicell overlay for the duration of infection.

RESULTS

Recovery of wild-type OROV strain BeAn19991. OROV is a negative-sense virus, and previously (27), we described the cloning of full-length antigenomic sense cDNA copies of its L, M, and S segments into the T7 RNA polymerase-driven plasmid backbone pTVT7R (0, 0) (31). This plasmid contains a single G residue immediately downstream of the T7 promoter sequence to aid efficient transcription. cDNA copies of OROV genome segments were cloned into pTVT7R in the antigenomic sense (Fig. 1A). To recover infectious OROV, BSR-T7/5 cells (29) were transfected with 1 μg of the pTVTOROVL, pTVTOROVM, and pTVTOROVS plasmids. Supernatant was harvested 7 days p.t. once CPE was visible, and success of the rescue attempt was determined by titration of infectious virus by plaque assay. The rescue of OROV was easily reproducible, yielding titers of 2.0×10^7, 4.5×10^6, and 2.3×10^7 PFU/ml in three independent experiments. As a control, BSR-T7/5 cells transfected with only pTVTOROVM and pTVTOROVS did not give rise to infectious virus. To test the authenticity of the recombinant OROV (rOROV), permissive Vero E6 cells were infected with the rescue supernatant and cell extracts were used for Western blotting (data not shown). Furthermore, rOROV-infected Vero E6 cells were fixed and stained at 24 h p.i. using a polyclonal anti-OROV antibody (a kind gift from Luiz Tadeu Moraes Figueiredo, University of São Paulo School of Medicine, Brazil). Substantial amounts of cytoplasmic OROV protein were detectable in the infected cells (data not shown), further confirming the successful recovery of infectious OROV.

The growth kinetics and plaque phenotype of rOROV were similar to those of the authentic wt virus (Fig. 1B to D). All experiments from this point on were carried out with rOROV.

Growth of recombinant OROV in mammalian cell lines. The growth properties of rOROV were tested in Vero E6 cells at MOIs ranging from 0.0001 to 1 PFU/cell. Previous work from our group has demonstrated that some viruses show a better fitness in certain cell types and at different MOIs, possibly due to the efficiency at which defective interfering particles are generated (32, 33). rOROV grew to similar titers by 48 h p.i. at all MOIs tested (Fig. 1E) and in a wide range of cell lines derived from several species (MOI, 0.001) (Fig. 1F), similar to other bunyaviruses (32, 33). Lower titers were obtained in human cell lines 2fTGH and HeLa than in A549 cells. Lower virus titers were also obtained from CPT-tert, QT-35, and MRK101 cells; however, due to the specific aims of the current study, these observations were not investigated further. rOROV formed plaques on the rodent, monkey, human, and sheep cell lines that were investigated (Fig. 1G). At 3 days p.i.

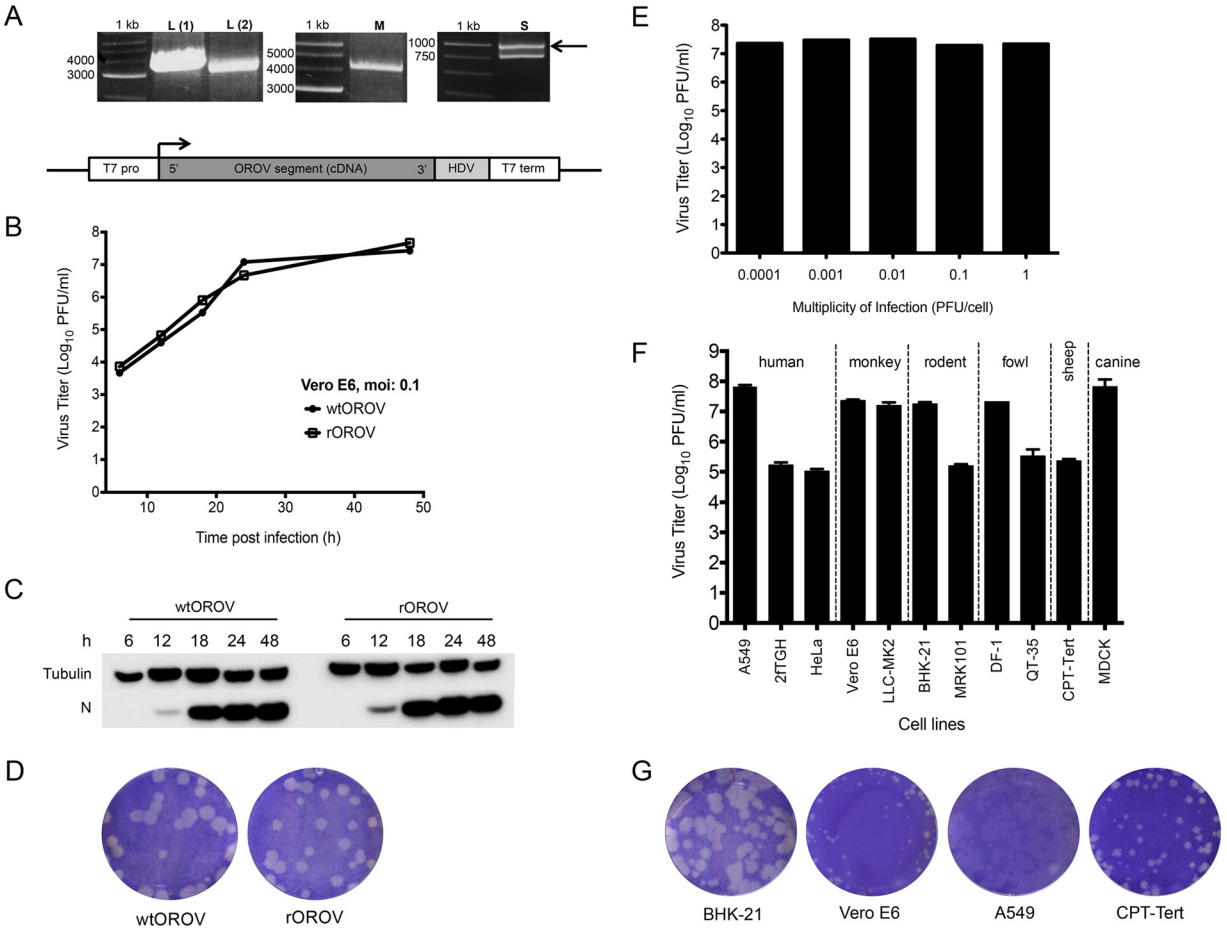

FIG 1 Characterization of recombinant OROV. (A) RT-PCR products derived from the L, M, and S segments of OROV strain BeAN19991. Amplified products were separated on a 1% agarose gel along with a 1-kb marker (Promega). Products were cloned into plasmids containing a T7-RNA polymerase promoter and a hepatitis delta ribozyme as shown in the schematic at the bottom. (B) Growth properties of wild-type (wt) and recombinant (r) OROV in Vero E6 cells. Cells were infected at an MOI of 0.1. At indicated time points samples were harvested and titers determined by plaque assay on BHK-21 cells. The graph shows results of a representative experiment. (C) Western blot showing N protein synthesis from the growth curve (A). Tubulin was probed as a loading control. (D) Comparison of plaque phenotypes of wtOROV and rOROV. A plaque assay was carried out on BHK-21 cells, and at 3 days p.i., cells were fixed and stained with crystal violet. (E) Effects of different MOIs on rOROV yields in Vero E6 cells. Infected cells were harvested 48 h p.i. and titrated on BHK-21 cells. A graph is presented for a representative experiment. (F) Comparison of rOROV growth in various cell lines. Indicated cells were infected at an MOI of 0.001 and at 48 h p.i. harvested and titrated on BHK-21 cells. Bars represent ranges from two experiments. (G) Comparison of rOROV plaque phenotypes on BHK-21, Vero E6, A549, and CPT-Tert cells. Infected cells were fixed and stained with crystal violet at 3 days p.i.

in BHK-21 cells, rOROV plaques were larger than in the other cell lines, and on A549 cells, the plaques were harder to visualize (Fig. 1G). Based on these results, BHK-21 cells were chosen for virus titration, while Vero E6 and A549 cells were chosen for the purpose of initial characterization of all recombinant viruses in this study. Vero E6 and BHK-21 cells both lack fully functional IFN systems (34–36), while A549 cells are IFN competent (37).

Generation of OROV mutants. Using our newly established OROV rescue system, we generated OROV mutant viruses as described below.

(i) NSm deletion. A mutant OROV lacking the entire NSm ORF from the M segment was generated. This was done by deleting the entire NSm coding region immediately after the first NSm transmembrane domain (TMD) and predicted cleavage site up to the third TMD, leaving the predicted cleavage site of the Gc protein intact (Fig. 2A). These sites were predicted using the TMHMM Server v. 2.0 and SignalP 4.1 Server algorithms (http://www.cbs.dtu.dk) based on work done by Xiaohong Shi (MRC-University of Glasgow, Centre for Virus Research) for the characterization of orthobunyavirus M segments (X. Shi and R. M. Elliott, submitted for publication). Primers delNSmOROVF and delNSmOROVR (Table 1) were designed to bind to positions 1475 to 1498 and 1036 to 1013 of the M segment, respectively. This allowed an excision PCR to be performed, thereby deleting the entire NSm region but leaving the first TMD site, so as not to alter the position of the Gc protein in the endoplasmic reticulum and Golgi, during folding. To rescue rOROVdelNSm virus, BSR-T7/5 cells were transfected with 1 μg of pTVTOROVL, pTVTOROVS, and pTVTOROVdelNSm plasmids. At 7 days p.t., infectious virus particles were recovered, titrated, and sequenced (Source Bioscience) to confirm the mutation.

(ii) NSs mutants. The following step was the creation of the NSs mutant viruses. As NSs lies in an overlapping reading frame within the N ORF, the positions at which mutations could be introduced were limited. The NSs ORF of OROV has four in-frame methionines; therefore, in an attempt to abrogate NSs tran-

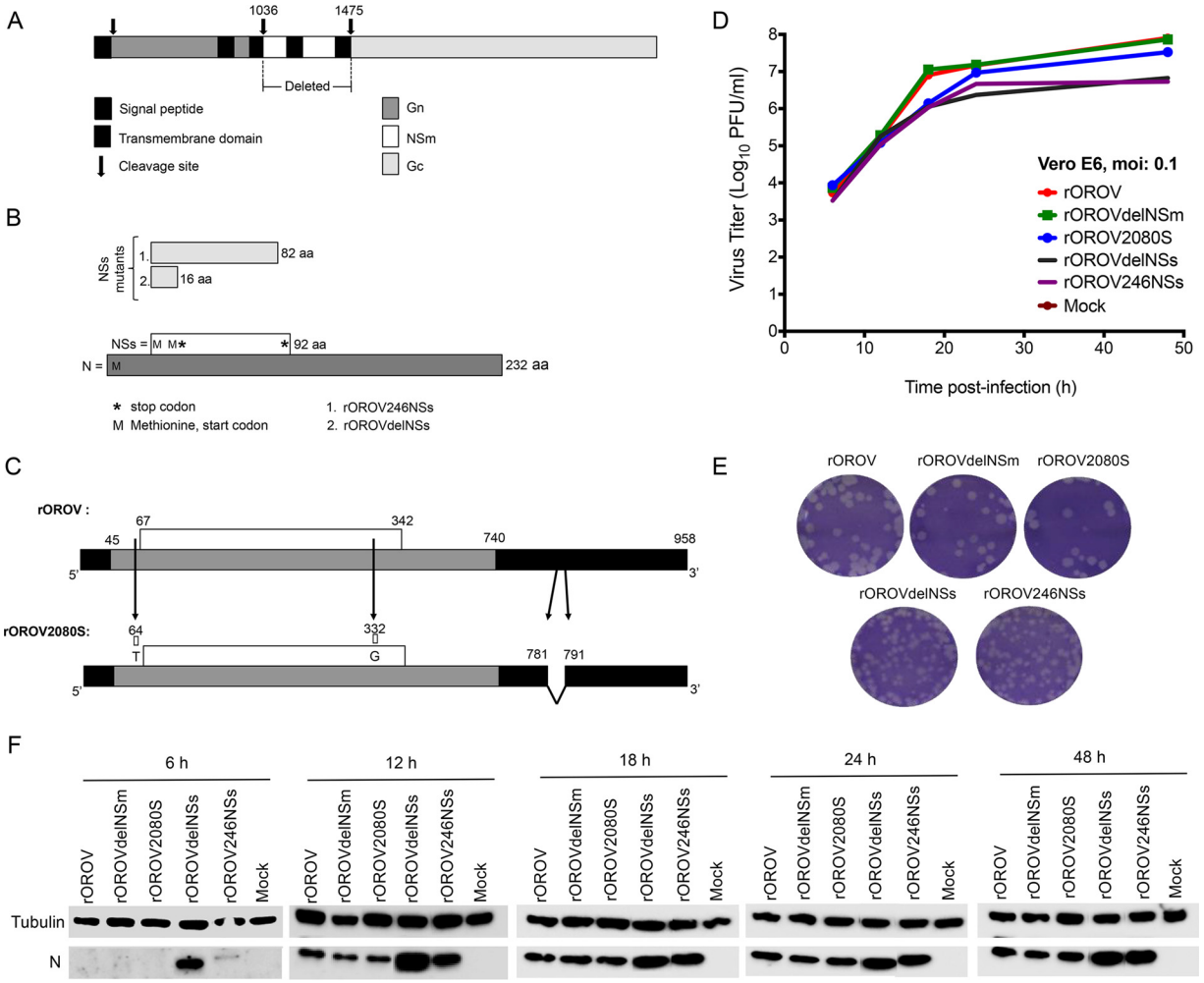

FIG 2 Creation of OROV mutant viruses. (A) Schematic of the M segment showing Gn, NSm, and Gc regions. The arrows depict where cleavage occurs. The patterned box indicates the signal peptide, and the black boxes represent transmembrane domains. Nucleotides 1036 to 1475 were deleted in order to generate delNSm M segment. (B) S segment products N and NSs. NSs is coded from an overlapping reading frame with N. Schematic shows how NSs mutants differ from the wt. rOROV246NSs has a stop codon (asterisk) placed at nucleotide (nt) position 314 of S segment cDNA, changing TTA to TAA and thereby deleting the last 8 aa. rOROVdelNSs has a stop codon at cDNA nt position 116, changing TGG to TAG so that a stop codon is generated immediately after the second start codon (methionine [M]). Numbers are amino acid lengths. (C) rOROV2080S S segment in comparison to wtOROV and rOROV S segment. Numbers are nucleotide positions. Arrows show where changes occur. First two positions generate a variation in the NSs OROF. Black highlights the UTRs. (D) Growth properties of recombinant viruses in Vero E6 cells. Cells were infected at an MOI of 0.1. Samples were harvested at the indicated time points and titrated on BHK-21 cells. The graph shows results of a representative experiment. (E) Plaque phenotype of recombinant viruses in BHK-21 cells. A plaque assay was carried out, and at 3 days p.i., cells were fixed and stained with crystal violet. (F) N production in recombinant viruses. Cell lysates from the growth curve (D) were probed for OROV-N and tubulin.

scription, the NSs start codon was left in place and instead a translational stop codon was inserted in frame immediately after the second methionine at position 17 (Fig. 2B, 2. rOROVdelNSs). At the nucleotide level, this is at position 115 and changes TGG (W) to TAG (stop), resulting in a 48-nt NSs ORF. The reason for this approach was that previous work done on BUNV revealed that when the start codon of NSs was removed, the virus was still capable of producing an NSs protein from a downstream methionine (38). The strategy used in this study for OROV is similar to the one used to create an SBV mutant lacking NSs (32). In addition to this, a C-terminally truncated NSs was also engineered. This was generated by introducing a stop codon at nt position 313, changing TTA (L) to TAA (stop). This resulted in a 246-nt NSs ORF and a protein sequence of 82 amino acids (aa), compared to 92 aa for wt NSs (Fig. 2B, 1. rOROV246NSs). Primers used in generating the plasmids are in Table 1. In order to rescue the NSs mutants (named rOROVdelNSs and rOROV246NSs), BSR-T7/5 cells were transfected with 1 μg of pTVTOROVL and pTVTOROVM and 1.5 μg of the mutant S segment (pTVTOROVdelNSs or pTVTORO246NSs). At 7 days p.t., infectious virus particles were recovered and titrated and the entire NSs ORF was sequenced (Source Bioscience) to confirm mutations.

(iii) S-segment mutant. In a previous work (24), we reported the isolation and sequencing of OROV clinical isolates that differ from the prototype strain (BeAn19991) in the S segment, as they lack 11 nt at position 781 to 791 in the 3′ untranslated region (UTR). The NSs ORFs of these viruses also contain a tandem AUG translation start codon created by a C-U variation at position 332 and a Gln-to-Arg change in the NSs ORF at position 89 (Fig. 2C, rOROV2080S). To test whether these variations altered the *in vitro*

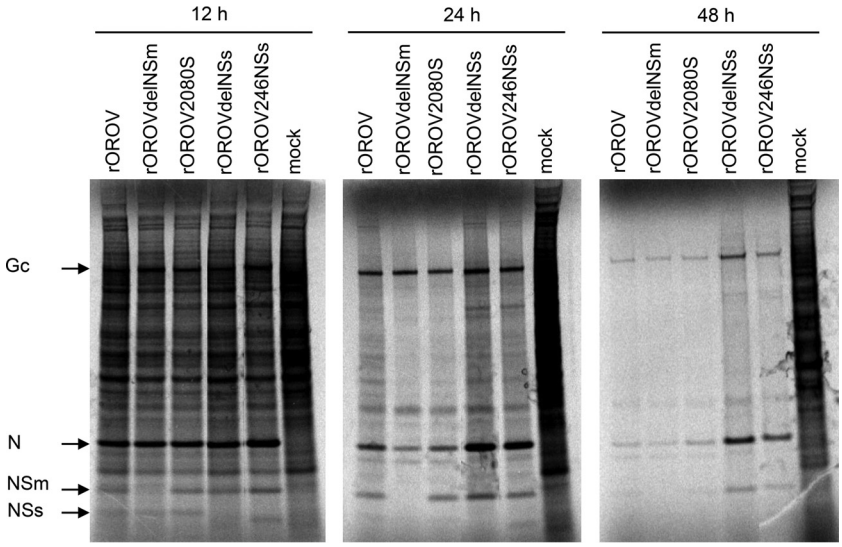

FIG 3 Host cell protein shutoff. Vero E6 cells were infected with rOROV, rOROVdelNSm, rOROV2080S, rOROVdelNSs, or rOROV246NSs or mock infected. Cells were infected at an MOI of 3 and incubated at 37°C. At the indicated time points, the cells were labeled with [^{35}S]methionine for 2 h. Cells lysates were then separated by SDS-PAGE. Arrows indicate the position of viral proteins Gc, N, NSm, and NSs.

growth properties of the rescued virus, a cDNA plasmid (designated pTVTOROV2080S) containing the S segment of clinical isolate BeH759025 (GenBank accession number KP691614 [24]) was generated using the same cloning strategy as for pTVTOROVS (27). In order to rescue this S-segment mutant (named rOROV2080S), BSR-T7/5 cells were transfected with plasmids pTVTOROVL, pTVTOROVM, and pTVTOROV2080S (1 μg each). At 7 days p.t., infectious virus particles were recovered and titrated and the entire S segment was sequenced (Source Bioscience).

All mutant viruses in this study were passaged three times at a low MOI in Vero E6 cells and sequenced. Introduced mutations were maintained, confirming the stability of these viruses. Subsequent experiments utilized viruses from passage two.

Growth properties of recombinant viruses in mammalian cell lines and their effect on host protein synthesis. Growth kinetics of rOROV, rOROVdelNSm, rOROVdelNSs, rOROV246NSs, and rOROV2080S were compared in Vero E6 cells at an MOI of 0.1. rOROV, rOROVdelNSm, and rOROV2080S replicate with similar efficiencies; however, mutants rOROVdelNSs and rOROV246NSs appeared attenuated and reached titers that were 1 log lower than that of rOROV (Fig. 2D). Western blotting revealed larger amounts of N protein from rOROVdelNSs at earlier time points, suggesting a possibly increased efficiency of the virus in translating N (Fig. 2F). Plaque morphologies of the recombinant viruses were then compared on BHK-21 cells. rOROV, rOROVdelNSm, and rOROV2080S produced plaques with a round morphology and were clear and similar to each other. The plaques of viruses rOROVdelNSs and rOROV246NSs, on the other hand, were smaller, with corrugated and ill-defined borders (Fig. 2E).

To investigate whether the recombinant viruses caused inhibition of host cell protein synthesis, Vero E6 cells were infected at an MOI of 3, and at 12, 24, and 48 h p.i., cells were radiolabeled with [^{35}S]methionine. Cell extracts were analyzed by SDS-PAGE. rOROV, rOROVdelNSm, and rOROV2080S, as well as the rOROVdelNSs and rOROV246NSs, demonstrated an ability to cause host translation shutoff by 24 h p.i. (Fig. 3). It was also observed that the last two viruses produced noticeably more N protein at this time point than did the other viruses. This result also confirmed that the mutant viruses rOROVdelNSm and rOROVdelNSs do not express NSm and NSs proteins, respectively, and that the rOROV246NSs virus expresses a truncated version of NSs (Fig. 3).

As rOROV2080S behaves similarly to rOROV and rOROV246NSs behaves similarly to rOROVdelNSs in terms of *in vitro* replication kinetics, only rOROV, rOROVdelNSm, and rOROVdelNSs were focused on for growth comparison in IFN-competent A549 cells. rOROV and rOROVdelNSm grew with similar kinetics and reached comparable titers, whereas rOROVdelNSs growth appeared more restrictive and at 48 h the viral titers were almost 2 logs lower than those of rOROV and rOROVdelNSm (Fig. 4A). Western blot analysis of N expression showed smaller amounts of protein in the rOROVdelNSs-infected cells (Fig. 4B). Next, the growth of rOROV, rOROVdelNSm, and rOROVdelNSs in A549 cells was compared to their growth in IFN-incompetent A549/V cells. These cells express the V protein of parainfluenza type 5 virus, thereby blocking type I IFN signaling via STAT1 degradation (39). Cells were infected at an MOI of 0.001, and titers were measured at 48 h p.i. Cells were also infected with BUNV or a BUNV mutant lacking the NSs protein (rBUNVdelNSs2) for comparison (40, 41). All viruses grew to higher titers in the IFN-incompetent cell line, similar to BUNV. rOROVdelNSs titers were over 1 log higher in A549/V cells than in A549 cells, although this difference was not as high as with rBUNVdelNSs2 (Fig. 4C). Western blotting for N confirmed lower levels of expression in A549 cells infected with rOROVdelNSs and rBUNVdelNSs2, corresponding with the yield assay (Fig. 4D).

OROV NSs protein inhibits type I IFN production in A549 cells. We measured IFN production in A549 cells in response to infection with rOROV, rOROVdelNSm, rOROV2080S, rOROVdelNSs, or rOROV246NSs at an MOI of 1. For comparison, we also infected cells with BUNV or rBUNVdelNSs2. At 24 h p.i., the medium from infected monolayers was collected, infec-

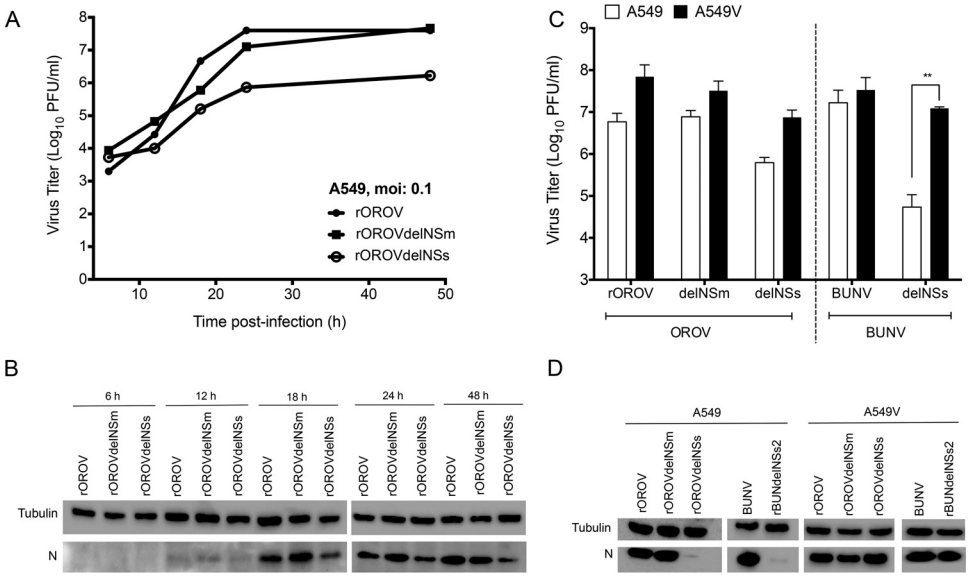

FIG 4 Growth properties of recombinant viruses in A549 cells. (A) Growth kinetics of rOROV, rOROVdelNSm, and rOROVdelNSs in A549 cells at an MOI of 0.1. At the indicated time points, samples were harvested and viral titers determined by plaque assay on BHK-21 cells. The graph presents results for one representative experiment. (B) Western blot for cell lysates from growth curve (A). Lysates were separated by SDS-PAGE and probed for OROV N and tubulin. (C) Comparison of growth properties in A549 and A549/V cells. Cells were infected at an MOI of 0.001 with the indicated viruses. Forty-eight hours p.i., viral titers were determined by plaque assay. BUNV was used for comparison. Bars indicate SDs ($n = 3$; **, $P < 0.01$ by Student's t test). (D) Western blot analysis for panel C. Cells lysates were probed for viral N protein. Tubulin was probed as a loading control.

tious virus was inactivated by UV treatment, and the amount of IFN present was measured in a biological protection assay as described previously (42). As expected, no IFN was produced from mock- or BUNV-infected cells, and rBUNVdelNSs2-infected cells produced considerable amounts of IFN. While rOROV, rOROVdelNSm, and rOROV2080S induced small amounts of IFN, rOROVdelNSs induced large amounts (Fig. 5A). rOROV246NSs, which lacks only 9 aa at the NSs protein C terminus, induced IFN to the same extent as rOROVdelNSs (Fig. 5A and B). Next, we used Western blotting to probe the A549 cell extracts for STAT1, phosphorylated STAT1 (pSTAT1), and the interferon-stimulated gene (ISG) protein MxA. pSTAT1 and MxA expression was detected in cells infected with rOROVdelNSs or rOROV246NSs but not in cells infected with rOROV, rOROV2080S, or rOROVdelNSm (Fig. 5C), confirming that OROV NSs is an IFN antagonist.

OROV is less sensitive to IFN-α treatment than BUNV. BUNV replication was previously shown to be highly sensitive to IFN-α (43). To test if OROV was equally sensitive, Vero E6 cells (which cannot produce but can respond to IFN [36]) were treated with increasing doses of universal type 1 IFN-α (0, 10, 100, 1,000, and 10,000 U/ml), either preinfection (− 24 or − 2 h) or postinfection (+ 2 or + 24 h). Cells were infected with BUNV or OROV at an MOI of 0.01, and IFN-α was maintained in the medium throughout the infection period. At 48 h p.i., the amount of infectious virus in the culture medium was estimated by plaque assays. While both viruses showed sensitivity to IFN, OROV was clearly less sensitive than BUNV (Fig. 6A). For example, pretreating cells with 10,000 U of IFN-α either 2 or 24 h preinfection completely inhibited BUNV replication, as did treating cells with 10,000 U at 2 h p.i. In contrast, there was only a 1- to 2-log reduction in the titers of OROV in cells pretreated for 2 h with 10,000 U of IFN-α prior to infection and a 3-log reduction in cells pretreated for 24 h. Furthermore, while pretreating cells with 1,000 U of IFN-α for 24 h preinfection completely inhibited BUNV, there was only a 2-log reduction in cells infected with OROV (Fig. 6A). We have repeated the experiment with rOROV using 10,000 U/ml of IFN and at MOIs of 0.001 and 0.01. At 24 or 48 h p.i. at both MOIs, rOROV replication was not completely inhibited, as observed with BUNV, with titers decreased by 2 to 3 logs compared to the values for untreated cells (data not shown). Viruses rOROVdelNSm, rOROV2080S, rOROVdelNSs, and rOROV246NSs demonstrate a sensitivity to IFN-α similar to that of rOROV (Fig. 6B), indicating that the increased resistance of OROV to IFN-α compared to that of BUNV is not due to expression of a functional NSs protein. Next, we investigated the plaque morphology on pretreated Vero E6 cells for rOROV and rOROVdelNSs in comparison to BUNV and rBUNVdelNSs2. A 1,000-U/ml concentration of IFN-α was maintained in the overlay during the infection period. No BUNV or rBUNVdelNSs plaques were observed when the plaque assays were performed in the presence of IFN-α. In contrast, rOROV and rOROVdelNSs plaques were observed in the presence of IFN-α, although they were considerably smaller than those on untreated cells (Fig. 6D). Taken together, these results demonstrate that in the tested cells and with the MOI of virus used, OROV is sensitive to IFN-α in a dose-dependent manner; however, it is significantly more resistant than BUNV. Furthermore, the NSs protein is not responsible for this increased resistance.

Replication of recombinant viruses in mosquito cell lines. We have also compared the growth kinetics of rOROV, rOROVdelNSm and rOROVdelNSs in mosquito cell lines U4.4 (*Aedes albopictus*) and Aag2 (*Aedes aegypti*). Interestingly, and unlike the situation in mammalian cells, rOROVdelNSs grows to similar levels as rOROV (Fig. 7). In both U4.4 and Aag2, it appears that rOROVdelNSm grows to slightly higher titers than the other

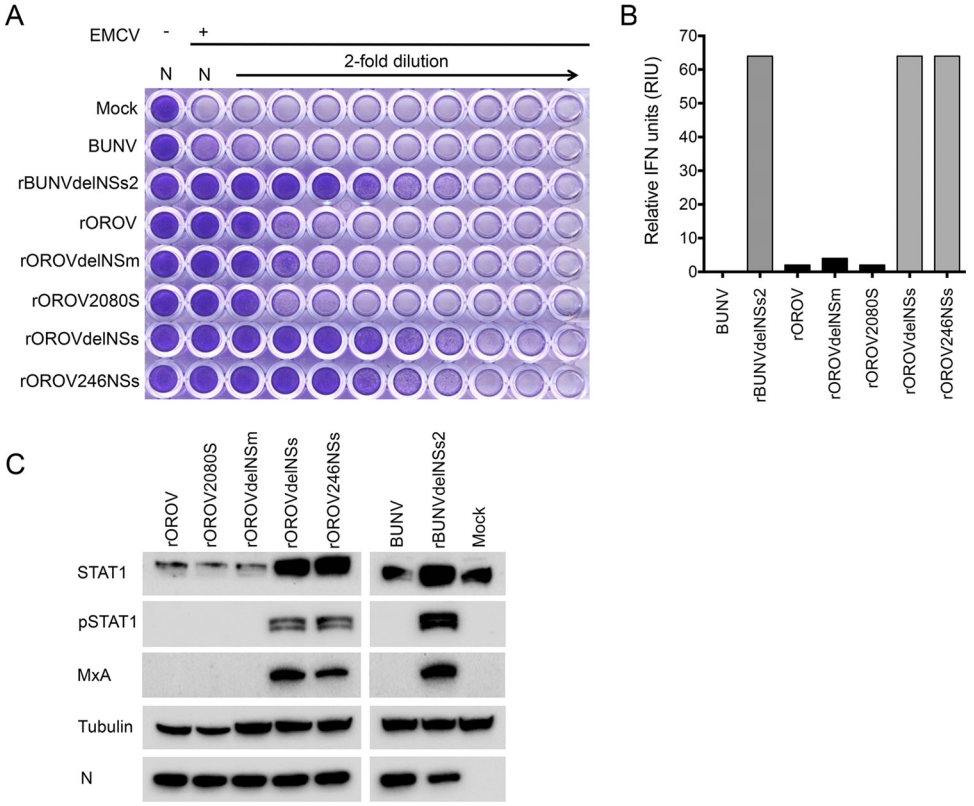

FIG 5 Biological interferon production assay. A549 cells were infected at an MOI of 1 with BUNV, rBUNdelNSs2, rOROV, rOROVdelNSm, rOROV2080S, rOROVdelNSs, or rOROV246NSs or mock infected. Supernatant was harvested at 24 h p.i., and cell extracts were separated by SDS-PAGE. (A) UV-inactivated supernatant was used to pretreat A549-N pro cells prior to infection with EMCV. At 3 days p.i., cells were fixed and stained with crystal violet. (B) Graph calculated from panel A, presenting relative IFN units expressed as 2N where N is the number of 2-fold dilutions that offered protection. (C) Cells extracts were probed for OROV N, STAT1, pSTAT1, and MxA. Tubulin was probed as a loading control.

viruses. Investigating this further was beyond the scope of the current study.

DISCUSSION

In this paper, we describe the successful recovery of OROV in cultured cells entirely from cloned cDNAs. OROV is a midge-borne orthobunyavirus that causes a febrile illness in the South American human population. The virus has caused over half a million infections, and though not fatal, its dengue-like symptoms can persist for weeks and in a few cases can progress into more severe symptoms, such as meningitis and encephalitis (18). OROV is closely related to SBV, another Simbu virus also spread by biting midges from the genus *Culicoides*. SBV causes severe fetal malformations in ruminants in Europe but has not been known to infect humans. Using the previously described reverse genetics system for SBV (32, 44) and our newly established OROV rescue system, we can begin to understand the basis for pathogenicity in humans and study reasons for such a species barrier. In addition to this, we can also begin to study the M-segment variations that are found among Oropouche species. OROV M-segment reassortants Iquitos and Madre de Dios viruses can cause disease in humans (25, 26), while Perdoes virus and the more divergent Jatobal virus have only been isolated from nonhuman primates (*Callithrix penicillata*) and the South American coati (*Nasua nasua*), respectively (24, 45). It is interesting that members of the Oropouche species display a broad phylogenetic diversity predominately due to the M segment. The variations observed in the M segments of these viruses could have resulted from either genomic reassortment or extensive adaptation to different hosts and habitats. Using the OROV reverse genetics system established in this study, it would now be possible to study in detail these differences in terms of pathogenesis, virulence outcome, and host range of these viruses. This work would contribute to understanding the evolution of clade A Simbu serogroup viruses within South America.

The recombinant OROV (rOROV) that we have generated replicates similarly to the authentic virus (wild-type OROV [wtOROV]), reaching titers of 10^7 PFU/ml (Fig. 1B). Using this system, mutant viruses lacking either the NSm or the NSs protein were also generated. Only some bunyaviruses encode these proteins, and the exact role played by the NSm protein in orthobunyavirus infections remains unclear. Work on BUNV NSm demonstrated that the protein can localize to the Golgi efficiently on its own (46) and may play a role in viral assembly (47). In Rift Valley fever virus (RVFV), the NSm protein is important for infection in mosquitoes by allowing the virus to cross the midgut barrier (48, 49). Similarly, in tospoviruses, the NSm protein has been shown to be important for virus cell-to-cell spread (50–52). Results from our work indicate that for OROV, the NSm protein is dispensable for virus replication in cultured cells, as rOROVdelNSm grows and replicates similarly to rOROV (Fig. 2D and E, 4, and 7). We have previously (24) discussed the sequence similarity of the M-segment genes between different OROV reassortants and noted

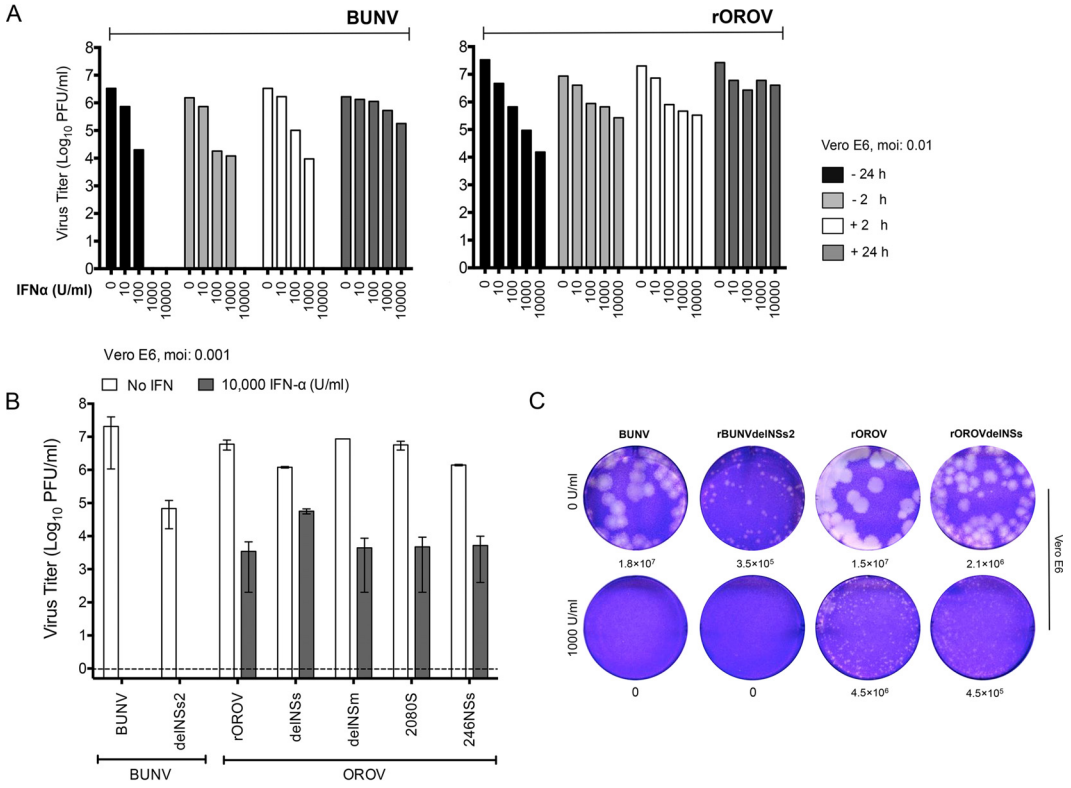

FIG 6 Sensitivity of OROV to IFN-α treatment. (A) IFN-α sensitivity test. Vero E6 cells were treated with increasing concentrations of IFN-α (0, 10, 100, 1,000, and 10,000) either before (−) or after (+) infection. Cells were infected with BUNV or rOROV at an MOI of 0.01. Forty-eight hours p.i., supernatant was harvested and viral titers were determined by plaque assay on BHK-21 cells. Graphs show results of a representative experiment. (B) Vero E6 cells were treated with 10,000 U/ml of IFN-α 24 h prior to infection with indicated viruses at an MOI of 0.001. Samples were harvested at 48 h p.i., and viral titers were determined by plaque assay on BHK-21 cells. Bars represent ranges from two experiments. (C) Vero E6 cells were treated (1,000 U/ml) or not (0 U/ml) with IFN-α 24 h prior to infection. A plaque assay for BUNV, rBUNVdelNSs2, OROV, or rOROVdelNSs was performed. Four days p.i., cells were fixed and stained with crystal violet.

that the NSm region of the M polyprotein of all these viruses is highly conserved compared to the Gn and Gc glycoproteins, which could indicate that this portion of the polyprotein is less prone to mutation due to a common, yet unknown, selective pressure. Future work could include performing mutations on the NSm coding sequence and monitor for effects on virus replication in more relevant primary cell lines and *in vivo* models, such as insects. Similarly, the rOROV2080S mutant generated in this study would also require *in vivo* characterization in order to determine if the S-segment difference observed between OROV isolates offers any advantage over the prototype BeAn19991 S segment, as the current study was not sufficient to determine this.

As with other NSs-encoding bunyaviruses, OROV NSs protein is an IFN antagonist, and by deleting the NSs ORF, OROV induces high levels of IFN and thus induces STAT1 phosphorylation and MxA expression (Fig. 5, rOROVdelNSs). Interestingly, the C-terminally truncated NSs mutant was also incapable of inhibiting type I IFN production (Fig. 5, rOROV246NSs). Work on BUNV and RVFV has demonstrated that NSs inhibits IFN-β activation downstream of transcriptional activation through disruption of DNA-dependent RNA polymerase II (RNAPII) activity (53–55). BUNV NSs interacts with subunit MED8 of the RNAPII regulatory module (56), preventing Ser2 phosphorylation and hence preventing elongation and 3′-end processing of the nascent mRNA transcript (57–59). This was initially thought to be due to an interaction of BUNV NSs C terminus (aa 83 to 91) with MED8; however, a BUNV NSs mutant lacking an N terminus of 21 amino acids is also unable to degrade RNAPII, indicating that both the C and the N termini are important for BUNV NSs function (38, 56, 60). The BUNV MED8 binding domain was mapped to a C-terminal amino acid motif LPS, which is conserved in orthobunyavirus NSs proteins (56); interestingly, OROV C-terminal mutant rOROV246NSs also lacks a similar motif, LPC (see Fig. S1A in the supplemental material). This LPC motif is conserved among only the clade A viruses in the Simbu serogroup (see Fig. S1B). Whether the inability of rOROV246NSs to inhibit IFN production is due to its lack of the MED8 binding domain will be investigated in follow-up studies. La Crosse virus (LACV) and SBV NSs function as IFN antagonists by targeting RNAPII for degradation by the proteasome (61–63). Mutations to the C terminus of SBV NSs have also been shown to affect the protein's ability to degrade RNAPII (63). In the phlebovirus RVFV, the NSs protein interacts with subunits of the general transcription factor TFIIH, which also has a role in RNAPI transcription (64). SFTSV NSs forms viral inclusion bodies in the cytoplasm and uses these to capture kinases TBK1 and IKKε and proteins STAT1 and STAT2 (65, 66). Recently, a study comparing 6-week-old C57BL/6 mouse knockout mutants demonstrated that mitochondrial antiviral-signaling protein (MAVS) activation plays a crucial role in type 1 IFN signaling during OROV infection (67); it would be interesting to see how the rOROVdelNSs and rOROV246NSs mutants replicate in such *in vivo* systems. Interestingly, both rOROVdelNSs and

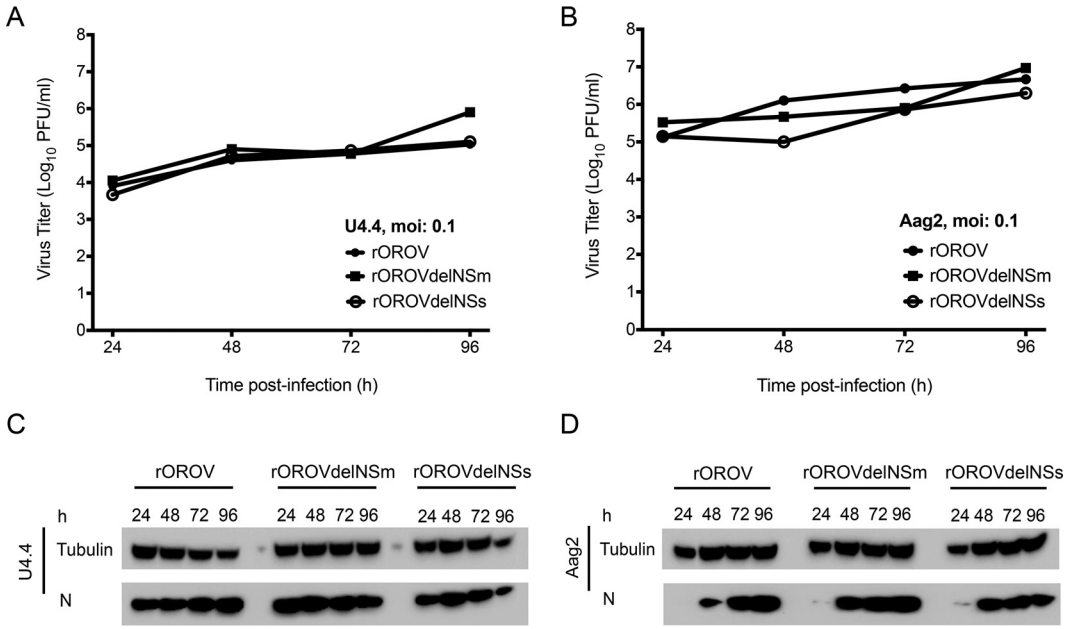

FIG 7 Growth kinetics in mosquito cells. Cells were infected with rOROV, rOROVdelNSm, or rOROVdelNSs at an MOI of 0.1. At the indicated time points, samples were harvested and viral titers were determined by plaque assay. Presented graphs are representative experiments. Cell extracts were separated by SDS-PAGE and probed for viral N and tubulin. (A) Replication in U4.4 cells; (B) replication in Aag2 cells; (C) N production in U4.4 cells; (D) N production in Aag2 cells.

rOROV246NSs are attenuated in Vero E6 (Fig. 2D) and in BHK-21 (Fig. 2E) cells, both of which lack fully functional IFN systems, and from radiolabeling experiments, we know that rOROVdelNSs is capable of causing translational shutoff in Vero E6 cells (Fig. 3). Using the OROV reverse genetics system, we can now begin to study protein-protein interactions and investigate the role of the NSs protein further.

This study also showed that while OROV is sensitive to IFN-α, to see maximal effects, cells have to be treated for 24 h prior to infection (Fig. 6A, rOROV). In contrast, BUNV is highly sensitive to IFN-α (Fig. 6A). These findings are consistent with previously published work demonstrating a resistance of OROV to the antiviral effects of IFN-α both *in vivo* and *in vitro* in comparison to other pathogenic orthobunyaviruses (68). The reasons for the differences in relative sensitivity of OROV and BUNV to IFN-α are under investigation, but the differences may, for example, be due to the differential effects of certain ISGs on these viruses or on the ability of OROV to more rapidly switch off host cell gene expression than BUNV. Whatever the reason, the increased resistance of OROV to IFN-α is not due to expression of the NSs protein, as rOROVdelNSs shows a sensitivity to IFN-α similar to that of OROV.

In conclusion, our present work has shown that we are able to generate infectious OROV entirely from cDNA and that similar to the case with other bunyaviruses, OROV NSs is an IFN antagonist. We have also demonstrated that the NSm protein appears to be nonessential for virus replication in the cultured cells that were tested. The work we have presented here will now enable us to study OROV in more detail in order to establish the molecular details involved in viral replication and pathogenesis, and potentially to generate attenuated vaccine strains. The work we present here is an important move forward toward understanding this important yet neglected human pathogen.

ACKNOWLEDGMENTS

We thank Xiaohong Shi for advice on creating rOROVdelNSm and Massimo Palmarini for OROV-N antibody and a batch of IFN-α. We thank Stephen Welch for reviewing the manuscript and Mark Tilston for proofreading it.

This paper is dedicated to the memory of Richard M. Elliott, who will forever hold a special place in our hearts as a friend, father figure, and mentor.

FUNDING INFORMATION

Wellcome Trust provided funding to Richard M. Elliott under grant number 99220. Medical Research Council (MRC) provided funding to Natasha Louise Tilston-Lunel under grant number 1101085. FAPESP-São Paulo Research Foundation provided funding to Gustavo Olszanski Acrani under grant number 2013/02798-0.

REFERENCES

1. **Elliott RM.** 2014. Orthobunyaviruses: recent genetic and structural insights. Nat Rev Microbiol **12:**673–685. http://dx.doi.org/10.1038/nrmicro3332.
2. **Elliott RM, Brennan B.** 2014. Emerging phleboviruses. Curr Opin Virol **5:**50–57. http://dx.doi.org/10.1016/j.coviro.2014.01.011.
3. **Nunes MR, Martins LC, Rodrigues SG, Chiang JO, Azevedo Rdo S, da Rosa AP, Vasconcelos PF.** 2005. Oropouche virus isolation, southeast Brazil. Emerg Infect Dis **11:**1610–1613. http://dx.doi.org/10.3201/eid1110.050464.
4. **Dixon KE, Travassos da Rosa AP, Travassos da Rosa JF, Llewellyn CH.** 1981. Oropouche virus. II. Epidemiological observations during an epidemic in Santarem, Para, Brazil in 1975. Am J Trop Med Hyg **30:**161–164.
5. **Pinheiro FP, Hoch AL, Gomes ML, Roberts DR.** 1981. Oropouche virus. IV. Laboratory transmission by *Culicoides paraensis*. Am J Trop Med Hyg **30:**172–176.
6. **Vasconcelos HB, Azevedo RS, Casseb SM, Nunes-Neto JP, Chiang JO, Cantuaria PC, Segura MN, Martins LC, Monteiro HA, Rodrigues SG, Nunes MR, Vasconcelos PF.** 2009. Oropouche fever epidemic in Northern Brazil: epidemiology and molecular characterization of isolates. J Clin Virol **44:**129–133. http://dx.doi.org/10.1016/j.jcv.2008.11.006.
7. **Baisley KJ, Watts DM, Munstermann LE, Wilson ML.** 1998. Epidemi-

ology of endemic Oropouche virus transmission in upper Amazonian Peru. Am J Trop Med Hyg **59:**710–716.
8. **Mourao MP, Bastos MS, Gimaqu JB, Mota BR, Souza GS, Grimmer GH, Galusso ES, Arruda E, Figueiredo LT.** 2009. Oropouche fever outbreak, Manaus, Brazil, 2007-2008. Emerg Infect Dis **15:**2063–2064. http://dx.doi.org/10.3201/eid1512.090917.
9. **Bastos Mde S, Figueiredo LT, Naveca FG, Monte RL, Lessa N, Pinto de Figueiredo RM, Gimaque JB, Pivoto Joao G, Ramasawmy R, Mourao MP.** 2012. Identification of Oropouche Orthobunyavirus in the cerebrospinal fluid of three patients in the Amazonas, Brazil. Am J Trop Med Hyg **86:**732–735. http://dx.doi.org/10.4269/ajtmh.2012.11-0485.
10. **Pinheiro FP, Travassos da Rosa AP, Travassos da Rosa JF, Bensabath G.** 1976. An outbreak of Oropouche virus disease in the vicinity of Santarem, Para, Brazil. Tropenmed Parasitol **27:**213–223.
11. **Pinheiro FP, Travassos da Rosa AP, Gomes ML, LeDuc JW, Hoch AL.** 1982. Transmission of Oropouche virus from man to hamster by the midge *Culicoides paraensis*. Science **215:**1251–1253. http://dx.doi.org/10.1126/science.6800036.
12. **Roberts DR, Hoch AL, Dixon KE, Llewellyn CH.** 1981. Oropouche virus. III. Entomological observations from three epidemics in Para, Brazil, 1975. Am J Trop Med Hyg **30:**165–171.
13. **Anderson CR, Spence L, Downs WG, Aitken TH.** 1961. Oropouche virus: a new human disease agent from Trinidad, West Indies. Am J Trop Med Hyg **10:**574–578.
14. **Pinheiro FP, Travassos da Rosa AP, Travassos da Rosa JF, Ishak R, Freitas RB, Gomes ML, LeDuc JW, Oliva OF.** 1981. Oropouche virus. I. A review of clinical, epidemiological, and ecological findings. Am J Trop Med Hyg **30:**149–160.
15. **Roberts DR, Pinheiro FDPP, Hoch AL, LeDuc JW, Peterson NE, Santos MAV, Western KA.** 1977. Vectors and natural reservoirs of Oropouche virus in the Amazon region. US Army Medical Research and Development Command, Washington, DC.
16. **Smith GC, Francy DB.** 1991. Laboratory studies of a Brazilian strain of *Aedes albopictus* as a potential vector of Mayaro and Oropouche viruses. J Am Mosquito Control Assoc **7:**89–93.
17. **Pinheiro FP, Pinheiro M, Bensabath G, Causey OR, Shope RE.** 1962. Epidemia de vírus Oropouche em Belém. Revista do Serv Especial Saude **12:**15–23.
18. **Pinheiro FP, Travassos da Rosa AP, Vasconcelos PF.** 2004. *Bunyaviridae*: other *Bunyaviridae*. Oropouche fever, p 2418–2423. *In* Feigin RD, Cherry J, Demmler GJ, Kaplan SL (ed), Textbook of pediatric infectious diseases, 5th ed. Saunders, Philadelphia, PA.
19. **Watts DM, Phillips I, Callahan JD, Griebenow W, Hyams KC, Hayes CG.** 1997. Oropouche virus transmission in the Amazon River basin of Peru. Am J Trop Med Hyg **56:**148–152.
20. **Mercer DR, Castillo-Pizango MJ.** 2005. Changes in relative species compositions of biting midges (Diptera: Ceratopogonidae) and an outbreak of Oropouche virus in Iquitos, Peru. J Med Entomol **42:**554–558. http://dx.doi.org/10.1093/jmedent/42.4.554.
21. **Rosa AP, Rodrigues SG, Nunes MR, Magalhaes MT, Rosa JF, Vasconcelos PF.** 1996. Outbreak of oropouche virus fever in Serra Pelada, municipality of Curionopolis, Para, 1994. Rev Soc Bras Med Trop **29:**537–541. (In Portuguese.)
22. **Pan American Health Organization.** 2010. Epidemiological alert. Outbreak of Oropouche fever. Pan American Health Organization, Washington, DC. http://www1.paho.org/hq/dmdocuments/2010/epi_alert_2010_22_June_Oropouche_Fever.pdf.
23. **Forshey BM, Guevara C, Laguna-Torres VA, Cespedes M, Vargas J, Gianella A, Vallejo E, Madrid C, Aguayo N, Gotuzzo E, Suarez V, Morales AM, Beingolea L, Reyes N, Perez J, Negrete M, Rocha C, Morrison AC, Russell KL, Blair JP, Olson JG, Kochel TJ.** 2010. Arboviral etiologies of acute febrile illnesses in Western South America, 2000–2007. PLoS Negl Trop Dis **4:**e787.
24. **Tilston-Lunel NL, Hughes J, Acrani GO, da Silva DE, Azevedo RS, Rodrigues SG, Vasconcelos PF, Nunes MR, Elliott RM.** 2015. Genetic analysis of members of the species Oropouche virus and identification of a novel M segment sequence. J Gen Virol **96:**1636–1650. http://dx.doi.org/10.1099/vir.0.000108.
25. **Aguilar PV, Barrett AD, Saeed MF, Watts DM, Russell K, Guevara C, Ampuero JS, Suarez L, Cespedes M, Montgomery JM, Halsey ES, Kochel TJ.** 2011. Iquitos virus: a novel reassortant orthobunyavirus associated with human illness in Peru. PLoS Negl Trop Dis **5:**e1315. http://dx.doi.org/10.1371/journal.pntd.0001315.
26. **Ladner JT, Savji N, Lofts L, Travassos da Rosa A, Wiley MR, Gestole MC, Rosen GE, Guzman H, Vasconcelos PF, Nunes MR, Lipkin WI, Tesh RB, Palacios G.** 2014. Genomic and phylogenetic characterization of viruses included in the Manzanilla and Oropouche species complexes of the genus Orthobunyavirus, family Bunyaviridae. J Gen Virol **95:**1055–1066. http://dx.doi.org/10.1099/vir.0.061309-0.
27. **Acrani GO, Tilston-Lunel NL, Spiegel M, Weidemann M, Dilcher M, da Silva DE, Nunes MR, Elliott RM.** 2014. Establishment of a minigenome system for Oropouche virus reveals the S genome segment to be significantly longer than reported previously. J Gen Virol **95:**513–523.
28. **Bridgen A, Elliott RM.** 1996. Rescue of a segmented negative-strand RNA virus entirely from cloned complementary DNAs. Proc Natl Acad Sci U S A **93:**15400–15404.
29. **Buchholz UJ, Finke S, Conzelmann KK.** 1999. Generation of bovine respiratory syncytial virus (BRSV) from cDNA: BRSV NS2 is not essential for virus replication in tissue culture, and the human RSV leader region acts as a functional BRSV genome promoter. J Virol **73:**251–259.
30. **Shi X, Elliott RM.** 2009. Generation and analysis of recombinant Bunyamwera orthobunyaviruses expressing V5 epitope-tagged L proteins. J Gen Virol **90:**297–306. http://dx.doi.org/10.1099/vir.0.007567-0.
31. **Johnson KN, Zeddam JL, Ball LA.** 2000. Characterization and construction of functional cDNA clones of Pariacoto virus, the first Alphanodavirus isolated outside Australasia. J Virol **74:**5123–5132. http://dx.doi.org/10.1128/JVI.74.11.5123-5132.2000.
32. **Elliott RM, Blakqori G, van Knippenberg IC, Koudriakova E, Li P, McLees A, Shi X, Szemiel AM.** 2013. Establishment of a reverse genetics system for Schmallenberg virus, a newly emerged orthobunyavirus in Europe. J Gen Virol **94:**851–859. http://dx.doi.org/10.1099/vir.0.049981-0.
33. **Brennan B, Welch SR, Elliott RM.** 2014. The consequences of reconfiguring the ambisense S genome segment of Rift Valley fever virus on viral replication in mammalian and mosquito cells and for genome packaging. PLoS Pathog **10:**e1003922. http://dx.doi.org/10.1371/journal.ppat.1003922.
34. **Emeny JM, Morgan MJ.** 1979. Regulation of the interferon system: evidence that Vero cells have a genetic defect in interferon production. J Gen Virol **43:**247–252.
35. **Chinsangaram J, Piccone ME, Grubman MJ.** 1999. Ability of foot-and-mouth disease virus to form plaques in cell culture is associated with suppression of alpha/beta interferon. J Virol **73:**9891–9898.
36. **Desmyter J, Melnick JL, Rawls WE.** 1968. Defectiveness of interferon production and of rubella virus interference in a line of African green monkey kidney cells (Vero). J Virol **2:**955–961.
37. **Spann KM, Tran KC, Chi B, Rabin RL, Collins PL.** 2004. Suppression of the induction of alpha, beta, and lambda interferons by the NS1 and NS2 proteins of human respiratory syncytial virus in human epithelial cells and macrophages [corrected]. J Virol **78:**4363–4369. http://dx.doi.org/10.1128/JVI.78.8.4363-4369.2004.
38. **van Knippenberg I, Carlton-Smith C, Elliott RM.** 2010. The N-terminus of Bunyamwera orthobunyavirus NSs protein is essential for interferon antagonism. J Gen Virol **91:**2002–2006. http://dx.doi.org/10.1099/vir.0.021774-0.
39. **Killip MJ, Young DF, Gatherer D, Ross CS, Short JA, Davison AJ, Goodbourn S, Randall RE.** 2013. Deep sequencing analysis of defective genomes of parainfluenza virus 5 and their role in interferon induction. J Virol **87:**4798–4807. http://dx.doi.org/10.1128/JVI.03383-12.
40. **Bridgen A, Weber F, Fazakerley JK, Elliott RM.** 2001. Bunyamwera bunyavirus nonstructural protein NSs is a nonessential gene product that contributes to viral pathogenesis. Proc Natl Acad Sci U S A **98:**664–669. http://dx.doi.org/10.1073/pnas.98.2.664.
41. **Hart TJ, Kohl A, Elliott RM.** 2009. Role of the NSs protein in the zoonotic capacity of Orthobunyaviruses. Zoonoses Public Health **56:**285–296. http://dx.doi.org/10.1111/j.1863-2378.2008.01166.x.
42. **Hale BG, Knebel A, Botting CH, Galloway CS, Precious BL, Jackson D, Elliott RM, Randall RE.** 2009. CDK/ERK-mediated phosphorylation of the human influenza A virus NS1 protein at threonine-215. Virology **383:**6–11. http://dx.doi.org/10.1016/j.virol.2008.10.002.
43. **Streitenfeld H, Boyd A, Fazakerley JK, Bridgen A, Elliott RM, Weber F.** 2003. Activation of PKR by Bunyamwera virus is independent of the viral interferon antagonist NSs. J Virol **77:**5507–5511. http://dx.doi.org/10.1128/JVI.77.9.5507-5511.2003.
44. **Varela M, Schnettler E, Caporale M, Murgia C, Barry G, McFarlane M, McGregor E, Piras IM, Shaw A, Lamm C, Janowicz A, Beer M, Glass M, Herder V, Hahn K, Baumgartner W, Kohl A, Palmarini M.** 2013.

Schmallenberg virus pathogenesis, tropism and interaction with the innate immune system of the host. PLoS Pathog **9:**e1003133. http://dx.doi.org/10.1371/journal.ppat.1003133.
45. **Figueiredo LT, Da Rosa AP.** 1988. Jatobal virus antigenic characterization by ELISA and neutralization test using EIA as indicator, on tissue culture. Mem Inst Oswaldo Cruz **83:**161–164.
46. **Shi X, Kohl A, Leonard VH, Li P, McLees A, Elliott RM.** 2006. Requirement of the N-terminal region of orthobunyavirus nonstructural protein NSm for virus assembly and morphogenesis. J Virol **80:**8089–8099. http://dx.doi.org/10.1128/JVI.00579-06.
47. **Shi X, Kohl A, Li P, Elliott RM.** 2007. Role of the cytoplasmic tail domains of Bunyamwera orthobunyavirus glycoproteins Gn and Gc in virus assembly and morphogenesis. J Virol **81:**10151–10160. http://dx.doi.org/10.1128/JVI.00573-07.
48. **Kading RC, Crabtree MB, Bird BH, Nichol ST, Erickson BR, Horiuchi K, Biggerstaff BJ, Miller BR.** 2014. Deletion of the NSm virulence gene of Rift Valley fever virus inhibits virus replication in and dissemination from the midgut of *Aedes aegypti* mosquitoes. PLoS Negl Trop Dis **8:**e2670. http://dx.doi.org/10.1371/journal.pntd.0002670.
49. **Crabtree MB, Kent Crockett RJ, Bird BH, Nichol ST, Erickson BR, Biggerstaff BJ, Horiuchi K, Miller BR.** 2012. Infection and transmission of Rift Valley fever viruses lacking the NSs and/or NSm genes in mosquitoes: potential role for NSm in mosquito infection. PLoS Negl Trop Dis **6:**e1639. http://dx.doi.org/10.1371/journal.pntd.0001639.
50. **Soellick T, Uhrig JF, Bucher GL, Kellmann JW, Schreier PH.** 2000. The movement protein NSm of tomato spotted wilt tospovirus (TSWV): RNA binding, interaction with the TSWV N protein, and identification of interacting plant proteins. Proc Natl Acad Sci U S A **97:**2373–2378. http://dx.doi.org/10.1073/pnas.030548397.
51. **Kormelink R, Storms M, Van Lent J, Peters D, Goldbach R.** 1994. Expression and subcellular location of the NSM protein of tomato spotted wilt virus (TSWV), a putative viral movement protein. Virology **200:**56–65.
52. **Storms MM, Kormelink R, Peters D, Van Lent JW, Goldbach RW.** 1995. The nonstructural NSm protein of tomato spotted wilt virus induces tubular structures in plant and insect cells. Virology **214:**485–493.
53. **Weber F, Bridgen A, Fazakerley JK, Streitenfeld H, Kessler N, Randall RE, Elliott RM.** 2002. Bunyamwera bunyavirus nonstructural protein NSs counteracts the induction of alpha/beta interferon. J Virol **76:**7949–7955. http://dx.doi.org/10.1128/JVI.76.16.7949-7955.2002.
54. **Kohl A, Clayton RF, Weber F, Bridgen A, Randall RE, Elliott RM.** 2003. Bunyamwera virus nonstructural protein NSs counteracts interferon regulatory factor 3-mediated induction of early cell death. J Virol **77:**7999–8008. http://dx.doi.org/10.1128/JVI.77.14.7999-8008.2003.
55. **Billecocq A, Spiegel M, Vialat P, Kohl A, Weber F, Bouloy M, Haller O.** 2004. NSs protein of Rift Valley fever virus blocks interferon production by inhibiting host gene transcription. J Virol **78:**9798–9806. http://dx.doi.org/10.1128/JVI.78.18.9798-9806.2004.
56. **Léonard VH, Kohl A, Hart TJ, Elliott RM.** 2006. Interaction of Bunyamwera Orthobunyavirus NSs protein with mediator protein MED8: a mechanism for inhibiting the interferon response. J Virol **80:**9667–9675. http://dx.doi.org/10.1128/JVI.00822-06.
57. **Eick D, Geyer M.** 2013. The RNA polymerase II carboxy-terminal domain (CTD) code. Chem Rev **113:**8456–8490. http://dx.doi.org/10.1021/cr400071f.
58. **Corden JL.** 2013. RNA polymerase II C-terminal domain: tethering transcription to transcript and template. Chem Rev **113:**8423–8455. http://dx.doi.org/10.1021/cr400158h.
59. **Robinson PJJ, Bushnell DA, Trnka MJ, Burlingame AL, Kornberg RD.** 2012. Structure of the Mediator Head module bound to the carboxy-terminal domain of RNA polymerase II. Proc Natl Acad Sci U S A **109:**17931–17935. http://dx.doi.org/10.1073/pnas.1215241109.
60. **Thomas D, Blakqori G, Wagner V, Banholzer M, Kessler N, Elliott RM, Haller O, Weber F.** 2004. Inhibition of RNA polymerase II phosphorylation by a viral interferon antagonist. J Biol Chem **279:**31471–31477. http://dx.doi.org/10.1074/jbc.M400938200.
61. **Verbruggen P, Ruf M, Blakqori G, Overby AK, Heidemann M, Eick D, Weber F.** 2011. Interferon antagonist NSs of La Crosse virus triggers a DNA damage response-like degradation of transcribing RNA polymerase II. J Biol Chem **286:**3681–3692. http://dx.doi.org/10.1074/jbc.M110.154799.
62. **Blakqori G, Delhaye S, Habjan M, Blair CD, Sanchez-Vargas I, Olson KE, Attarzadeh-Yazdi G, Fragkoudis R, Kohl A, Kalinke U, Weiss S, Michiels T, Staeheli P, Weber F.** 2007. La Crosse bunyavirus nonstructural protein NSs serves to suppress the type I interferon system of mammalian hosts. J Virol **81:**4991–4999. http://dx.doi.org/10.1128/JVI.01933-06.
63. **Barry G, Varela M, Ratinier M, Blomstrom AL, Caporale M, Seehusen F, Hahn K, Schnettler E, Baumgartner W, Kohl A, Palmarini M.** 2014. NSs protein of Schmallenberg virus counteracts the antiviral response of the cell by inhibiting its transcriptional machinery. J Gen Virol **95:**1640–1646. http://dx.doi.org/10.1099/vir.0.065425-0.
64. **Assfalg R, Lebedev A, Gonzalez OG, Schelling A, Koch S, Iben S.** 2012. TFIIH is an elongation factor of RNA polymerase I. Nucleic Acids Res **40:**650–659. http://dx.doi.org/10.1093/nar/gkr746.
65. **Ning YJ, Feng K, Min YQ, Cao WC, Wang M, Deng F, Hu Z, Wang H.** 2015. Disruption of type I interferon signaling by NSs protein of severe fever with thrombocytopenia syndrome virus via hijacking STAT2 and STAT1 into inclusion bodies. J Virol **89:**4227–4236. http://dx.doi.org/10.1128/JVI.00154-15.
66. **Ning YJ, Wang M, Deng M, Shen S, Liu W, Cao WC, Deng F, Wang YY, Hu Z, Wang H.** 2014. Viral suppression of innate immunity via spatial isolation of TBK1/IKKepsilon from mitochondrial antiviral platform. J Mol Cell Biol **6:**324–337. http://dx.doi.org/10.1093/jmcb/mju015.
67. **Proenca-Modena JL, Sesti-Costa R, Pinto AK, Richner JM, Lazear HM, Lucas T, Hyde JL, Diamond MS.** 2015. Oropouche virus infection and pathogenesis are restricted by MAVS, IRF-3, IRF-7, and type I interferon signaling pathways in nonmyeloid cells. J Virol **89:**4720–4737. http://dx.doi.org/10.1128/JVI.00077-15.
68. **Livonesi MC, de Sousa RL, Badra SJ, Figueiredo LT.** 2007. In vitro and in vivo studies of the interferon-alpha action on distinct Orthobunyavirus. Antiviral Res **75:**121–128. http://dx.doi.org/10.1016/j.antiviral.2007.01.158.